EXPERIMENTAL AND THEORETICAL STUDIES ON THE PERIPHERAL ZONE OF THE ERYTHROCYTE MEMBRANE

by

Frank Jürgen Nordt, B.S.

A THESIS

Presented to the Department of Biochemistry
and the Graduate Division of the
University of Oregon Health Sciences Center
in partial fulfillment of
the requirements for the degree of

Doctor of Philosophy
August 1979

APPROVED:

[redacted]

Professor in Charge of Thesis

[redacted]

Chairman, Graduate Council

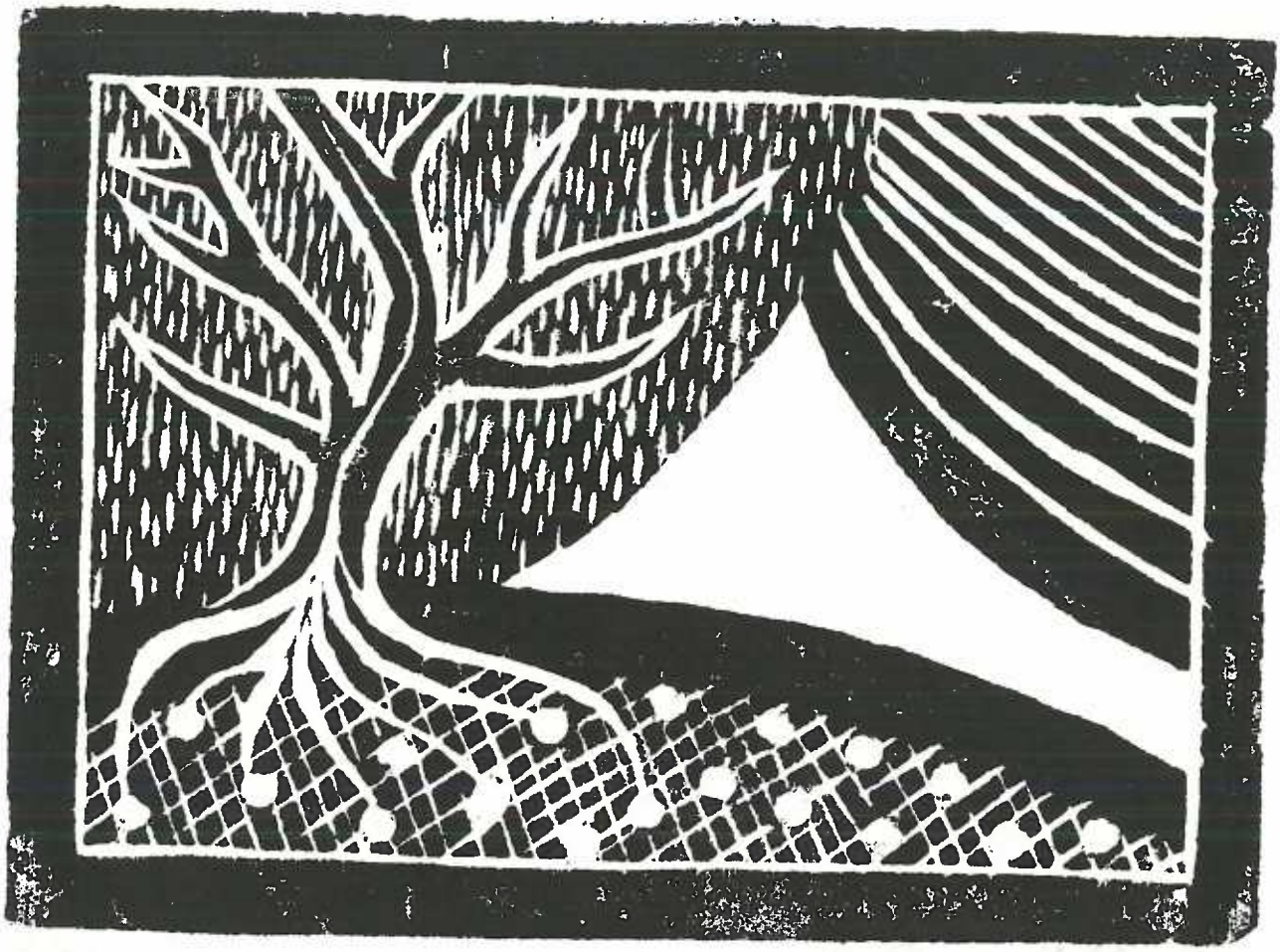

ACKNOWLEDGMENTS

I wish to thank my supervisor, Dr. G.V.F. Seaman, from whose advice, criticism and encouragement I have benefitted greatly. His generosity throughout our association is also gratefully acknowledged. I am indebted to Dr. Robert J. Knox and Charles F. Zukoski IV for many helpful discussions as well as assistance with some experiments. I am especially grateful to Janet Cowan whose talents and skills in deciphering my manuscripts are unparalleled. Her encouragement and good spirits are also deeply appreciated. I also wish to thank Pam Ewing and Karen Berger for their secretarial assistance and Clover Redfern for her typing the final manuscript.

Finally I wish to express my gratitude to my wife, Joan, and daughter, Kirsten, for their patience and understanding throughout the period during which this research was performed.

TO JOAN, KIRSTEN AND INGRID

TABLE OF CONTENTS

Chapter | Page

LIST OF FIGURES

LIST OF TABLES

CHAPTER 1

INTRODUCTION

Diseases in which shortened red cell life span is a characteristic feature have provided impetus to studies on the mechanism of red cell aging, recognition and elimination. How does the intact organism recognize a senescent red cell? Normal erythrocytes are biocompatible until they are recognized as effete or damaged and are sequestered and catabolized by the reticuloendothelial system. Current hypotheses on the mechanisms of red cell aging, recognition and destruction invoke the supposition that alterations in the membrane and surface properties of red cells upon aging are responsible for this eventual recognition and elimination. The role of sialic acid, a major terminal carbohydrate moiety at the exoface of human red cell membrane glycoproteins and the major surface charge contributor of the red cell, has been receiving increasing attention, stimulated in part by the work of Ashwell and Morell on the rapid and specific elimination of desialylated circulating plasma glycoproteins. Neuraminidase, an enzyme which specifically cleaves sialyl residues, has been used to treat red cells to produce changes in cell surface properties which mimic some aspects of cellular senescence. This, together with reported decreases in sialic acid levels in old as compared to young cells and reported decreases in surface charge density, led to the

examination of the evidence for selective losses of sialic acid from red cells as well as the action of neuraminidase on the surfaces of red cells. Subsequently the observation was made that red cells treated with neuraminidase had anomalous electrokinetic properties which were not consistent with the view that simple loss of sialic acid was the only consequence of interaction with the enzyme. The thematic questions around which the subject matter of this thesis revolves are: 1) what is the nature of the anomalous electrophoretic properties of neuraminidase treated human erythrocytes and, 2) what implications may they have on the hypothesis that sialic acid is a major determinant of red cell life span.

The following section of this chapter outlines the theoretical underpinnings of cellular electrophoresis. The second chapter details some of the methodology common to much of the work, followed in the third chapter by description of equipment and experimental procedures utilized in gathering electrophoretic data. Included are sections detailing innovations in the design of equipment as well as the development of low zeta potential gel surface coatings for the elimination of electroosmotic flow in analytical particle electrophoresis. The fourth chapter describes the electrokinetic properties of human red blood cells, particularly after fixation with formaldehyde where the theoretical and experimental effects of cellular conductivity on their electrokinetic properties are considered. The following two chapters

deal directly with the sialic acid content of young and old erythrocytes, its relationship to surface charge density, and the interaction of Vibrio cholerae neuraminidase with the surfaces of human erythrocytes. The seventh chapter lists the conclusions which have been drawn from this work.

1.1 History and Theory of Electrophoresis

Prior to the 19th century, interest in phase boundaries and the nature of surfaces was primarily academic. Spurred by advances in electrochemistry and the advent of sources of steady direct current, Ferdinand Frédéric Reuss made a series of observations in 1807 on the relative positive charge of water in contact with powdered clay or quartz, on which he reported in Moscow in 1808 (1). Without being aware of it nor having a satisfactory explanation for the phenomena which he observed, Reuss in fact discovered electroosmosis.

In 1852 Wiedemann (2) attempted to describe quantitatively the relationship in electroosmosis between the amount of liquid transported and the magnitude of current and electromotive force applied. In 1859 Quincke (3) was the first to postulate the existence of a phenomenon which is the opposite of electroosmosis, namely, a liquid made to flow along a stationary charged surface should give rise to a potential difference between the ends of the surface. This phenomenon was later termed the streaming potential. The reciprocal phenomenon to

electrophoresis, namely the sedimentation potential, which arises as a result of an electric field which is created when charged particles move relative to a stationary fluid, was first qualitatively observed by Dorn in 1878 (4).

Quincke (5) later turned his attention to the movement of particles in an electric field, i.e., electrophoresis, and determined that most substances in contact with water are negatively charged. The validity of this conclusion has since been borne out. Quincke further observed that the net direction and velocity of movement of particles in aqueous media in a closed glass tube is due to the vector sum of the separate movements of the fluid and the particle.

Interest in biological surfaces was stimulated by Kühne's experiments on muscle fibers in 1860 (6). The swelling of muscle tissue which takes place at the negative pole, on application of a current, was correctly interpreted as being due to electroosmosis, which further indicated that the charge on muscle tissue was negative. Similar results were obtained on nervous tissue.

During this early period semiempirical laws were advanced to explain the electrical and mechanical forces at play, where interfaces move with respect to one another. Both inorganic as well as biological materials were shown to act as if they were charged when in contact with aqueous media. Furthermore, it was found that the vast majority of surfaces are negatively charged. Up until this point (1878) however,

no satisfactory theory had been developed to account for the origin of surface electric charge nor for the interrelationship of the variety of variables which play a role in electrokinetic phenomena. Thus, the theories advanced over the next few decades, i.e., the late nineteenth and early twentieth centuries, will be examined with special emphasis on electrophoresis.

The net surface charge of a particle is governed principally by ionization of surface groups, ion ad- or desorption or chemical reaction of surface groups with a component in the suspending medium. The surface charge affects the distribution of ions in the medium by attracting ions of opposite charge (counter or gegen-ions) toward the surface while repelling ions of like charge (co-ions) away from the solid-solution interface.

Thermal (Brownian) motion of ions opposes the electrical forces which determine the distribution of ions around the charged surface. In order to maintain overall electroneutrality of the system there exists a diffuse neutralizing region of excess counterions in the vicinity of the surface (see Fig. 1-1). The distance over which this diffuse double layer of charge extends into the ionic medium is directly related to the density of population of ions and their valency, in bulk solution. The extension of the double layer decreases in proportion to the square root of the ionic strength of the medium in contact with the surface.

Figure 1-1. a) and b) Schematic representation of the distribution of ions in the diffuse part of an electrical double layer near a negatively charged surface. The counter-ion concentration close to the surface is much greater than the co-ion concentration. At a relatively large distance (x) from the surface the counter- and co-ion concentrations become equal to their bulk solution values, n_0.

(a)

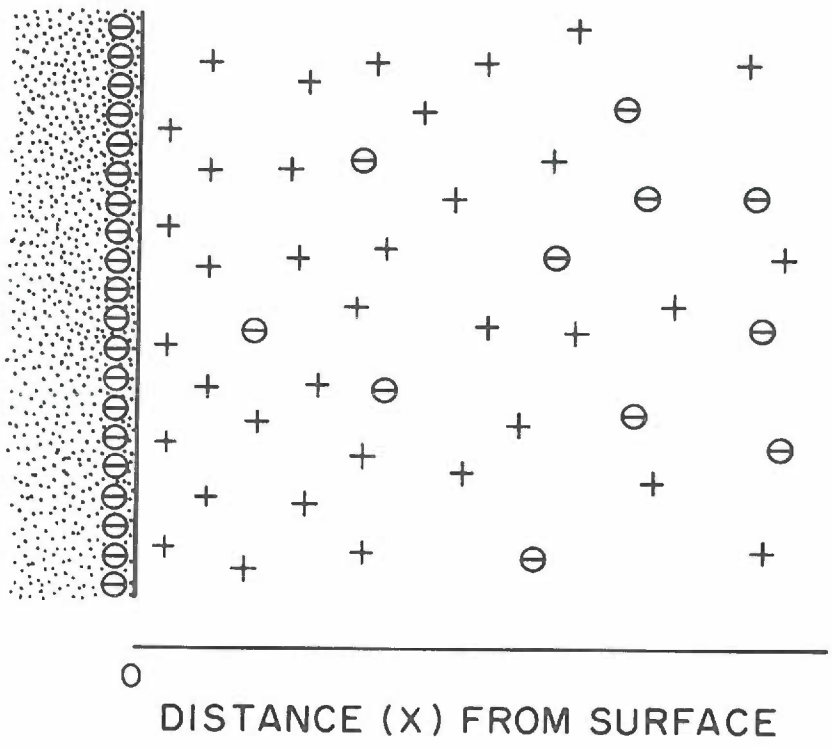
O
DISTANCE (X) FROM SURFACE

(b)

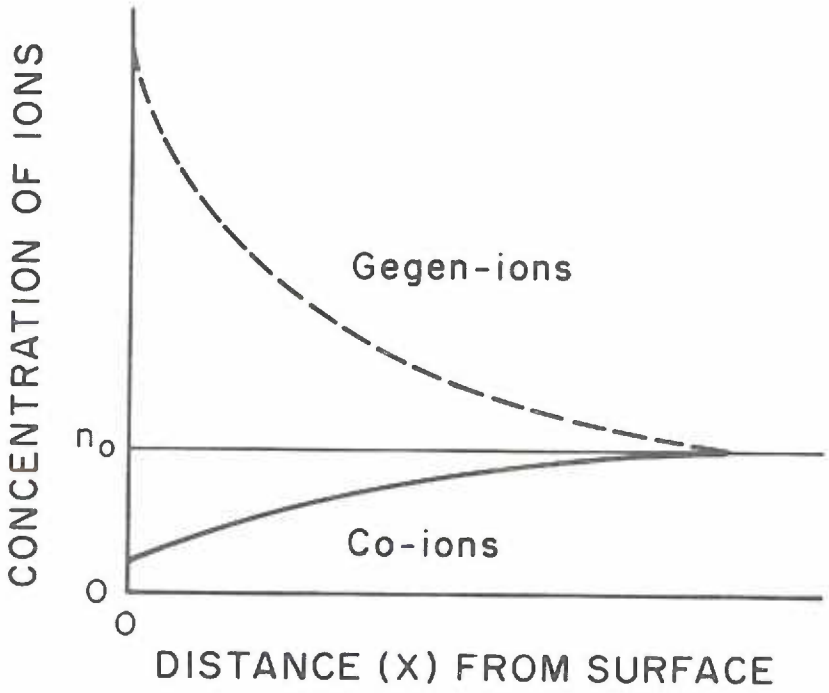
CONCENTRATION OF IONS
Gegen-ions
n_o
Co-ions
O
O
DISTANCE (X) FROM SURFACE

On application of an external force such as an electric field to a particle-double layer system, movement of the particle will result, in a direction dictated by the polarity of the field (electrophoresis). The counterions in the double layer will move in the opposite direction carrying solvent molecules along with them thus exerting viscous drag on the particle. The lower the ionic concentration in the bulk phase, the more diffuse will be the double layer, the less viscous drag will be exerted by it on the particle and the greater will be the electrophoretic velocity of the particle. The electrophoretic mobility of the particle is defined as the electrophoretic velocity of the particle divided by the magnitude of the electric field. The relationship between the experimentally determined electrophoretic mobility (u) and the electrostatic potential (ζ) present at the plane of hydrodynamic slip was first formulated by von Smoluchowski (7) as:

$$\frac{v_e}{X} = u = \frac{\varepsilon \zeta}{4\pi\eta} \qquad 1\text{-}1$$

where v_e is the velocity of the particle in an externally applied electric field of strength, X, and ε and η are the dielectric constant and viscosity of the bulk suspending medium, respectively.

The following equations dealing with electrokinetic phenomena have been well summarized by a number of authors (8, 9, 10, 11). Consider the motion of a fluid lamina in the diffuse part of the double

layer region relative to that of a nonconducting charged surface in the presence of an externally applied electric field X the lines of force of which run parallel to the surface. Then the electrical force on the ions which is transferred to the molecules of the suspending medium in the lamina of thickness, dx, is:

$$\rho X A dx \qquad 1\text{-}2$$

where ρ is the charge density in the liquid and A the area of the lamina. The electrical force is opposed by a viscous retardation force which at the distance, x, from the surface is given by

$$-A(\eta \frac{dv}{dx})_x \qquad 1\text{-}3$$

At a point $(x + dx)$ the force may be written as:

$$A(\eta \frac{dv}{dx})_{x+dx} \qquad 1\text{-}4$$

where η and dv/dx, in both Eqs. 1-3 and 1-4, is the viscosity and velocity gradient, respectively. Equation 1-4 may be expanded by means of a Taylor series:

$$A(\eta \frac{dv}{dx})_{x+dx} = A(\eta \frac{dv}{dx})_x + A[\frac{d}{dx}(\eta \frac{dv}{dx})]_x dx \qquad 1\text{-}5$$

Combining Eqs. 1-3 and 1-5 the total viscous retardation force on the lamina is:

$$A\left[\frac{d}{dx}\left(\eta\frac{dv}{dx}\right)\right]_x dx \qquad 1\text{-}6$$

For an infinite flat surface, the charge may be assumed to vary only in the direction normal to the surface and the dielectric constant, ε, is assumed to be independent of both the potential, ψ, and the charge density, ρ. Poisson's equation in one dimension may thus be utilized, i.e.,

$$\frac{d^2\psi}{dx^2} = -\frac{4\pi\rho}{\varepsilon} \qquad 1\text{-}7$$

At terminal velocity, the electrical forces will be equally balanced by the viscous forces. This may be represented mathematically by rearranging and substituting for ρ in in Eq. 1-2 and combining the result with Eq. 1-6:

$$\frac{X}{4\pi}\frac{d}{dx}\left(\varepsilon\frac{d\psi}{dx}\right) = \frac{d}{dx}\left(\eta\frac{dv}{dx}\right) \qquad 1\text{-}8$$

To obtain the potential at any distance x from the surface Eq. 1-8 may be multiplied by x and the result integrated by parts over the region $x = 0$ to $x = \infty$ which leads to:

$$\frac{X}{4\pi}\left[x\left(\varepsilon\frac{d\psi}{dx}\right)\Big|_0^\infty - \int_0^\infty \varepsilon\frac{d\psi}{dx}\,dx\right] = \left[x\left(\eta\frac{dv}{dx}\right)\Big|_0^\infty - \int_0^\infty \eta\frac{dv}{dx}\,dx\right] \qquad 1\text{-}9$$

Since at $x = \infty$, both dv/dx and $d\psi/dx$ are zero the first terms on either side of Eq. 1-9 drop out. Integrating the remainder the following is obtained:

$$\eta v \Big|_0^\infty = \frac{X\varepsilon}{4\pi} \psi \Big|_0^\infty \qquad 1\text{-}10$$

Changing the frame of reference by setting the velocity of the fluid at the surface, $-v$, equal to the velocity of the surface relative to that of the fluid, v_e, the Smoluchowski equation relating the electrophoretic mobility, u, to the potential at the surface is obtained:

$$\frac{v_e}{X} = u = \frac{\varepsilon\psi}{4\pi\eta} \qquad 1\text{-}11$$

When a particle undergoes electrophoresis it carries with it a thin, probably monomolecular, layer of fluid and specifically adsorbed counterions (Stern layer) which shield the actual surface potential. As a result the potential which may be calculated from the electrophoretic mobility with Eq. 1-11 does not actually represent a surface potential, but rather a potential at some distance away from the surface. The plane which coincides with this distance is the electrophoretic surface or plane of hydrodynamic shear. Since knowledge of the hydrodynamic behavior near charged interfaces is scant, the exact location of the slip plane remains uncertain. For this reason, ψ, the surface potential in Eq. 1-11 is replaced by ζ, the zeta potential giving:

$$\frac{v_e}{X} = u = \frac{\varepsilon\zeta}{4\pi\eta} \qquad 1\text{-}12$$

For example, the zeta potential of particles whose charge stems from entities which are an integral part of the surface, such as ionized functional groups, will generally be of the same sign as the surface potential but of somewhat smaller magnitude. However, if the particle charge stems primarily from specifically adsorbed counterions, the zeta potential may in fact be of opposite sign to the actual surface potential. Debye and Hückel (12) corroborated Smoluchowski's Eq. 1-12 except for the fact that instead of $1/4\pi$, they obtained a factor $1/6\pi$. The explanation for the apparent discrepancy is due to Henry (13) who showed that for weakly charged particles ($\zeta < 25$ mV):

$$u = \frac{\varepsilon\zeta}{6\pi\eta} f(\kappa a, \sigma_2/\sigma_1) \qquad 1\text{-}13$$

where $1/\kappa$ is the thickness of the double layer, a is the radius of curvature of the particle under investigation, and σ_2 and σ_1 are the specific conductivities of the particle and the suspending medium, respectively.

Von Smoluchowski in his analysis had assumed that the external electric field deformed around the particle such that it was everywhere parallel to the particle surface. On the other hand Hückel assumed that the lines of force of the external field ran straight from one

Figure 1-2. a) Schematic representation of a diffuse electrical double layer near a negatively charged surface with specifically adsorbed hydrated counter-ions. The centers of the specifically adsorbed ions, which may be dehydrated in the direction of the surface, are located between the surface and the Stern plane, S, at X_1. The electrophoretic surface or shear plane, D, at X_2, is located at the plane demarcated by the outer edge of the hydrated adsorbed ions.

b) Schematic illustration of the electrical potential at various distances from the surface. Notice the ζ potential in this example is less than the surface potential, ψ_0, and Stern potential, ψ_1. This is due to counter-ions shielding the actual surface charge. In some cases the ζ potential may actually be of opposite sign to the surface potential, e.g., in the case of adsorption of surface active counter-ions. In other cases the ζ potential may be of greater magnitude than the surface potential, e.g., in the case of adsorption of surface active co-ions.

(a)

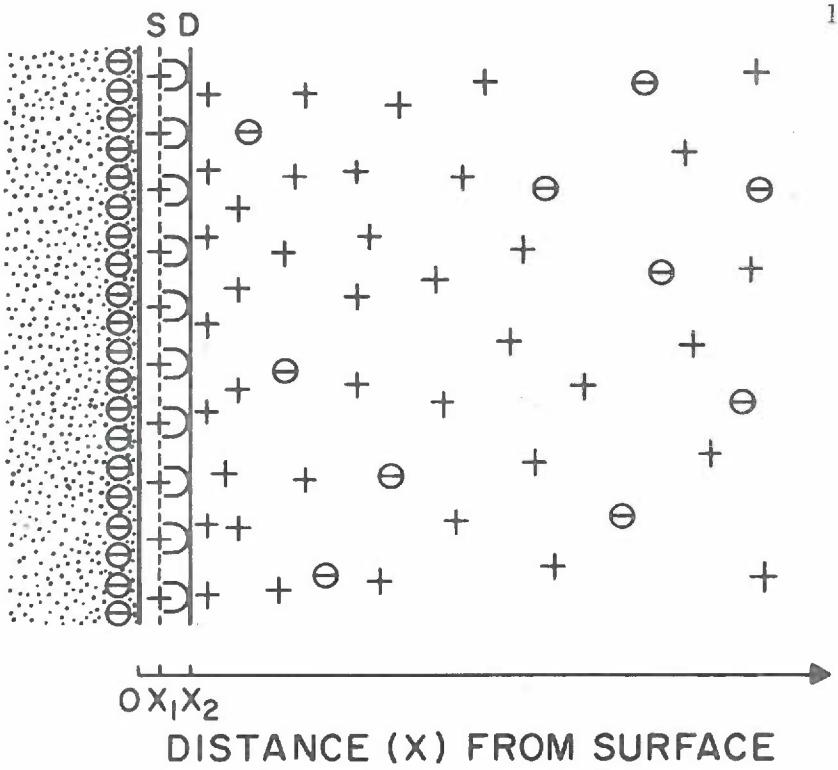
S D
O X1 X2
DISTANCE (X) FROM SURFACE

(b)

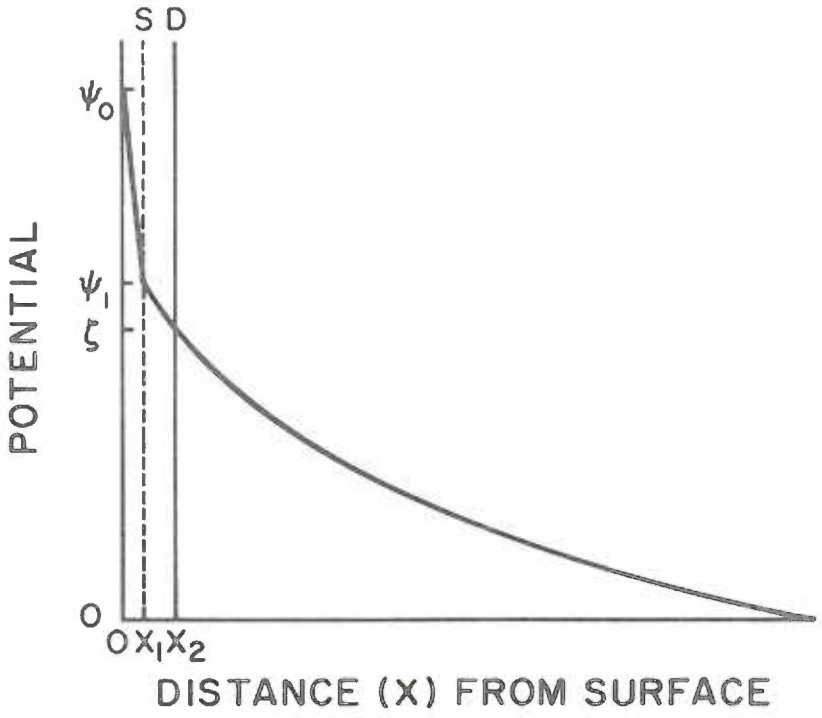
S D
Ψ0
Ψ1
ζ
POTENTIAL
0
O X1 X2
DISTANCE (X) FROM SURFACE

electrode to the other, i.e., the particle acted as a conductor (see Fig. 1-3). For a nonconducting particle Eq. 1-13 reduces to:

$$u = \frac{\varepsilon \zeta}{6 \pi \eta} f(\kappa a) \qquad 1-14$$

From the definition of κ and a, it can be seen that κa is a measure of the ratio of the particle radius to the thickness of the double layer. In the limiting case of $\kappa a \rightarrow \infty$, i.e., when the double layer is very thin in comparison to the radius, Henry (13) showed that $f(\kappa a) = 3/2$ in which case Eq. 1-14 further reduces to Eq. 1-12, the Smoluchowski equation. On the other hand when $\kappa a \rightarrow 0$, $f(\kappa a) = 1$ and the result of Hückel is obtained (see Fig. 1-4).

Henry's analysis for a particle whose double layer thickness is small in comparison to its local radii of curvature, suggests that the electrophoretic mobility of this particle is independent of its shape. Strictly speaking however, his derivation is valid only for spheres and cylinders. Nevertheless, Eq. 1-12 is valid for a particle of arbitrary shape. This has been rigorously proven by Morrison (14). Moreover these assertions have also been borne out experimentally. Abramson (15) for example, has summarized data of numerous investigators pertaining to the independence of the electrophoretic mobility of particles on their shape and size. Similar conclusions have been drawn for biological cells. A number of examples exist which indicate that the

Figure 1-3. a) The lines of force of an external electric field in the presence of a particle, the conductivity of which is equal to that of the suspending medium.

b) The lines of force around a nonconducting particle in a conducting medium.

(a)

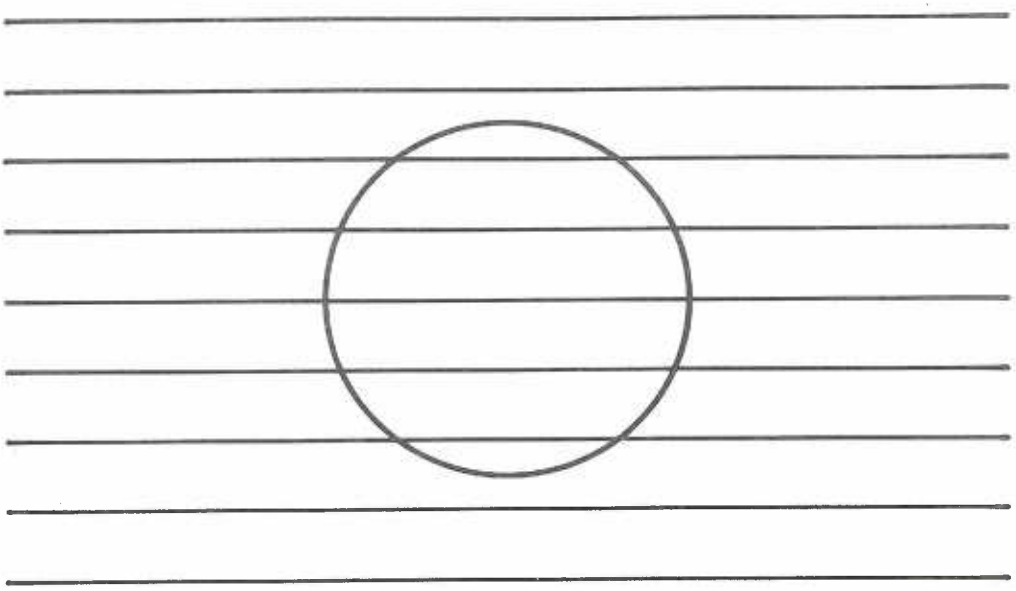

(b)

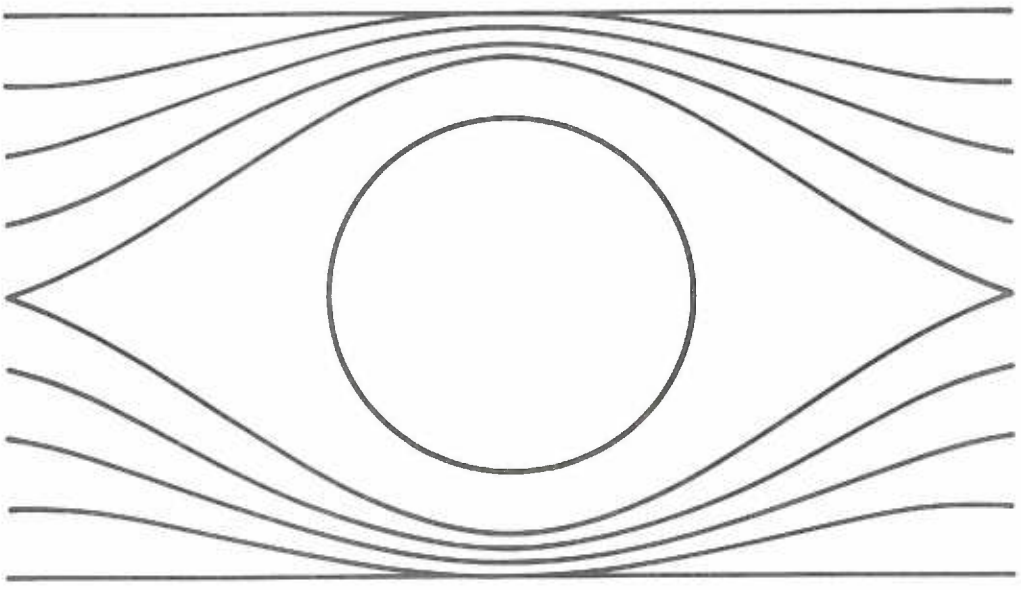

Figure 1-4. A plot of Henry's function $f(\kappa a, \sigma_2/\sigma_1)$ as a function of $\log \kappa a$ for a nonconducting (——) and conducting spherical particle (– – –) and for a nonconducting cylindrical particle oriented perpendicularly to the field (·····) and oriented parallel to the field (– · –).

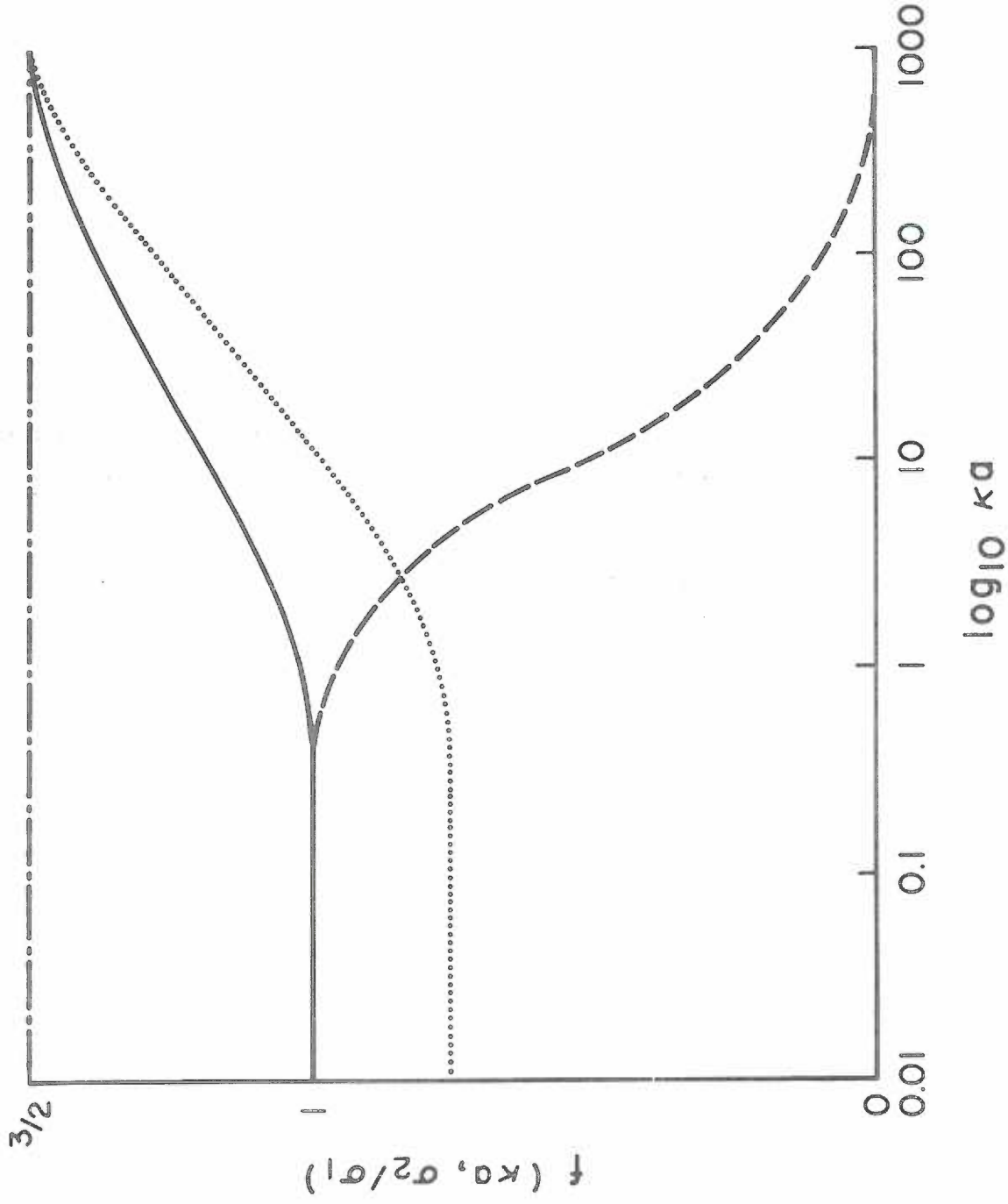
3/2
1
0
f (κa, σ2/σ1)
0.01
0.1
1.0
10
100
1000
log10 κa

surface shape of erythrocytes does not influence their mobility. Furchgott and Ponder (16) have shown that normal biconcave discoid red cells have the same mobility as sphered cells. The mobility of sickled cells is also identical to that of normal cells (17, 18). In the absence of evidence to the contrary, it must be concluded that the electrophoretic velocity of large colloidal particles, whose radii of curvature are large in relationship to the thickness of their double layers, is independent of their macroscopic shape.

1.2 Kinetics of Electrophoresis

As noted, the electrical forces acting on a charged particle are due to the net charge per unit area of surface and they are balanced by viscous forces on reaching a steady state velocity such that the total force on a particle undergoing electrophoresis is zero. An important question is the time required for a particle to reach its terminal equilibrium velocity since the time constant should only be a small percentage of the measurement time, otherwise serious errors in estimating an electrophoretic mobility would arise.

For the sake of simplicity, the case for a spherical particle with large κa will be considered. The forces acting on a particle at rest in a viscous medium to which a constant force, E, is applied at time, $t = 0$, may be described by the second order differential equation:

$$m \frac{dx^2}{dt^2} = E - b \frac{dx}{dt} \qquad 1\text{-}15$$

where m is the mass of the particle and b is the damping coefficient which from Stokes' law takes the form $6\pi\eta a$, where η and a are the viscosity of the medium and radius of the particle, respectively.

If E is the electrical force acting on the particle using Henry's adaptation (13) of Debye and Hűckel's analysis (12), Eq. 1-15 may be rewritten as:

$$m \frac{dx^2}{dt^2} + 6\pi\eta a \frac{dx}{dt} = \frac{3}{2} \varepsilon X a \zeta \qquad 1\text{-}16$$

where

X = magnitude of the electric field applied at $t = 0$.

ζ = zeta potential of the particle.

ε = dielectric constant of the suspending medium.

The solution to Eq. 1-16 is:

$$v(t) = v_0(1-e^{-t/\tau}) \qquad 1\text{-}17$$

where

$v(t)$ = velocity at time t.

v_0 = terminal or steady state velocity

and

τ = the relaxation time which is defined by the relationship

$$\tau = \frac{m}{b} = \frac{m}{6\pi\eta a} \qquad 1\text{-}18$$

The mass m, of a spherical particle is given by:

$$m = \frac{4}{3}\pi a^3 \rho_c \qquad 1\text{-}19$$

where ρ_c = the density of the particle.

Thus, substituting for m in Eq. 1-18 the relaxation time becomes:

$$\tau = \frac{2a^2\rho_c}{9\eta} \qquad 1\text{-}20$$

As an example, for the human red cell the following parameters:

$$a = 7 \times 10^{-4} \text{ cm}$$

$$\rho_c = 1.09 \text{ g} \cdot \text{ml}^{-1}$$

$$\eta = 0.903 \times 10^{-2} \text{ dyne} \cdot \text{sec} \cdot \text{cm}^{-2} \quad \text{for} \quad 0.150 \text{ M NaCl}$$

were substituted into Eq. 1-20 and τ was calculated to be on the order of 13 μsec. Thus, the kinetics of electrophoresis are very rapid indeed.

To this point a further retardation force, the so-called relaxation effect, has been neglected. The relaxation effect arises as a result of a particle, in the presence of an external electric field,

constantly being ahead of the center of its own ionic atmosphere. Overbeek and Wiersema (9) have shown however, that the magnitude of this relaxation effect is negligible for zeta potentials < 25 mV.

In the derivation of Eq. 1-12 it was assumed that the viscous retardation force acting on the surface under consideration was a monotonically decreasing linear function of distance from the particle. Thus, the equation is valid only for particles suspended in media whose rheological behavior is Newtonian and which also exhibit laminar flow. Furthermore, bulk viscosity and dielectric constant values within the double layer were assumed. However, these assumptions may not be valid if the surface potential near the shear plane is high enough to decrease significantly the dielectric constant and/or increase the medium viscosity by dipole orientation. Investigation has shown the effect of a high surface potential on the dielectric constant, ε, to be insignificant, but its effect on the viscosity within the double layer may, in some special instances, be significant, although only at high electrolyte concentrations. Again for particles having low zeta potentials, like most biological particles, these effects are negligible (9). Furthermore, recently Hunter and Alexander (19) and Stigter (20) have criticized the values obtained for the viscoelectric effect by Lijklema and Overbeek (21) as being grossly overestimated.

Thus Eq. 1-12 may be used with confidence for a nonconducting particle, of arbitrary shape and low surface potential, which has a

double layer of small dimension in comparison to its radius of curvature and which is suspended in Newtonian fluids at particle concentrations low enough that two or more particles do not interact hydrodynamically or electrostatically.

1.3 Relationship between the Zeta Potential and Surface Charge Density

The relationship between the charge density of a surface and the surface potential was first derived by Gouy (22) and later Chapman (23). The Boltzmann equation (1-21) is used to give the average number of ions (n_+ and n_- in the case of a uni-univalent electrolyte) per unit volume at a distance x from a plane infinite surface, in terms of the potential ψ at distance x, and the number of ions of each ionic species per unit volume, n_0, in bulk solution.

$$n_+ = n_0 \exp[+\frac{ze\psi}{kT}] \quad \text{and} \quad n_- = n_0 \exp[-\frac{ze\psi}{kT}] \qquad 1\text{-}21$$

The parameters z, e, k and T represent the valence of charge of the ionic species, the electronic charge, Boltzmann's constant and the absolute temperature, respectively. Since the charge at point x is comprised of only ions the charge density, ρ, is given by:

$$\rho = ze(n_- - n_+) \qquad 1\text{-}22$$

Substituting the values for n_+ and n_- from Eq. 1-21 into Eq. 1-22 we obtain:

$$\rho = zen_0[\exp(-\frac{ze\psi}{kT}) - \exp(+\frac{ze\psi}{kT})] \qquad 1\text{-}23$$

The hyperbolic sine is defined by $(\exp^{x} - \exp^{-x})/2 = \sinh x$. Thus Eq. 1-23 may be reduced to:

$$\rho = -2zen_0 \sinh \frac{ze\psi}{kT} \qquad 1\text{-}24$$

Now ρ is also, as shown previously, related to ψ by the Poisson equation:

$$\frac{d^2\psi}{dx^2} = -\frac{4\pi\rho}{\varepsilon} \qquad 1\text{-}7$$

Combining Eq. 1-24 with Eq. 1-23 gives the Poisson-Boltzmann equation:

$$\frac{d^2\psi}{dx^2} = \frac{8\pi zen_0}{\varepsilon} \sinh \frac{ze\psi}{kT} \qquad 1\text{-}25$$

If $(ze\psi/kT) \ll 1$, i.e., if the electrical energy $ze\psi$ is much less than the thermal energy kT, i.e., $\psi \leq 25$ mV, $\sinh(ze\psi/kT) \simeq ze\psi/kT$ giving:

$$\frac{d^2\psi}{dx^2} = \kappa^2\psi \qquad 1\text{-}26$$

where $\kappa = [8\pi z^2 e^2 n_0/\varepsilon kT]^{1/2}$ is the Debye-Hückel reciprocal length parameter. The solution to Eq. 1-26 is given by Gouy (22) and Chapman (23) with the following boundary conditions $\psi = \psi_0$ when $x = 0$ and $\psi = 0$ when $d\psi/dx = 0$ at $x = \infty$ as:

$$\psi = \psi_0 \exp(-\kappa x) \qquad 1\text{-}27$$

It may be seen from this equation that the potential ψ at $x = 1/\kappa$ has dropped to $1/e = 0.37$ of the potential at the surface (ψ_0). Therefore $1/\kappa$ is a good measure for the extension of the double layer and is often referred to as "the thickness of the double layer". The parameter κ may be calculated on the basis of molar ionic concentration, i.e.,

$$\kappa = \left[\left(\frac{4\pi e^2}{1000\varepsilon kT} \right) N_A \sum_i c_i z_i^2 \right]^{1/2} \qquad 1\text{-}28$$

where c_i is the molarity of the ion of type i and N_A is Avogadro's number. More commonly κ is evaluated on the basis of ionic strength, I, as defined by Lewis and Randall (24):

$$I = 1/2 \sum c_i z_i^2 \qquad 1\text{-}29$$

Thus:

$$\kappa = \left[\frac{8\pi e^2 I N_A}{1000\varepsilon kT} \right]^{1/2} \qquad 1\text{-}30$$

It is readily seen from Eqs. 1-28 and 1-30 that either a decrease in ionic valence or concentration (ionic strength) leads to an expansion of the double layer (see Fig. 1-5) as well as an increase in zeta potential at the plane of shear due to a more diffuse double layer.

Now the total surface charge, σ_0, must equal the total space charge in the diffuse double layer and be of opposite sign to maintain electroneutrality, i.e.,

$$\sigma_0 = -\int_0^\infty \rho dx \qquad 1\text{-}31$$

Substituting the Poisson-Boltzmann relation for ρ (Eq. 1-7) we obtain:

$$\sigma_0 = \frac{\varepsilon}{4\pi} \int_0^\infty \frac{d^2\psi}{dx^2} dx \qquad 1\text{-}32$$

Integration, with boundary conditions equal to $d\psi/dx = 0$ at $x = \infty$ and $\psi = \psi_0$ at $x = 0$, and substitution of the differential of Eq. 1-27 results in the relationship:

$$\sigma_0 = -\frac{\varepsilon}{4\pi} \frac{d\psi_0}{dx} = \frac{\kappa\varepsilon\psi_0}{4\pi} \qquad 1\text{-}33$$

Replacing ψ_0 by ζ as for Eq. 1-12 we obtain:

Figure 1-5. Schematic illustration of the effect of decreasing the double layer thickness, $1/\kappa$, on the ζ potential by increasing the ionic strength of the suspending medium.

I = High ionic strength; low ζ potential.

II = Intermediate ionic strength; intermediate ζ potential.

III = Low ionic strength; high ζ potential.

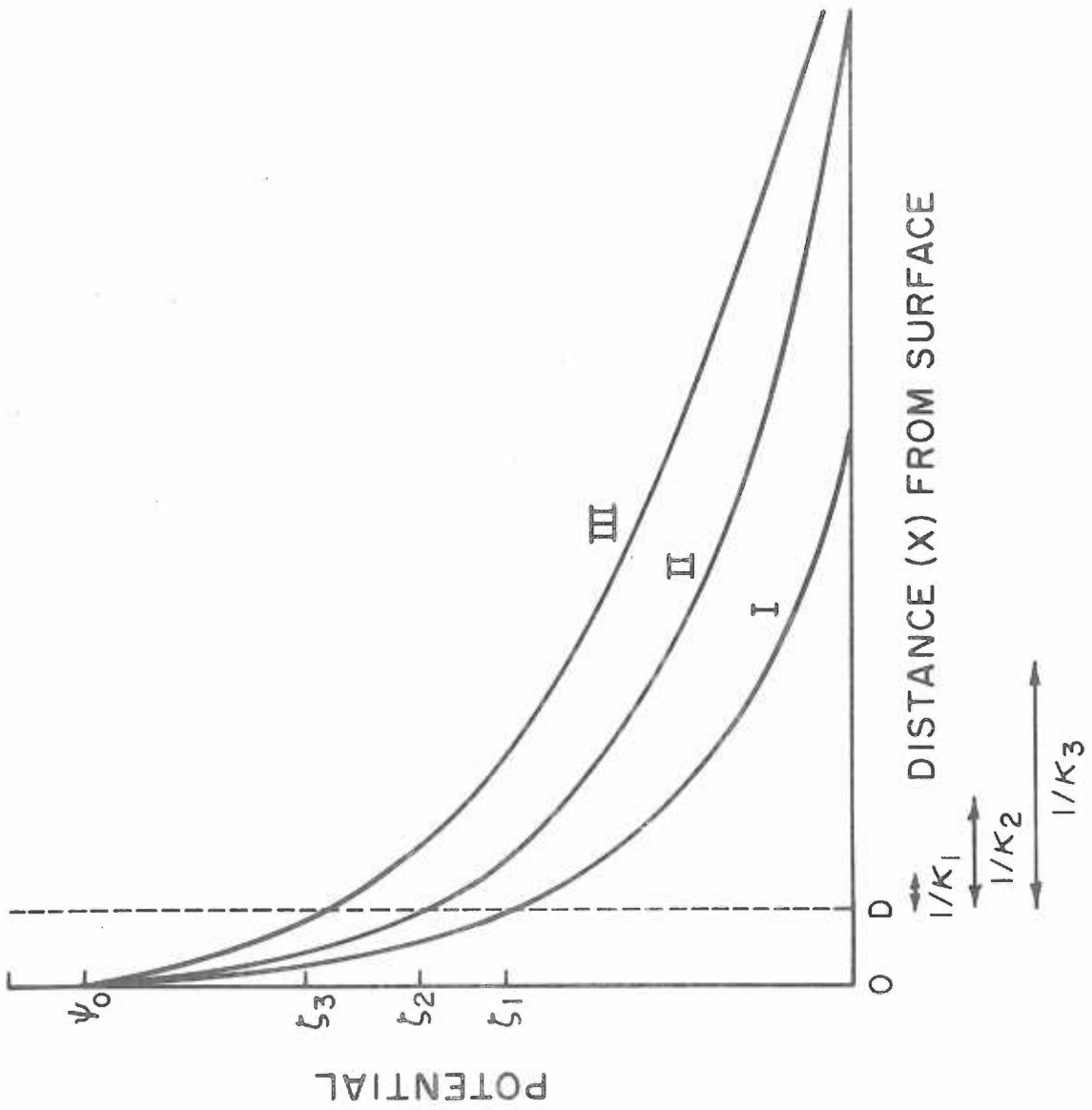
POTENTIAL
ψ_o
ζ_3
ζ_2
ζ_1
O
D
DISTANCE (X) FROM SURFACE
$1/\kappa_1$
$1/\kappa_2$
$1/\kappa_3$
I
II
III

$$\sigma_0 = \frac{\kappa\varepsilon\zeta}{4\pi} \qquad 1\text{-}34$$

Combining Eq. 1-34 and Eq. 1-12 the relationship between charge density and mobility is obtained:

$$u = \frac{\sigma_0}{\kappa\eta} \qquad 1\text{-}35$$

It is again evident from Eq. 1-35 and Eq. 1-34 that the mobility and the zeta potential depends on the double layer thickness, $1/\kappa$, i.e., the lower the ionic strength the greater will be the zeta potential as well as the mobility for a given surface charge density.

Under conditions where zeta potentials > 25 mV are encountered, i.e., $ze\psi_0/2kT < 1$, Eq. 1-25 may still be solved (22, 23) in which case:

$$\psi = \frac{2kT}{ze} \ln\left[\frac{1+\gamma \exp[-\kappa x]}{1-\gamma \exp[-\kappa x]}\right] \qquad 1\text{-}36$$

when $d\psi/dx = 0$ at $x = \infty$ and $\psi = \psi_0$ at $x = 0$, where

$$\gamma = \exp\frac{[(ze\psi_0/2kT)-1]}{[(ze\psi_0/2kT)+1]} \qquad 1\text{-}37$$

and

$$\sigma_0 = \left[\frac{2n_0\varepsilon kT}{\pi}\right]^{1/2} \sinh\left[\frac{ze\psi_0}{2kT}\right] \qquad 1\text{-}38$$

Again replacing ψ_0 by ζ and inserting molar concentration terms and I for ionic strength, Eq. 1-38 may be simplified to give:

$$\sigma_0 = 2\left[\frac{N_A kT}{2000\pi}\right]^{1/2}[\varepsilon I]^{1/2} \sinh\left[\frac{e\zeta}{2kT}\right] \qquad 1\text{-}39$$

for uni-univalent electrolytes.

The Gouy-Chapman equation (1-39) requires critical examination. It does not provide a precise means of calculating surface charge densities from zeta potentials since a number of questionable assumptions are embodied in its derivation.

The first assumption which is questionable is that charge is spread uniformly over a surface. In fact, we know that surface charge is at least due to discrete point sources and to a better approximation ionic entities, which have a definite volume. If the ionic volume is neglected the Boltzmann equation predicts unrealistically high concentrations of ions near the surface, especially in the presence of relatively high potentials and bulk ion concentrations. Corrections for ionic volumes have been examined by Haydon (25) and Overbeek and Wiersema (9) who concluded that the magnitude of such corrections would be small for low surface potentials. Haydon (26) has also found on theoretical examination of the Gouy-Chapman equation that it would produce underestimates of surface charge densities in the case of surfaces which are penetrable to counterions. Consequently Haydon

(26) introduced a term, α, which he defined as the function of the total space within the double layer available to counterions. Equation 1-39 is multiplied by the term $[1+(1-\alpha)^{1/2}]$ to yield:

$$\sigma_0 = [1+(1-\alpha)^{1/2}] \cdot 2\left|\frac{NkT}{2000\pi}\right| [\varepsilon I]^{1/2} \sinh\left|\frac{e\zeta}{2kT}\right| \qquad 1\text{-}40$$

In the limit where $\alpha = 1$, Eq. 1-40 reduces to Eq. 1-39, i.e., none of the space within the double layer is available to counterions. In the case $\alpha = 0$, the value for the surface charge density would actually be twice that calculated with the unmodified equation.

The largest error in surface charge density calculations is probably associated with the uncertainty in the value of the α factor. Most biological surfaces are penetrable to counterions and use of the unmodified Gouy-Chapman equation will lead to underestimates of surface charge density. Yet it seems unwise to select an arbitrary value of α in most calculations, since in all probability it would be incorrect. Correction for α may always be made when and if an experimental or theoretical basis for selecting an α value becomes available.

The assumption embodied in the Poisson equation as in the Smoluchowski equation (Eq. 1-12) is that the dielectric constant within the double layer is equal to that of the bulk solution. This cannot be the case for the following two reasons. First, the molecules of the

liquid are oriented by the electric field produced by the surface charge. Secondly, the charge of small ions within the double layer have a similar orientation effect on solvent molecules. This effect increases in the direction toward the surface due to the increase in ionic concentration in that direction. Fortunately, as stated previously, for particles having low zeta potentials these effects are small (21).

The free energy of interaction between ions within the double layer as well as in bulk solution needs also to be considered. In bringing an ion from infinity to its final position within the double layer, work must be performed against the ion's own atmosphere. This fact is neglected by the Poisson-Boltzmann relationship. A further energy term, which is also inherently neglected, arises from ion polarization. In transferring an ion from bulk solution where the external electric field is zero to a point within the double layer where the electric field has a finite value the ion becomes polarized.

A number of investigators have attempted to estimate the magnitude of these errors in surface charge density calculations. Haydon (25) has reviewed these attempts at correction and concludes the following:

a. To a certain extent the corrections tend to compensate each other, i.e., the potential is increased by the ionic volume and dielectric saturation and decreased by the polarization and self-atmosphere effects.

b. The net correction for a nonconducting surface with the relatively high surface potential of 100 mV will be on the order of ~ 3% with the ionic volume correction the main contributor. At the charge densities and potentials encountered in most types of biological cell suspensions the corrections would be very small indeed.

For the variety of reasons, which have been briefly dealt with above, it can be seen that the Gouy-Chapman treatment of the diffuse double layer is not precise. However, given the usual lack of knowledge of the molecular surface architecture of colloidal particles, application of more sophisticated models of double layer structure in surface charge density calculations would hardly be fruitful at this time. Nevertheless, the results of numerical estimates of surface potential or surface charge density may be used for comparative purposes.

Electrophoretic methods may provide significant information on the fine structure and ionic composition of the diffuse solid-liquid interfacial region of colloidal particles, including biological cells. The mobility of a particle is only a reflection of its net surface charge density and thus no information on the spatial distribution of charges on the surface can be obtained by simple mobility measurements. Yet the structure and ionic composition of the double layer region of particles or cells may still be investigated by measuring the dependence

of their mobility on the pH or ionic strength of the suspending medium or on the specific effects produced by a variety of surface modification agents, including chemical reagents and/or enzymes. For example, study of the relationship between the electrophoretic mobility of particles and the ionic strength of the suspending medium at constant pH may aid in distinguishing whether the surface charge is arising from adsorption of ions from the suspending medium or from ionogenic groups which are an integral part of the molecular structure of the surface. Changing of the ionic strength of the suspending medium will vary $1/\kappa$, i.e., the thickness of the double layer. Thus, for an ion penetrable surface the spatial distribution of surface charge groups normal to the surface may be investigated, i.e., groups which lie deep within the double layer would not contribute to the zeta potential at high ionic strength, whereas they would contribute at lower ionic strengths. If the surface charge of the particles under investigation stems from integral ionogenic surface groups, information on their pK values, which may aid in their specific identification may be obtained by gathering data on the mobility of the particles as a function of pH of the suspending medium. Introduction, elimination or blockage of specific surface groups or structures by functional group-specific reagents or enzymes, in conjunction with electrokinetic studies, and in applicable situations, analysis of the reaction products, will also aid in the determination of surface molecular fine structure.

CHAPTER 2

GENERAL METHODOLOGY

This chapter describes in detail some of the materials and procedures which are common to much of the work presented throughout this thesis. Specialized variations of these methods are covered in their own appropriate section.

2.1 Materials

All chemicals used were reagent grade quality unless otherwise noted. Water was distilled from the city water supply with a custom made two stage pyrex still and stored in glass jugs connected in series with glass tubing and teflon joints. Typically the pH value of the water was about 6 and its conductivity, as measured with a Radiometer Type CDM2f conductivity meter in conjunction with a CDC 104 conductivity cell, ranged between 1.5 and 2.5 x 10^{-6} mho $\cdot$ cm^{-1}.

2.2 Ostwald Viscometry

Glass capillary viscometers which pass a precise volume of fluid through a capillary by application of an accurately reproducible force may be utilized for determining the kinematic viscosity of a fluid. The kinematic viscosity, of a fluid, is defined as the ratio of dynamic viscosity to fluid density. The force is provided by the

pressure of the hydrostatic head due to different fluid levels in the viscometer itself.

The dynamic viscosity, η (Poise), is defined as the ratio of shear stress, τ (dynes $\cdot$ cm^{-2}), to shear rate, D (sec^{-1}):

$$\eta = \frac{\tau}{D} \qquad 2\text{-}1$$

For Newtonian fluids, τ increases linearly with D and η is independent of D. Experimentally the dynamic viscosity may be determined from the kinematic viscosity, ν, (centistokes, cS). The parameters are related by:

$$\nu = ct - \frac{B}{t} = \frac{\eta}{\rho} \qquad 2\text{-}2$$

where c is the viscometer constant relating the flow time t (sec) of the fluid to its kinematic viscosity and B, which is a correction term, sometimes referred to as the coefficient of the kinetic energy of efflux of the fluid. B is defined by the relationship:

$$B = 3.98 \frac{V}{\ell} \qquad 2\text{-}3$$

where V is the volume of the fluid which flows in time t (ml $\cdot$ sec^{-1}) and ℓ (cm) is the length of the capillary of the viscometer (27). For the viscometers used in these studies $V \cong 1.3 \times 10^{-2}$ ml $\cdot$ sec^{-1} and $\ell \cong 9$ cm. Thus, $B/t \cong 7 \times 10^{-5}$ cS in Eq. 2-2 and may thus be neglected since kinematic viscosities on the order of 1 cS

were usually encountered in this work. Thus, Eq. 2-2 reduces to the relation

$$\nu = ct \qquad 2\text{-}4$$

and

$$\eta = \nu\rho = \rho ct \qquad 2\text{-}5$$

For the determination of kinematic viscosities, 5.0 ml of the fluid to be tested was introduced via a pipette into the Ostwald viscometer which had been cleaned[1] with Dichrol (Scientific Products), a sulfuric acid-dichromate cleaning solution, and rinsed with about 500 ml of distilled water and dried with reagent grade methanol. The viscometer was clamped vertically in a large water bath (~ 20 L capacity), the temperature of which was maintained at 25.0°C ± 0.1°C. The fluid to be tested was allowed to equilibrate to the temperature of the bath for about 10 minutes. The fluid was then sucked up into the timing arm of the viscometer, and the length of time for the fluid to pass between the etched marks of the viscometer was recorded. Triplicate measurements were usually taken and the results were bracketed by timing of a standard fluid. Doubly distilled water usually served as the standard fluid. To constitute acceptable data the timings were required to be within 1 to 2% of each other. If this was not

---

[1] A clean glass surface was pragmatically defined as one which would drain evenly without beading when distilled water was applied.

the case, the viscometer was recleaned and the tests were repeated.

The viscometer constant was calculated from the flow times of distilled water with the aid of Eq. 2-4 and the accepted value for the kinematic viscosity of water at 25.0°C, i.e.,

$$\nu^{25}_{H_2O} = \frac{\eta^{25}_{H_2O}}{\rho^{25}_{H_2O}} = \frac{0.8904}{0.9971} = 0.8930 \qquad \text{(Ref. 28)}$$

The density of the test fluid was measured pycnometrically at the specified temperatures. Dynamic viscosities could then be calculated by use of Eq. 2-5.

2.3 Determination of Density of Liquids by Pycnometry

Densities of various liquids were determined at specific temperatures by pycnometry which consists of finding the weight of liquid occupying a known volume defined by the shape of a given vessel, i.e., a pycnometer. Gay-Lussac pycnometers having capacities of about 10 ml were used. On calibration these types of pycnometers are capable of an accuracy of about $\pm$ 1 x 10^{-4} g $\cdot$ ml^{-1}. The volume of these pycnometers depends somewhat on the amount of pressure exerted on the ground joint, thus care was exercised in replacing the stopper with about the same pressure as was used in calibrating the vessels.

The pycnometers were filled with a Pasteur pipette with the calibrating liquid or sample. The pycnometer was then immersed up to the ground glass neck in a water bath at the desired temperature, ±0.1°C. Usually the pycnometer was filled with the liquid at a temperature slightly below the temperature of the water bath. Thus, on thermostating some of the liquid would be forced out through the capillary. The liquid remaining on the flat surface of the stopper was quickly wiped off with absorbant tissue. After a few more minutes if no further changes in the liquid level had taken place it was assumed that the pycnometer, as well as the liquid, were in temperature equilibrium with the water bath. The pycnometer was then quickly dried with absorbant tissue and weighed on an analytical balance to ±0.1 mg.

The weight of fluid occupying the pycnometer was determined by difference, i.e., the weight of the empty pycnometer was subtracted from the weight of the filled pycnometer. The volume of a pycnometer was determined by dividing the weight of reagent grade mercury contained in the pycnometer by its density (29) at a specified temperature. In this manner the coefficient of expansion of glass with temperature was taken into account. Densities of experimental samples, at specified temperatures, were obtained by dividing the weight of the test fluid by the volume of the pycnometer as determined by the mercury calibration. Pycnometers were cleaned in a manner similar to that

which was used for Ostwald viscometers, and the same standards for cleanliness applied.

2.4 Statistical Procedures

2.4.1 Sample Standard Deviation

Sample standard deviations were calculated to provide an estimate of the dispersion of data about a mean value. In some instances, to provide an estimate of the actual error about a mean value, the standard error was calculated from the standard deviation as described by Young (30). To provide an estimate of the magnitude of the ratio of the standard deviation to the mean, a fractional standard deviation can be calculated which may also be expressed as a percent standard deviation.

2.4.2 Linear Regression Analysis

Linear regression analysis (30) was utilized to fit data to straight lines of the form $y = mx + b$, where y and x are dependent and independent variables, respectively, and m and b are the regression coefficients and y intercept, respectively. An indication of the quality of fit was obtained by calculating a correlation coefficient r. Values of r close to ± 1.00 indicated a better fit than values close to zero.

2.5 Measurement of Cell Concentration by Electronic Sensing Zone Instruments

Measurements of various hematological parameters are often expressed in a variety of units in the literature, some of which are ambiguous. As a hypothetical example, the sialic acid content of red cells may be expressed as x grams of sialic acid per ml of red cells in one report. Another report may state there are 2x grams of sialic acid per ml of red cells. It could be inferred that the red cells described in the latter report contained twice as much sialic acid as those described in the first. On the other hand, the mean cellular volume of the cells in the sample containing 2x grams of sialic acid per ml of red cells may be half that of the cells which contain x grams per ml red cells, such that the sialic acid content per cell is actually the same in both cases. To prevent such ambiguities, hematological parameters, in the work to be presented, will be expressed on a per cell basis, if possible. This, however, requires accurate determination of red cell concentrations.

The measurement of particle (cell) concentrations, as well as particle volumes by electronic sensing zone instruments, has found wide application in recent years. These instruments are capable of providing rapid and very accurate data on particle concentrations. The accuracy of volume measurements however, is somewhat less certain, nor is accuracy easily determined. The instruments, available

commercially, all operate on the same principle which stems from an application of Ohm's law. The transducer of these instruments consists of a cylindrical aperture, manufactured either from ruby or glass which separates two electrode compartments. The aperture or orifice may have a diameter of ~10-1000 μm, but is usually in the range of 30-100 μm in diameter for enumeration and sizing of mammalian blood cells, for example. The length of the orifice is usually equal to one to two times its diameter.

The particles being measured are suspended in the outer electrode compartment and are forced through the aperture. On application of a potential (V) across the orifice, the major resistance (R) to the flow of current (I) is provided by the narrow aperture itself, plus a small hemispherical volume at either end of the orifice, thus the name "sensing zone instrument".

When a particle enters the orifice sensing zone, the resistance will increase by an amount which is proportional to the volume of the particle, its shape, its ionic electrical conductivity and its pathway through the aperture. These parameters and the magnitude of the resistance changes have been considered in detail by Grover et al. (31) and Kachel et al. (32).

The instrument available for the work described here was an Electrozone-Celloscope/PDP-8/M mini-computer analysis package (Particle Data Inc., Elmhurst, IL) which is pictured in Fig. 2-1, and

Figure 2-1. Electrozone Celloscope/PDP-8/M minicomputer analysis package.

1) Electrozone-Celloscope
2) Transducer-Aperture
3) Current Control
4) Linear Amplifier Gain Control
5) Lower Threshold Control
6) Mode Selector (Σ mode cancels Upper Threshold Control 7)
7) Upper Threshold Control
8) Lin/Log Amplifier Control
9) Mercury Manometer Metering Section
10) Aperture Viewing Microscope
11) Class 100 Laminar Flow Clean Bench
12) Digital Equipment Corporation Decwriter I/O Terminal
13) Oscilloscope
14) Digital Equipment Corporation PDP-8/M central processing unit (CPU)
15) Digital Equipment Corporation RX8 Floppy Disk mass storage subsystem

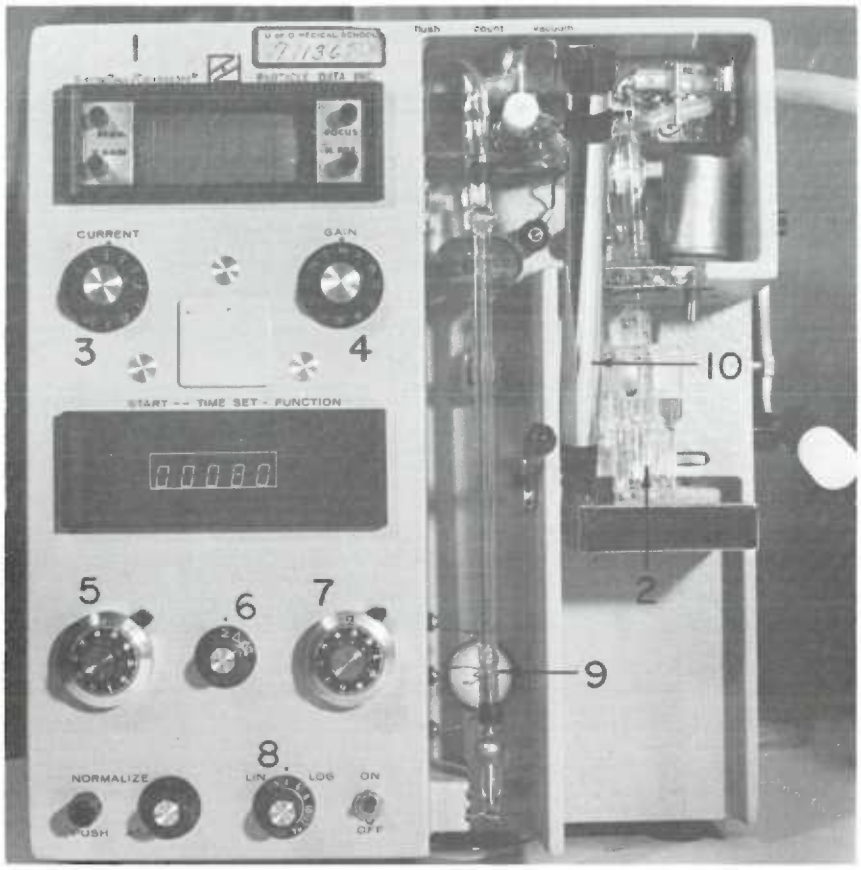
1
CURRENT
GAIN
3
4
START -- TIME SET - FUNCTION
5
6
7
8
NORMALIZE
PUSH
LIN
LOG
ON
OFF
10
2
9


1
13
12
15
14
11

depicted block diagramatically in Fig. 2-2. Changes in aperture resistance in this instrument are measured in conjunction with a constant current source, the output level of which can be controlled by the operator. On passage of a particle through the aperture, there is a decrement in the potential across the orifice which is proportional to the change in resistance in the orifice due to the presence of the particle. It is this voltage decrement which constitutes the output of the transducer. The decrement in V is detected as a pulse which is amplified in series by a preamplifier, a linear amplifier and a logarithmic amplifier. The degree of linear amplification of the pulse is determined by the gain control of the instrument. The logarithmic amplifier can be utilized to determine the dynamic range of particle sizes which will be detected. In other words, a given log amplifier setting approximates the number of doublings of particle volume between the largest and smallest particles which are detected by the instrument. For example, at the extreme log settings of 4 and 14 the ratios of the volumes of the largest to the smallest particles, which are sized, are 2^4:1 and 2^{14}:1, respectively.

The analog information, i.e., the amplified pulses, are digitized by an analog to digital converter and passed on to the computer where the information is analyzed and stored in one of 128 registers. The particle size to which these registers correspond are predetermined by the operator. The computer also keeps track of the number of

Figure 2-2. Block diagram of the Electrozone Celloscope /PDP-8 /M particle count and size analysis system.

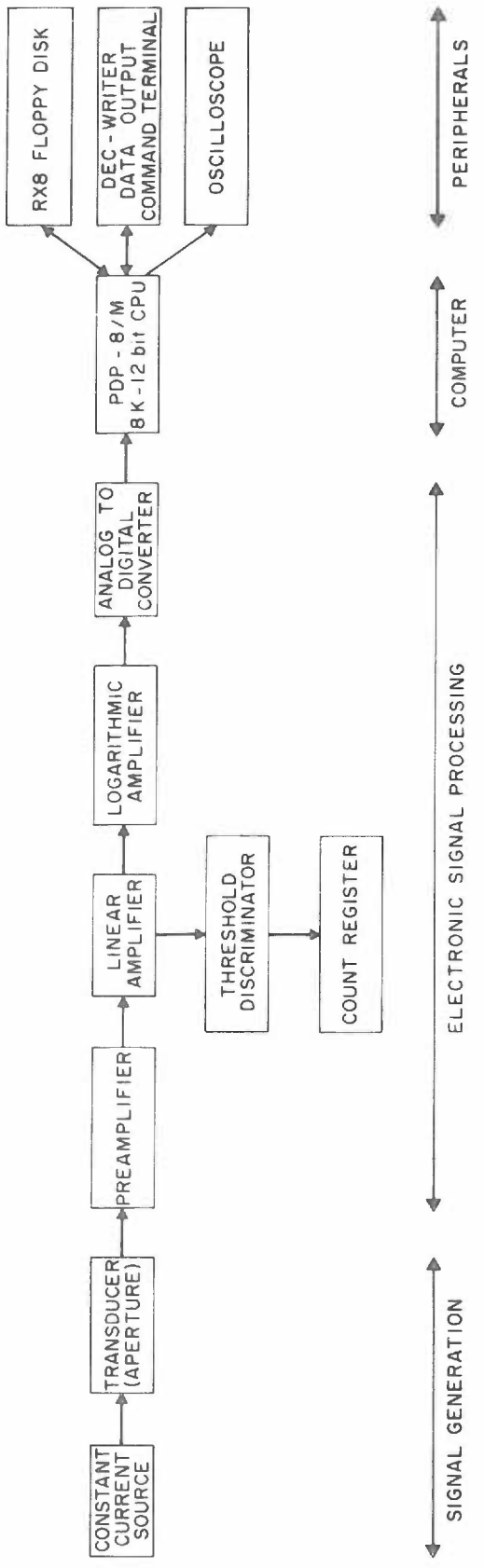
CONSTANT CURRENT SOURCE
TRANSDUCER (APERTURE)
PREAMPLIFIER
LINEAR AMPLIFIER
LOGARITHMIC AMPLIFIER
ANALOG TO DIGITAL CONVERTER
PDP - 8/M 8K - 12 bit CPU
THRESHOLD DISCRIMINATOR
COUNT REGISTER
RX8 FLOPPY DISK
DEC - WRITER DATA OUTPUT COMMAND TERMINAL
OSCILLOSCOPE
SIGNAL GENERATION
ELECTRONIC SIGNAL PROCESSING
COMPUTER
PERIPHERALS

particles in each register. This information is reconverted back to analog information which is transmitted to an oscilloscope, where the operator may observe the accumulation of size distribution data almost simultaneously as it is being collected. The information may also be stored rapidly for later retrieval, on a flexible-media mass storage subsystem, similar in size and appearance to 45-rpm phonograph records (RX8 Floppy Disk system, Digital Equipment Corp., Maynard, MA).

Upper and lower threshold controls on the Celloscope allow the screening out of voltage pulses due to electronic noise. The upper threshold control may be disabled by operating the instrument in the Σ mode, selected by the mode control switch.

It can readily be seen how this instrument may be used to enumerate particles in a suspension. Each time a particle traverses the orifice a signal is generated. By controlling the volume of a particle suspension which is analyzed and by summation of the signals, the number of particles per unit volume of a suspension may be determined. This is subject to the condition that the suspension undergoing analysis is sufficiently dilute that two particles are rarely inside the aperture simultaneously. In this event, often referred to as coincidence loss, two particles will register as only one. By taking into account dilution factors the particle concentration of a suspension, such as blood, may easily be determined.

As will become evident, determination of mean cellular volumes will be an issue in this thesis in a number of instances. Since the issue of electronic volume determination of particles has been brought up, the applicability of the technique to measuring mean cellular volumes of red cells will be discussed here also.

Determination of particle volumes by electronic sensing zone instruments, although simple in principle as outlined above, becomes complex, especially if the particles are non-ideal, i.e., if they are deformable and deviate from ideal shapes, such as spheres or cylinders. Human erythrocytes, the particles of interest in this thesis, fall into the category of non-ideal particles.

For example, it has long been noted that the volume distribution of human erythrocytes as determined by sensing zone instruments, had bimodal characteristics. Although the source of the bimodality was the subject of much debate, it has now been found that it was due to artifacts, arising from particles traversing the orifice by all possible pathways. Cells traversing the orifice near its edge remain there longer than particles traversing axially through the aperture. This longer transit time gives rise to artifactually large voltage pulses and thus artifactually large volumes. Furthermore, cells traversing near the axis of the orifice are deformed to a greater degree than cells which traverse the orifice near its edge (32). These shape changes, which approximate changing oblate ellipsoids to prolate ellipsoids are

also associated with changes in resistance in the orifice (32). The shape of red cells will also be affected by the magnitude of flow rates through the orifice, i.e., higher flow rates will result in higher rates of shear, near and within the orifice, which will cause increasing degrees of cellular deformation giving rise to shape factor changes which in turn result in changes in orifice resistance. Without special hydrodynamic focusing equipment by which cells may be directed through the axis of the orifice at controlled flow rates, absolute volume determinations by electronic sensing zone instruments are subject to considerable error (up to 50%). Volume determinations of one cell sample relative to that of another may also be in error if the cells are not equally deformable and/or are not very similarly shaped. As a result, cell volumes were routinely measured by a micro-hematocrit technique described in Section 5.2.2 rather than by electronic means.

Cell concentrations, however, were routinely measured electronically. The exact instrumental settings and orifice size of the Electrozone-Celloscope, for the enumeration of red cells, were chosen empirically. The current settings were maintained at levels low enough so as to prevent appreciable heat buildup in the orifice and possible fragmentation of red cells. This amounted to maintaining aperture currents below 1 mA for a 30 μm orifice. The gain setting of the linear amplifier of the instrument and the setting of the logarithmic amplifier were adjusted such that the entire population of

particles, i.e., the smallest to the largest, fell between the upper and lower limits of detection of the instrument, as graphically depicted on the oscilloscope screen. Typical instrument settings were: Current = 1/8, Gain = 8 1/2; Logarithmic Amplifier = 8; Mode = Σ; Lower threshold discriminator = 30. The gain setting of the linear amplifier and the lower signal discriminator were adjusted such that electronic noise signals, resulting from too low signal to noise ratios, were not registered. Typically, 100 µl of a particle suspension, as controlled by the mercury manometer metering section, constituted one analysis. A minimum of two dilutions of a sample were prepared and each dilution was analyzed at least in triplicate. The fractional standard deviation of the mean number of particles counted was required to be less than 0.01 for the data to be considered acceptable. The dilutions were made such that particle concentrations were about 3×10^5 ml^{-1} so as to minimize ($\leq$ 1%) coincidence losses. Isoton II (Coulter Electronics, Hialeah, Florida), a specially filtered, balanced electrolyte solution was used as the diluent for red blood cell counting. According to the manufacturer, the solution consists of: NaCl-7.93 $g \cdot L^{-1}$, Na_2EDTA-0.3 $g \cdot L^{-1}$, KCl-0.40 $g \cdot L^{-1}$, NaH_2PO_4-0.19 $g \cdot L^{-1}$, Na_2HPO_4-1.95 $g \cdot L^{-1}$, and NaF-0.50 $g \cdot L^{-1}$.

Background counts due to electronic noise and particulate contamination of the Isoton II in the size range of the particles to be counted was always maintained at < 1% of the total number of particles

counted. The sample preparation, including the particle enumeration itself, was performed within a class 100 clean bench (Integrated Air Systems, Burbank, CA) so as to eliminate extraneous particulate matter. Accuvettes (Coulter Electronics, Hialeah, FL) served as sample containers. They allowed the orifice to be observed through a built-in microscope on the Celloscope apparatus, to ensure that it remained unobstructed during sample analysis.

Red cell suspensions were prepared for dilution and subsequent enumeration, gravimetrically. As an example, for a blood sample containing ~5 x 10^6 red cells per mm^3, approximately 30 mg of suspension would be weighed out on an analytical balance and diluted with 10.00 ± 0.02 ml of Isoton II. One hundred µl of this suspension would be transferred to a fresh Accuvette containing 10.00 ± 0.02 ml Isoton II. This would result in an electronic count of about 15,000 cells per 100 µl diluted suspension. The volume of the blood suspension (V_s) weighed out initially was calculated from the mass of the suspension (m_s) and the density of the suspension (ρ_s), i.e.,

$$V_s = \frac{m_s}{\rho_s} \qquad 2\text{-}6$$

The density of the suspension in turn was calculated according to the relationship:

$$\rho_s = [1-(f \cdot Hct)]\rho_{media} + [f \cdot Hct \cdot \rho_{RBC}] \qquad 2\text{-}7$$

where

ρ_s = suspension density

f = packing efficiency factor = 0.99

Hct = suspension hematocrit

ρ_{media} = media density (determined pycnometrically)

ρ_{RBC} = red cell density[1/]

The hematocrit (Hct) was expressed as the fraction of the total volume of a red cell suspension occupied by red cells only. Hematocrits were measured in microhematocrit tubes following centrifugation in an MSE microhematocrit centrifuge at 15,000 g for 5 minutes. The packing efficiency of native red cells even at such high centrifugal fields is not quite 100%, i.e., some interstitial fluid remains. To correct for this, hematocrits were multiplied by a packing efficiency correction factor (f) which for native cells is 0.99 (33).

2.6 The Thiobarbituric Acid Assay for Free Sialic Acids

The thiobarbituric acid assay was introduced for the determination of 2-deoxyribose (34) and was modified by Warren (35) and subsequently, Aminoff (36), for the assay of sialic acid. It is the most

---

[1/] See Section 5.1.2 for details on the experimental determination of red cell density.

sensitive as well as the most specific of the colorimetric methods for unbound sialic acid. That is, glycosides containing sialic acid do not react. The mechanism of the TBA-sialic acid assay has been investigated by Paerels and Schut (37), who have identified β-formylpyruvic acid as the chromogen which reacts with thiobarbituric acid in hot acidic solution to form the red pigment of interest. Its absorption maximum is at 549 nm.

The assay procedure, although simple, is fraught with pitfalls which may result in a lack of accuracy and/or reproducibility. The following reagents are necessary:

1) 0.025 M periodic acid in 0.125 N H_2SO_4 which should be stored in a brown bottle at room temperature.
2) 0.154 M sodium arsenite in 0.050 M HCl prepared by first dissolving the arsenite in 50 ml of 1 M HCl which is then diluted to 100 ml with distilled water.
3) 0.010 M 2-thiobarbituric acid adjusted to pH 9 with 1 M NaOH in order to convert the insoluble acid to the soluble sodium salt.
4) Acidified n-butanol. Prepared by mixing 475 ml n-butanol with 25 ml of 12 M HCl.
5) Sialic acid standard. A 0.647 mM stock solution of sialic acid in water. (N-Acetylneuraminic acid, A-Grade, Calbiochem-Behring Corp., La Jolla, CA).

Typically, a sufficient amount ($\leq$ 100 µl) of either a blank test sample or standard solution (containing 5-20 µg of sialic acid) were put into a 12 ml conical glass centrifuge tube with a screw top teflon lined cap. If < 100 µl of supernatant fluid, standard or blank were used, sufficient distilled water or appropriate buffer was added such that the total volume amounted to 100 µl. To each tube, 250 µl of the periodate reagent were added and the tubes were mixed and subsequently incubated in a 37°C water bath. After 30 minutes the samples were removed from the bath and 200 µl of the arsenite reagent were added to reduce the excess periodate. After waiting for one to two minutes, or until the color of liberated iodine had disappeared, 2.0 ml of the thiobarbituric acid reagent were added and the samples were mixed well and immediately incubated in a boiling water bath for 7.5 minutes. (Timing was not started until the bath was at a full boil.). After this the samples were cooled in an ice bath for ~5 minutes at which time 5.0 ml of cold acidified n-butanol were added. The samples were returned to the ice bath for an additional 3-5 minutes and then shaken vigorously to extract the chromogen into the organic phase. The tubes were then centrifuged at ~500-1000 g for 10 minutes in a refrigerated centrifuge at 5-10°C, insuring that the centrifugation temperature was at or above the initial sample temperature in order to facilitate the phase separation. Maintenance of the temperature, at which phase separation took place, at or above the initial temperature of the two

phase system, prevented the organic phase from becoming turbid. Turbidity arose if the organic phase, which was saturated with water from the aqueous phase, was exposed to temperatures lower than those at which it became saturated with water. This was because the solubility of water in acidified n-butanol decreases with decreasing temperature with resultant formation of immiscible droplets and thus turbidity. Turbidity may also arise from emulsion stabilization due to surfactant constituents of the sample.

Optical densities were measured in a double beam spectrophotometer at 549 nm in cuvettes with a 1 cm light path, against a distilled water blank. Optical densities were corrected for reagent contributions, by carrying a distilled water, or appropriate buffer, blank through all sample processing steps.

The amount of sialic acid in the test samples was calculated on the basis of the standard samples carried through the assay procedure. The number of micrograms of sialic acid per absorbance unit was calculated, assuming 100% recovery of the standard. The result was multiplied by the absorbance of the test samples to determine the number of micrograms of sialic acid that were contained in the assayed volume of test sample. The total sialic acid released per red cell by VCN, for example, was calculated from:

$$\frac{\text{Total NANA released}}{\text{Total number of red cells}}$$

$$= \frac{[\text{NANA} \cdot \text{ml}^{-1} \text{ supernatant fluid}]\{V[1-(f \cdot \text{Hct})]+V_E\}}{[\text{RBC} \cdot \text{ml}^{-1}][V]}$$

$$= \frac{[\text{NANA} \cdot \text{ml}^{-1} \text{ supernatant}][V_S]}{[\text{RBC} \cdot \text{ml}^{-1}][V]} \qquad 4\text{-}6$$

where

f = the packing efficiency factor (0.99 for fresh red cells)

Hct = the fraction representing the packed cell volume of the red cell suspension

V = the volume of stock red cell suspension

V_E = the volume of enzyme solution added

V_S = the final volume of supernatant fluid

The linearity of the absorbance versus the amount of sialic acid in the range of 5-40 μg per sample was established (Fig. 2-3). Furthermore, the ratio of the optical density of a sample at 549 nm to its optical density at 532 nm was tested to determine whether substances which interfere with the assay were present in the samples. Malonaldehyde, a chromogen produced in the TBA assay from 2-deoxyribose and certain unsaturated lipids, has a maximum absorption at 532 nm. If these substances had been present, Warren (35) has suggested a method which could be used to correct sialic acid

Figure 2-3. Representative standard curve illustrating the linearity of the TBA assay. The amounts of N-acetylneuraminic acid indicated, were added to each sample and the assay was carried out as described in the text.

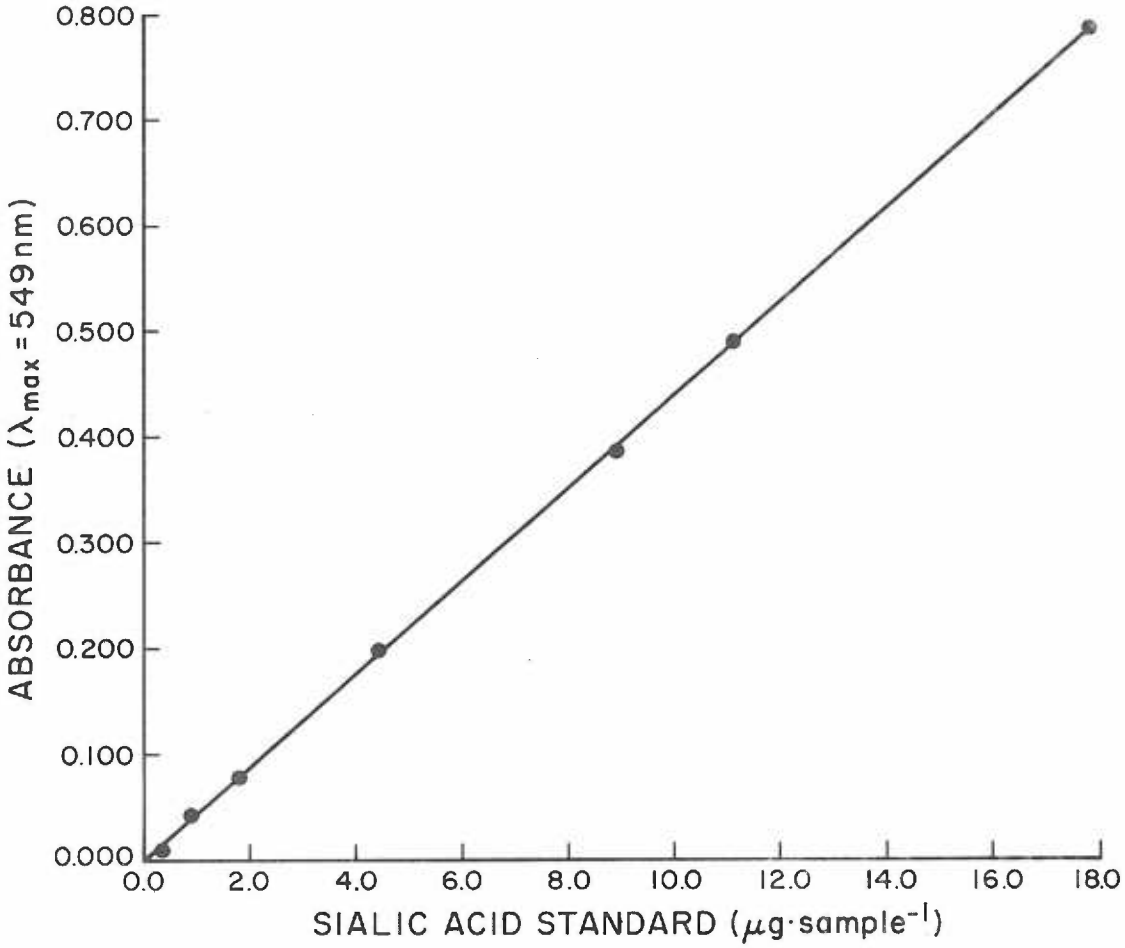
0.800
0.700
0.600
0.500
0.400
0.300
0.200
0.100
0.000
ABSORBANCE (λ_{max} = 549 nm)
0.0
2.0
4.0
6.0
8.0
10.0
12.0
14.0
16.0
18.0
SIALIC ACID STANDARD ($\mu g \cdot sample^{-1}$)

measurements from the above cited OD ratio. Aminoff (36) has investigated a number of substances which have been found not to interfere with the assay and they include:

N-acetylglucosamine (1 mg)
N-acetylmuramic acid (50 μm)
Arabinose (1 mg)
Aspartic Acid (0.1 mg)
Fructose (0.2 mg)
Glucosamine-HCl (1 mg)
Glucosaminic acid (1 mg)
Histidine-HCl (1 mg)
Ribose-5-phosphate (0.1 mg)
Serine (0.1 mg)
Threonine (1 mg)
Sialomucoids

2.7 Protein Assays

2.7.1 Amidoschwartz 10B Dye Binding Assay for Protein

The Amidoschwartz 10B assay for protein is a rapid indirect spectrophotometric method of determining protein in dilute solutions (2-120 $\mu g \cdot ml^{-1}$) (38). The method is insensitive to a number of non-proteinaceous substances often present in protein solutions which interfere with other methods such as that of Lowry (38).

The following reagents and materials are required:

1) Protein standard: crystallized bovine serum albumin (BSA) may serve as a standard and should be dissolved in the same buffer in which the unknown quantity of protein is dissolved. The concentration of BSA should be approximately

10 $mg \cdot ml^{-1}$. The exact concentration is determined spectrophotometrically. The extinction coefficient for a 1% (w/v) solution of BSA at 278 nm is 6.6 (39).

2) 1 M Tris-HCl pH 7.5 containing 1% (w/v) sodium dodecyl sulfate (SDS).
3) 0.367 M trichloroacetic acid (TCA) and 0.03 M TCA.
4) 0.1% (w/v) Amidoschwartz 10B in methanol:glacial acetic acid:water in a volume ratio of 45:10:45, respectively.
5) Destaining solution consisting of methanol:glacial acetic acid:water in a volume ratio of 90:2:8, respectively.
6) Eluent solution prepared by dissolving 1.0 g NaOH and 0.0186 g disodium ethylenediaminetetraacetate dihydrate in 1 L ethanol:water (50:50 volume ratio).
7) Millipore membrane filters (Millipore Corp., Bradford, MA) of the HAWP series, either 25 or 47 mm in diameter, pore size of 0.45 μm.

The assay procedure consists of placing a standard, test or blank sample containing a maximum of 30 μg of protein into glass test tubes. Water or appropriate buffer solution was added to obtain a final volume of 270 μl to which 30 μl of the 1 M Tris-HCl-SDS solution was added. The protein was precipitated by addition of 100 μl of the 0.367 M TCA solution. The samples were mixed and allowed to stand at room temperature for 5 minutes. The acidified samples were then taken up in

glass Pasteur pipettes and filtered through a Millipore membrane at predetermined spots. The wetted area was maintained < 7 mm in diameter. The test tubes were rinsed with a total of 400 µl of 0.037 M TCA which was also filtered such that the sample transfer from the test tube to the Millipore membrane was quantitative. The whole filter membrane was rinsed twice with 2 ml aliquots of 0.037 M TCA after which the membrane was stained for 2-3 minutes in the Amidoschwartz 10B solution. The filter membrane was then rinsed with water for 30 seconds and destained in a series of three 200 ml aliquots of the destaining solution. The areas on the membrane where protein was deposited became visible as blue spots on an almost colorless background.

After destaining, the filter membrane was again rinsed for 1-2 minutes in water and placed face up on several layers of absorbant paper. The stained spots were cut out with a cork borer and the disks were transferred to 8 x 60 mm glass test tubes. The blue dye was then quantitatively extracted with 600-1000 µl of the eluent solution for ~10 minutes. The tubes were vortexed 3-5 times during this period to aid in the dye extraction. For each test sample, including the blank, a series of BSA samples containing approximately 1.5, 5 and 15 µg protein were run on the same filter membrane. The eluent volume was held constant for any one set of disks.

The absorbance of the eluent solutions containing extracted dye was measured against blank eluent solution at 630 nm in a double beam spectrophotometer. A standard curve (Fig. 2-4) was prepared from the absorbances of the standard protein samples. The amount of protein in the unknown sample was calculated from the least squares linear regression line of the standard curve.

The response factor per μg of BSA per ml of eluent solution was found to be in the range of 0.026 absorbance units ±15%. The accuracy of the method is reported to be ~ ±25%, except for low molecular weight proteins such as insulin.

2.7.2 Quantitation of Protein by Dye Binding to Coomassie Blue G-250

This dye binding method which was first described by Bradford (40) is simpler and more rapid than the Amidoschwartz 10B assay. The method involves binding of protein to the dye Coomassie Blue G-250 in solution. The binding of the dye to protein is accompanied by a shift in the absorption maximum of the dye from 465 nm to 595 nm. The increase in optical density at 595 nm is monitored. The following reagents and materials are required:

1) 100 mg of Coomassie Blue G-250 dissolved in 50 ml of 95% (v/v) ethanol. To this solution 100 ml of 85% (w/v) ortho-phosphoric acid was added. The resulting solution is diluted to 1 L with water

Figure 2-4. Linearity of the Amidoschwartz dye binding assay. The amounts of BSA indicated were added to each sample and the assay was carried out as described in the text.

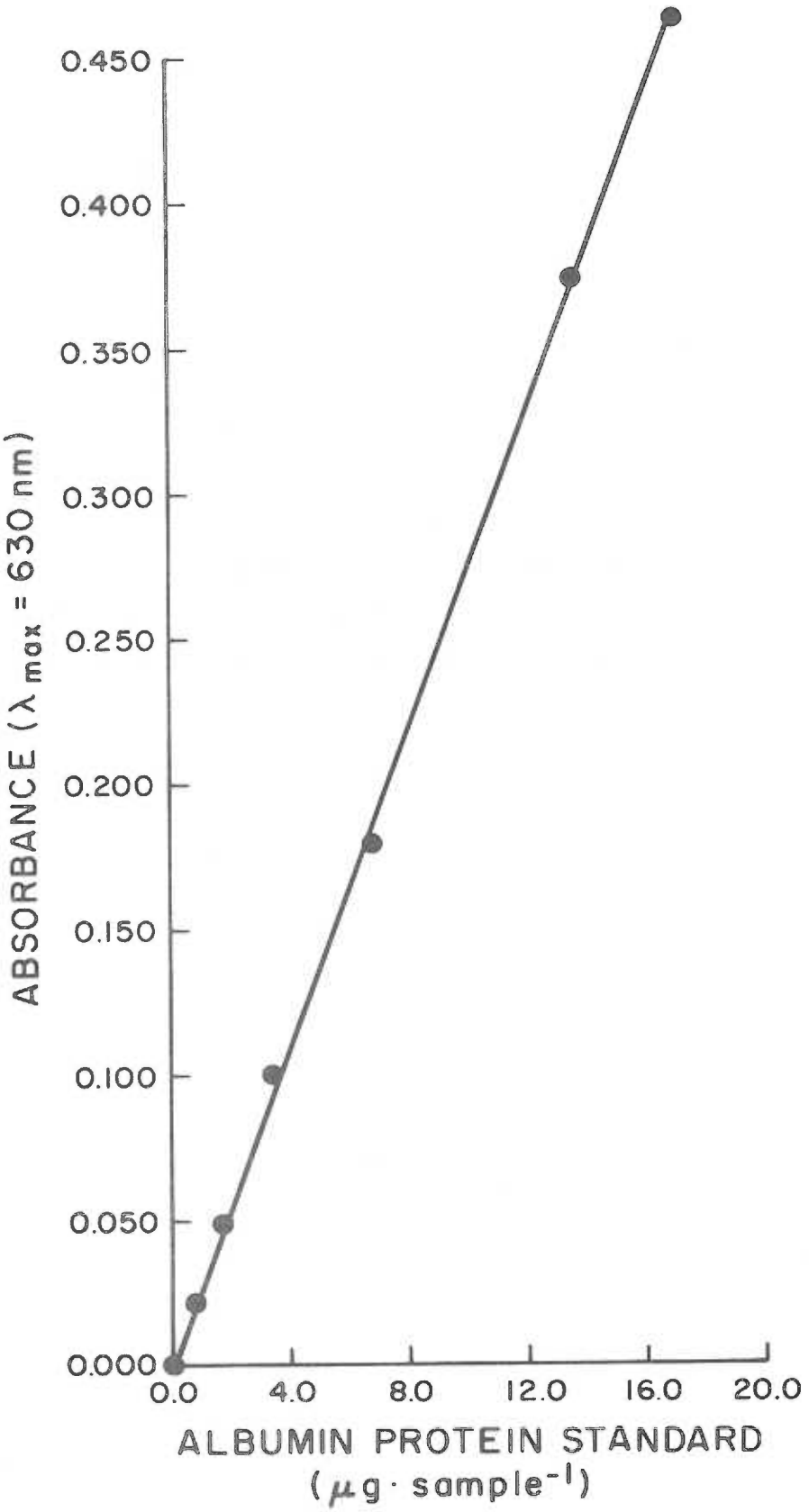
0.450
0.400
0.350
0.300
0.250
0.200
0.150
0.100
0.050
0.000
ABSORBANCE (λ max = 630 nm)
0.0
4.0
8.0
12.0
16.0
20.0
ALBUMIN PROTEIN STANDARD
(μg · sample-1)

and gravity filtered through Whatman No. 42 filter paper.

2) A standard solution of BSA was prepared as described under the Amidoschwartz assay.

The standard assay consisted of transferring up to 100 µl of protein solution containing 1-10 µg of protein (10-100 µg protein per ml) to 12 x 100 mm glass test tubes. A standard curve was constructed using BSA samples containing 20, 40, 60, 80 and 100 µg ml^{-1} BSA. If less than 100 µl of protein solution were utilized the volumes were adjusted to 100 µl with either appropriate buffer solution or water. (Glass Hamilton syringes should be utilized since variable results were obtained using automatic pipettes with plastic tips, presumably because of considerable adsorption of protein to the tips.) One ml of the Coomassie Blue reagent was added to the protein solutions and the absorbance was measured at 595 nm against a blank prepared from 100 µl of buffer plus 1 ml of Coomassie Blue reagent.

The development of the color complex, i.e., the formation of the protein-dye complex, is complete after ~2 minutes after addition of the Coomassie Blue reagent. The complex is stable for ~1 hour but the most precise measurements are obtainable between 5-20 minutes after addition of the dye. The sensitivity of the assay system is ~0.02 absorbance units per µg of protein in the final assay volume of 1.1 ml. Again, a standard curve was constructed (Fig. 2-5) and the amount of protein in the test samples was calculated from a linear

Figure 2-5. Standard curve for the Coomassie Brilliant Blue G-250 dye binding assay for protein. The amounts of BSA indicated were added to each sample and the assay was carried out as outlined in the text.

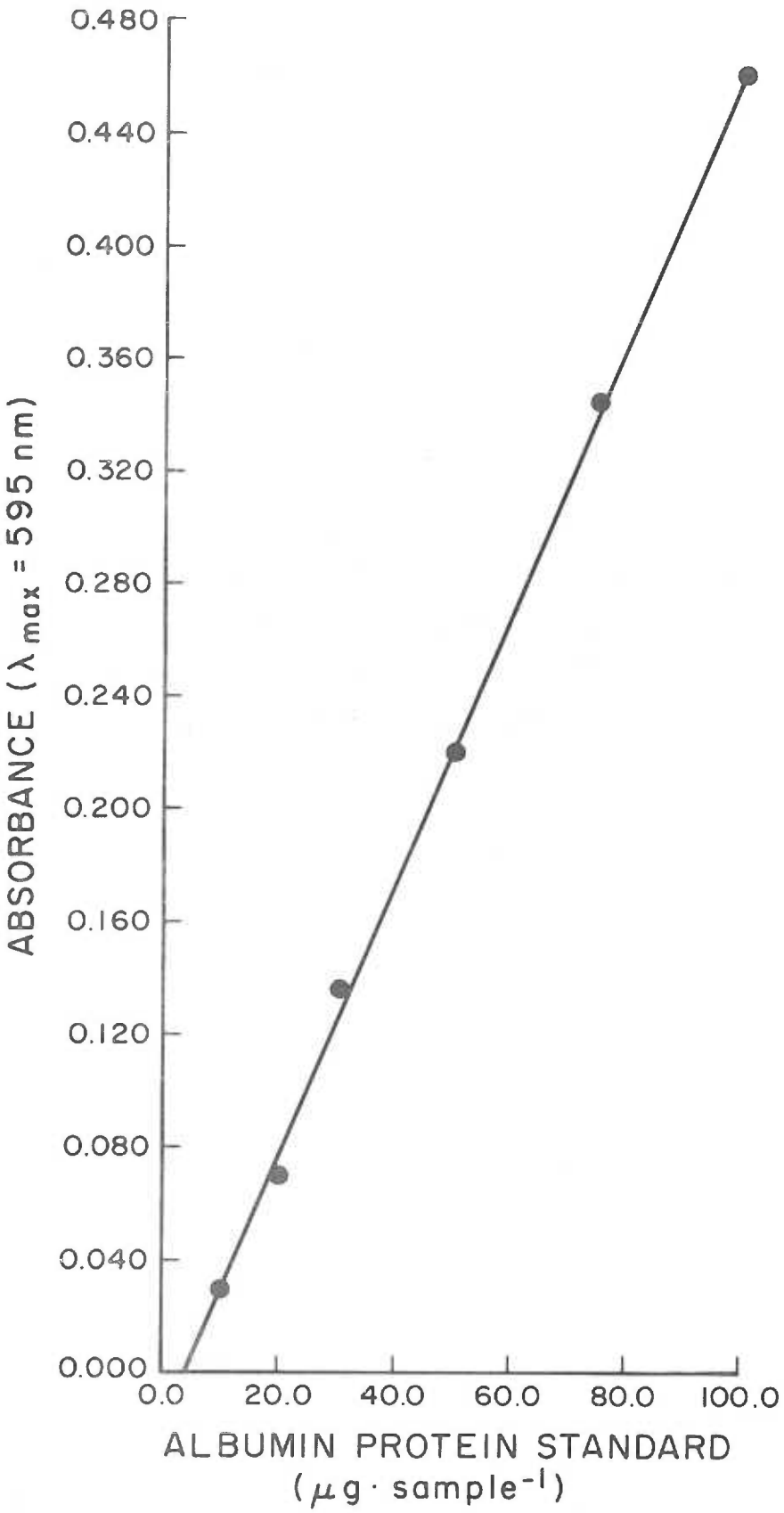
0.480
0.440
0.400
0.360
0.320
0.280
0.240
0.200
0.160
0.120
0.080
0.040
0.000
ABSORBANCE (λ max = 595 nm)
0.0
20.0
40.0
60.0
80.0
100.0
ALBUMIN PROTEIN STANDARD
(μg · sample-1)

regression fit of the data obtained on the BSA standard samples.

2.7.3 Protein Nitrogen Determination by the Microkjeldahl-Nessler Procedure

The microkjeldahl-Nessler assay (41) is a rapid method for the estimation of nitrogen in a protein sample. The number of μg of protein in a test sample may be obtained by multiplying the number of μg of nitrogen determined to be present by the factor 6.25. This assumes that the average percentage of nitrogen in a typical protein is ~16% (w/w). Due to the fact that all nitrogen present in a sample is measured by this method, extraneous nitrogeneous substances in the sample will yield falsely high values and they should, if possible, be excluded.

The following reagents and materials are necessary:

1) Nessler's reagent may be prepared according to the following recipe (41):
   a) Prepare 1.2 L of a 3.13 M NaOH solution.
   b) Prepare 30.0 ml of a 9.04 M solution of KI and transfer it to a filter flask.
   c) Add 33.8 g of iodine to the KI solution and mix well.
   d) Save ~0.5-1.0 ml of the KI-I_2 solution for subsequent back titration.
   e) Add 450 g of mercury to the KI-I_2 solution. The flask should now be stoppered and a piece of rubber tubing

which has been attached to the side arm of the flask should be pinched off.

f) The flask is now vigorously shaken inside of a fume hood and the pressure is released by opening the pinch clamp on the rubber tubing. This procedure is repeated until the solution is pale amber to slightly green. Excess mercury may then be decanted.

g) The solution is now tested for excess iodine by adding a few drops of it to a few drops of a 1% (w/v) corn starch solution in a spot test plate. If the test is negative as indicated by the absence of a brown color, a few drops of the solution saved in step d) should be added until iodine becomes barely visible in the spot test as a pale brownish color.

h) The KI-I_2-Hg solution is now added to the NaOH solution and mixed. This solution is then diluted to 1.8 L with water and stored in a brown bottle for 7-10 days prior to use. The solution is stable for one to two years. Since a sediment will form, care should be exercised by allowing the solution to clear prior to use if it has been agitated.

2) Concentrated sulphuric acid diluted 1:1 by volume with water.

3) 30% (w/v) hydrogen peroxide.

The assay procedure consists of digesting at least 1 ml, but always less than 2 ml, of the protein solution or blank with 200 µl of the sulfuric acid solution in a 12 x 100 mm test tube or a microkjeldahl flask containing a few small teflon boiling chips, over a low gas flame. Completion of digestion is indicated by clearing of the solution, and condensation of sulfuric acid in the neck of the flask.

On completion of the digestion the flask was cooled and 2-3 drops of hydrogen peroxide were added to complete the oxidation. The flask was then reheated to drive off the peroxide and water to prevent formation of a red mercurical precipitate on addition of the Nessler reagent. The sample was cooled again and diluted with 4.0 ml of water and mixed with 8.0 ml of the Nessler reagent which had been diluted 1:1 (v/v) with water. The absorbance of the nesslerized sample or blank was measured at 442 nm after 1 hour against a water blank.

A standard curve (Fig. 2-6) was prepared by using an $(NH_4)_2SO_4$ standard prepared by first drying the salt at 150°C in an oven for 2 hours. A 100 µg nitrogen per ml standard sample may be prepared by using a 3.57×10^{-2} M aqueous $(NH_4)_2SO_4$ solution and diluting it ten fold, by volume, with water. The $(NH_4)_2SO_4$ standard, as well as a blank sample were run through the entire procedure.

Figure 2-6. A standard curve illustrating the linearity of the microkjeldahl assay for nitrogen. The indicated amounts of nitrogen were added to each sample in the form of $(NH_4)_2SO_4$ and the assay was carried out in the manner described in the text.

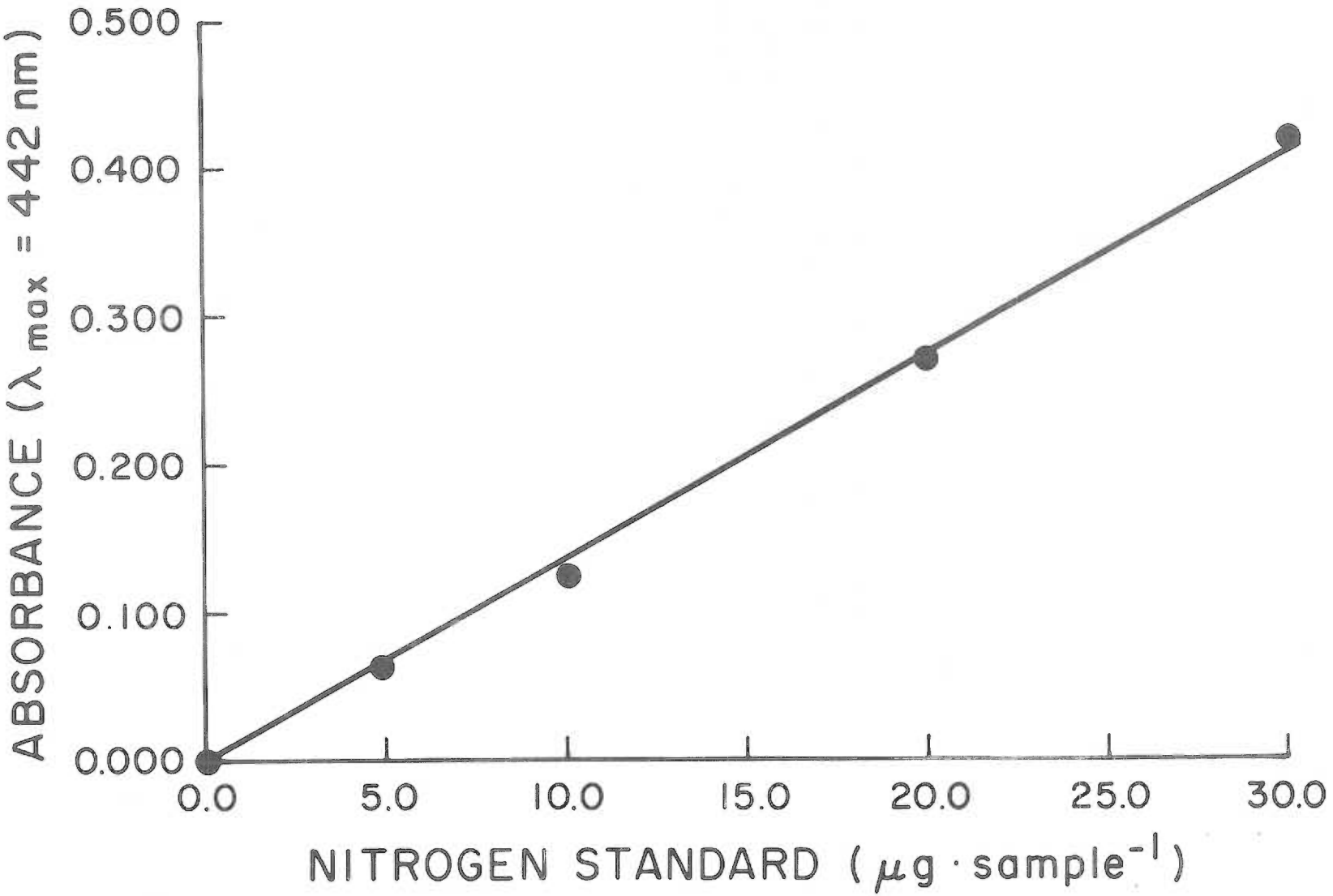
ABSORBANCE (λ max = 442 nm)
0.500
0.400
0.300
0.200
0.100
0.000
0.0
5.0
10.0
15.0
20.0
25.0
30.0
NITROGEN STANDARD (μg · sample^{-1})

CHAPTER 3

ANALYTICAL PARTICLE ELECTROPHORESIS

Analytical particle electrophoresis also known as microelectrophoresis (42), cellular electrophoresis (43), cell electrophoresis (44), microcataphoresis (45), and microscopic electrophoresis (46) is the method of choice for determining the electrophoretic mobility of particles that are large enough, and possess a refractive index sufficiently different from that of the suspending medium, to be visible in a light microscope. In some instances the electrophoretic mobility of submicroscopic colloids, e.g., proteins, has been successfully determined in a microelectrophoresis apparatus by adsorption of the colloid onto a suitable carrier particle. The results in some cases agree quite well with those obtained by the moving boundary or U-tube method or may be unreliable due to incomplete coverage of the carrier particle or conformational changes of the adsorbant molecules on interaction with the carrier.

3.1 Principles of Operation

The electrophoretic mobility of a particle or cell is obtained by measuring the electrophoretic velocity, v_e, of the particle per unit electric field strength, X, which is acting on the particle.

The electrophoretic velocity of particles suspended in an ionic medium is determined by an observer monitoring particle movement within a light transparent chamber with the aid of a microscope which is equipped with an ocular containing a graticule. This graticule is calibrated such that each square or division corresponds to a known physical distance at the point of focus of the microscope within the electrophoresis chamber. Thus v_e, is determined by measuring the time, t, in seconds, required by a particle to traverse one graticule division, i.e.,

$$v_e = \frac{[\mu m][\text{graticule division}]^{-1}}{[t][\text{graticule division}]^{-1}} = \frac{\mu m}{sec} \qquad 3-1$$

The electric field strength, X, is the electrical potential, V, measured in practical volts, divided by the effective length, in cm, over which the potential is measured, i.e., the electrical length (Section 3.3.1). Thus

$$X = \frac{V}{cm} \qquad 3-2$$

and the electrophoretic mobility, u, may be calculated with the use of Eq. 1-1, Section 1.1 and is usually expressed as $\mu m\ sec^{-1}\ V^{-1}\ cm$ or in some instances as $cm^2\ sec^{-1}\ V^{-1}$.

3.2 The Electrophoresis Chamber

Microelectrophoresis chambers regardless of ultimate geometric configuration have usually been constructed from glass. Conceivably they might be constructed using any rigid light transparent materials which may include plastics. Mehrishi (47) for example has described a cell, the electrode compartments of which were fabricated from Plexiglas. However, the actual column in which the particle suspension is housed is made of glass. Two types of electrophoresis chamber geometry are in general use namely the cylindrical and the rectangular types. Observation chambers employing, often complex, variations of these primary designs have been described in the literature (48). In many cases, these designs were developed in order to eliminate practical problems such as the forced return flow of fluid due to electroosmosis (48). In practice, however, they created as many problems as they were intended to eradicate.

Seaman (49) has compared a number of features of the basic cylindrical chamber design with features of chambers having a rectangular cross section. These comparisons are repeated in Table 3-1 from which it can be easily concluded that the cylindrical chamber design is superior for most applications, including all of those described in this thesis.

Table 3-1. Comparison of features of cylindrical and rectangular analytical particle electrophoresis chambers.

Feature	Cylindrical Chamber	Rectangular Chamber
1. Theory for electroosmotic flow in the chamber.	Satisfactory and exact solution to the hydrodynamic equations. The stationary annuloid (level) is located symmetrically at 0.293 of the tube radius from the wall.	No exact solution to the hydrodynamic equations. At ratios of cell width to cell depth > 20:1 the stationary levels are located at 0.21 and 0.79, respectively, of the total cell depth.
2. Experimental location of the stationary level	Optical refraction effects may necessitate application of an optical correction.	With glass plates of optical quality accurate location of the stationary levels is possible.
3. Form of the electroosmotic flow parabola	In chambers with a 2-3 mm bore the parabola is not steep in the region of the stationary level, so small focus setting errors do not produce significant errors in the electrophoretic mobility.	The condition of a 20:1 width/depth ratio normally necessitates a chamber of small depth (~0.5 mm), and consequently the profile for the parabole is steep at the stationary levels such that setting errors for the focus may lead to appreciable errors in the electrophoretic mobility.
4. Phase contrast optics	Not normally possible.	Readily incorporated.
5. Optical definition of particles	Moderate.	Good.

Table 3-1. Continued.

Feature	Cylindrical Chamber	Rectangular Chamber
6. Stability of the contents of the chamber during a run	The symmetrical chamber with uniform heat exchange minimizes the effects of thermal convection.	Asymmetric chamber prone to thermal instability and convective effects.
7. Effects of particle sedimentation	Larger particles sediment fairly rapidly out of the curved stationary level. Not suitable for dense particles or ones larger than about 20-25 μm diameter.	If the chamber is mounted in vertical alignment any sedimenting particles will remain in focus at the stationary level.
8. Construction	Relatively easily made in one piece so that heterogeneities in the surface properties of the glass are not likely to arise.	Optical quality plates with the same surface characteristics are necessary to prevent a distorted electro-osmotic flow parabola.
9. Measurement of field strength	The electric field is uniform and parallel to the axis of the tube so absolute results may be obtained.	The shape of the chamber precludes an electrode geometry which will produce a uniform applied electrical field. Absolute results are difficult or impossible to obtain.
10. Volume of dispersion sample required	For platinum electrode systems, 5-10 ml. For Ag/AgCl reversible electrodes, ~1 ml. With injection technique, ~0.1 ml.	Usually more than for the cylindrical chambers.
11. Cleaning of the chamber	Easy and rapid.	Difficult to achieve and slow to carry out because of the "corners".

3.2.1 The Cylindrical Chamber Apparatus

Although numerous cylindrical electrophoresis chamber designs have been described in the literature the design for chambers used here is primarily based on that of Alexander and Saggers (50). Their design was extensively modified by Bangham et al. (51) and Seaman and Heard (52). Due to a number of difficulties encountered with these versions, further modifications were made leading to the chamber pictured and shown schematically in Figures 3-1 and 3 2, respectively. This design is described by Seaman (49) and was constructed by A. Ryall of the Oregon Graduate Center, Beaverton, Oregon according to the specification given in Fig. 3-2. Its main features include the incorporation of a Ag/AgCl/KCl reversible electrode system. This system is preferable to others such as $Zn/ZnSO_4$ or $Cu/CuSO_4$ due to the appreciable solubility of these toxic metal ions compared to Ag^+.

Sintered glass disks are fused in, and separate the electrode compartments from the sample compartment. This in essence minimizes the diffusion of electrode products into the sample area. Furthermore, the sintered glass disks allow high ionic strength electrolytes, e.g., 1 M KCl to be used in the electrode compartments so that essentially 100% of the potential drop between the electrodes takes place across the sample compartment.

Figure 3-1. All-glass cylindrical electrophoresis chamber incorporating fused in sintered glass disks as first described by Seaman (49).

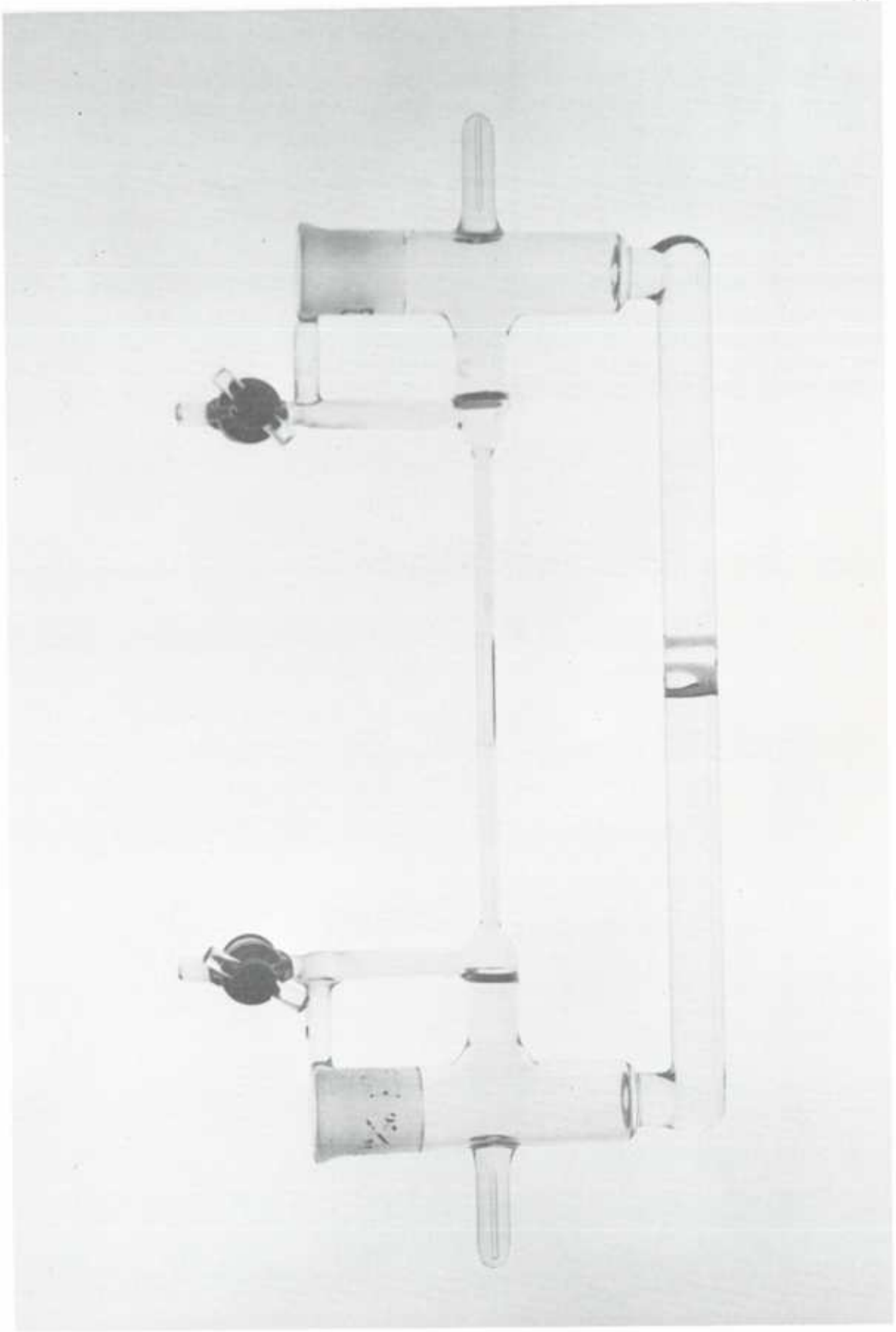

Figure 3-2. Schematic illustration including dimensional specifications (cm) of the all-glass electrophoresis chamber shown in Figure 3-1, incorporating a Ag/AgCl/KCl reversible electrode system.

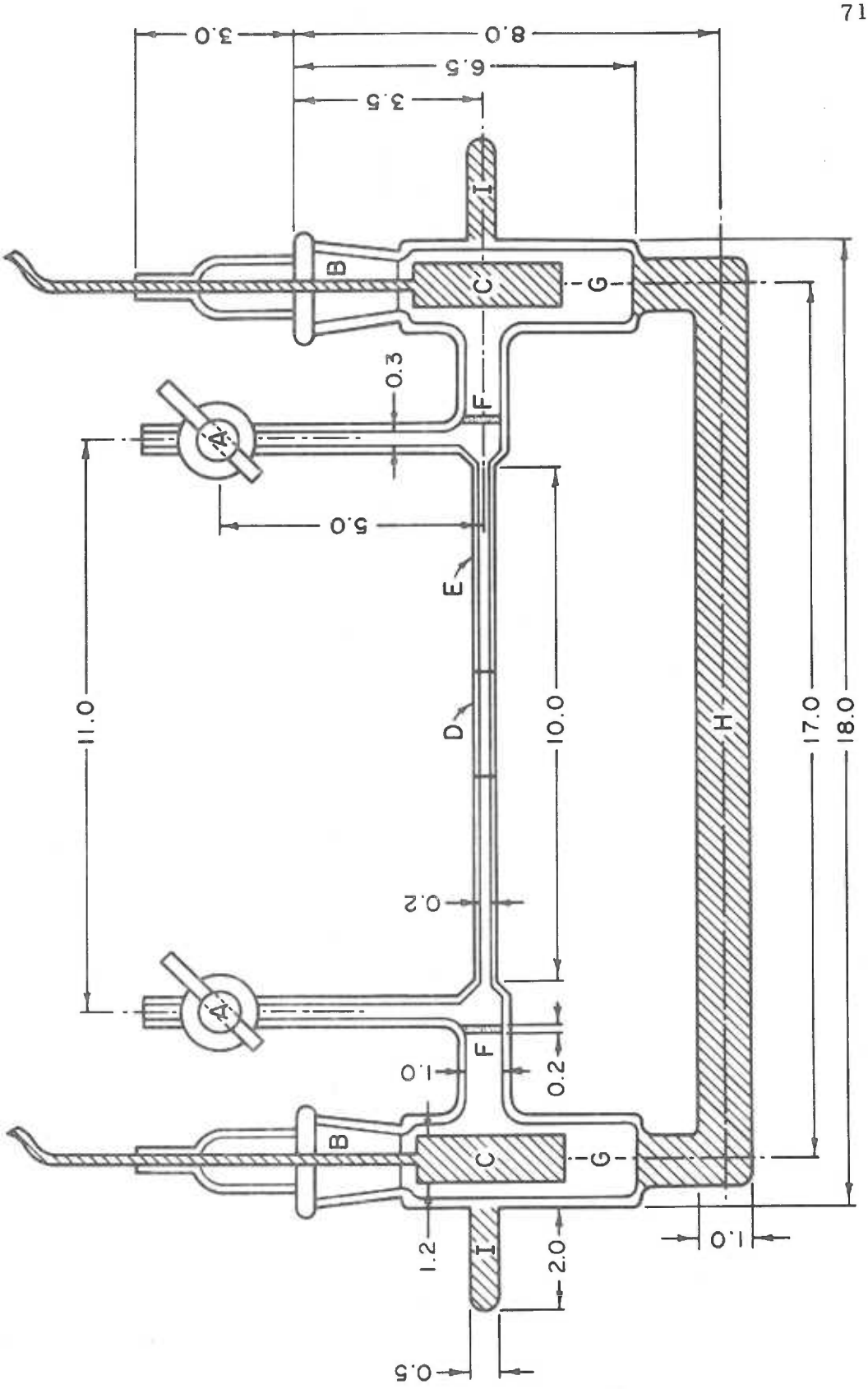
3.0
8.0
6.5
3.5
I
B
C
G
0.3
F
A
5.0
E
11.0
D
10.0
H
17.0
18.0
0.2
A
F
0.1
0.2
B
C
G
1.2
I
2.0
0.1
0.5

The sample compartment itself consists of a precision, uniform bore glass tube of ~2 mm diameter. The tubes were purchased from Rank Bros., Bottisham, England and had optical flats ground on the outside walls by the manufacturer to a thickness of ~100 μm or less. Optical flats improve the definition of the particles which are to be observed. Together with the fact that the chamber and microscope are immersed in water, the optical flats also reduce the effects of refraction, by the planoconcave lens-like nature of the tube, sufficiently to eliminate the necessity for applying optical corrections like those described by Henry (53).

The chamber was sealed positively by two stopcock keys at the top of the fillports. The chamber was also designed so that it was easily filled with Pasteur pipettes and easily cleaned in situ. The total sample volume of the chamber was ~2 ml.

After use in some of the initial studies it became apparent that the above described chamber design also suffered from a series of design deficiencies. These deficiencies were remedied by developing a modified, miniaturized version of the chamber shown in Fig. 3-1 and 3-2. This novel design is illustrated in Fig. 3-3 and 3-4. In incorporates the following features which distinguish it from the 1975 design (49):

a. The volume of the electrode compartments has been minimized both by substantially decreasing their physical size and

Figure 3-3. Mini-all-glass cylindrical microelectrophoresis chamber.

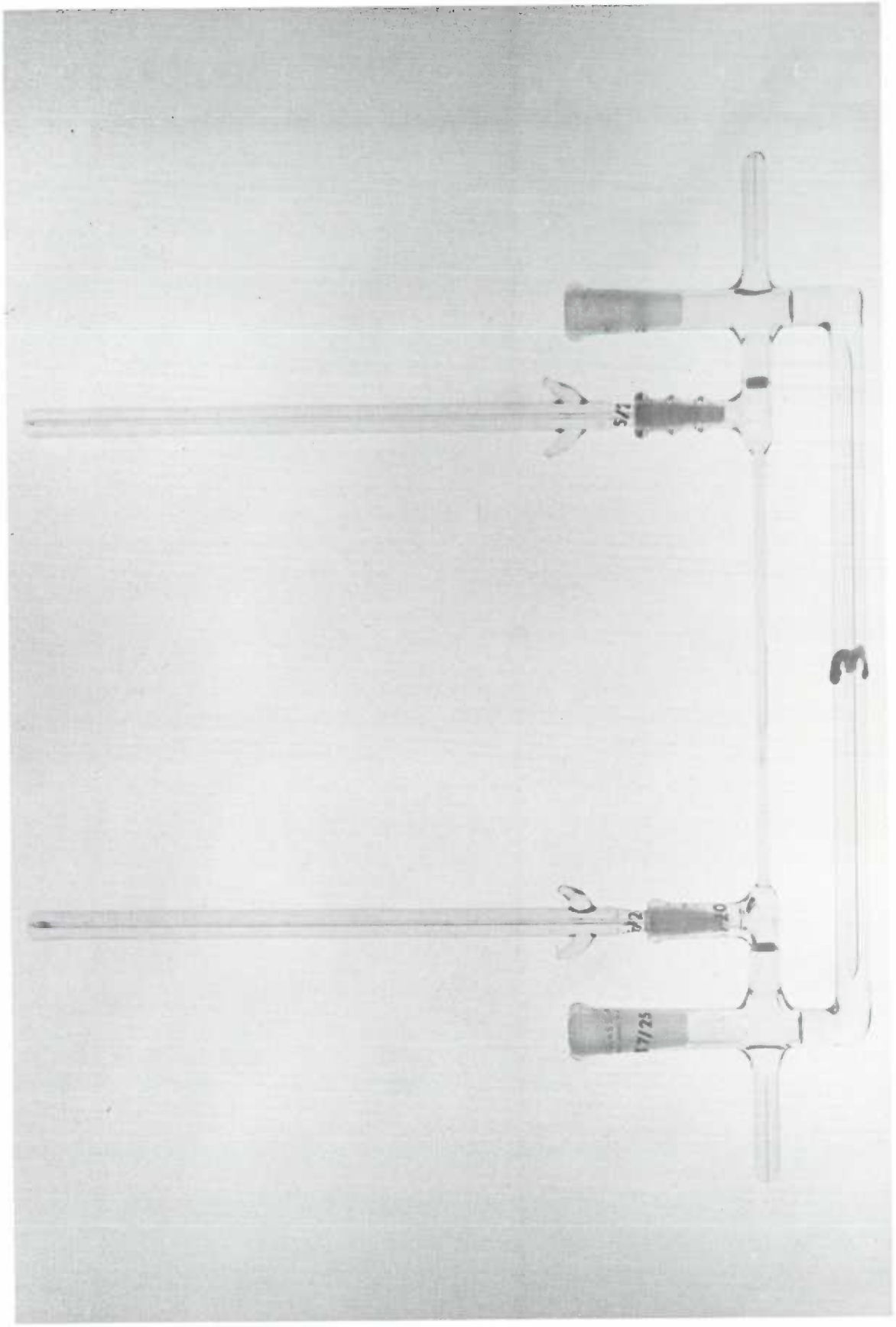

Figure 3-4. Dimensional specifications (cm) for the mini-all-glass electrophoresis chamber incorporating solid Ag/AgCl electrodes, fused in sintered glass disks and capillary standard taper stoppers.

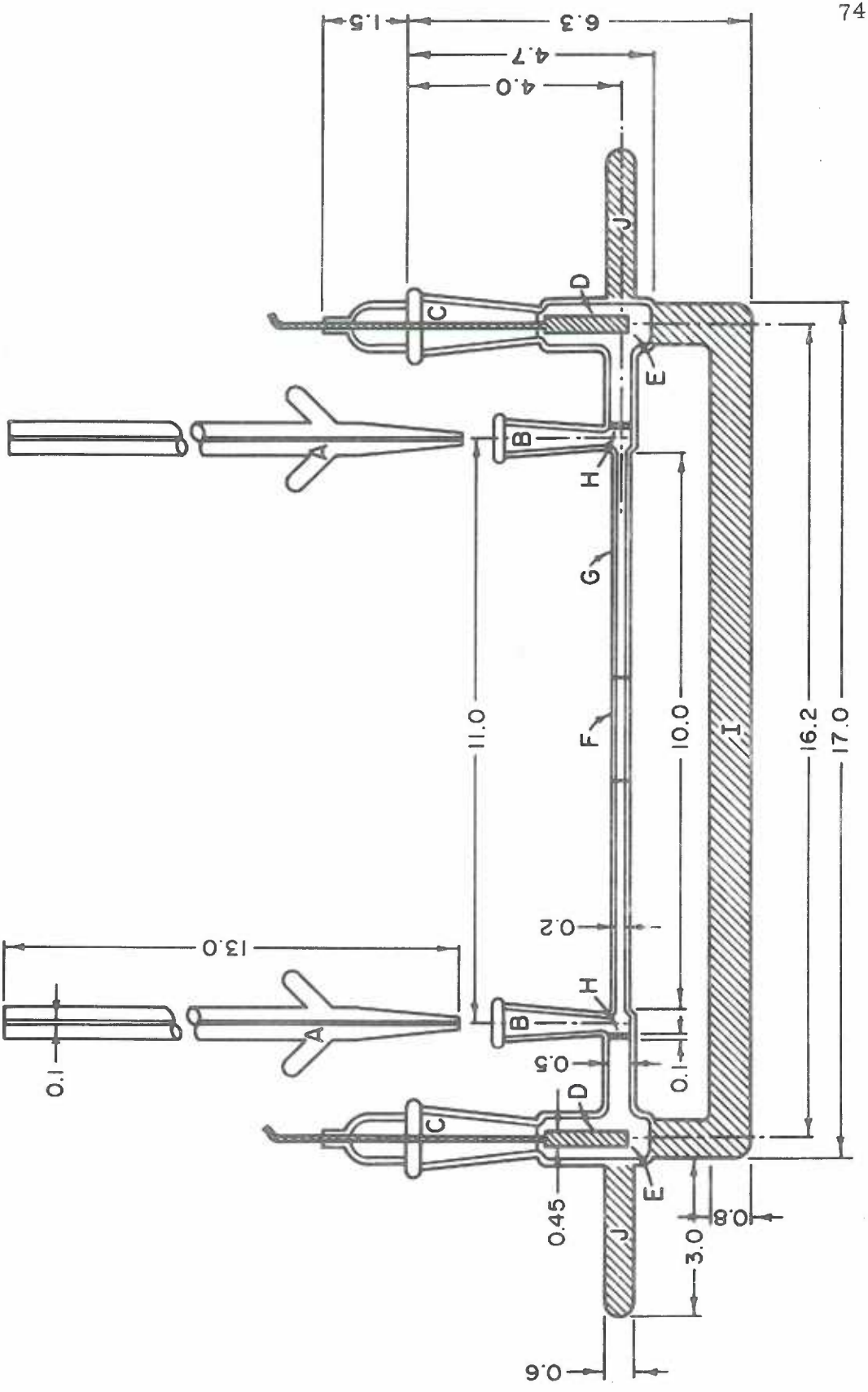
1.5
6.3
4.7
4.0
J
D
C
E
A
B
H
G
F
I
11.0
10.0
16.2
17.0
0.2
13.0
0.1
0.5
0.1
0.45
0.8
3.0
0.6

by using solid silver electrodes instead of hollow cylinder electrodes. The former displace more fluid thus decreasing the effective volume of the electrode compartments.

b. The above change allowed for a four fold reduction in area of the sintered glass disks from ~0.8 cm^2 to ~0.2 cm^2. This minimized the diffusion of KCl out of the electrode compartments and concomitant convective disturbances. The change also minimized electroosmotic flow through the disks which again minimized hydrodynamic disturbances within the sample compartment.

c. Electrodes were constructed from one piece of silver by turning a stock piece of silver on a lathe. This eliminates having to spot weld the electrode wire to the electrode body and provides for an overall more robust electrode which will stand up to many more replatings than those used previously.

d. The fill ports of the 1975 chamber design were reduced in length and the stop cocks replaced by stoppers. This was done to: 1) reduce the hydrostatic pressure heads which were present when the sample compartment was filled; 2) reduce the total required experimental sample volume by more than half, i.e., a minimum of 0.8 to 1.0 ml is necessary to fill the new type chamber; and 3) facilitate a technique referred to as "microinjection".

The technique entails introduction of a sample directly into the region where measurements are made, which involves only a small portion of the whole sample compartment. The equipment requirements are minimal, namely a piece of polyethylene tubing, ~15 cm long and having an inner diameter of ~0.2 mm, is gently heated and bent to ~30° angle about 1-2 cm from one end. The other end of the tubing is fitted over a 20 gauge syringe needle attached to a tuberculin syringe. The electrophoresis chamber is filled with particle free buffer and closed off at one end with one of the stoppers. The buffer is allowed to come to temperature equilibrium. If the buffer has been stored in a refrigerator, degassing the solution under reduced pressure will help to minimize bubble formation in the chamber. The polyethylene tubing may thus be filled with a suspension containing 10^6-10^7 particles per ml. To minimize sample requirements, as well as the probability of introducing air bubbles into the chamber, a 3-5 cm column of suspending medium is drawn into the tubing followed by ~1 cm of the particle suspension. The tubing should then be fed through the open chamber port into the capillary tube as far as the optical flat where the end of the tubing may be seen through the microscope. The particle sample may then be injected as the tubing is withdrawn gradually and the microscopic field checked for the presence of particles. The second stopper is then inserted. At this point a check should be made to determine whether particles are drifting

horizontally or are sedimenting more or less rapidly than normal. If convection is apparent the procedure must be repeated.

Convective disturbances are a major problem if the injection procedure is improperly carried out. The major sources of convection are density differences between the injected sample suspension and the suspending medium which may result from differences in temperature or small differences in media composition. Consequently, it is imperative that the medium used to suspend the particle sample be drawn from the same stock as is used to fill the chamber and that temperature differences be minimized. The microinjection technique allows for the maximum conservation of samples available only in small quantities.

e. Finally, instead of running a completely closed system the new chamber design allows for running a half open system by utilizing ground glass full length standard taper joints with a 13 cm long 1 mm inner diameter capillary stem. The opening at the end of one of the capillary stems is further reduced in an oxygen flame to a point where air barely passes through the capillary. The other capillary is completely closed off. This eliminates drifts arising from convective and mechanical disturbances due to air currents or temperature fluctuations. This half open system also allows for slight expansion of the sample suspension which is bound to take place on application

of an electric current, thus further stabilizing the system.

The newly designed chamber like the previous one was built according to specifications give in Fig. 3-4 by A. Ryall, Oregon Graduate Center, Beaverton, Oregon. Electrodes made of 99.99% pure silver were turned on a lathe by Dr. P. Blume, Good Samaritan Hospital and Medical Center, Portland, Oregon. All standard taper glassware as well as matched medium porosity sintered glass disks were obtained from Lab Glass, Inc., Vineland, New Jersey.

Although the new type chamber described above was used for the majority of the work a second type of chamber employing platinum black electrodes (54) was also utilized for electrophoretic analyses of particles or cells suspended in media of less than physiological ionic strength. This chamber is depicted in Fig. 3-5. Due to the fact that platinum is extremely inert and available in ultra-pure form, sintered glass disks need not be incorporated to separate the electrodes from the sample. The drawback to using platinum electrodes is that they polarize appreciably above ionic strengths of 0.05 g-ions $\cdot L^{-1}$. Furthermore appreciable sample volumes, up to 10 ml, are necessary. Thus platinum chambers cannot be used if only small amounts of material are available.

Figure 3-5. Schematic illustration of the all glass cylindrical electrophoresis chamber incorporating platinum electrodes. The chamber is especially suited for work at low ionic strengths viz., <0.050 g-ions $\cdot L^{-1}$. Dimensions are given in cm.

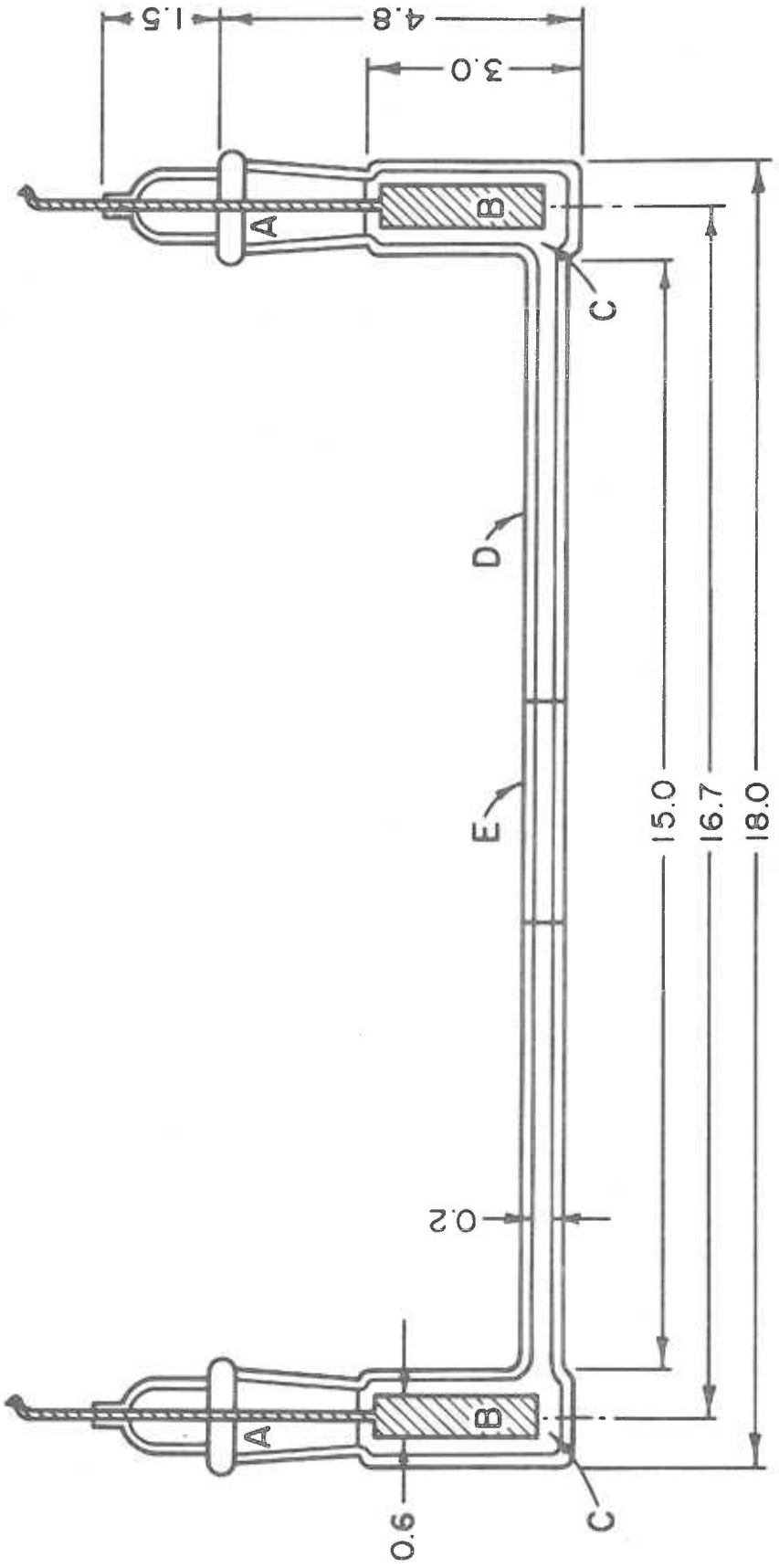
1.5
4.8
3.0
A
B
C
D
E
15.0
16.7
18.0
0.2
0.6

3.2.2 Plating of Ag/AgCl Reversible Electrodes

Silver electrodes were plated with silver chloride to minimize electrode polarization which if it occurred would result in decreased electrical field strengths in the measuring chamber.

Typically a bright silver electrode was cleaned with ethanol and rinsed with water to remove organic deposits. The electrode was then etched in nitric acid diluted 1:1 with distilled water to produce an even white mosaic appearance. It was then placed in a 100-150 ml beaker containing 0.01 M HCl along with a stir bar and a second silver electrode surrounding the first. The electrode to be plated was then connected to the positive pole and the other to the negative pole of a DC power supply. A current of < ~3 mA was applied for 2-3 hours after which the electrode had taken on a dark even grayish appearance.

3.2.3 Plating of Platinum Electrodes

Platinum electrodes were plated with finely divided platinum (platinum black). This greatly increases the effective surface area of the electrodes thus making them reversible and usable up to ionic strengths of 0.05 g-ions $\cdot L^{-1}$ for an electrode which ostensibly has a 1 cm^2 surface area.

Typically the electrodes were rinsed in ethanol to remove oily organic contamination followed by distilled water. They were then

dipped into a chromic-sulfuric acid cleaning solution for ~5 minutes and again thoroughly rinsed with water. Alternatively the electrodes were cleaned by burning contamination off in an oxygen flame. The electrodes were thus suspended in the plating solution consisting of 58 mM chloroplatinic acid ($H_2PtCl_6 \cdot 6H_2O$) and 1 mM lead acetate in water and plated at ~5 mA for 10-15 minutes. The current was reversed approximately every 30 seconds.

To leach the plating solution out of the electrodes they were placed in 0.05 M sulfuric acid with passage of current for ~15 minutes. The current was reversed at ~1-2 minute intervals.

3.2.4 Cleaning of the Chamber

Typically the chamber was cleaned with an alcoholic potassium hydroxide solution prepared by diluting 10 ml of a 30 M solution of KOH in water with 95% v/v ethanol to give a final volume of 100 ml. The chamber was completely filled with this solution and allowed to stand for several hours, preferably overnight. The chamber was then thoroughly rinsed with distilled water. Cleaning solutions containing chromate ions are not recommended due to the fact that these ions are toxic and desorb exceedingly slowly from glass. Cleaning of the chamber is especially important when using cell suspensions which may leak proteins. These will coat the sample tube of the chamber

unevenly leading to disturbed fluid flow profiles and inaccurate and/or variable data.

3.2.5 Calibration of the Sample Capillary Tube

Before the capillary tube is actually incorporated into a chamber its radius must be accurately measured. The radius is needed to compute the position of the annuloid where the velocity of the electrolyte fluid in the presence of an electric field is zero. This annuloid is also known as the stationary level and is discussed further in Section 3.6. The radius is also used in measuring and computing the electrical length of the chamber (Section 3.3.1).

The radius for capillary tubes of uniform bore was calculated from the length and mass of a mercury column in the sample tube according to:

$$R = \left[\frac{m_{Hg}}{\rho_{Hg}^{22} \pi \ell} \right]^{1/2} = \left[\frac{m_{Hg}}{(42.54\ g/ml) \cdot \ell} \right]^{1/2} \qquad 3\text{-}3$$

where m_{Hg} is the mass of mercury in g, ℓ is the length of the column in cm and ρ_{Hg}^{22} is the density of mercury at 22°C (approximately room temperature).

Typically the tube was weighed on an analytical balance with enough clay to plug the ends of the tube. The tube was then filled with mercury to give a 7-9 cm long column. The ends were plugged and

the tube was reweighed. Thus the mass of the mercury could be determined. The length of the mercury column (±0.01 mm) was measured with a traveling microscope (Precision Tool and Instrument Co., Ltd., Thornton Heath Surrey, England, Microscope Type 2158). The meniscus was taken into account at one end of the column and not the other to obtain a true column length.

3.3 Equipment and its Setup

The general requirements for peripheral equipment have been described by a number of authors (49, 55). The apparatus as it was generally used and operated in the collection of the electrophoretic data is described below.

An electrophoresis chamber of the type described in detail in Section 3.2.1 was immersed in a 17 L capacity water bath, the temperature of which was controlled to within ±0.1°C by a 200 watt heating element connected to a relay via a mercury thermostat.

The water bath was well stirred to minimize temperature gradients, which if they had occurred over a range of ±0.5°C would have given rise to significant measurement errors. These would have resulted from either uneven heating and cooling of the sample compartment of the electrophoresis chamber giving rise to gravity driven thermal convections, or alterations in the viscosity and/or conductivity of the suspending medium.

The electrophoresis chamber rigidly mounted in a holder was aligned within the water bath in front of a microscope. Initially the chamber was levelled so that the sample compartment capillary tube (hereafter referred to simply as the "tube") was parallel with the surface of the water in the bath. This eliminated the effects of any non-vertical gravitational velocity components during operation. Secondly the length of the tube was set at a right angle to the axis of the microscope assembly. As this adjustment is not critical it was made visually.

A cylindrical chamber microelectrophoresis apparatus is pictured and schematically illustrated in Figs. 3-6 and 3-7 respectively and may be referred to for the following discussion.

Vertical alignment of the chamber was achieved via a screw traverse. The distance traveled was indicated by a dial test indicator (Mercer, St. Albans, England, 0.002 mm division^{-1}). The aim was to position the tube such that the optical axis of the microscope intersected the longitudinal axis of the tube. This was accomplished by locating and positioning the black-white inner glass-air interface at the top or bottom of the tube so that it bisected the field of view in the ocular. As an aid for bringing the interface into sharp focus the tube was often filled with distilled water which produced a white-white glass-fluid interface which was often demarcated by colored fringes. With the aid of the vertical adjustment screw, the chamber was moved

Figure 3-6. Typical cylindrical chamber microelectrophoresis apparatus employed for the collection of mobility data.

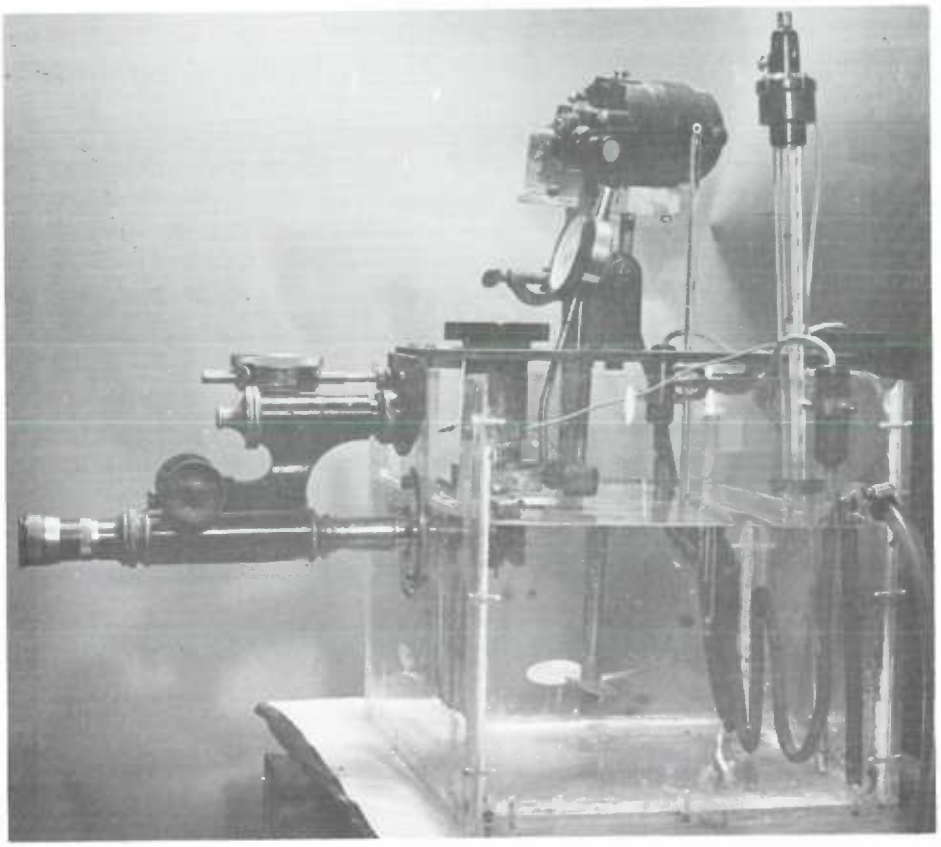

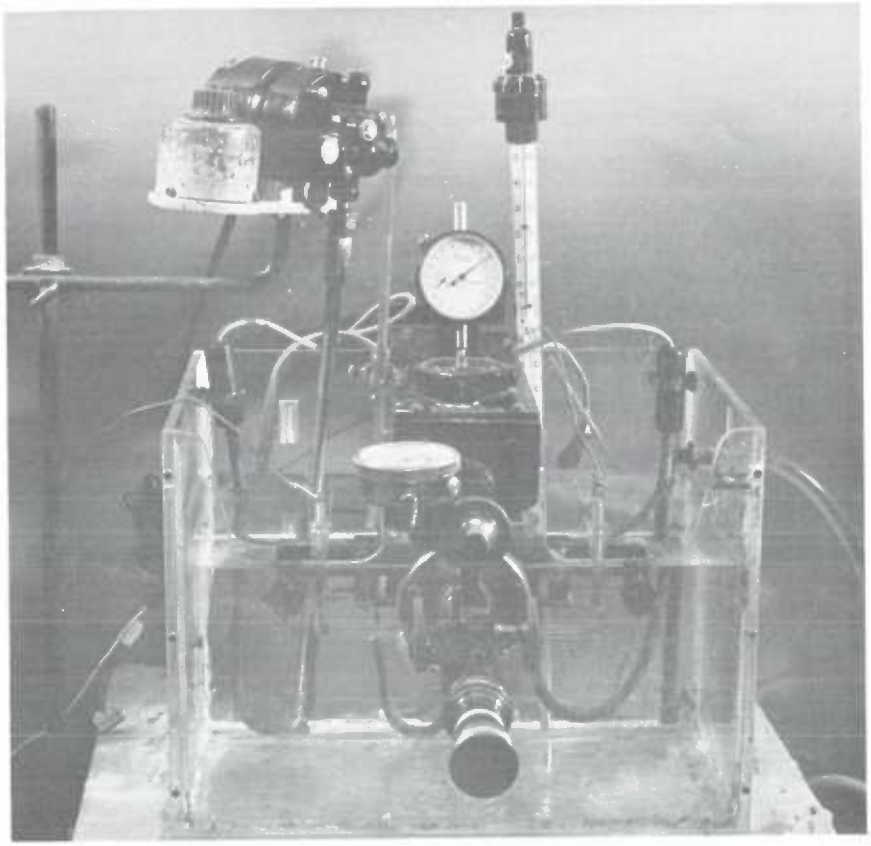

Figure 3-7. Schematic illustration of a cylindrical microelectrophoresis apparatus.

1) Ocular with graticule
2) Microscope tube
3) Coarse adjustment for microscope
4) Fine adjustment for microscope
5) Dial test indicator for horizontal positioning
6) X40 objective
7) Electrophoresis chamber and chamber holder
8) Vertical adjustment screw
9) Dial test indicator for vertical positioning of chamber
10) Stirrer
11) Heater
12) Light source
13) Tank leveling screws

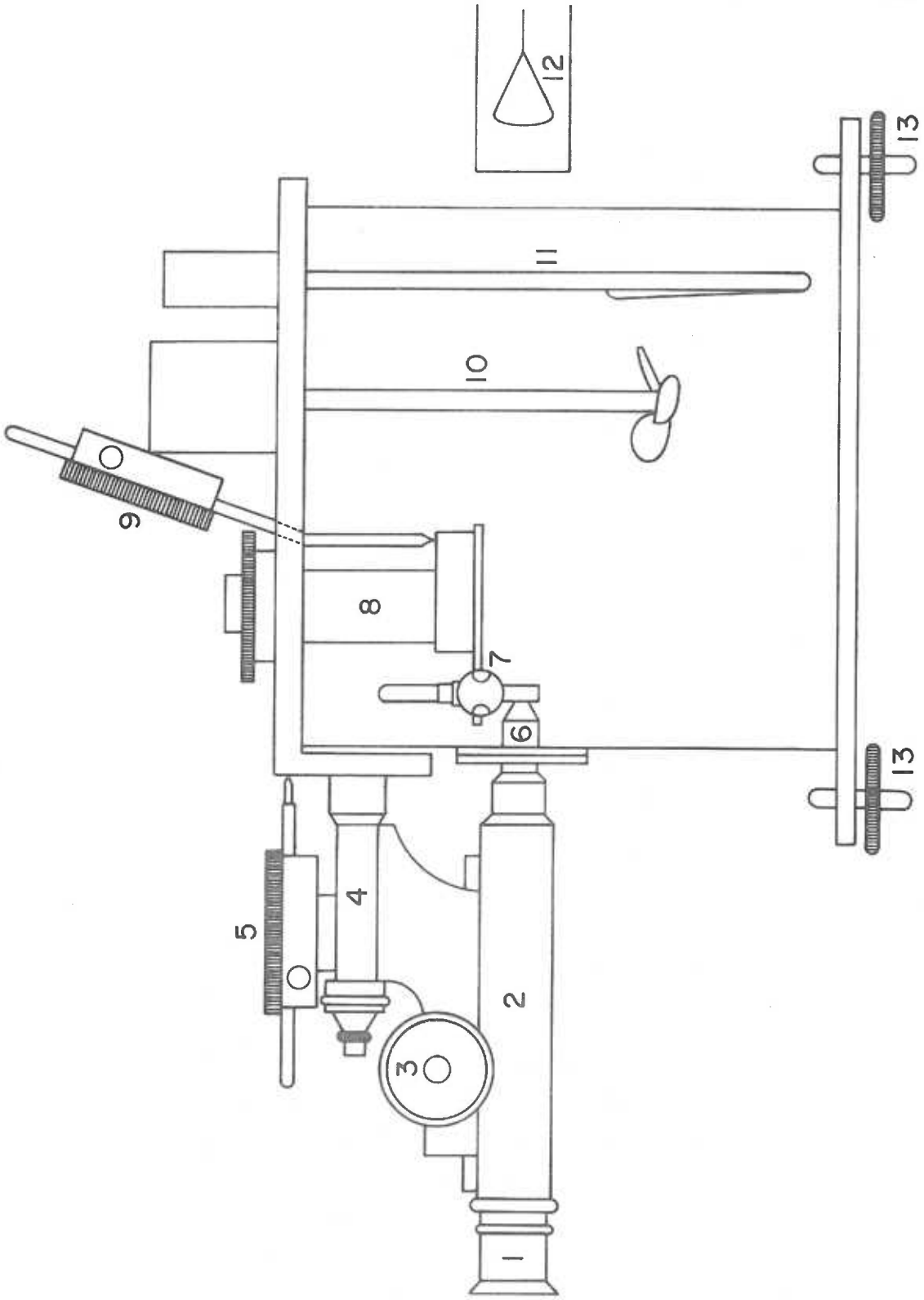
12
13
11
10
9
8
7
6
13
5
4
2
3
1

appropriately either up or down so that the second interface was brought into position and bisected the field of view. The distance traveled, which corresponded to the bore of the tube, was noted on the dial test indicator. The chamber was then moved back to half the total distance. Thus the tube was centered on the optical axis of the microscope.

The horizontal stationary level adjustment was made with the aid of the fine adjustment of the microscope and the horizontal dial test indicator. The inside proximal wall of the tube was located and focused on with the microscope. This was most easily accomplished by filling the tube with a relatively concentrated salt solution, e.g., 1 M KCl or 1 M NaCl, aspirating it until the solution dried, with the resultant deposition of microcrystals of salt on the wall, which then served as a focusing aid. The microscope was then moved toward the axis of the tube for a distance of 0.293 R, where R, is the radius of the tube. (For the determination of R see Section 3.2.5.) All of the apparatus used in the studies presented in this thesis were of similar design to that depicted in Fig. 3-6 and were manufactured either by Rank Bros., Bottisham, England or by Dr. G.V.F. Seaman, University of Oregon Health Sciences Center, Portland, Oregon.

3.3.1 Calibration of the Assembled Apparatus

The effective electrical length, ℓ_e, was measured using standard KCl solutions. KCl was dried at 150-200°C for ~2 hours and a 0.100 M solution was prepared. The electrode compartments of the electrophoresis chamber were filled with 1 M KCl making sure that no trapped air remained in the sintered glass disks which would increase their resistance and result in aberrant current and voltage readings. The electrodes were inserted into the compartments using a light coat of silicone grease to obtain a good seal. The water bath was maintained at 25.0 ± 0.1°C. The sample compartment was rinsed thoroughly and filled with the 0.100 M KCl solution which also had previously been equilibrated to 25.0 ± 0.1°C. The current through the chamber was measured, on application of a given voltage, with a digital multimeter (Hewlett Packard 3435A). Electrical field strengths were kept at $< 5\ V \cdot cm^{-1}$ which resulted in current readings of < 3 mA. The electrical length was then calculated according to the equation:

$$\ell_e = \frac{K_{sp} V \pi a^2}{I} \qquad 3\text{-}4$$

where K_{sp} is the specific conductivity of 0.100 M KCl, V is the applied voltage, a is the chamber tube radius and I is the current through the chamber. The most critical aspect of the procedure is the accuracy of the voltage and current measurements. Voltage should be accurate to within ± 1 V and the current accurate to within ±0.04 mA.

3.3.2 Graticule Calibration

A Bausch and Lomb graticule (No. 31-16-11) the squares of which were 0.05 mm on a side was calibrated with a stage micrometer scale (American Optical 0.01 mm unit^{-1}). A magnification of X400 was typically utilized for the collection of electrophoretic data (X40 water immersion objective + X10 ocular). At this magnification one graticule width corresponds to 10-15 μm actual physical length when the microscope was focused on an object, i.e., a particle or a cell.

3.3.3 Performance Monitoring of Electrophoresis Apparatus

The apparatus calibration and operation were routinely checked before and after examination of experimental samples with either native or formaldehyde-fixed human red blood cells suspended in 0.150 M aqueous sodium chloride adjusted to pH 7.4 ± 0.2 with aqueous 0.150 M sodium bicarbonate solution. Either native or formaldehyde-fixed human erythrocytes were utilized. Both types of cells have the same mobility in physiological ionic strength saline (56). A mean

mobility of -1.08 ± 0.05 μm sec^{-1} V^{-1} cm for a set of ten measurements was taken to indicate acceptable performance of the apparatus. A mechanical or electronic stopwatch accurate to within 0.1 second was used in determining electrophoretic velocities.

3.3.4 Accuracy of Electrophoretic Measurements

The electrophoretic mobility values of particles or cells are subject to a number of variables including: Brownian movement, errors in focusing at the stationary level, calibration errors, timing errors, temperature, uncontrolled convection arising from joule heating, asymmetry of electroosmotic flow due to heterogeneity in the surface properties of the glass of the sample tube and in the case of cells, biological variation. The principal source of error is inaccuracy in focusing at the stationary level. This will be discussed in more detail in Section 3.6. The sample standard deviation of 10-20 individual cells is ~0.05 μm sec^{-1} V^{-1} cm when measured in 0.150 M aqueous sodium chloride solution and ~0.10 μm sec^{-1} V^{-1} cm when measured at an ionic strength of 0.0150 g-ions $\cdot$ L^{-1}. The precision of the method should be on the order of 1%.

3.4 Performance of Electrophoretic Mobility Measurements

Electrophoretic mobility measurements were made by timing only those cells which appeared to be in focus with the microscope set

at the stationary level position. Typically the cells were timed over a number of graticule divisions such that the total elapsed transit time was on the order of 6-10 seconds. This was to minimize errors arising from the operator's reaction time being a considerable percentage of the total elapsed time. In some cases these restrictions could not be adhered to due to extremely low electrophoretic mobilities. The transit times were recorded to the nearest 0.1 second. The direction of the electric field was reversed after every measurement. Usually a data set consisted of ten readings after which the chamber was refilled with a fresh sample. In practice the mean mobility and standard deviation for the data set was calculated by combining Eq. 3-1 and Eq. 3-2 to obtain a factor, F, which was divided by the time required for a particle to traverse one graticule division in the ocular of the microscope, i.e.,

$$\frac{[\mu m][\text{graticule division}]^{-1}}{[X]} = \frac{[\mu m][\text{graticule division}]^{-1}[cm]}{[V]} = F \qquad 3\text{-}5$$

$$\frac{[F]}{[\text{sec}][\text{graticule division}]^{-1}} = u = \mu m \ \text{sec}^{-1} \ V^{-1} \ cm \qquad 3\text{-}6$$

3.5 Elimination of Electroosmotic Flow in Analytical Particle Electrophoresis by Low Zeta Potential Gel Surface Coatings

Interest in surface coatings which will markedly reduce or eliminate the zeta potential at an electrophoresis chamber wall stems

from the practical issue of eliminating electroosmotic flow during electrophoresis.

In any closed glass electrophoresis chamber containing an electrolyte the negative charge of the glass wall results in an increase in concentration of cations close to the glass surface. Application of an external electric field results in movement of these cations along with some of the solvent molecules (H_2O) near the wall toward the cathode (electroosmosis) and a concurrent forced return flow through the center of the tube. In order to make reliable measurements of the electrophoretic mobility of a particle such as a cell it is imperative that the microscope be focused at the cylindrical annuloid in the chamber where no net flow of fluid occurs during electrophoresis (stationary level). Since this annuloid is infinitely thin, electroosmotic flow will always contribute to experimental error. Figure 3-8 illustrates the general features of laminar electroosmotic fluid flow for a closed cylindrical tube including the parabolic fluid flow profile, regions of electroosmotic flow, return fluid flow and the location of the stationary level.

3.5.1 Electroosmotic Fluid Flow and Associated Errors

As previously described in Section 1.1, application of an electric field to a suspension of charged particles or cells contained in a closed cylindrical chamber will result in electrophoresis of the particles.

Figure 3-8. Electroosmotic fluid flow in a closed cylindrical tube. (a) A longitudinal crossectional view of the fluid velocity profile and fluid streamlines for a tube with radius, R (fluid velocity is plotted in terms of V_s, the fluid flow at the tube wall). (b) A transverse crossection where maximum electroosmotic fluid flow is shown by dense shading, and the unshaded area shows the region of the stationary level where fluid flow tends to zero. (c) Fluid flow parabola which is a plot of fluid velocity vs. distance from the tube wall.

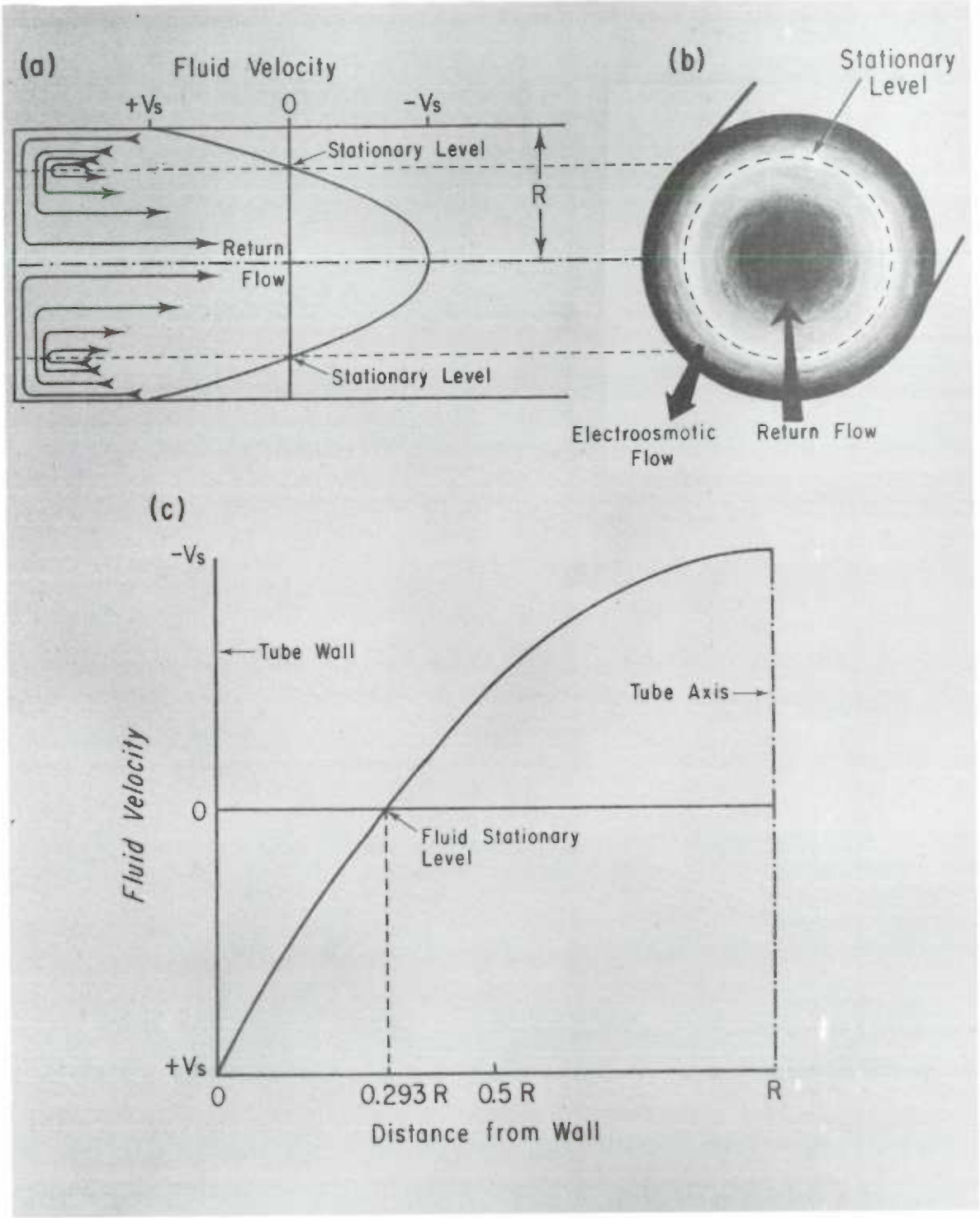
(a)
Fluid Velocity
+Vs
0
-Vs
Stationary Level
R
Return
Flow
Stationary Level
(b)
Stationary
Level
Electroosmotic
Flow
Return Flow
(c)
-Vs
Tube Wall
Tube Axis
Fluid Velocity
0
Fluid Stationary
Level
+Vs
0
0.293 R
0.5 R
R
Distance from Wall

The observed velocity, v_o, of a particle at an arbitrary position in the tube will be the sum of its electrophoretic velocity, v_e, and the velocity of the suspending medium, v_w:

$$v_o = v_e + v_w \qquad 3\text{-}7$$

Furthermore Bangham et al. (51) based on a treatment by Lamb (57) have shown that v_o of a particle is related to its distance, r, from the axis of the tube by the relationship:

$$v_o = v_e + v_s\left[\frac{2r^2}{a^2} - 1\right] \qquad 3\text{-}8$$

where v_s is the fluid velocity at the tube wall and a is the radius of the tube. By setting

$$\frac{2r^2}{a^2} = 1 \qquad 3\text{-}9$$

in Eq. 3-8 v_o will equal v_e. Solving Eq. 3-9 for r results in $r = 0.707a$. On substituting for r in Eq. 3-8 the solution shows that at a distance of $0.707a$ from the tube axis $v_o = v_e$ and $v_w = 0$. In theory, electrophoretic mobility measurements which are made at the stationary level are not subject to error as a result of fluid flow. However, as briefly discussed already, errors do result in practice as a result of:

1) the finite size of the particles which cannot be contained in an infinitely thin stationary level;
2) focusing errors at the stationary level, i.e., lack of appropriate optical corrections to rectify the effects of refraction and aberration, depth of focus, and shape and size of the focal field relative to the radius of curvature of the stationary level.

The magnitude of errors in v_e as a result of fluid flow may be estimated by differentiating Eq. 3-8, i.e.,

$$dv_o = \frac{4v_s r}{a^2} dr \qquad 3-10$$

Dividing both sides of Eq. 3-10 by the electric field strength, X, results in a relationship between the experimentally observed electrophoretic mobility, u_o (see Eq. 1-12), at small radial increments from the stationary level in terms of the electroosmotic mobility, u_s:

$$\Delta u_o = \frac{4u_s r}{a^2} \Delta r \qquad 3-11$$

If the fractional error in the true electrophoretic mobility, u, due to fluid flow is defined as δ, then:

$$\delta = \frac{\Delta u_o}{u} = \frac{4u_s r}{a^2 u} \Delta r \qquad 3\text{-}12$$

The results of estimates of δ are shown in Fig. 3-9 which is interpreted as follows. If the electrophoretic mobility, u, is measured for particles at 20 μm from the stationary level in a 2 mm bore diameter capillary, there will be a fractional error, δ, in the mobility value obtained. Its magnitude will depend on the relative magnitudes of both the electrophoretic and electroosmotic mobility, u and u_s respectively. For example, a particle with $u = 2.0$ and $u_s = 2.1$, the observed electrophoretic mobility, u_o, at 20 μm from the stationary level would deviate from the true mobility, u, by 6%, i.e., $\delta = 0.06$.

In a clean glass chamber u_s at pH 7 may be in the range of 5-6 μm sec^{-1} V^{-1} cm and 2-3 μm sec^{-1} V^{-1} cm at ionic strengths of 0.0150 and 0.150 g-ions $\cdot$ L^{-1}, respectively. It can be seen that the fractional errors at such electroosmotic mobilities may be appreciable. These errors may, however, be considerably reduced by decreasing the surface charge of the chamber walls. It may be seen also from Fig. 3-9 that it is not necessary to reduce u_s to zero in order to make the errors negligible unless the electrophoretic mobilities to be measured are near zero. In practice, any reduction in u_s facilitates data collection, reduces operator errors in judging whether

Figure 3-9. Estimated electroosmotic mobilities, u_s, which produce fractional errors, δ, in the absolute values of electrophoretic mobility, u_e at 20 μm from the stationary level in a 2.0-mm bore capillary tube.

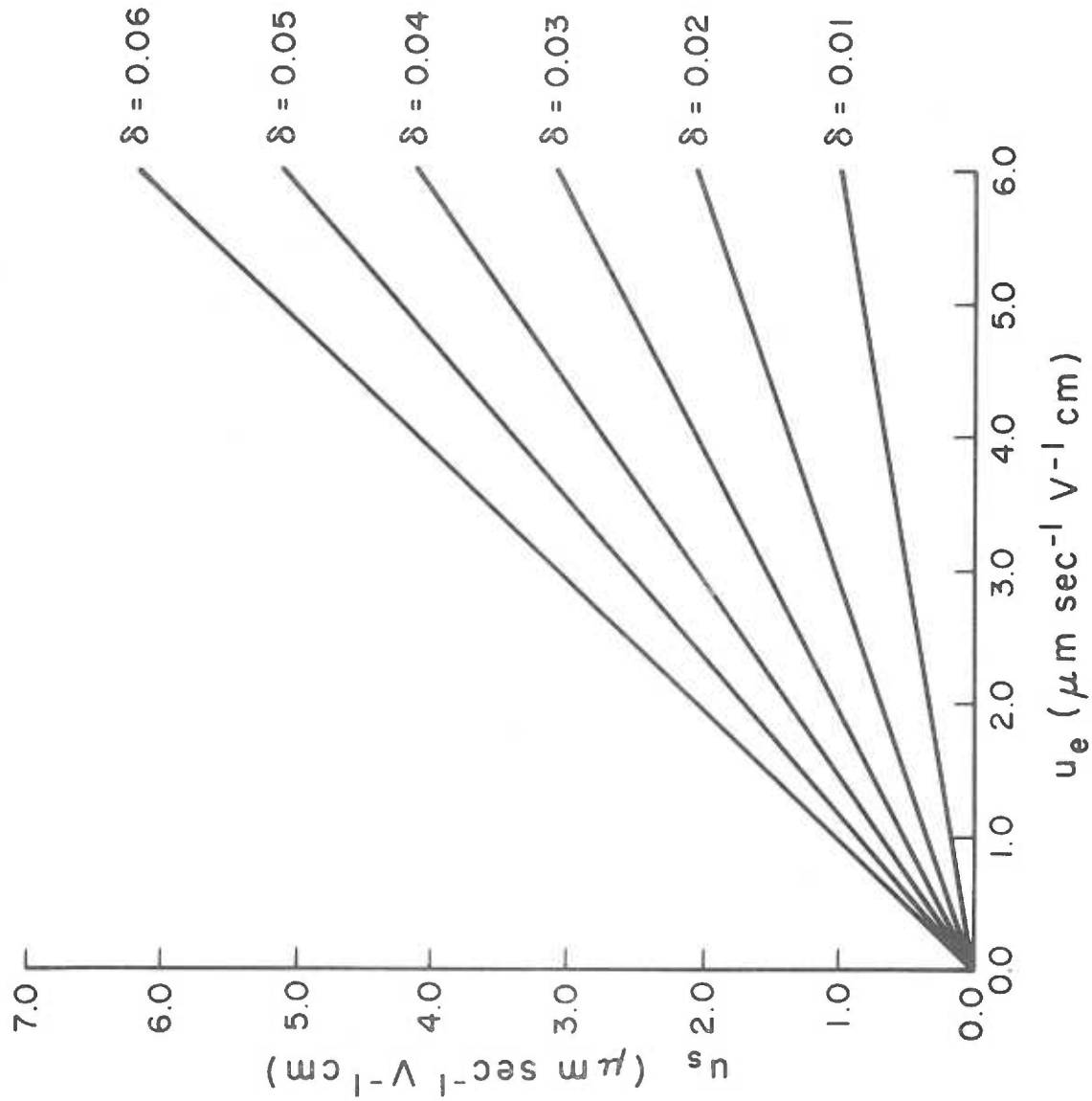
δ = 0.06
δ = 0.05
δ = 0.04
δ = 0.03
δ = 0.02
δ = 0.01
0.0
1.0
2.0
3.0
4.0
5.0
6.0
7.0
u_s (μm sec^{-1} V^{-1} cm)
u_e (μm sec^{-1} V^{-1} cm)

particles are in focus, minimizes errors in setting the stationary level and minimizes the influence of changes in the location of the stationary level due to asymmetric contamination of the wall surface by adsorbed substances or to heterogeneous distribution of charge on an uncontaminated wall. In preparative particle electrophoresis or in automated analytical techniques where measurements are made at locations other than the stationary level (58) it is necessary to reduce u_s to almost zero. Reduction of electroosmotic flow to low levels may also facilitate free boundary electrophoresis of the Tiselius type (59) where boundary spreading due to electroosmotic flow may introduce uncertainty and errors on analysis of the data.

3.5.2 Origin of and Strategy to Eliminate Chamber Wall Charge

The negative charge of borosilicate glass surfaces is reported to originate from the ionization of surface groups which are an integral part of the glass. Two types of sites are present, the first with a pk_a of ~7 and the second with a pk_a of 5.1 (60). The weaker acidic site is due to the silanol group, $\rangle$Si-OH, while the stronger acidic site is most likely the boranol group, $\rangle$B-OH.

The wall charge may be reduced or eliminated by:

1) use of adherent or adhesive films (61).

2) Covalent bonding of materials to the surface (61).

3) physical adsorption of substances (62).

The geometry of the electrophoresis chamber precludes the use of adhesive films to eliminate the surface charge which leaves two alternative general approaches, namely:

1) covalent bonding to surface groups to eliminate the negative groups by chemical modification (total charge zero) or to introduce positive groups such that the net charge is zero, or a combination of these types of surface modification.
2) to use substances, usually macromolecules, which physically adsorb to the glass surface, thereby shifting the electrophoretic plane of shear out from the original glass surface to the new macromolecular surface. By this means the charge on the original surface will have a negligible influence on ion distribution at the new plane of slip during electrophoresis (63).

The vast number of surface reactions encompassed by the above two approaches can be severely restricted by an examination of the criteria required for a satisfactory surface coating or modification. The following properties of the surface coating should be considered in judging its general suitability and application limitations:

1) Physical properties:
   a) transparent to light, at least over the same range of wavelengths as the original glass.

b) small coating thickness relative to the radius of the electrophoresis tube.

c) capable of being applied uniformly.

d) an electrical conductance not significantly greater than that of the particle suspending medium.

e) low fixed or acquired electrostatic charge in buffers.

f) poor surface for gas bubble nucleation and formation.

g) nonadhesive to particles or biological cells to be examined in the coated tube.

2) Chemical and biological properties:

a) hydrophilic to minimize adsorption of components from samples.

b) compatible with system to be examined, e.g., non-toxic towards living cells.

c) not subject to attack or degradation by any biological specimens under test.

d) does not desorb or change the electrokinetic properties of the particles under examination.

3) Electrokinetically stable (64) for duration of studies to:

a) buffers up to physiological ionic strenghts (~0.150 g-ions $\cdot L^{-1}$).

b) pH range, 2 to 11.

c) temperature range ~0-50°C.

d) shear rates encountered when filling or cleaning the electrophoresis tube.

Taking the above criteria into consideration possible coating materials or surface modifiers include:

1) Polysaccharides [agarose; dextran; ficoll; glycogen; methylcellulose; and starch].
2) Methacrylates and acrylamides [2-hydroxyethylmethacrylate (HEMA) (65); 2,3-dihydroxyporpylmethacrylate (DHPMA) (65); and polyacrylamide].
3) Polymeric alcohols [polyethylene glycol (PEG); and polyvinyl alcohol (PVA)].
4) Silane derivatives as either sub-layer agents or primary coatings [γ-glycidoxypropyltrimethoxysilane (Dow Corning, Z6040) (66); γ-aminopropyltriethoxysilane (Union Carbide, A-1100) (66); γ-methacryloxypropyltrimethoxysilane (Dow Corning, Z6030) (66); and vinyltrimethoxysilane (Dow Corning) (66)].

To date, polysaccharides have offered many promising features as coatings. They are hydrophilic, have small numbers of charged groups and are generally biocompatible. As a class they may be crosslinked and their residual charge groups eliminated or chemically reduced by procedures such as those used by Porath et al. (67) on agarose. In addition, polysaccharides may be derivatized or oxidized

and mixtures used to produce coatings with either a net negative, net positive or net zero charge.

Electrophoretic testing of the efficacy, stability, and completeness of various surface treatments, modifications, or coatings may be carried out in various ways including,

1) After coating the inside of the electrophoresis chamber, the electroosmotic flow is calculated from experimental measurements of the electrophoretic velocities of standard particles at various levels within the chamber.
2) The electrophoretic mobilities of coated or modified particles made from the same material as the electrophoresis chamber are measured by standard analytical electrophoresis.
3) The zeta potential of coated tubes may also be determined from electroosmotic flow or streaming potential measurements (68).

The first approach is the more desirable test of any coating procedure. However, for screening purposes the second approach significantly reduces the time needed for initial survey and testing of coatings and/or procedures.

3.6.3 Materials and Methods

3.5.3.1 Standard Particles. Corning #7740 borisilicate particles were used as a model system for screening the effectiveness of

polysaccharide derivatives as low zeta potential surface coatings for glass. The particles were prepared by W. J. Patterson (Marshall Space Flight Center, Huntsville, Alabama) by grinding Corning #7740 glass tubing for 11 hours in distilled water in an aluminum oxide ball mill. The mill was initially cleaned by several short term grindings and rinsings with distilled water.

Clean particles of suitable size for electrophoretic measurements were obtained by repeated sedimentation of particles in aqua regia, each time removing those particles which had sedimented. Initially, the particles were suspended in 600 ml of 3% v/v aqua regia, a concentrate of which was prepared by mixing 18 ml of concentrated nitric acid and 82 ml of concentrated hydrochloric acid. The particles were allowed to sediment for 60 minutes. Particles remaining in suspension were centrifuged and the foregoing process was repeated. The supernatant suspension of particles was then centrifuged at ~16000 g and the particles were resuspended in ~3 volumes of 3% v/v aqua regia and left to stand overnight. The particles were centrifuged again and the aqua regia was aspirated and the particles were resuspended in 6 M HCl at ~60 °C and sonicated for ~60 minutes in a sonicator bath. Possible organic contaminants were removed by sequential resuspension and centrifugation of the glass particles in toluene-ethanol and isopropanol. A 5:1 v/v mixture of toluene-ethanol was utilized. The ethanol was included to remove any remaining water

associated with the glass particles. The particles were then washed six times with 0.0150 M aqueous NaCl at 60°-70°C.

The electrophoretic mobility of the particles was monitored throughout the cleaning procedure. The size of the particles was estimated by light microscopy.

3.5.3.2 Coating Materials. Methylcellulose (Cow Methocel MC, 8000 cps Premium, Lot MM-110786), agarose (Bio-Rad Laboratories, gel electrophoresis grade, Lot 63683), and dextran (Pharmacia, Lot 4386, MW 2×10^6), as well as their diethylaminoethyl (DEAE) and triethylaminoethyl (TEAE) derivatives were screened as low zeta potential gel surface coatings.

DEAE-methylcellulose was prepared from methylcellulose by modification of the method of Peterson and Sober (69). Methylcellulose (60 g) was dissolved in 170 ml of 5.9 M NaOH and made 0.05 M with respect to sodium borohydride to prevent air oxidation of the polymer.

This mixture was reacted with diethylaminoethylchloride hydrochloride (40 g) (recrystallized from methanol) for 40 minutes at 55°-63°C. Two further batches of methylcellulose were prepared with 7 g and 35 g respectively, of diethylaminoethylchloride hydrochloride. These preparations will be referred to as "lower" and "higher" degree amino substituted methylcellulose derivatives. After 40 minutes, the reaction mixtures were cooled in an ice bath and 250 ml of 2 M NaCl

were added. The batches were then dialysed exhaustively against distilled water to remove excess sodium hydroxide. After the penultimate change of water the pH rose from ~pH 6 to ~pH 7 after 16 hours of dialysis. Following dialysis, the batches, which were in clear gel form, were warmed in a water bath. The derivatives were then precipitated by addition of 6 liters of cold reagent grade acetone and filtered through coarse sintered glass filters. Unexpectedly, the "higher" substituted derivative clogged the filter. Therefore, the acetone was removed under reduced pressure. The resulting gel was broken up in a Waring blender and lyophilized overnight, after which it was again ground to a fine powder. The yields were 45.5 and 43.7 g of the "lower" and "higher" substituted derivatives, respectively.

DEAE-agarose was prepared according to the method of Ragetli and Weintraub (70). Agarose (24 g) in 68 ml of 5.9 M NaOH was stirred and cooled on ice and was reacted with diethylaminoethyl-chloride hydrochloride dissolved in 110 ml dioxane-water (4.3:1 v/v) by slow addition over a period of 20 minutes. On completion of the addition of reactant, the mixture was heated to 55°C for 0.5 hours and then cooled to room temperature after which 180 ml of 2 M NaCl was added. The reaction mixture was further diluted with water to ~8 liters total volume and the gel was allowed to settle overnight. The supernatant fluid containing fine gel particles was discarded and

the remaining resin was filtered through a coarse sintered glass filter. The colorless cake was lyophilized overnight giving a total yield of 6.1 g.

DEAE-dextran (MW ~2 x 10^6, Lot 5469) was obtained as such from Pharmacia.

The DEAE derivatives of methylcellulose, agarose and dextran were converted to their TEAE analogs with redistilled ethylbromide (Eastman Kodak) by the procedure that Schell and Ghetie (71) used on agarose. DEAE-dextran, DEAE-methylcellulose and DEAE-agarose (10 g, 10 g and 3 g respectively) were refluxed for 5 hours with 70 ml absolute ethanol made 0.092 M with respect to ethyl bromide. The derivatives were washed with ethanol, filtered through a medium or coarse sintered glass filter and treated with 0.25 M NaOH in 95% v/v ethanol mixed in a ratio of 1:4. TEAE-methylcellulose and the TEAE-agarose were precipitated with reagent grade acetone and filtered through a coarse fritted glass filter. TEAE-dextran which remained in solution was dialysed against water to remove excess sodium hydroxide. The solution was then evaporated to near dryness and lyophilized. Yields of TEAE-dextran, TEAE-agarose and TEAE-methylcellulose were 3.0, 1.5 and 2.5 g respectively.

In order to determine, quantitatively, the degree of substitution of the methylcellulose with DEAE functional groups, the nitrogen contents of both the "lower" and "higher" substituted derivatives were

determined for the lyophilized materials by the microkjeldahl method (72). The DEAE-methylcellulose (10 mg) was weighed and wrapped in ashless filter paper (Whatman, No. 542) and introduced into a microkjeldahl flask. A Selenium bead (0.1 g) was added as a catalyst in addition to 2 ml of concentrated sulfuric acid. The solution was heated until clear. One or two drops of 30% H_2O_2 was added after the flask had cooled. The liberated ammonia was distilled into a 0.647 M boric acid solution containing 1.5% v/v methyl red (0.1% w/v in ethanol) and bromcresol green (0.1% w/v in ethanol) which had been combined in the ratio of 1:5, respectively. This boric acid mixed-indicator solution, containing the ammonia, was titrated with 0.0100 M HCl until a pink endpoint was reached. Blanks containing filter paper only were run as controls. Samples of ammonium sulfate, dried in an oven for 2 hours at 150°C served as standards.

3.5.3.3 Effectiveness of Derivatives as Low Zeta Potential Coatings. The effectiveness of each of the primary gels and their DEAE and TEAE derivatives were evaluated as low zeta potential gel surface coatings by suspending glass particles in a saline solution (0.0150 M aqueous NaCl buffered with 0.0150 M aqueous $NaHCO_3$ to pH 7.2 ± 0.1) containing a 0.1% w/v concentration of a given derivative and measuring the electrophoretic mobility of the particles at 25.0°C.

Agarose was not appreciably soluble in aqueous media at room temperature. Therefore, in order to coat glass particles with

agarose, the mixture of glass particles and agarose was heated to 86°C. At this temperature the agarose was water soluble. Subsequently the solution was cooled to 25°C and the borosilicate particles were electrophoretically characterized.

The electrophoretic mobilities of particles suspended in media containing coating materials were corrected for the bulk medium viscosity effects of the polymer derivatives according to the relationship:[1/]

$$\frac{u_1 \eta_1}{\eta_2} = u_2 \qquad 3\text{-}13$$

where u_1 and η_1 are the mobility of the particles and viscosity of the suspending medium containing the polymers, respectively, and η_2 is the viscosity of the plain suspending medium and u_2 is the viscosity corrected electrophoretic mobility. Alternatively, mobilities were viscosity corrected using an equation analogous to Eq. 3-13,

---

[1/] Equation 3-13 stems from the Helmholtz-Smoluchowski relationship (Eq. 1-12). Particles which have identical surface properties and are suspended in two media of differing viscosities whose bulk dielectric constants are not significantly different would be expected to have different electrophoretic mobilities, i.e., $u_1 = \varepsilon\zeta/u\pi\eta_1$ and $u_2 = \varepsilon\zeta/u\pi\eta_2$. Therefore $u_1\eta_1 = u_2\eta_2 = \varepsilon\zeta/4\pi$ and Eq. 3-13 follows by simple rearrangement. Polysaccharide polymers of the types and concentrations used in the coating experiments would not be expected to have an effect on the bulk dielectric constants of the solutions (63).

substituting the kinematic viscosities, for the dynamic viscosities. This substitution was only performed when the densities of the suspending media were not significantly different. This would be the case for the very low polymer concentrations utilized in the coating experiments.

Bulk viscosities of the polymer solutions were measured at 25.0 ± 0.1°C with an Ostwald viscometer having a flow time for water of ~80 seconds, essentially according to the methods outlined in Section 2.2.

3.5.3.4 Tenacity of Coatings. As a test of tenacity of the coatings, the particles were washed one to three times in dilute saline media (0.0150 M aqueous NaCl). The effect of the washes were assessed by measuring the electrophoretic mobility of the particles in 0.0150 M aqueous NaCl-$NaHCO_3$, pH 7.2 and noting any changes. In attempts to improve the stability of the DEAE methylcellulose coatings, epichlorohydrin was tested as a potential crosslinking reagent.

The hydroxyl groups present on DEAE-methylcellulose were used as reactive groups to link individual molecules together into a gel-like network. It has been found that for gel formation, epoxide addition with the resultant formation of ethers is most suitable (73). Ethers are relatively unreactive and thus give stable derivatives, and the reactions may be carried out in aqueous media and under mild conditions.

An epoxide reacts with an alcohol in the presence of acid or base according to the following reaction (74):

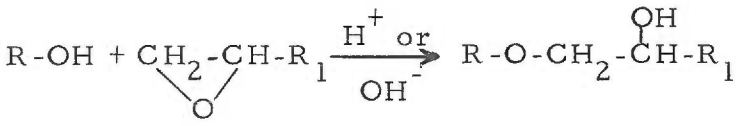

In order to crosslink two alcohols a bifunctional epoxide is required. Though epichlorohydrin is not a diepoxide it nevertheless reacts as if it were one (73). The reactions of epichlorohydrin with two alcohols in the presence of base are as follows:

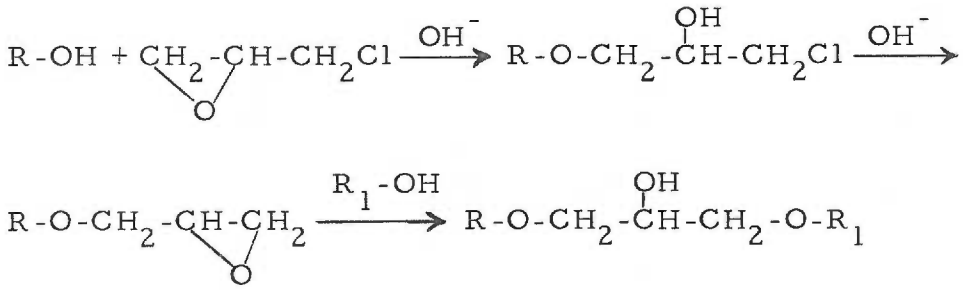

In the case of a polyfunctional alcohol such as DEAE-methylcellulose a three-dimensional gel network will be formed. In the actual procedure here a modification of Flodin's procedure was used (73). A 0.2% (w/v) solution of the "higher" modified DEAE-methylcellulose in water was prepared to which glass particles were added to make a milky white suspension. The particles were subsequently centrifuged, the supernatant decanted and the particles were suspended in 1.40 M

NaOH to which sodium borohydride (0.5 g per 100 g DEAE-methylcellulose) had been added to prevent oxidation of the polymer. This suspension was mixed with redistilled epichlorohydrin (Eastman Kodak) (10% v/v) and incubated at 70°C in a water bath for 4 hours. The particles were subsequently centrifuged, washed three times in 0.0150 M aqueous NaCl-$NaHCO_3$, pH 7.2 ± 0.1 and characterized electrophoretically. The effect of further washes on the electrophoretic mobility of the particles was monitored.

Finally, the internal surface of an all glass cylindrical electrophoresis chamber was coated with DEAE-methylcellulose and then treated with epichlorohydrin. The chamber was filled with a 0.2% w/v solution of DEAE-methylcellulose in 1.4 M sodium hydroxide containing 0.5 g sodium borohydride per 100 g DEAE-methylcellulose and 1.0% (v/v) epichlorohydrin. The chamber was incubated in a 70°C water bath overnight. The chamber was then thoroughly rinsed out with water and 1 M KCl and set up in the usual manner.

The effect of the coating on the electroosmotic flow was assessed by measuring the electrophoretic mobility of native glass particles in media of varying ionic strengths at a series of distances from the inner chamber wall.

3.5.4 Results and Discussion

Glass particles for electrophoresis and surface modification obtained by the repeated sedimentation procedure, had a sedimentation rate of < 0.3 mm $\cdot$ min^{-1}. These particles were ≤ 5 μm in diameter.

The cleaning procedure increased the electrophoretic mobility of the glass particles from -2.49 ± 0.33 μm sec^{-1} V^{-1} cm in 0.0150 M aqueous NaCl-$NaHCO_3$ pH 7.2 ± 0.1 for crude uncleaned particles, to -5.58 ± 0.25 μm sec^{-1} V^{-1} cm for particles taken all the way through the cleaning procedure. Attempts at further cleaning treatments failed to increase the electrophoretic mobility further.

The increase in zeta potential upon cleaning is most likely due to the removal of adsorbed foreign substances which either shield or neutralize the surface charge groups of the glass. The latter mechanism, i.e., neutralization of surface charge groups, may particularly be operative in the case under consideration. Since the glass was ground in an aluminum oxide ball mill it is likely that aluminum ions would be present at the glass surface which would result in a lowered zeta potential (75, 76). Thus in this case electrophoretic analyses also served as a monitoring aid in assessing the effectiveness of various cleaning procedures.

The electrophoretic mobilities of borosilicate glass particles at 25.0°C in 0.0150 M aqueous NaCl-$NaHCO_3$ pH 7.2 ± 0.2, coated

electroosmotic flow in his free zone electrophoretic equipment (77). The use of the TEAE derivatives in general was thought unwise after questions and uncertainties arose as to the actual degree of quaternization achieved with ethyl bromide derivatization of the DEAE derivatives (78). Furthermore, the TEAE derivatives were no more effective in modifying the charge properties of the model particles than were the DEAE derivatives. The charge reversal of the borosilicate particles by the dextran derivatives were found to be too drastic, and thus, potentially, but not immediately, useful in producing a nearly uncharged electrophoresis chamber surface. These considerations prompted further studies to be limited to the DEAE derivatives of methylcellulose. The rationale was to produce a substance which had enough cationic groups to enhance binding to a glass surface but did not possess an excess of positive groups which would only produce a positively charged surface and thus defeat the purpose of the coating. In addition, it was sought to further stabilize the adsorbed layer by chemical crosslinking of individual molecules.

Thus, two preparations of DEAE-methylcellulose were prepared and evaluated, each containing lower and different levels of amino group substitution than the particular derivative with which the data presented in Table 3-2 was obtained. The nitrogen content of the lower and higher amino substituted methylcellulose derivatives were found to be 0.37 and 1.28 mg per gram, respectively, by microkjeldahl

Figure 3-10. The electrophoretic mobility of bare borosilicate glass particles (——) and crosslinked DEAE-methylcellulose coated particles (– – –) as a function of pH of the suspending medium. Migration toward the cathode is positive. The ionic strength of the suspending medium is 0.015 g-ions $\cdot L^{-1}$.

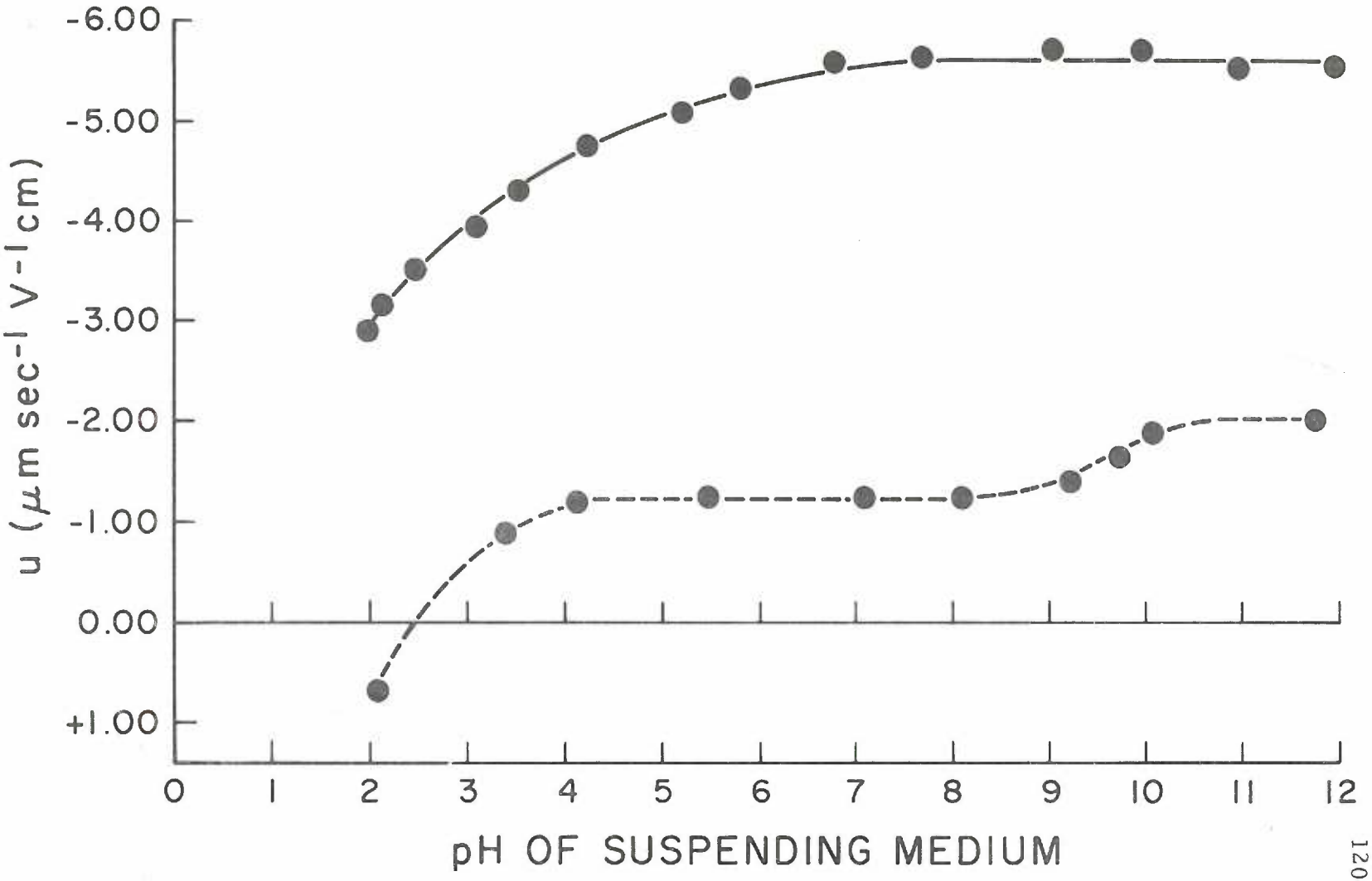
-6.00
-5.00
-4.00
-3.00
-2.00
-1.00
0.00
+1.00
u (μm sec⁻¹ V⁻¹ cm)
0
1
2
3
4
5
6
7
8
9
10
11
12
pH OF SUSPENDING MEDIUM

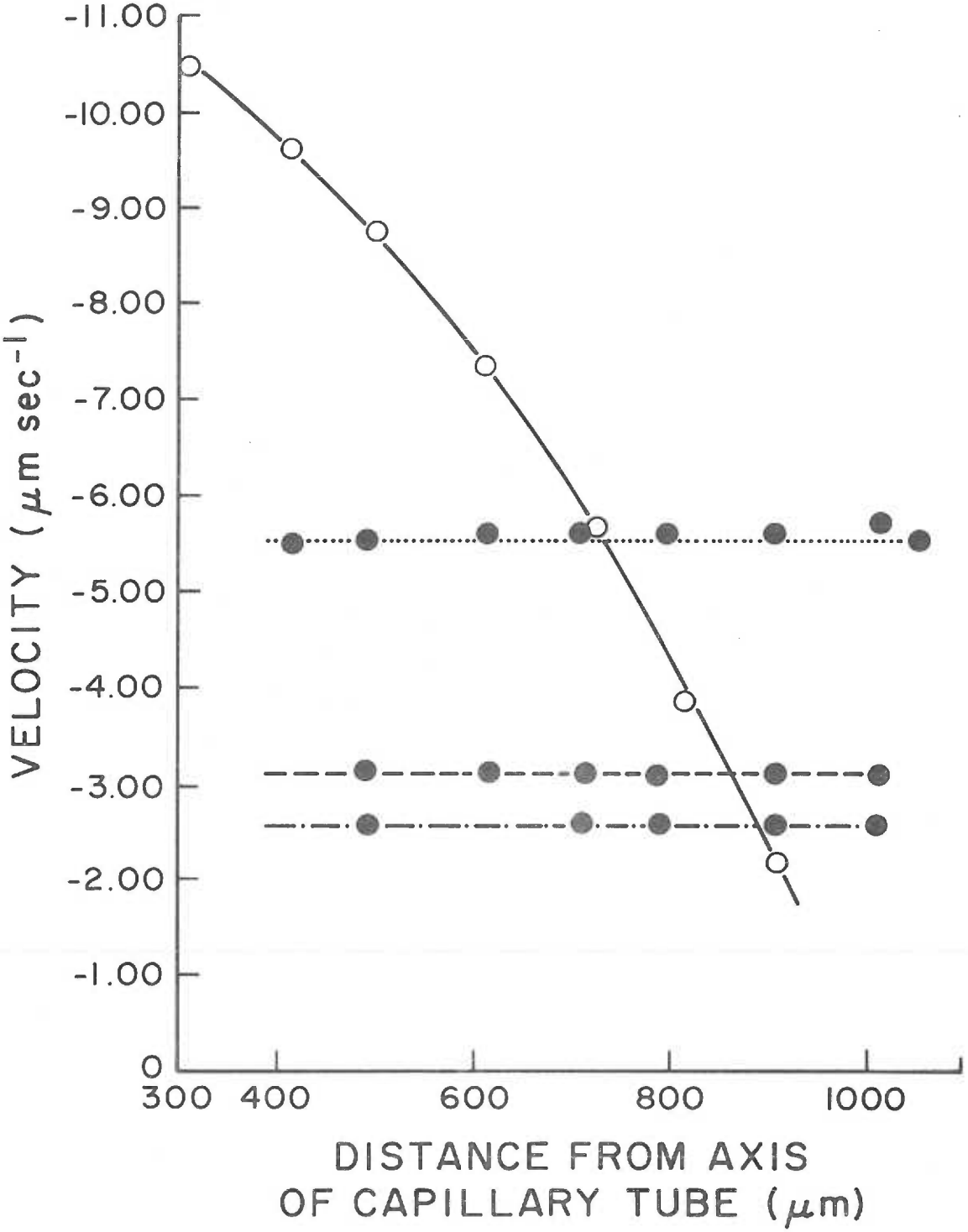
-11.00
-10.00
-9.00
-8.00
-7.00
-6.00
-5.00
-4.00
-3.00
-2.00
-1.00
0
VELOCITY (μm sec⁻¹)
300
400
600
800
1000
DISTANCE FROM AXIS
OF CAPILLARY TUBE (μm)

for up to 15 hours. Calculation of the electroosmotic flow at the wall of the chamber by means of Eq. 3-8 yielded values which ranged between -0.09 and +0.12 $\mu m\ sec^{-1}\ V^{-1}\ cm$ over the range of ionic strengths investigated. The solid line in Fig. 3-11 represents the electrophoretic velocity of the bare glass particles in an uncoated glass chamber and shows the extreme dependence of particle velocity on position in the chamber for an uncoated chamber.

Use of the Eq. 3-2 for the results obtained for the bare glass chamber yield an average value for the electroosmotic flow of $+5.9\ \mu m\ sec^{-1}\ V^{-1}\ cm$ corresponding to an electrophoretic mobility of -5.9 which agrees well with the observed value of $-5.6\ \mu m\ sec^{-1}\ V^{-1}\ cm$ for bare borosilicate glass particles. After 24 hours the chamber coated with crosslinked DEAE-methylcellulose showed an increase in negative surface charge which resulted in an electroosmotic flow of $-1.21\ \mu m\ sec^{-1}\ V^{-1}\ cm$ for the aqueous 0.0150 M NaCl medium as a result of slow desorption of the coating.

This at present is a complicating factor since slow desorption, aside from leading to gradual reappearance of electroosmotic flow, may also lead to the possibility of contamination of any indicator particles during the course of an electrophoretic experiment. Nevertheless, these studies have significantly advanced the development of single stage coatings which are easy to apply, do not require a sublayer nor elaborate pre-treatment procedures and which will remain

electrokinetically stable for considerable periods of time. These types of coatings have since found application, especially in preparative electrophoresis of both test particles and living cells particularly in the zero gravity environment of space, i.e., in the National Aeronautics and Space Administration (NASA) sponsored Appollo-Soyuz Text Project of 1975 (83).

CHAPTER 4

THE ELECTROKINETIC PROPERTIES OF THE NATIVE AND FORMALDEHYDE FIXED HUMAN ERYTHROCYTE

The human red cell has been much more extensively studied by electrophoresis than other cell types. Early work on the electrophoresis of human erythrocytes and mammalian erythrocytes in general has been reviewed by Abramson (46). Noteworthy is the fact that the electrophoretic mobility of red cells is constant within a species. Electrophoretic mobilities of red cells are also quite stable. There are no significant changes in mobility of cells suspended in physiological ionic strength media over a period of at least 24 hours. Furthermore, at physiological pH the mobility of red cells is not affected by the presence of hemoglobin in the suspending media which confirmed earlier observations that red cells adsorbed little if any hemoglobin at pH 7.4 (84, 85). Neither the age nor the race of the donor is important in determining the electrophoretic mobility of human red cells in a given buffer. It was noted as early as 1914 (86) that the electrophoretic mobility of mammalian red cells was dependent on the bulk pH of the suspension and that at certain pH values the cells had an "isoelectric point". Numerous investigators have since found that the "isoelectric points" vary, depending on the length of time the cells are suspended at a give pH value. In fact, if measurements are made rapidly after addition of acid to a suspension, i.e., before significant

amounts of hemolysis occurs, no "isoelectric point" can be observed down to a pH value of 3.6 (87). Thus, when a complicated system, such as a cell is under investigation, it makes little sense to refer to true isoelectric points as one would in the case of proteins. Furthermore, on the basis of studies performed by Heard and Seaman (64) it may be concluded that the pH values at which the isoelectric points of human red cells would lie, would be outside the region of electrokinetic stability of the cells, i.e., in a pH region where irreversible, time-dependent changes in the surface properties of the cells occur.

In the case of biological surfaces the electrical surface charge is usually acquired by ionization of functional groups of molecules which are an integral part of the membrane surface. Typically these groups may include:

$$R\text{-}COOH \rightleftharpoons R\text{-}COO^- + H^+$$

$$R\text{-}O\text{-}\underset{\underset{OH}{|}}{\overset{\overset{O}{\|}}{P}}\text{-}OH \rightleftharpoons R\text{-}O\text{-}\underset{\underset{OH}{|}}{\overset{\overset{O}{\|}}{P}}\text{-}O^- + H^+$$

$$R\text{-}NH_2 + H^+ \rightleftharpoons R\text{-}NH_3^+$$

$$R\text{-}O\text{-}\underset{\underset{O}{\|}}{\overset{\overset{O}{\|}}{S}}\text{-}OH \rightleftharpoons R\text{-}O\text{-}\underset{\underset{O}{\|}}{\overset{\overset{O}{\|}}{S}}\text{-}O^- + H^+$$

Surface charge may originate from ad- or desorption of ions from the suspending medium or chemical reaction of surface groups

with a component of the suspending medium. These latter two mechanisms play only a minor role in governing the charge properties of biological surfaces.

Bungenberg de Jong (88) has shown that the charge group responsible for the electrokinetic behavior of a specific particle may be identified and distinguished from another type of charge group present on a different particle, by the respective electrophoretic responses of the particles to a variety of simple cations and/or anions. For example, a colloidal particle, which has as its predominant ionogenic species a specific functional group, will require characteristic concentrations of counterions to be present in the suspending medium to reverse its charge. The order and position of an isovalent series of counterions in terms of their effectiveness in reversing the charge on a given type particle, will often be characteristic, and aid in the identification of the functional group responsible for that charge. Some useful information has been gained on the ionogenic composition of biological surfaces, but the method has been criticized as being unreliable, especially with regard to surfaces which have more than one type of charge group present (89). Furthermore, many of the ions used in such investigations are toxic and often form complexes in aqueous media at neutral pH. In some cases the method has led to erroneous conclusions. For example, Winkler and Bungenberg de Jong (90) and later Bangham et al. (75) reported the major ionogenic group

at the shear plane of the human erythrocyte surface to be a phosphate group rather than a carboxyl group as later shown by Cook et al. (91). Both of the former studies were based on the circumstantial evidence of charge reversal spectra, rather than a direct correlation between erythrocyte charge and a specific charge bearing molecule(s) or reaction of putative charged functional groups with specific reagents. This type of evidence was obtained in the early 1960's. Seaman and Heard (92), partially on the basis of a report by Ponder (93), that trypsin treatment of human erythrocytes results in a decrease in electrophoretic mobility, suggested that this decrease was due in part to a diminution in the number of α-carboxyl groups effective at the plane of shear. This hypothesis was given impetus by evidence that treatment of red cells with the carboxyl group modifying reagent, N-bromosuccinimide (94), resulted in a decrease in electrophoretic mobility (92). Cook et al. (95) subsequently reported the isolation of a sialoglycopeptide from the supernatant fluid of a human erythrocyte suspension which was incubated with trypsin. This led them to suggest that sialic acid, the structure of which had recently been elucidated (96, 97), may be partially responsible for the surface charge of the erythrocyte. Contemporarily, Gottschalk (98, 99) recognized an enzymatic component, first observed by Burnet et al. (100) in filtrates of Vibrio cholerae and Clostridium perfringens culture media, which was capable of specifically cleaving the α-O-ketosidic linkages between

substituted terminal neuraminic acids and penultimate carbohydrate residues of glycoproteins.

It was this enzymatic component which was also responsible for destroying the receptor sites for influenza viruses at the surfaces of human erythrocytes, hence its original name, Receptor Destroying Enzyme or RDE (100). Ada and Stone (101) demonstrated that in addition to destroying red cell receptors for viruses, Vibrio cholerae culture filtrates containing RDE were also capable of reducing the net negative surface charge of human red cells by more than 80% as measured by analytical particle electrophoresis. Furthermore, Klenk and Uhlenbruck (102) found that RDE would cleave acylated sialic acids from red cell ghosts isolated from various mammalian species as well as human red cells in which case the particular sialic acid was identified as N-acetylneuraminic acid (103). This led Klenk (104) to suggest that perhaps the negative charge of the erythrocyte could be due to an acylated neuraminic acid. This in fact was confirmed first by Cook et al. (91) who isolated sialic acid in crystalline form after release from native human erythrocytes by treatment with a purified preparation of RDE which has since been termed neuraminidase (99) or sialidase (104). The enzyme is classified as acylneuraminyl hydrolase EC 3.2.1.18.

Although neuraminidases may be obtained from a number of sources including myxo and paramyxo viruses, bacteria, protozoa and

different organs of vertebrates. The most common source remains the Vibrio cholerae organism. This is mainly because of the broad specificity of this enzyme. It hydrolyzes α 2→3 (105), α 2→4 (106), α 2→6 (105), and α 2→8 (107) linkages of α-O-ketosidically linked sialic acids in contrast to Clostridium perfringens neuraminidase which is specific only for α 2→3 and α 2→6 linkages (108). This makes the Vibrio chloerae enzyme especially suitable in studies where quantitation of total sialic acid is an issue and where the types of linkages present may not be known. Furthermore, the enzyme is obtainable commercially in highly purified form at relatively low cost, in constrast to the Clostridium perfringens enzyme (109). It should be pointed out however, that the enzymes having a narrow range of specificity may be useful in the future when it might be desirable to quantitate or determine the function of sialic acids having specific linkages.

Cook et al. (91) measured the decrease in electrophoretic mobility associated with the release of sialic acid from human red cells after treatment with Vibrio cholerae neuraminidase and found that at least 80% of the charge could be attributed to the ionizable carboxyl group of the N or O, N acylated molecule, the structure of which is:

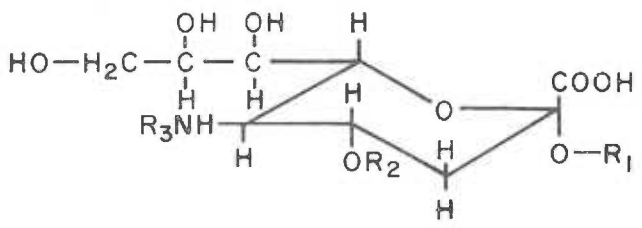

where R_1 represents a penultimate carbohydrate residue; R_2 is usually hydrogen or an acetyl moiety; and R_3 is an acetyl group in the case of human erythrocytes. Eylar et al. (110) confirmed the results of Cook et al. (91) and showed that all of the sialic acid is located in the peripheral zone of the erythrocyte and is also enzymatically releasable since similar amounts of sialic acid may be hydrolysed from red cell ghosts by mild treatment with sulfuric acid. This has also been confirmed more recently by Aminoff et al. (123). Furthermore, Steck et al. (110) have shown that very little sialic acid is present on the inside of the human red cell membrane. This is also consistent with the view that the carbohydrate portions of glycopropteins associated with the membrane are situated at the exoface of the erythrocyte membrane (111).

The experimental quantity of sialic acid released from the membrane may be compared to the theoretical quantity expected to be released, based on a given reduction in surface charge density for a given number of cells. The Gouy-Chapman equation (Eq. 1-39) may be utilized to calculate erythrocyte charge density changes assuming for example that the carboxyl group of each sialic acid moiety corresponds to one electron charge which is effective at the electrophoretic plane of shear. On the basis of such calculations yields of sialic acid were obtained which are about twice those expected from theoretical considerations. As has been pointed out in Section 1.3 the Gouy-Chapman

theory may yield underestimates of surface charge density of systems having ion-penetrable surfaces, such as the red cell. Even though only arbitrary values of α may be assigned to Eq. 1-40, it is unlikely that α would equal zero, in which case the charge density would just be twice that found from conventional theory.

Another possible explanation for the discrepancy is that the carboxyl groups of some of the sialic acid molecules are esterified and thus do not contribute to the surface charge density. No experimental evidence however, exists to support this conjecture. A further possibility is that conformational changes in the red cell membrane upon neuraminidase treatment may invalidate the one to one correspondence between the number of sialyl residues released into the suspending medium and the number of electron charges lost. However, the most likely explanation for the discrepancy is that the action of neuraminidase is not restricted to the electrophoretic surface of the cell and that sialic acid moieties, which are situated relatively deep within the peripheral zone and thus electrokinetically not very effective, are also released. For example, at physiological ionic strength the effective thickness of the double layer, $1/\kappa$, as calculated with the aid of Eq. 1-28 is only ~8 Å, such that groups greater than 20 Å away from the plane of shear would make little, if any, contribution to the zeta potential of the cell.

Seaman et al. (112) have investigated the distribution of charge groups over the electrophoretic surface of the human erythrocyte. Using the small divalent calcium ion as a molecular caliper an assessment was made of the relative proportions of single and double site interactions as depicted in the following schemes:

$$R\text{-}COO^- + Ca^{+2} \rightarrow R\text{-}COOCa^+ \qquad \text{(Single Site)}$$

$$\begin{matrix} R\text{-}COO^- \\ R\text{-}COO^- \end{matrix} + Ca^{+2} \rightarrow \begin{matrix} R\text{-}COO \\ R\text{-}COO \end{matrix} \!\!>\!\! Ca \qquad \text{(Double Site)}$$

Predominantly single site interactions would result in charge reversal whereas predominantly double site interactions would lead to charge neutralization. From extrapolation of the calcium ion adsorption isotherm it was found that charge reversal can be obtained (112). This implied adsorption by a significant number of sites of a single calcium ion per singly charged ionogenic group. This is consistent with the relatively low charge density of human erythrocytes and points to relatively wide separations between each ionic site.

Further studies have shown the red cell to behave essentially as a macropolyanion, i.e., negative functional groups, particularly those of sialic acid, constitute all of the surface charge groups which are detectable by electrophoresis (92, 113). For example, there is no change in the electrophoretic mobility of human red cells suspended in

physiological ionic strength media in the pH range of 4.5 to 9 (64). This is indicative of the absence of molecules bearing functional groups which have a pK in this pH range, e.g., primary amino groups. Variations in mobility above pH 9 are due to irreversible changes in the electrokinetic properties of the cells and are thus of doubtful significance (113). There is also no change in the electrokinetic behavior of red cells following chemical modification with reagents which might be expected to react with cationic groups, such as amino groups, and thus effectively eliminate them from contributing to cellular surface charge. Reagents in this category include formaldehyde (56), acetaldehyde (56), 2,4-dinitrofluorobenzene (114) and tosyl chloride (92). The electrophoretic mobility of aldehyde treated cells as a function of pH of the suspending medium over a range of ionic strength has been reported to be identical to that of native cells in the region where the latter are electrokinetically stable (56). Stabilization of erythrocytes with aldehydes, for relatively long periods of time, has taken on an increasingly important role. In addition to electrokinetic studies, aldehyde fixed cells have been used to investigate the role of deformability in the rheological behavior of erythrocyte suspensions (115) and in dextran-mediated aggregation of erythrocytes (116). Furthermore, aldehyde fixation has been employed widely in electron microscopic investigations on the physicochemical nature of the red cell surface (119, 120). For the types of investigations cited to yield valid data, the

method of fixation must produce cells which have reproducible properties which are not changed with time. Because the rate of fixation of cells with acetaldehyde is quite slow and glutaraldehyde is expensive and, in addition, fixation with it leads to an increased net negative charge at physiological pH, formaldehyde has become the preferred reagent for fixation.

4.1 Cellular Conductivity and the Electrokinetic Properties of Formaldehyde Fixed Human Erythrocytes

Various methods of preparing formaldehyde fixative solutions have been described. Heard and Seaman (56) reported that formalin, due to its substantial methanol content, was unsatisfactory as a fixation agent. These authors, therefore, recommended that fixative solutions be prepared by sublimation of paraformaldehyde and absorption of the gas into a suitable buffer. Vassar et al. (117), on the basis of a report by Pease (118), suggested that the preparation of the formaldehyde fixative solutions be simplified by dissolving commercially available paraformaldehyde directly in an appropriate buffer. Fixation of red cells by this method led to fixed cells which had lower mobilities than the native red cells in low ionic strength media. Furthermore, at low ionic strengths the electrokinetic properties of these cells also changed with the length of time that they were stored.

The variety of changes which take place in the physicochemical properties of the human erythrocyte on fixation with aldehydes have been documented by a number of investigators (56, 117, 121, 122). Furthermore, the work of Carstensen et al. (124) has shown that substantial increases in the conductivity of red cells take place on fixation with glutaraldehyde. As has been pointed out in Section 1.1 the electrophoretic mobility of a particle theoretically depends on the ratio of the conductivity of the particle to that of its environment, i.e.,

$$u = \frac{\varepsilon\zeta}{4\pi\eta}\left[\frac{1}{1+\frac{\sigma_2}{2\sigma_1}}\right] \qquad 4\text{-}1$$

where u is the electrophoretic mobility, ζ is the potential at the surface of shear relative to the bulk medium, η and ε are the viscosity and dielectric constant of the suspending medium and σ_2 and σ_1 are the conductivities of the particle and suspending medium, respectively. For nonconducting particles Henry's correction factor reduces to unity and the equation reduces to the Helmholtz-Smoluchowski relationship:

$$u = \frac{\varepsilon\zeta}{4\pi\eta} \qquad 4\text{-}2$$

The necessity for stabilized red cell preparations for studies, which require exposure of red cells to conditions under which native

cells are not stable, led to an investigation designed to elucidate the underlying reasons for the anomalous behavior of red cells fixed by the method recommended by Vassar et al. (117) and the role, if any, of cellular conductivity in determining the electrokinetic properties of formaldehyde fixed erythrocytes.

4.1.1 Materials and Methods

4.1.1.1 Preparation of Formaldehyde Fixatives.

Paraformaldehyde was obtained from Matheson, Coleman and Bell, Lots A5H17 and 11F12. The paraformaldehyde was converted directly to the formaldehyde monomer by heating in doubly distilled water to ~70°C. Typically a 1.00 M solution of formaldehyde was prepared, filtered through Whatman No. 1 filter paper and diluted with a concentrated aqueous solution of sodium chloride or phosphate buffered saline to give a final solution of 0.500 M formaldehyde in either 0.150 M NaCl or 0.140 M NaCl-0.051 M Na_2HPO_4-0.009 M NaH_2PO_4 (PBS). In another experiment the PBS fixative was prepared with the addition of 1.0 mM EDTA. In addition, the formaldehyde was first generated by heating paraformaldehyde to 203-210°C as recommended by Heard and Seaman (56). The generated formaldehyde gas was dissolved in water to a concentration of $\leq$ 5.00 M. The solution was assayed for formaldehyde by the sodium sulfite method (125) and subsequently diluted with PBS or NaCl to give a final ionic strength of 0.150 g-ions $\cdot L^{-1}$ and a

formaldehyde concentration of 0.500 M.

Because of its accuracy, simplicity and rapidity, the sodium sulfite method is well suited for the determination of formaldehyde in aqueous solution. The method is based on the quantitative liberation of sodium hydroxide when formaldehyde reacts with sodium sulfite to form the formaldehyde-bisulfite addition product, i.e.,

$$HCHO_{(aq)} + Na_2SO_3 + H_2O \rightarrow NaOH + HCH(NaSO_3)OH$$

The liberated sodium hydroxide was titrated with a standard hydrochloric acid solution.

Typically 50 ml of a 1.0 M Na_2SO_3 solution plus 3 drops of phenolphthalein indicator solution (0.1% w/v in ethanol) were placed in a 250 ml Erlenmeyer flask. The solution was neutralized by addition of a few drops of a 1.00 M standard hydrochloric acid solution. An accurately measured volume of a formaldehyde solution was added (usually 10.00 ml) to this solution which was then titrated with the standard acid to a phenolphthalein end point. One ml of a 1.00 M solution of hydrochloric acid is equivalent to 0.03003 g formaldehyde and the molarity of the formaldehyde in the sample was determined according to the following equation:

$$\text{Molarity of HCHO} = \frac{[\text{moles of HCl}]}{[\text{volume of HCHO sample}]} \qquad 4\text{-}3$$

$$= \frac{[\text{volume HCl (L)}][\text{Molarity HCl}(M\,L^{-1})]}{[\text{volume HCHO (L)}]}$$

4.1.1.2 Preparation of Formaldehyde Fixed Red Blood Cells.

Human blood was obtained from healthy adult volunteers by venipuncture. The blood was anticoagulated with EDTA (final concentration 4.0 mM) and washed three times with 0.150 M aqueous NaCl solution buffered to pH 7.4 and 0.150 M aqueous $NaHCO_3$ solution (standard saline).

Red cells to be fixed in formaldehyde, prepared by direct dissolution of paraformaldehyde, were washed once more in either standard saline or PBS depending on the final salt composition of the fixative (standard saline or PBS). The cells were then packed by centrifugation at ~2500 g after which they were suspended in ~50 volumes of 0.500 M formaldehyde in either standard saline or PBS. The pH of the formaldehyde-standard saline fixative solution was initially adjusted to pH 7.9 with 1 M $NaHCO_3$. The pH of the suspension was monitored for two hours, at 0.5 hour intervals, following addition of the fixative and readjusted to pH 7.4 with 1 M $NaHCO_3$ as necessary. Cells fixed in PBS-fixative required no additional pH adjustments. In one experiment the cell samples were equally divided after 24 hours and one-half of the cells were suspended in fresh fixative solution.

The pH of the other samples, in standard saline fixative, was readjusted to pH 7.4 with 1 M $NaHCO_3$. Red cells fixed with formaldehyde generated as per Heard and Seaman (56) were treated in a similar fashion. In another experiment the concentration of formaldehyde in PBS was varied from 0.500 to 0.583 to 0.666 M to determine the effect of formaldehyde concentration on the extent of hemolysis in the cell preparations.

4.1.1.3 Analytical Particle Electrophoresis. Electrophoretic mobilities were measured either in a cylindrical chamber apparatus equipped with Ag-AgCl electrodes (Fig. 3-3) for cells in 0.150 M NaCl or in a cylindrical chamber equipped with platinum electrodes (Fig. 3-5) for cells suspended in lower inoic strength media. Typically, NaCl media of two different ionic strengths were used, namely, 0.150 and 0.0150 g-ions $\cdot L^{-1}$ with the pH adjusted to 7.4 ± 0.2 by $NaHCO_3$ of equivalent ionic strength. Media of lower than physiological ionic strength, utilized for electrophoresis of native red blood cells, were rendered isotonic by the addition of sorbitol. Chambers were positioned in a constant-temperature water bath at 25.0 ± 0.1°C and were operated at voltage gradients < 6 volts$\cdot cm^{-1}$ with currents < 3 mA to minimize joule heating and resultant convective instabilities. Mobility measurements on fixed cells were made > 5 days after fixation.

4.1.1.4 Conductivity Measurements. Conductivity measurements were made at 25.0 ± 0.1°C in a microelectrophoresis chamber

(Fig. 3-3). This chamber, when properly calibrated, acts as an excellent conductivity cell, as it separates the experimental sample from the electrodes and their electrochemical reaction products; the electrodes themselves are completely reversible and the time needed for experimental conductivity determinations amounted to a few seconds once the cell suspension had been placed in the chamber.

Conductivities of samples, consisting of red cell suspensions having a variety of red cell volume fractions, were calculated according to the following equation:

$$\sigma = \left[\frac{\ell_e}{\pi a^2}\right]\frac{I}{V} \qquad 4\text{-}4$$

where σ is the conductivity of the sample in mho $\cdot$ cm^{-1}, ℓ_e is the electrical length of the chamber, a is the radius of the chamber capillary tube, I is the current passing through the chamber at a constant applied potential, V. The quantity $\ell_e/\pi a^2$ is a chamber constant and was determined using standard potassium chloride solutions. Currents and voltages were measured using a Systron Donner multimeter, Model 7205.

Red cell suspension samples were prepared by washing fresh or formaldehyde fixed red cells three times in standard saline. For measurements carried out at low ionic strength the samples were washed an additional three times in 0.0150 M NaCl-$NaHCO_3$, pH 7.4

rendered isotonic with 0.247 M sorbitol. Five to eight different cell suspensions having red cell volume fractions varying from ~0.01 to ~0.4 were placed into the sample compartment of the chamber. Currents in mA were recorded on application of 50.0 volts across the chamber. The conductivity of the suspending medium was determined before and after each set of suspension conductivities was determined. No significant change in the electrical length of the chamber was noted during the course of the experiments.

Cellular conductivities were calculated from Fricke's equation (126) for a suspension of homogeneous spheroids:

$$\frac{\frac{\sigma}{\sigma_1} - 1}{\frac{\sigma}{\sigma_1} + x} = \frac{\frac{\sigma_2}{\sigma_1} - 1}{\frac{\sigma_2}{\sigma_1} + x} \cdot \rho \qquad 4\text{-}5$$

where σ, σ_1 and σ_2 are the specific conductivities of the suspension, the suspending medium, and the suspended particles, respectively; ρ is the volume fraction occupied by the suspended particles; and x is a shape factor which is a function of the ratio σ_2/σ_1 as well as the axial ratios of the spheroids. A plot on the left-hand side of Eq. 4-5 vs ρ yielded a straight line from the slope of which σ_2 was calculated. The shape factor of human red cells was determined by assuming that their shape approaches that of an oblate ellipsoid. For human red cells the axial ratio is ~1/4 (127) which for

nonconducting particles results in x being equal to 1.1 (126). As a final approximation, this value of x was used together with Eq. 4-5 in finding the conductivity ratio σ_2/σ_1. A new value of x, corresponding to this ratio was determined from a plot of x vs σ_2/σ_1 for an axial ratio of 1/4 as provided by Fricke (216) and substituted into Eq. 4-5 to determine a new conductivity ratio. This iteration converged rapidly to give constant values of σ_2.

4.1.1.5 The Packing Efficiency of Formaldehyde Fixed Red Cells. The volume fraction (ρ) of each cell sample was calculated from the mean cellular volume (MCV) and the number of cells per ml of sample, which was measured electronically as described in Section 2.5. The MCV's of fresh red cells were determined from the hematocrit and electronic cell count measurements of a concentrated cell suspension, as outlined in Sections 2.5 and 5.2.2. A hematocrit packing efficiency correction factor of 0.99 was included in the calculation. The MCV of formaldehyde fixed cells was determined similarly except that the packing efficiency correction factor was 0.65. This factor was determined by a polymer dilution technique as follows: The total volume of a cell suspension is given by

$$V_T = V_C + V_{IS} + V_{SN} \qquad 4\text{-}6$$

where V_T is the total volume, V_C is the cellular volume, V_{IS}

is the interstitial fluid volume and V_{SN} is the supernatant fluid volume. The packing efficiency factor, f, is equal to true hematocrit divided by observed hematocrit, i.e.,

$$f = \frac{V_C/V_T}{(V_C+V_{IS})/V_T} \qquad 4\text{-}6$$

If a given volume of a polymer solution of specific concentration is added to a cell pack of known volume the interstitial fluid volume may be determined from

$$\frac{C_I}{C_F} = \frac{V_{SN}+V_{IS}}{V_{SN}} \qquad 4\text{-}7$$

where C_I and C_F are the initial and final concentrations of polymer in the supernatant fluid after mixing and recentrifuging the cell pack, i.e.,

$$V_{IS} = V_{SN}\left(\frac{C_I}{C_F} - 1\right) \qquad 4\text{-}8$$

The volume of the cell pack, V_{CP}, is equal to

$$V_{IS} + V_C \quad \text{or} \quad V_C = V_{CP} - V_{IS} \qquad 4\text{-}9$$

Substituting this result into the Eq. 4-6 we obtain

$$f = V_{CP} - V_{IS}/V_{CP} \qquad 4\text{-}10$$

and substituting for V_{IS} from Eq. 4-8

$$f = V_{CP} - [V_{SN}(\frac{C_I}{C_F} - 1)]/V_{CP} \qquad 4\text{-}11$$

In this way f was calculated using a dextran T-70 (Pharmacia) solution, the initial and final concentrations of which were determined polarimetrically. The cells were centrifuged in 30 ml siliconized Corex glass test tubes at 25°C at 3000 g for 30 minutes. Brooks (33) has found that dextran T-70 neither adsorbs extensively nor enters human erythrocytes such that bulk polymer concentration changes reflect dilution by interstitial fluid rather than adsorption or filling of intracellular spaces.

4.1.1.6 Aluminum and Iron Contamination Analyses. Paraformaldehyde samples, before and after sublimation as well as the reddish residues remaining in the sublimation vessel, were analyzed qualitatively for aluminum according to the tests recommended by the IUPAC (128). Aluminon supplied in a spot test kit (BDH Chemicals Ltd., Poole, England) was utilized for the aluminum analysis. Quantitative analysis for iron was performed using potassium ferrocyanide. Formaldehyde fixative solutions were also analyzed quantitatively for aluminum contamination by atomic absorption analysis

using a Model 555 Instrumentation Laboratory Inc. atomic absorption spectrophotometer.

4.1.1.7 Miscellaneous. Osmolalities of media were measured in a Precision Systems freezing point depression osmometer. The possible presence of organic impurities in the formaldehyde solutions was investigated by scanning its spectrum from 200 nm to 340 nm using a Beckman Model 25 spectrophotometer.

4.2 Results

The electrophoretic mobility of human red blood cells fixed and stored at room temperature in 0.500 M formaldehyde-PBS solution, prepared essentially according to the method of Vassar et al. (117), was measured at intervals up to ~10 months. During this time the mobility of these cells in standard saline remained constant at -1.10 ± 0.04 μm sec^{-1} V^{-1} cm (Fig. 4-1). However, the mobility of these cells in 0.015 M NaCl-$NaHCO_3$ pH 7.4 ranged from -2.79 μm sec^{-1} V^{-1} cm initially to values as low as -2.05 μm sec^{-1} V^{-1} cm on prolonged storage. Typically the initial mobilities were 10 to 20% lower than those reported by Heard and Seaman (56) for formaldehyde fixed and native red cells in 0.015 g-ions · L^{-1} ionic strength media. For some cell samples the decrease in mobility was time dependent and a plateau was reached 4-6 months after fixation (Fig. 4-1).

Figure 4-1. Electrokinetic stability of human red cells fixed and stored in 0.500 M formaldehyde in PBS. The fixative was prepared according to the method of Vassar et al. (117). Mean mobilities are plotted for cells washed and suspended in 0.150 M NaCl-$NaHCO_3$ pH 7.4 ± 0.2 (closed symbols) and in 0.0150 M NaCl-$NaHCO_3$ pH 7.4 ± 0.2 (open symbols) following various time periods of storage.

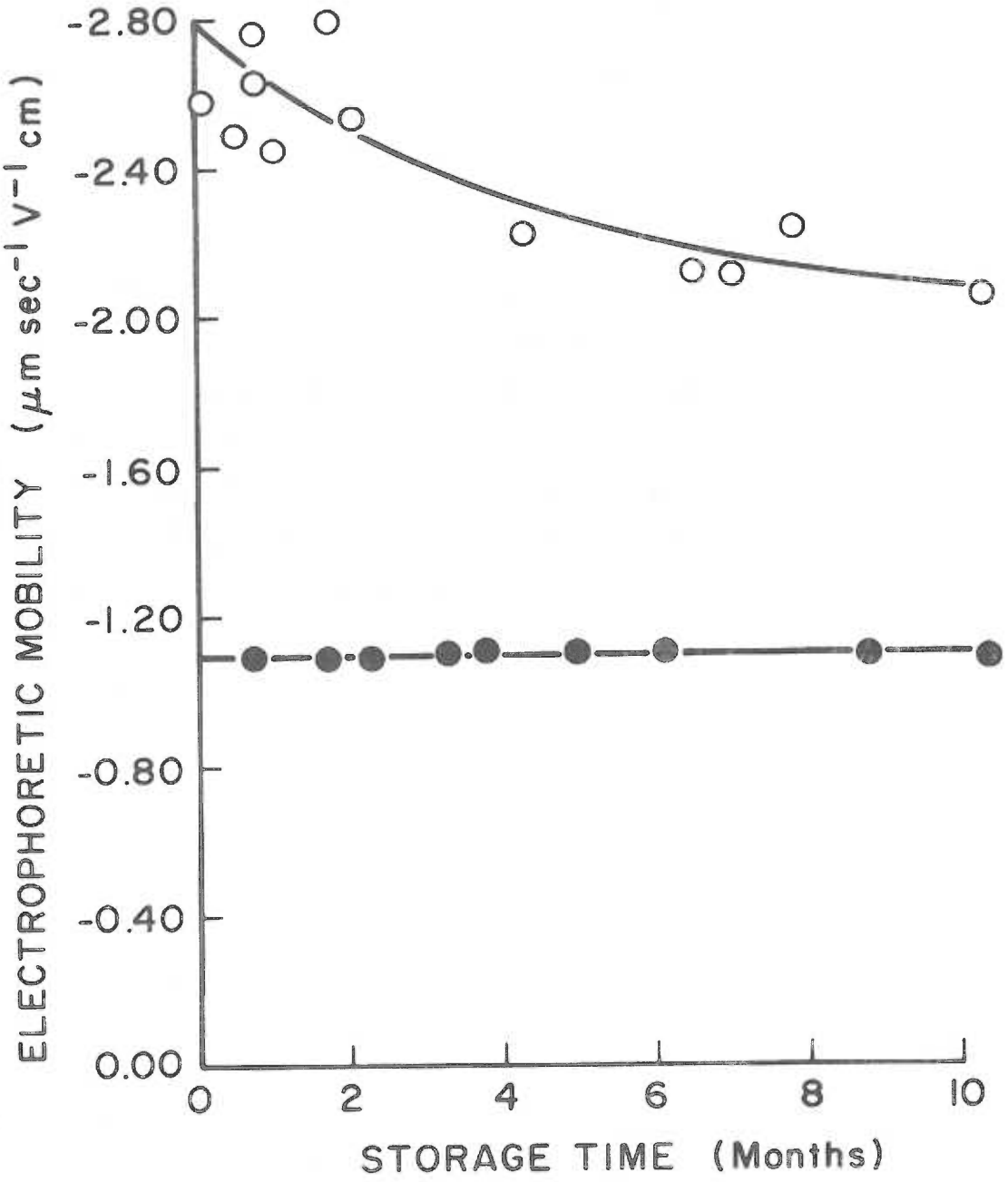
-2.80
-2.40
-2.00
-1.60
-1.20
-0.80
-0.40
0.00
0
2
4
6
8
10
ELECTROPHORETIC MOBILITY (μm sec⁻¹ V⁻¹ cm)
STORAGE TIME (Months)

Experiments were performed to duplicate the experimental methods and conditions of Heard and Seaman (56) and Vassar et al. (117) in order to identify the possible reasons for their divergent results. Table 4-1 shows the results of a typical experiment in which blood was taken from one donor and the cells fixed in isotonic saline or PBS containing formaldehyde generated by sublimiation or by direct dissolution of paraformaldehyde. It can be seen readily that the salt composition of the fixative makes no significant difference in the plateau mobility values of the fixed cells in either physiological or low ionic strength saline. However, the results depend significantly on the method of formaldehyde generation. If paraformaldehyde is first sublimed as recommended by Heard and Seaman (56) the mobility values are in close agreement with those originally reported.

It can also be seen that changing the fixative after 24 hours influences the final mobility values only slightly. However, it was also found that the extent of hemolysis which was slight ($< 0.2\%$) in 0.500 M formaldehyde solutions could be virtually eliminated by utilizing a 0.583 M formaldehyde concentration thus removing the necessity for the precautionary measure of changing the fixative after 24 hours. The extent of hemolysis in 0.666 M formaldehyde solutions was visually much greater than in either 0.500 M or 0.583 M solutions.

Figure 4-2 shows the electrophoretic mobility of formaldehyde fixed cells prepared according to the method of Heard and Seaman (56)

Table 4-1. Electrophoretic mobilities of fresh native and formaldehyde fixed human erythrocytes.

Ionic Strength of Suspending Medium ($g\text{-ions} \cdot L^{-1}$)	Electrophoretic Mobility ($\mu m\ sec^{-1}\ V^{-1}\ cm$)[1,2]	Aldehyde Treatment (0.500 M Formaldehyde)	Method of Formaldehyde Generation from Paraformaldehyde[3]	Salt Composition of Fixative (NaCl or PBS)[4]
0.150	1.08 ± 0.04 (2)	none		
0.150	1.10 ± 0.04 (20)	+	o and Δ	NaCl and PBS
0.0150	2.76 ± 0.07 (20)	none		
0.0150	2.79 ± 0.10 (20)	+	o	NaCl (+)
0.0150	2.75 ± 0.10 (20)	+	o	NaCl (-)
0.0150	2.80 ± 0.14 (20)	+	o	PBS (+)
0.0150	2.73 ± 0.13 (20)	+	o	PBS (-)
0.0150	2.37 ± 0.18 (30)	+	Δ	NaCl (-)
0.0150	2.58 ± 0.13 (30)	+	Δ	PBS (-)

[1] Mean mobility ± sample SD; the number of individual cells measured appears in parentheses.

[2] No significant variation in electrophoretic mobility from the listed values was detected for those cell samples fixed with formaldehyde prepared by sublimation of paraformaldehyde one month after fixation.

[3] Formaldehyde monomers were generated from stock paraformaldehyde either by sublimation and collection of the gas in water (o) or by direct dissolution of paraformaldehyde in water (Δ).

[4] + or - in parentheses indicates whether fixative solution was changed 24 hours after initial addition.

Figure 4-2. Electrokinetic stability of human red cells fixed and stored in 0.500 M formaldehyde in PBS. The media was prepared by the method of Heard and Seaman (56). As in Figure 4-1 closed and open symbols refer to mean mobilities of cells washed and suspended in 0.150 and 0.0150 M NaCl-$NaHCO_3$ pH 7.4 ± 0.2, respectively.

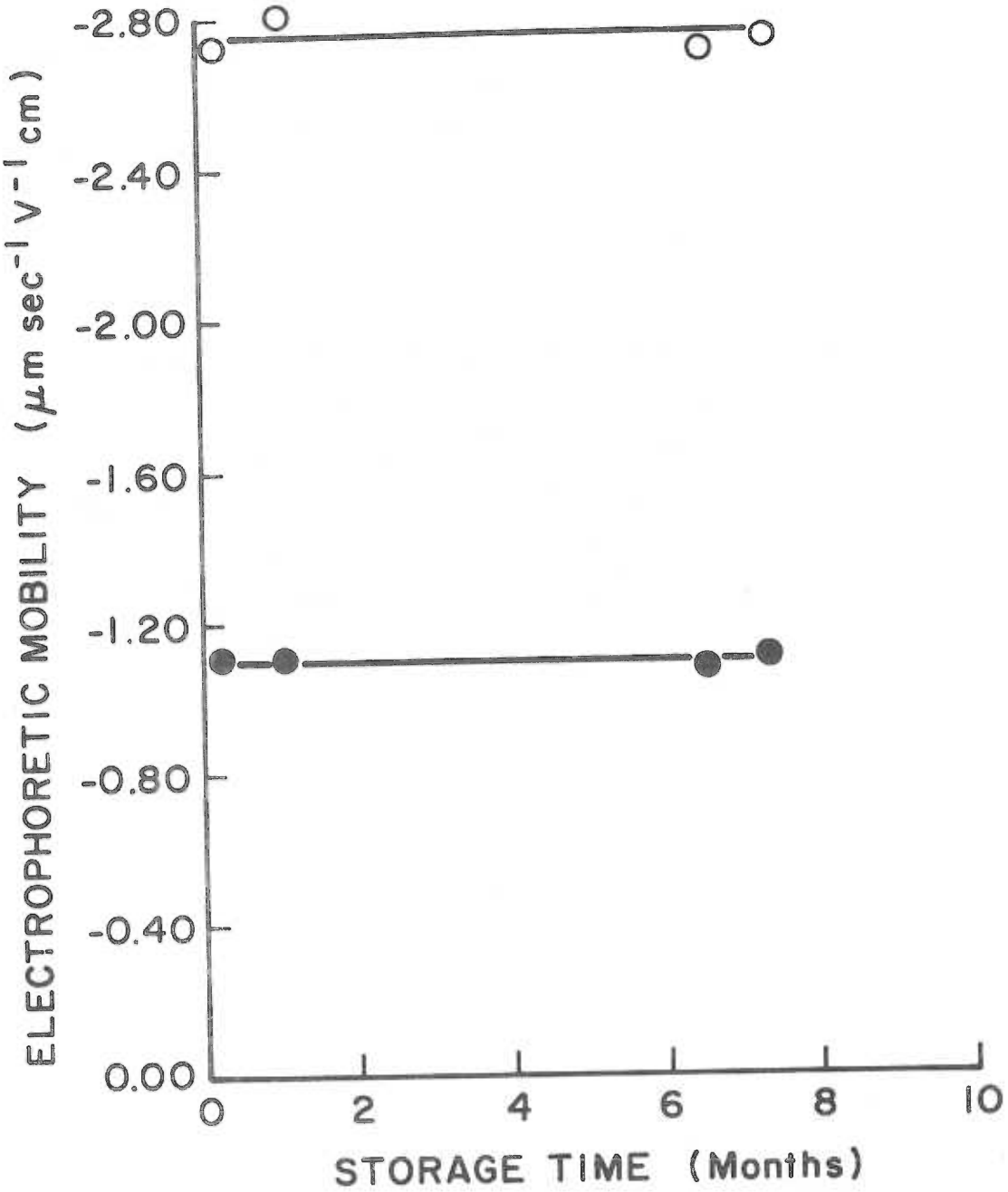
-2.80
-2.40
-2.00
-1.60
-1.20
-0.80
-0.40
0.00
ELECTROPHORETIC MOBILITY (μm sec⁻¹ V⁻¹ cm)
0
2
4
6
8
10
STORAGE TIME (Months)

in PBS as a function of storage time. The electrophoretic mobility of these cells in standard saline remains constant at -1.10 ± 0.04 μm sec^{-1} V^{-1} cm which is identical to the results depicted in Fig. 4-1. In addition, the mobility of these cells in 0.0150 M NaCl, pH 7.4 remains constant on lengthy storage in contrast to the electrokinetic behavior of cells fixed according to the method of Vassar et al. (117) (Fig. 4-1).

After sublimation of paraformaldehyde reddish-brown deposits remained in the sublimation vessel. These residues gave a strong positive qualitative test for the presence of aluminum. Atomic absorption analysis showed the commercial paraformaldehyde preparations used in this study to be contaminated with at least 7 ppm aluminum. No iron could be detected by either a ferrocyanide spot test or by atomic absorption analysis. Spectral scans of the formaldehyde fixation solutions in the region 200 nm to 340 nm indicated no major organic contamination. A single absorption peak was observed at 200 nm.

The electrokinetic behavior of erythrocytes fixed in media prepared by direct dissolution of paraformaldehyde with the addition of 1.0 mM EDTA was identical to cells fixed in media prepared by first subliming paraformaldehyde. The electrophoretic mobility of the cells fixed in the EDTA-containing medium was -1.09 ± 0.04 μm sec^{-1}

V^{-1} cm in standard saline and -2.79 ± 0.11 μm sec^{-1} V^{-1} cm in 0.015 M NaCl pH 7.4.

The course of heat-induced depolymerization of paraformaldehyde to formaldehyde in PBS and the stability of the fixative solution following storage at room temperature were examined by freezing point depression measurements. A 0.500 M formaldehyde concentration corresponds to ~0.250 M NaCl. The osmolality of PBS is 287 mOsm·kg^{-1} such that a 100% yield of formaldehyde from paraformaldehyde to give 0.500 M HCHO should result in a fixative osmolality of ~800 mOsm·kg^{-1}. Fixative preparations of 0.50 M paraformaldehyde in PBS gave values ranging from 755 to 780 mOsm·kg^{-1}. The osmolality of the fixative was followed during the heating step in a water bath up to ~70°C. Greater than 90% of the final plateau value of the osmolality was obtained by the time the fixative had reached 65°C. Plateau values were reached after the temperature of the fixative was held for several minutes at 65°C. No increase in osmolality was seen by further heating to 70°C. The suspension of paraformaldehyde became clear when the hydrolysis had proceeded to > 95% of the plateau osmolality. The pH and osmolality of the fixative solution stored sealed in glass at room temperature remained the same for at least two months indicating that repolymerization of the formaldehyde

does not occur to a measurable degree under these conditions.

Figures 4-3 and 4-4 show the effect of fixation on the conductivity of erythrocytes suspended in standard saline and 0.0150 M NaCl-$NaHCO_3$-0.247 M sorbitol, pH 7.4. It can be seen clearly that a change in conductivity of the suspension occurs on fixation of the cells with formaldehyde. The high degree of linearity of the data in these figures as well as their reproducibility lends support to the use of Fricke's relationship (Eq. 4-5) for the calculation of cellular conductivities. The results of such calculations are presented in Table 4-2. This table shows that fresh red cells at physiological ionic strength act essentially as nonconductors and cells fixed with formaldehyde have conductivities which are only ~6 and 9 times greater than their native counterparts in high and low ionic strength media, respectively.

Suspensions made from formaldehyde fixed cells washed three times in 0.150 M NaCl and three times in 0.0150 M NaCl-$NaHCO_3$-0.247 M sorbitol, pH 7.4, at a wash ratio of $\geq$ 10:1, had abnormally high conductivities. It was found that these suspensions had a conductivity greater than that of the suspending medium if they were not allowed to stand and equilibrate for a considerable time period in the

Figure 4-3. Plots of conductivity ratio function as a function of the volume fraction, ρ, for cells suspended in 0.150 M $NaCl$-$NaHCO_3$, pH 7.4. The conductivity ratio function is $-(\frac{\sigma}{\sigma_1} - 1 / \frac{\sigma}{\sigma_1} + x) \times 10^2$ where σ is the conductivity of the suspension, σ_1 the conductivity of the suspending medium and x the shape factor of the cells. The cellular conductivity, σ_2, was calculated from the slope of the lines which were fit to the data by least squares analysis. ● native human erythrocytes and ▲ human erythrocytes fixed with formaldehyde solutions prepared according to Heard and Seaman (56).

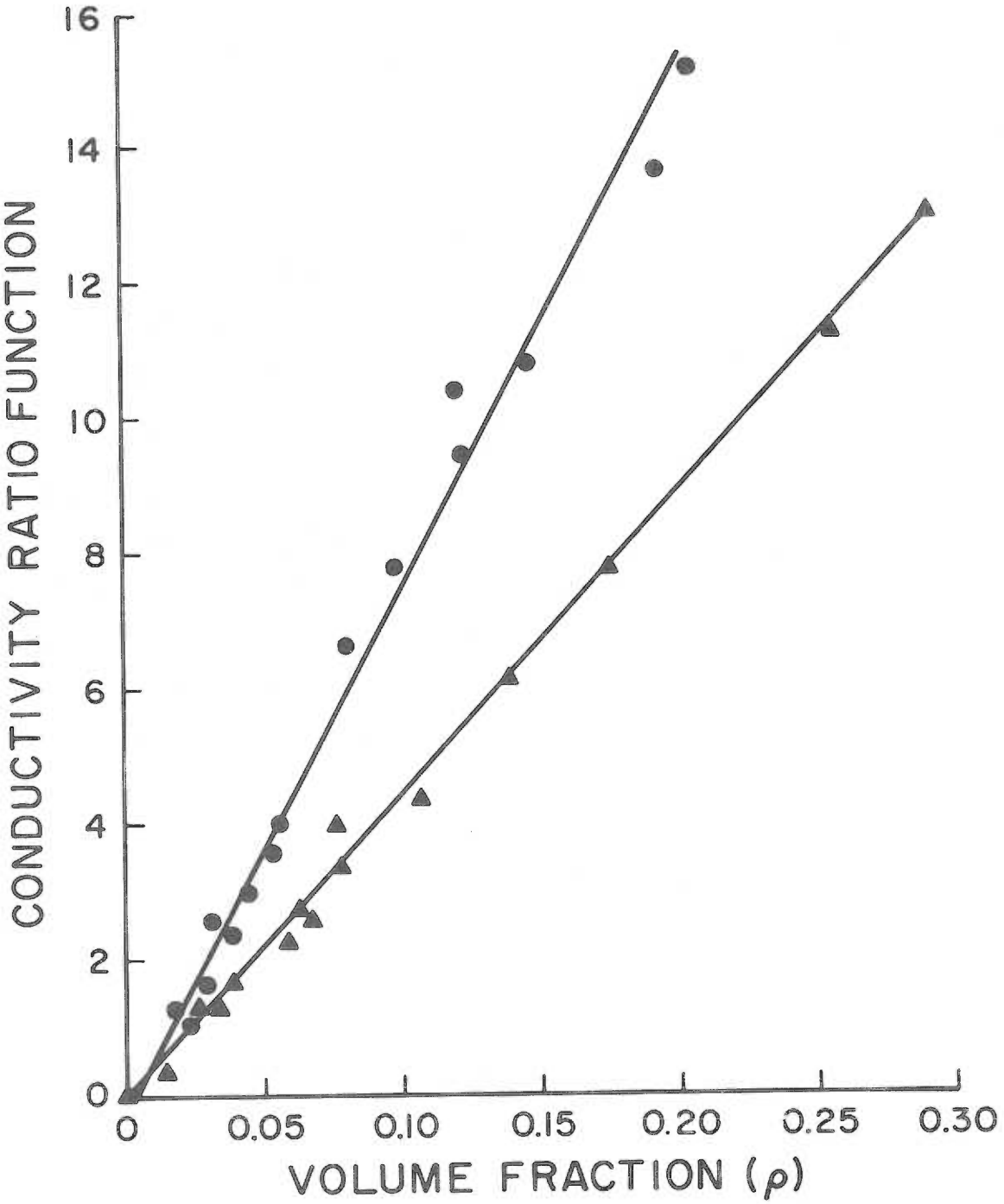
CONDUCTIVITY RATIO FUNCTION
VOLUME FRACTION (ρ)
0
2
4
6
8
10
12
14
16
0
0.05
0.10
0.15
0.20
0.25
0.30

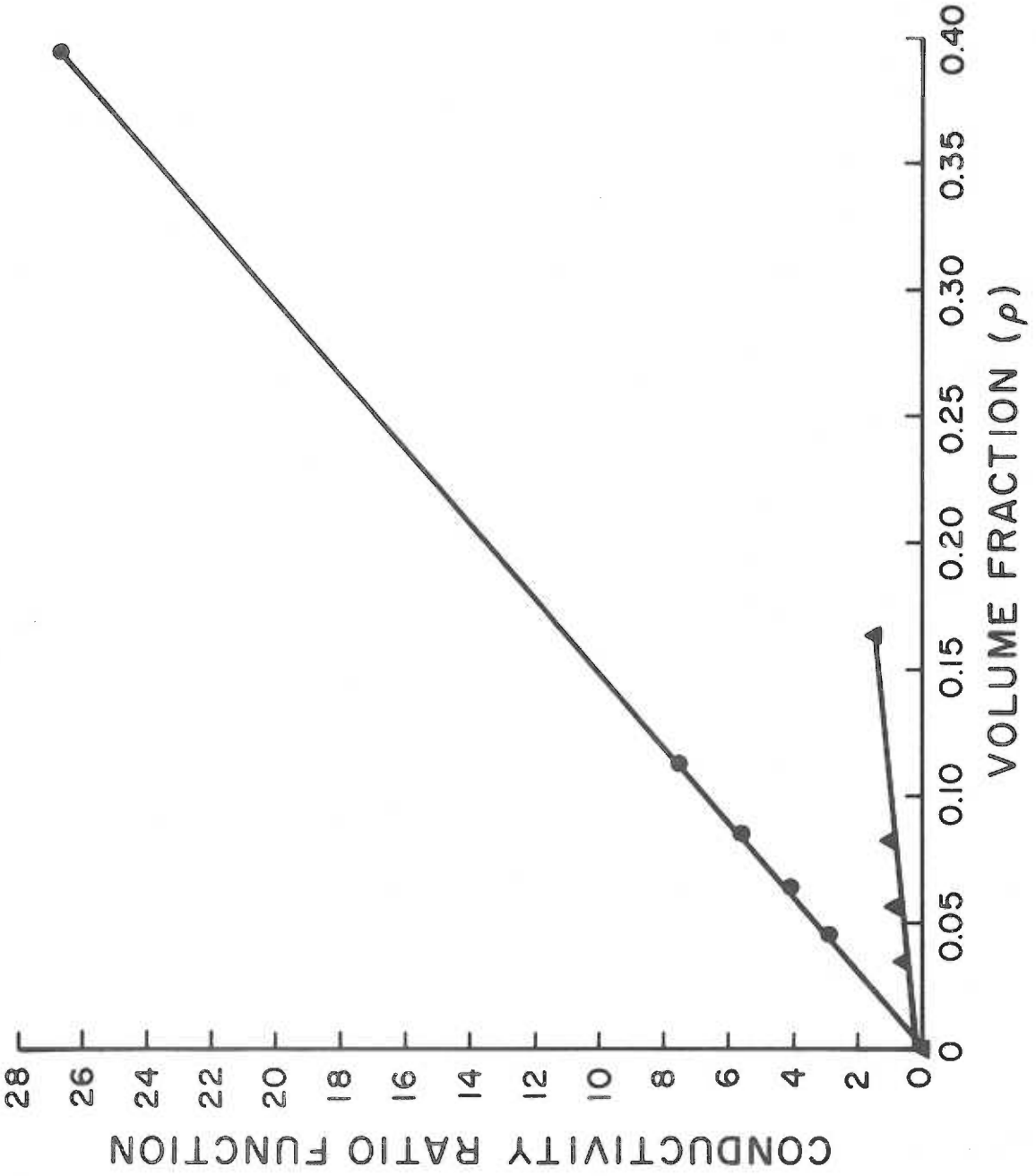
CONDUCTIVITY RATIO FUNCTION
0
2
4
6
8
10
12
14
16
18
20
22
24
26
28
VOLUME FRACTION (ρ)
0
0.05
0.10
0.15
0.20
0.25
0.30
0.35
0.40

Table 4-2. The conductivity of native and formaldehyde fixed human erythrocytes[1/] suspended in physiological and low ionic strength media.

Cell Sample	Suspending Medium (pH 7.4)	Suspending Medium Conductivity x 10^2 (σ_1-mho·cm^{-1})	Cellular Conductivity x 10^3 (σ_2-mho·cm^{-1})
Native erythrocytes	standard saline	1.52	0.65
Fixed erythrocytes	standard saline	1.52	3.92
Native erythrocytes	0.0150 M NaCl-$NaHCO_3$-0.247 M sorbitol	0.166	0.15
Fixed erythrocytes	0.0150 M NaCl-$NaHCO_3$-0.247 M sorbitol	0.166	1.30

[1/] Fixation was performed with media prepared as per Heard and Seaman (56).

low ionic strength media before finally being washed in low ionic strength media. The results shown in Fig. 4-4 were obtained on cells stored 24 hours in 0.0150 M NaCl-$NaHCO_3$-0.247 M sorbitol, pH 7.4, and then washed therein three times further prior to making up the experimental samples. These observations also underscore the need for thorough washing of cell suspensions for conductivity measurements.

The MCV of both fresh and formaldehyde fixed human red cells was found to be approximately 88-90 μm^3 in good agreement with earlier results. These MCV values also indicate that the formaldehyde fixation of human red cells is an isovolemic process.

4.3 Discussion

Aqueous formaldehyde solutions have long been utilized as fixatives for the preservation of tissue. Red cells fixed with formaldehyde retain many of the same properties as native cells. For example, their morphology is indistinguishable from unfixed cells when viewed under a microscope. Furthermore, many surface properties remain unchanged including interaction of a number of red cell antigens with their corresponding antibodies (129). Nevertheless, a number of surface properties do change with fixation (129, 130), e.g., loss of agglutinability in the presence of appropriate antisera.

Fixation with formaldehyde has also been used to stabilize red cells such that they might be used under conditions where the native cell would hemolyze. Fixation followed by electrokinetic analysis has lead to results which show that the electrophoretic mobility of these cells is invariant over a wide range of pH. In addition, no differences in electrophoretic mobility between the fixed cells and native cells were observed over the range of ionic strengths and pH value where the native cells are stable.

It is generally accepted that formaldehyde reacts at room temperature initially with amino groups of proteins to form methylolamines, which then react more slowly to form a methylene bridge between primary or secondary amino groups (131) according to the following schemes:

$$R\text{-}NH_2 + HCHO \rightarrow R\text{-}NH\text{-}CH_2OH$$

$$R\text{-}NH\text{-}CH_2OH + HCHO \rightarrow R\text{-}N\text{-}(\text{-}CH_2OH)_2$$

$$R\text{-}N\begin{matrix}CH_2OH\\CH_2OH\end{matrix} + 2\ R'\text{-}NH_2 \rightarrow R\text{-}N\begin{matrix}CH_2\text{-}NH\text{-}R'\\CH_2\text{-}NH\text{-}R'\end{matrix}$$

Moreover, formaldehyde may react with guanidyl, imidazole, indole as well as phenolic groups. Amide groups may also react but only under relatively harsh reaction conditions. Levy (132) has investigated the equilibria in the formol titration and found the

equilibrium constants for the formation of the dimethylolamines from amino acids to be relatively large and Frankel-Conrat et al. (133) have remarked that formaldehyde adducts of proteins are stable although some derivatives may give up their formaldehyde "readily" in the presence of dimedone (133), a reaction which requires the use of a catalyst and reflux conditions in ethanol (134). Conditions such as these are certainly not encountered in work with formaldehyde treated red cells.

The unchanged electrokinetic properties of human red cells on treatment with formaldehyde, together with the fact that formaldehyde reacts primarily with potential cationic groups, viz., amino groups, thus eliminating them from contributing to the surface charge of erythrocytes, has been used in support of other data (64, 92) which show the human erythrocyte to behave as a macropolyanion in electrophoresis. It should be emphasized here that the electrophoretic method is accurate only to about 2-3%. If the red cell has 1.3 to 2.6×10^7 anionic sites per red cell (the former figure having been calculated from Eq. 1-40 with $\alpha = 1$ and the latter with $\alpha = 0$, then 2-3% of this number may represent cationic groups, i.e., $3.9\text{-}7.8 \times 10^5$ sites.

Although the method of Vassar et al. (117), because of its relative simplicity, has been used for a period of a few years in this laboratory it became apparent that red cells fixed by this method,

using currently available paraformaldehyde reagents behave electrokinetically as expected at physiological ionic strength but had mobilities which were 10-20% lower than originally reported by Heard and Seaman (56) in media of low ionic strength, i.e., 0.0150 g-ions $\cdot L^{-1}$. Figure 4-1 shows that the electrophoretic mobility of red cells suspended in 0.0150 M NaCl, pH 7.4, within one month of fixation, is quite variable. In addition, there is a decrease in the mobility of the cells which increases with the length of time of storage of the preparation. This type of variability, if not accounted for, renders fixed red cells unsatisfactory as standard particles for the performance evaluation of electrophoretic equipment. Other types of particles, e.g., polystyrene latices, are less suitable standard particles for biological experiments since their electrokinetic properties are exceedingly sensitive to impurities in suspending media (135).

The results presented in Table 4-1 and Fig. 4-1 confirm the original studies conducted by Heard and Seaman (56). The differences between the method of Vassar et al. (117) and the procedure of Heard and Seaman (56) are shown to be primarily due to the elimination of non-volatile impurities by initially subliming the paraformaldehyde in the Heard and Seaman (56) method. The reddish residues remaining in the reaction vessel after sublimation of paraformaldehyde reinforced the suspicion that paraformaldehyde contains impurities. A clue to the possible identity of the impurities was given by Walker (136)

who reported aluminum to be one of the major contaminants of commercial paraformaldehyde preparations. We confirmed that the paraformaldehyde was contaminated with aluminum by both qualitative and quantitative means. Other metals may also be present in the paraformaldehyde since positive interference by a number of metals, including Cu^{+2} and Ni^{+2} and Ga^{+3} has been reported for the assay used (128).

The mechanism by which such impurities produce the anomalous electrokinetic properties of fixed erythrocytes requires some comment. It is well known, for instance, that specific binding of cations such as aluminum to negatively charged cells or particles will lead to a decrease in their electrophoretic mobility or even charge reversal (17, 75). The effectiveness of a particular cation as a charge reversal agent is a strong function of its valency, the trivalent cations being much more effective than divalent cations. Metal impurities such as aluminum would also account for the fact that red cells fixed in the sodium chloride solution of formaldehyde prepared by direct dissolution of paraformaldehyde had a lower mobility than cells fixed in the comparable PBS medium (Table 4-1), since the phosphate would to some extent react with metal ions and effectively lower their concentration thus making them unavailable to bind to the surfaces of the cells. This interpretation is further supported by the fact that addition of EDTA to fixatives prepared directly from paraformaldehyde is

as effective as sublimation in eliminating the anomalously low and variable electrokinetic properties of cells prepared by the method of Vassar et al. (117).

Seaman and Pethica (17, 76) found that metal cation concentrations necessary for charge reversal of red cells were higher in physiological ionic strength media than in low ionic strength media. Thus, at high ionic strength and very low concentrations of contaminating multivalent cations, the effect on the electrophoretic mobility of red cells may be obscured and undetectable, yet quite noticeable at low ionic strengths. This is precisely the case in our study where the mobility of cells prepared directly from paraformaldehyde was -1.10 ± 0.04 $\mu m\ sec^{-1}\ V^{-1}\ cm$ in 0.150 M NaCl as expected, but significantly lower than anticipated in 0.0150 M NaCl (Table 4-1 and Fig. 4-1).

It has been pointed out by Vassar et al. (117) as well as by Bowes and Carter (137) that artifacts in fixed red cells may arise from the deposition of aldehydic polymers on their surfaces. This was not the case in this study since it was demonstrated spectrophotometrically that no measurable degree of polymerization took place in the fixatives. Furthermore, this is consistent with data presented by Walker (138) that polymerization of formaldehyde does not take place to a significant degree in aqueous solutions at concentrations similar to those used in this study.

Our data, which show the native human erythrocyte to have negligible conductivity at physiological ionic strength, are in close agreement with dielectric dispersion measurements (139). Similarly, the data agree closely with those of Carstensen et al. (140) who set the upper limit on the ratio of the conductivity of red cells to that of the suspending medium (σ_2/σ_1) to be ~0.1 at low ionic strength. However, even though similar results were obtained, Carstensen et al. (140) used relatively high (> 80%) volume fractions in determining the conductivity of the suspensions, which makes their estimate of σ_2/σ_1 approximate at best, since their data analysis was valid only for spheres at low volume concentrations (126). In contrast, in the analysis here, the shape factor and its dependence on the conductivity ratio σ_2/σ_1 was taken into account.

It has generally been accepted that treatment of human erythrocytes with formaldehyde does not alter their electrokinetic properties as first reported by Heard and Seaman (56). This observation has been used as supporting evidence that the normal human red cell behaves electrokinetically as a macropolyanion (92). These authors argued that if there were a significant number of positively charged groups in the peripheral zone of the erythrocyte, e.g., amino groups, they would be blocked by reaction with formaldehyde and effectively eliminated from contributing to the surface charge of the red cell and as a result the electrophoretic mobility would be expected to increase.

The data presented in Table 4-2 would suggest that the analysis and interpretation of electrophoretic mobility data obtained on formaldehyde fixed erythrocytes is more complex than might be anticipated. The zeta potentials of formaldehyde fixed erythrocytes, if they were to be corrected for the contribution of conductivity with the aid of Eq. 4-1, would be ~11% and 39% greater than for native red cells at ionic strengths of 0.150 and 0.0150 g-ions $\cdot L^{-1}$, respectively. This could imply that formaldehyde fixation of red cells leads to the elimination of a significant number of cationic charge groups in the peripheral zone of the red cell.

The use of conductivity data alone to draw such conclusions is not warranted however, especially in the face of considerable other experimental evidence which shows that cationic charge groups make up less than ~5% of the number of anionic groups. The fact alone that the electrophoretic properties of the formaldehyde fixed human red cell are identical to those of the native cell, within experimental error, seems unlikely to be fortuitous.

Most important however, is the consideration of the applicability of Henry's equation per se to the system under study. Overbeek and Wiersema (9) have commented that in electrophoresis even metallic particles may be treated as insulators since under ordinary field strengths employed such particles cannot conduct a current. In other words, since metallic particles cannot conduct ions, any current which

The total current passing through the volume element will be equal to the sum of the individual currents passing through each circuit element, i.e.,

$$I_T = I_{RBC} + I_M \qquad 4\text{-}12$$

where I_T is the total current, I_{RBC} is the current passing through the cell and I_M is the current passing through the suspending medium. The resistances of the circuit elements may be calculated from the specific conductivity, κ, of the red cells and the suspending medium, respectively, utilizing the following relationship:

$$R = \frac{[1/\kappa][\ell]}{[A]} \qquad 4\text{-}13$$

where ℓ is the length of the resistor and A is its cross sectional area. For the sake of simplicity, the red cell is assumed to be a cylinder of 8 μm diameter and length. Taking the field strength in electrophoresis to be a reasonable 5 $V \cdot cm^{-1}$ the potential across the cell, would be 4 mV. The potential drop across the volume element of the suspending medium containing that cell would also be 4 mV. However, since the suspending medium occupies the whole of the diameter of the capillary tube, i.e., 2 mm, the cross sectional area of the fluid volume element under consideration is 3.14×10^{-2} cm^2. With Ohm's law and the resistances which were calculated with the

aid of Eq. 4-13, the currents, I_{RBC} and $I_{M'}$ carried by the red cell and the volume element of saline, respectively were calculated. The results are presented in Table 4-3. The amount of current carried by the red cells is ~6 orders of magnitude less than that carried by the suspending medium.

In summary, it is concluded that red cells fixed with formaldehyde, in accordance to the methods of Heard and Seaman (56) or in the presence of EDTA, have the same electrophoretic mobilities at physiological as well as low ionic strength as fresh native erythrocytes. This is not the case for cells fixed as per Vassar et al. (117). Furthermore, it is shown that although there is a measurable increase in conductivity on fixation of red cells with formaldehyde the increase is insignificant in terms of how much current either native or fixed red cells will carry under the conditions encountered in cellular electrophoresis.

Table 4-3. Resistances and current fluxes through native and formaldehyde fixed human erythrocytes under conditions encountered in cellular electrophoresis.

Cell Sample	Suspending Medium	R_M [1] (Ω)	R_{RBC} [2] Ω ($\times 10^{-6}$)	I_M [3] (Amperes) $\times 10^{3}$	I_{RBC} [4] (Amperes) $\times 10^{9}$
Native red cells	standard saline	1.68	2.45	2.38	1.6
Fixed red cells	standard saline	1.68	0.41	2.38	9.8
Native red cells	0.015 M $NaCl$-$NaHCO_3$-0.247 M sorbitol	15.3	10.6	0.26	0.4
Fixed red cells	0.015 M $NaCl$-$NaHCO_3$-0.247 M sorbitol	15.3	1.22	0.26	3.3

[1] Resistance of a volume element of the suspending medium, the length of which is equal to that of a red cell, i.e., ~8 μm and whose cross sectional area is equal to that of an electrophoresis chamber capillary of 2 mm diameter, i.e., 3.14×10^{-2} cm^2.

[2] Resistance of red cells assuming that they have an idealized shape of a cylinder 8 μm in diameter and 8 μm in length.

[3] Current passing through the suspending medium.

[4] Current passing through the red cells.

CHAPTER 5

SIALIC ACID AT THE RED CELL SURFACE: ITS RELATIONSHIP TO CELL AGE AND SURFACE CHARGE DENSITY

Since the discovery of sialic acids at the surfaces of mammalian erythrocytes by Cook et al. (91) and Eylar et al. (142) their occurrence has been found to be almost ubiquitous. Their presence has been reported in all species of vertebrates and in certain invertebrates as well (143). There has been considerable interest in elucidating the functional role of sialic acids in glycoproteins per se as well as in the glycoproteins at cell surfaces especially those of the red cell surface.

Chemically sialic acids are usually acylated derivatives of chemically unstable, neuraminic acid (5-amino-3, 5-dideoxy-D-glycero-D-galacto-nonulosonic acid) (144). The N-acetyl derivative, the main sialic acid constituent of human red cells, and the N-glycolyl derivative of neuraminic acid, constitute the main structural backbone of about 17 types of sialic acid known to occur naturally (144). At least one form of sialic acid has been found to be associated with the erythrocyte membranes of all animal species thus far examined and as many as four types have been reported for rabbit red cells where N-acetylneuraminic acid and N-glycolylneuraminic acid, as well as their O-acetylated counterparts were isolated from stroma preparations (145). In the case of human erythrocytes 95-100% of the sialic acid is in the form of N-acetylneuraminic acid (142).

Almost invariably the sialic acids are in bound form occupying the terminal nonreducing ends of oligosaccharide chains which in turn are structural components of cell surface glycoproteins or glycolipids. Human red cell membrane glycolipids contain only extremely small quantities of sialic acid (147). In fact the amounts are so small that in some studies they have remained undetected (148). Wintzer and Uhlenbruck (146) have reported that the glycolipids in native human erythrocytes are relatively resistant to the action of neuraminidase whereas Kościelak et al. (147) reported no difficulties in liberating sialic acid from isolated glycolipid fractions. It may be that the sialoglycolipids are arranged in the cell membrane in such a way that the enzyme is sterically hindered from reaching the residues. In any case, sialic acids present on glycolipids of human red cells represent a very small percentage of the overall quantities associated with glycoproteins. Generally speaking, fucose replaces sialic acid in being the terminal sugar residue on the carbohydrate chains of human red cell membrane glycolipids. The significance of this is not known. Nevertheless, it is of interest that both fucose and sialic acid are located in the most peripheral regions of the cell where they may have the most influence. Both have the most complex biosynthetic pathways of all carbohydrate components of either glycoproteins or glycolipids (149). If the complexity of the biosynthetic mechanisms have resisted

evolutionary change it may be because the end products have very specific roles.

One of these roles may be for sialic acid to act as a masking group for penultimate cryptic determinants which if exposed signal certain properties of a molecule and evoke specific biologic responses. For example, in 1974 Ashwell and Morell (150) advanced the hypothesis that for many if not most circulating glycoproteins, sialic acid is essential for their continued viability in the circulation. This they deduced from a series of elegant experiments in which neuraminidase was utilized to cleave sialic acid and expose the penultimate nonreducing sugar, usually galactose, which in turn serves as a specific determinant for hepatic recognition and catabolism of the asialo molecules. On injection of radioactively labeled asialoceruloplasmin essentially all of the label disappeared from the circulation in a matter of minutes. Normal ceruloplasmin has a half life of ~56 hours. The label was found to be concentrated in the liver, particularly the parenchymal cells and none in Kupffer cells (151). The nonparticipation of Kupffer cells distinguishes the sequestration process of asialoglycoproteins from the clearing and subsequent phagocytosis of foreign materials or particles. Further evidence that the processes are different is provided by the fact that the survival time of foreign colloids is proportional to the amount with which the system is challenged, whereas

elimination of asialoceruloplasmin is not proportional to the dose injected (152).

In contrast to plasma glycoproteins, normal human red cells circulate in the bloodstream for 110-120 days and the degree of random destruction is low (153). Senescent cells are eliminated by phagocytic cells of the reticuloendothelial system (RES) primarily in the spleen, but also in the liver and bone marrow (154). The characteristics of the old red cell which lead to its disposal are not understood but are thought to involve changes in one or more physicochemical properties of the cell. For instance it has been suggested that decreases in electrophoretic mobility and hence in surface charge density accompany aging in vivo (155, 166) and reflect alterations in the cell surface which play a critical role in the recognition and elimination of effete erythrocytes by the RES (157). The purported decrease in surface charge density has been correlated with diminished sialic acid levels in senescent cells (158, 159, 160) and also with the fact that reinjection of red cells desialylated with neuraminidase in vitro results in a markedly shortened red cell life span in a variety of animals including dogs and goats (123), mice (161), rats (162), rabbits (163) as well as humans (164). These observations have given impetus to the hypothesis that the macrophages of the RES are tuned to recognize altered surface charge. In this hypothesis the charge characteristics of sialic acid are considered important, rather than its

role as a masking agent, although this role has not been ruled out either. Another hypothesis holds that loss of red cell membrane sialic acid on aging allows adsorption of plasma immunoglobulins, particularly IgG, onto the cell surface which in turn leads to recognition and elimination of the cells by autologous macrophages (165). Whether IgG binds because of decreased electrostatic repulsion or because of specific recognition of cryptic determinants remains unclear.

The mechanism of recognition and sequestration of effete red cells is of importance not only from the practical point of view of understanding and dealing with clinical disorders involving shortened red cell life span but is important in the larger sense of understanding and dealing with cellular senescence in general. In the latter case the red cell is a useful model because it is readily isolable and available, and has in essence no capacity to repair or regenerate damaged cell structures or components, and in humans, the degree of random destruction (accidental death regardless of age) is low (153). The cell, thus, has a defined life span and after ~1.6×10^5 recirculations (153) it is functionally worn out and eliminated, and thus, is somewhat analogous to the mechanical wearing of an automobile tire.

The human red cell also has a relatively short life span, which makes it ideal from an experimental point of view, and there already exists a wealth of data on its properties. Initial studies will be described which were undertaken to establish the relationship between the

reported reductions in sialic acid content and the electrophoretic mobility for in vivo aged cells, since there were no reports of studies in which both parameters were determined for the same cell preparations. Further studies were focused on determining the absolute quantity of neuraminidase susceptible sialic acid present on human red cells separated according to age by density fractionation procedures. It is difficult to fully interpret the experiments on the drastically reduced life span in vivo of red cells treated with neuraminidase in vitro, without fully understanding the effects of the enzyme preparation on the cell surface. Thus, studies will be described which were aimed toward characterizing the neuraminidase cell-surface interaction more fully.

5.1 Erythrocyte Fractionation

In order to study aging of erythrocytes, reliable methods are necessary for separating whole red cell populations into age fractions. Three principal methods of separating red cells in vitro into groups of different mean age exist, namely, simple centrifugation or centrifugation on density gradients, graded osmotic hemolysis and countercurrent distribution. The basis for the centrifugal methods lies in the fact that an increase in cell density has long been correlated with cell age (166, 167, 168). Increases in osmotic fragility of red cells with aging (169, 170) form the basis for separating cells into age groups by

graded osmotic shock, with the drawback that the oldest cells are destroyed first. Walter and Albertsson (171) have described systems consisting of two phase aqueous polymer solutions, e.g., dextran and polyethylene glycol, for separation or partitioning erythrocytes into age groups. However, equipment which provides for multiple partitioning of cells, i.e., counter-current distribution equipment, remains fairly expensive and is limited to processing only small quantity samples. Thus, this technique has remained relatively unexplored.

Over the years the centrifugal methods have become the most common methods for age fractionation of cells. In the work described here, both a one-step procedure and a discontinuous density gradient procedure were used. Nevertheless, caution should be exercised in interpreting studies using the centrifugal approaches, especially those using artificial gradients, as there is the inherent assumption that the cells, and especially the cell surface, is not significantly altered by the methods themselves. Furthermore, the presence of contaminating cell types, e.g., leukocytes or reticulocytes may present additional problems since the levels of activity, especially of those enzymes which are used as red cell age markers, are many fold higher in leukocytes and reticulocytes (172) and may give rise to spurious results (173).

The major problem in erythrocyte fractionation lies in obtaining age fractions which are relatively pure, especially of cells towards the

end of their life span, which in essence are those of highest interest. The centrifugal methods provide cell fractions which vary continuously in their density. Because of this it may be argued that density separation is actually an inappropriate choice of method for obtaining effete cells. Yet it remains the method of choice since all other methods suffer from similar, or worse, shortcomings, e.g., graded osmotic hemolysis destroys the oldest cells first.

5.1.1 Methods of Cell Fractionation

Blood was drawn from adult volunteers and was anti-coagulated with trisodium citrate dihydrate or ethylenediamine tetraacetate dihydrate (EDTA), the final concentrations of which were 13 mM and 4 mM, respectively. The blood was fractionated within a period of 4-6 hours after collection by use of phthalate water immiscible ester mixtures or by a high speed, one-step, centrifugal method pioneered by Rigas and Koler (174) and modified by Murphy (175).

5.1.2 Phthalate Ester Method

The anti-coagulated whole blood was washed three times at room temperature and centrifuged at ~2500 g for 10 minutes in standard saline to remove plasma proteins which might give rise to aggregation of cells with differing densities such that these aggregates would behave as large cells of intermediate density. The buffy coat material

was carefully aspirated after each wash to remove residual leukocytes. After the final wash the sample hematocrit was maintained at a high level (> 80%) in order to process a maximum amount of sample. Approximately 2.5 ml of blood was introduced into polypropylene tubes (10 x 78 mm) containing 0.7 ml of a mixture of dimethyl and dibutyl phthalate (Eastman Kodak). These tubes were centrifuged in an HB-4 Sorvall rotor in a Sorvall RC2-B temperature controlled centrifuge at 25°C at 16,300 g for 50 minutes.

The density of the ester mixtures were determined pycnometrically at 25.0°C ± 0.1°C. In an effort to determine whether cells had been centrifuged to equilibrium, fractions which were less dense than a particular ester mixture were recentrifuged.

Initial experiments were performed to determine the range of densities of a whole red cell population. Following these experiments, ester mixtures of specific densities were chosen in order to obtain approximately the 2 to 10% least and most dense cells from samples of whole blood. Following centrifugation, the cell samples were carefully separated from the ester mixtures with a Pasteur pipette and resuspended in their own plasma. This was done to "wash" the esters off the cell surface since they are not miscible with aqueous media. Subsequently, the cells were washed three times in an aqueous sodium chloride-potassium chloride-phosphate buffer solution, the exact

formulation of which was: 0.140 M NaCl, 3 mM KCl, 1 mM KH_2PO_4 and 8 mM Na_2HPO_4.

The extent of fractionation of the blood was estimated by measuring the packed cell column heights above and below the esters following centrifugation and calculating the percentage of the whole population to which a particular fraction corresponded, e.g., 5% of the least dense or most dense cells.

5.1.3 Fractionation by High-Speed Centrifugation

Simple centrifugation of red cells in the absence of artificial gradients (167) have been used for a number of years for age fractionation of red cells but was found by Rigas and Koler (174) to lead to relatively impure cell fractions. They improved on the earlier methods (167) by using ultracentrifugal field strengths to obtain stratification of erythrocytes according to their age. Murphy (175) considered that density centrifugation of cells requires movement of individual cells over one another and through a packed cell mass which would, in part, be influenced by the viscosity of the suspension as well as individual cell deformability. The required movement of the cells would be retarded at the relatively low temperatures of $\leq 5°C$ used in earlier work (174, 176). This is due to the inverse relationship between temperature and the viscosity of most fluids, including blood. Murphy (175) also showed that the deformability of red cells was

diminished at low temperature which would further hinder the stratification process. An additional consideration involved the use of a fixed-angle rotor rather than a swinging bucket rotor, since the density stratification process involves movement of cells in both directions. Murphy convincingly argues that an angle-head rotor would enhance separation of cells of different densities because of the internal circulation which results from the differences in forces at the outer and inner walls of the tube. That is, the less dense cells would rise on the inner wall of the tube in contrast to the more dense cells, which would be forced downward at the outer wall. These considerations were borne out experimentally. Centrifugation at 3 °C using a fixed angle rotor at 39, 000 g for one hour resulted in a similar degree of separation to that achieved in an ultracentrifuge at 170, 000 g for 24 hours in a swinging bucket rotor. Furthermore, maximal separation was obtained by centrifuging at 30°C for one hour at 27, 000 g, in comparison to higher and lower temperatures. Centrifugation beyond one hour or at higher speeds did not enhance the separation. For these reasons, this method was chosen to obtain cell fractions of different densities in the work described here.

Venous blood was drawn from adult human volunteers and anticoagulated with EDTA (final concentration 4 mM). The blood was centrifuged at ~2, 000 g at 4°C for 20 minutes, after which buffy coat material was aspirated. The cells were resuspended in their own

plasma and the procedure was repeated. The packed cells (hematocrit 85-90%) were transferred to 16 x 100 mm polypropylene tubes in 11 ml aliquots and centrifuged in an SS-34 Sorvall rotor for one hour at 27,000 g at ~30°C in a Sorvall RC-2B centrifuge. Cell fractions corresponding to approximately the top and bottom 5% were collected with a Pasteur pipette fashioned so that it had an opening ~3-4 mm in diameter. The pipette was held just below the surface of the red cell mass and moved slowly around the edge of the tube. On taking various percentage fractions off the cell column, some cells would invariably adhere to the side of the test tube. In order to avoid contamination of the more dense fractions, the adherent cells were swabbed off with a "Q-tip" moistened in saline. It should also be pointed out that the absolute temperature at which the fractionation was carried out, i.e., within one or two degrees of the specified temperature is not as important as maintaining a constant temperature. Fluctuations in temperature give rise to convection which leads to poor fractionation.

Following centrifugal fractionation, the red cells were washed three times in 20-30 volumes of pH 7.4 phosphate buffered saline, 0.144 M aqueous NaCl and 0.010 M aqueous potassium phosphate buffer.

5.1.4 Validation of Fractionation Technique

The efficiency of various age fractionation techniques has often been tested by radioactive labeling of newly formed erythrocytes. $^{59}Fe^{+2}$ particularly has been used for this purpose (174, 167, 177). As the cohort-labeled population ages, however, this isotope is recycled immediately into young erythrocytes which makes it especially unsuitable in experiments where accurate dating of red cells is necessary (178, 176). On the other hand, ^{14}C-glycine is also incorporated into newly synthesized hemoglobin of newly formed cells and is not significantly reutilized after cell destruction (176). However, injection of ^{14}C-glycine into human subjects is precluded. Nevertheless, it is well established that if the centrifugal technique results in a stratification of erythrocytes according to their density, the radiolabel methods would bear out that a separation according to *in vivo* age had been achieved. To validate a fractionation technique it would suffice to establish that a fractionation according to density has taken place. This may be accomplished experimentally as follows. For both whole populations of red cells and density fractionated cells a portion of the cell fraction of interest was taken up into siliconized glass micro-hematocrit centrifuge tubes followed by mixtures of dimethyl and dibutyl phthalate ester. These esters were supplied in a kit (Gravikit, Miles-Yeda, Ltd., Rehovot, Israel) consisting of a series of samples

of ester mixtures with each sample differing in density from the other by 0.004 $g \cdot ml^{-1}$. The microhematocrit tubes were then centrifuged for 30 minutes in an MSE microhematocrit centrifuge with its lid open. Cooling was provided by compressed air to maintain approximately a constant centrifuge head temperature. The percentage of cells of greater density than a particular ester mixture was calculated from the number of mm of a red cell column above and below the esters.

Estimates of cell density based on the density of hemoglobin show that the measured cell density is predominantly a function of hemoglobin concentration, i.e., the more dense cells have a higher mean cellular hemoglobin concentration (179, 176). In the study by Piomelli et al. (176), it was conclusively shown, by both $^{59}Fe^{+2}$ and ^{14}C-glycine labeling, that the more dense cells were the older cells. Thus, measuring the MCHC of cell fractions obtained by centrifuging a whole population of cells would also effectively establish that a density separation was achieved.

Certain red cell enzymes, particularly acetylcholinesterase and glutamic-oxaloacetic transaminase, have also been used as markers of the in vivo age of red cells (179, 180, 181). Red cell glutamic-oxaloacetic transaminase, (GOT, L-aspartate: 2 oxoglutarate amino-transferase EC 2.6.1.1.) the activity of which decreases with cell age, has been found to be the most sensitive of these markers (180). The GOT levels for the density fractions of cells obtained by either the

phthalate ester method or the simple high speed centrifugation method were independently measured by other personnel from this laboratory using the method of Karmen (182) as modified by Henry et al. (183).

The use of enzymes such as GOT as indicators of cell age has been challenged on the basis that graded enzymatic activities in density fractions may reflect graded contamination of these fractions with metabolically more active cells, i.e., white cells and reticulocytes (173). Caution should be exercised in placing too much confidence in red cell enzyme activity levels as primary indicators of cell age. Thus, validation of age fractionations of red cells by centrifugal means should be performed using more than one indicator of cell age, especially if radioactive labeling techniques are not employed.

Other hematologic characteristics of red cell fractions obtained by density centrifugation methods were also measured. These fraction characteristics included the percentage of reticulocytes, the mean cellular hemoglobin content (MCH), the mean cellular volume (MCV), and the sialic acid (NANA) content. Isolated reports on the variance of these parameters with cell age exist in the literature often with considerable disagreement. For example, a reduction (176, 184), an increase (185), and no variation (186) of MCV with cell age have been reported.

5.2 The Mean Cellular Values (MCV, MCH, MCHC)

All mean cellular values are calculated from three basic experimentally determined values, viz., the hematocrit, the hemoglobin content per unit volume of suspension, and red cell concentration.

5.2.1 Hemoglobin Content

The hemoglobin content of red cells was measured as the amount of hemoglobin in grams, per unit volume, in a red cell suspension. Hemoglobin was spectrophotometrically assayed at 540 nm by conversion of hemoglobin to cyanmethemoglobin according to Eilers (187). Reagents and cyanmethemoglobin standards were manufactured by Hycel and purchased from Scientific Products. Typically, 0.02 ml of blood was diluted with 5.0 ml of a reagent containing 0.6 mM $K_3Fe(CN)_6$, 0.8 mM KCN, 1 mM KH_2PO_4 and 0.5 ml $\cdot$ L^{-1} Sterox SE (Hartman-Laddon Co., Philadelphia), a nonionic detergent which enhances hemolysis and prevents turbidity due to plasma protein precipitation. The absorbance of the resulting cyanmethemoglobin solution was measured at 540 nm in a Beckman Model 25 spectrophotometer against a blank reagent solution. A calibration curve (Fig. 5-4) using standard cyanmethemoglobin solutions was prepared and expressed mathematically as a linear equation using least squares regression

analysis. The absorbance of the test sample was substituted into the equation and the concentration of hemoglobin in the test sample was calculated in $g \cdot dl^{-1}$.

5.2.2 Mean Cellular Volume (MCV in $\mu m^3 \cdot RBC^{-1}$)

The MCV is derived from the Hct, the packing efficiency factor (f), and the cell concentration ($RBC \cdot ml^{-1}$). Assuming that the Hct for a particular cell sample is 0.45 and the cell concentration is 5×10^6 $RBC \cdot ml^{-1}$, the MCV will be:

$$MCV = \left[\frac{(0.45)(0.99)}{5 \times 10^6 \text{ RBC} \cdot \text{mm}^{-1}}\right]\left[\frac{1 \times 10^9 \ \mu m^3}{mm^3}\right] = 89 \ \mu m^3 \cdot RBC^{-1} \qquad 5\text{-}1$$

5.2.3 Mean Cellular Hemoglobin (MCH in $pg \cdot RBC^{-1}$)

The mean cellular hemoglobin is a measure of the amount of hemoglobin contained in an average red cell of a particular population. Assuming that there are 15 g of hemoglobin per deciliter of a particular blood sample, and its cell concentration is 5×10^6 $RBC \cdot ml^{-1}$ then:

$$MCH = \left[\frac{15 \text{ g} \cdot \text{dl}^{-1}}{5 \times 10^6 \text{ RBC} \cdot \text{mm}^{-3}}\right]\left[\frac{1 \text{ dl}}{1 \times 10^5 \text{ mm}^3}\right] = 30 \text{ pg} \qquad 5\text{-}2$$

5.2.4 Mean Cellular Hemoglobin Concentration (MCHC in $g \cdot dl^{-1}$)

The MCHC parameter is an estimate of hemoglobin in an average red cell of a particular population, i.e., it is the ratio of the weight of hemoglobin to cell volume, and was calculated as follows, (again assuming 15 $g \cdot dl^{-1}$ hemoglobin and Hct = 0.45 and f = 0.99):

$$MCHC = \frac{[15\ g \cdot dl^{-1}]}{[0.99][0.45]} = 33.7\ g \cdot dl^{-1} \qquad 5\text{-}3$$

5.3 Reticulocyte Counts

Reticulocytes were enumerated in whole populations of red cells and on density fractions by the New methylene blue method (188). The reticulocyte, being an immature cell, contains remnants of the protein synthesizing machinery of its developing precursor stem cell. It is these remnants, particularly the ribosomes and ribonucleic acids, which on reaction with certain dyes, such as New methylene blue, precipitate as blue granules or filaments. Since reticulocytes lose the basophilic material during the maturation process, during the first one to two days in the circulation, the staining technique is specific and may be utilized for the enumeration of reticulocytes.

The staining solution consisted of 1.0 g New methylene blue (Basic Blue 24 CCI 52030, Matheson Coleman and Bell) dissolved in 100 ml

of sodium citrate-saline solution which was prepared by mixing a 0.100 M solution of sodium citrate dihydrate with 0.150 M NaCl in the ratio of 1:4 v/v, respectively. After maximum dissolution of the dye the mixture was gravity filtered through qualitative filter paper. The solution was then ready for use.

One drop of the staining solution was mixed with two drops of the red cell suspension of interest (Hct ~50%). The mixture was incubated in a small test tube at 37°C for 15-20 minutes. The red cells were then resuspended and a smear was prepared on a glass slide. The film was then examined under a microscope at a X1000 magnification using an oil immersion objective. Typically, a sufficient number of microscopic fields were surveyed until at least 50 reticulocytes were counted. The total number of red cells were counted in two to three fields of view to obtain a representative number of red cells per field. This representative number was multiplied by the number of fields surveyed for the reticulocyte count and divided into the number of reticulocytes counted. To obtain the percentage of reticulocytes, the last result was multiplied by 100.

5.4 Neuraminidase Treatment of Red Cells and Sialic Acid Assay

Membrane bound N-acetylneuraminic acid (NANA) was released from red cells by treatment with Vibrio cholerae neuraminidase (VCN,

acylneuraminyl hydrolase EC 3.2.1.18). The enzyme which is prepared as described by Schick and Zilg (189) was supplied in 0.05 M sodium acetate buffer, pH 5.5, containing 0.15 M NaCl and 0.01 M $CaCl_2$ (enzyme buffer) in 1 ml vials containing 500 units of activity where one unit is the amount of enzyme required to release 1 μg of N-acetylneuraminic acid from human α_1-acid glycoprotein in 15 minutes at 37°C. The enzyme was manufactured by Behringwerke, Marburg/Lahn, FGR and is currently available from the Calbiochem-Behring Corp., La Jolla, CA.

Typically, a stock suspension of erythrocytes was prepared at an hematocrit of ~20% in phosphate buffered saline (PBS, 0.144 M NaCl and 0.01 M potassium phosphate buffer, pH 7.4). The cell concentration of the suspension was determined according to the methods outlined in Section 2.5 and usually adjusted to ~2×10^9 cells $\cdot$ ml^{-1}. An aliquot of ~1.2 ml was weighed and 0.3 ml of 500 units $\cdot$ ml^{-1} VCN in enzyme buffer was added to the cell suspension at 37°C to give a final VCN concentration of ~100 units per ml of the final suspension volume. The suspension was mixed and incubated for one hour at 37°C in a water bath during which time it was agitated at least twice at regular intervals. A control suspension was incubated in the same manner except that an equivalent volume of pH 5.5 enzyme buffer was added instead of enzyme. Following the incubation, samples were centrifuged for 10 minutes at ~1000 g at room temperature and

supernatant fluids were sampled for analysis of liberated sialic acid. As a test for the completeness of removal of sialic acid by VCN an unfractionated red cell population was treated and then re-treated with VCN.

As a routine, sialic acid was assayed by the thio-barbituric acid (TBA) assay (36). Alternatively, to test the reliability and accuracy of the TBA method, the alkaline Ehrlich (36) and resorcinol (190) methods were also used to quantitate sialic acid. These latter two assays were performed by research assistants in the laboratory, as were the tests for the presence of interfering substances in the assay of sialic acid in the VCN digests. Experiments on the presence of interfering substances involved treatment of supernatant fluids with trichloroacetic acid (TCA) (for precipitation and removal of proteins from solution) followed by ether extraction. The supernatant fluid samples were mixed with a 70% w/v solution of TCA in water to give a final concentration of 9-10% w/v TCA. The resultant mixture of supernatant fluid and precipitated protein was cooled in an ice bath for ~15 minutes, followed by centrifugation and decantation of the supernatant fluid. The fluid was then extracted three times at room temperature with 2 volumes of diethyl ether which had been saturated with water. The weight of the supernatant fluid after each of the steps was recorded in order that the final volume and dilution factors could be computed.

5.5 Analytical Particle Electrophoresis

Whole populations and cells fractionated according to age on the basis of their density were electrokinetically characterized in both physiological ionic strength and low ionic strength saline media, essentially according to the methods outlined in Section 3.5. Specifically, the cells were washed three times in 0.15 M NaCl-$NaHCO_3$, pH 7.4 ± 0.2 and suspended therein for electrophoresis at high ionic strength. For low ionic strength work, the cells were washed two additional times in 0.030 M NaCl-$NaHCO_3$, pH 7.4 ± 0.2 rendered isotonic with 0.220 M sorbitol and also suspended therein for electrokinetic analysis.

5.6 Results

It is well known that the density of fluids is dependent upon temperature. Thus, it may easily be envisioned that the efficiency of density fractionations of blood using discontinuous phthalate ester density gradients will, in part, depend upon the maintenance of constant temperatures during the centrifugation. Experimentally determined absolute densities of whole populations or density fractions of red cells will also be a function of temperature.

The densities of dimethyl and dibutyl phthalate as a function of temperature are presented in Fig. 5-1. The temperature coefficients,

Figure 5-1. The dependence of density on temperature of dimethyl and dibutyl phthalate.

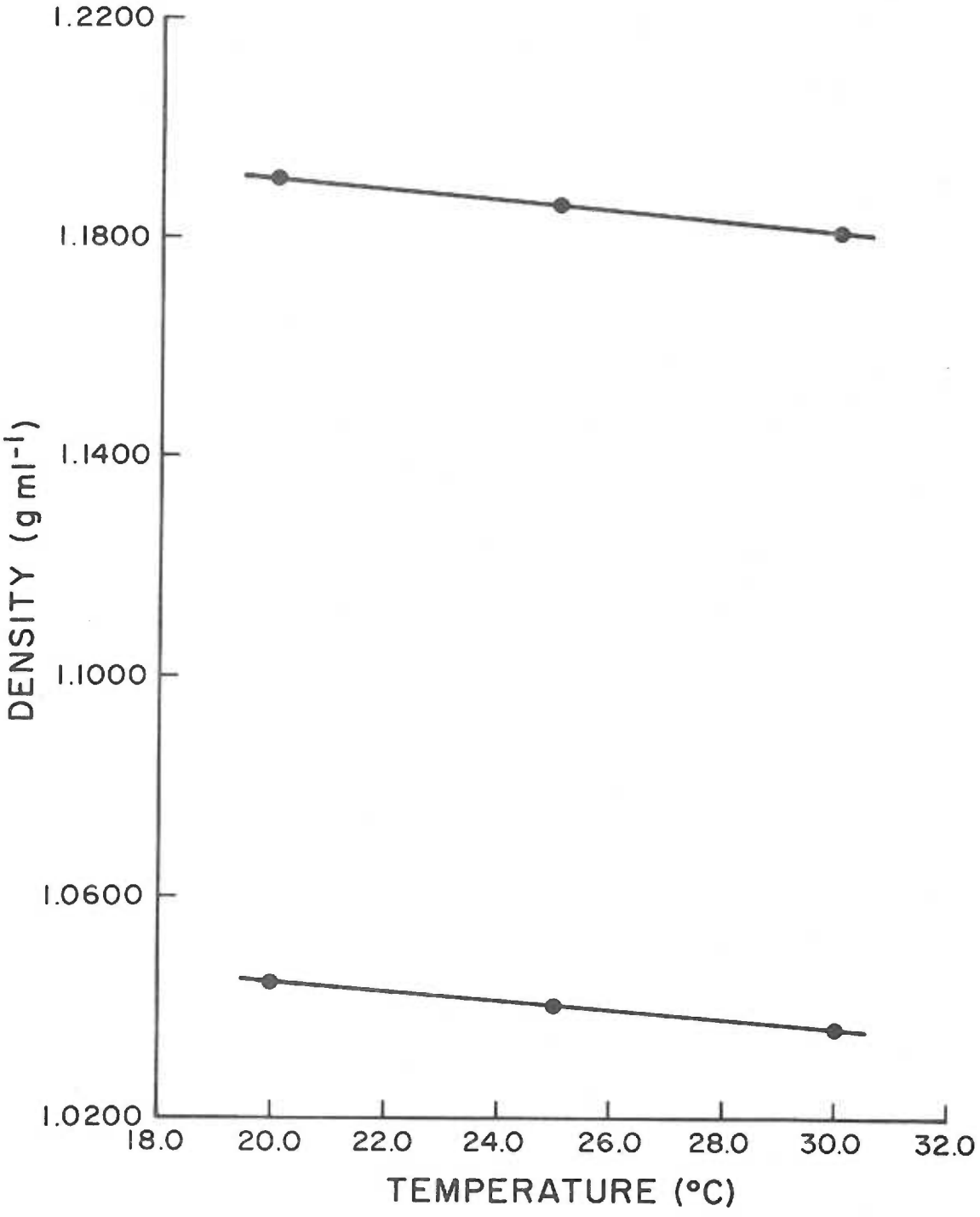
1.2200
1.1800
1.1400
1.1000
1.0600
1.0200
DENSITY (g ml⁻¹)
18.0
20.0
22.0
24.0
26.0
28.0
30.0
32.0
TEMPERATURE (°C)

calculated from the best fit line through the data points obtained by least squares linear regression analysis, for dibutyl phthalate and dimethyl phthalate are 8×10^{-4} g · ml^{-1} · °C^{-1} and 9×10^{-4} g · ml^{-1} · °C^{-1}, respectively. That is, the variation of the densities of the esters with temperature is, within experimental error, colinear. The densities of phthalate ester mixtures as a function of the ratio of dimethyl to dibutyl phthalate, are shown in Fig. 5-2. The data were utilized in preparing ester mixtures having specified values of density, such that the density distribution of a whole population of red cells might be experimentally determined. Such a density distribution of a whole population of human red cells is depicted in Fig. 5-3. It should be noted that the mean density of this particular sample of cells is 1.091 g · ml^{-1}. This is in relatively good agreement with values ranging from 1.089 to 1.107 g · ml^{-1} reported in the literature (191).

Using the data in Fig. 5-3, it may be convincingly stated that maintenance of a constant specified temperature during centrifugation is imperative in order to obtain accurate cell density distribution data. An error of 5°C for example, would shift the curve in Fig. 5-3 by ~0.004 g · ml^{-1} or approximately by 30% of the density range into which 90% or more of all the red cells fall.

In the phthalate ester fractionation technique the cells to be fractionated are always layered on top of the ester mixture. Therefore,

Figure 5-2. The density of mixtures of dibutyl phthalate and dimethyl phthalate as a function of their composition at 25.0°C.

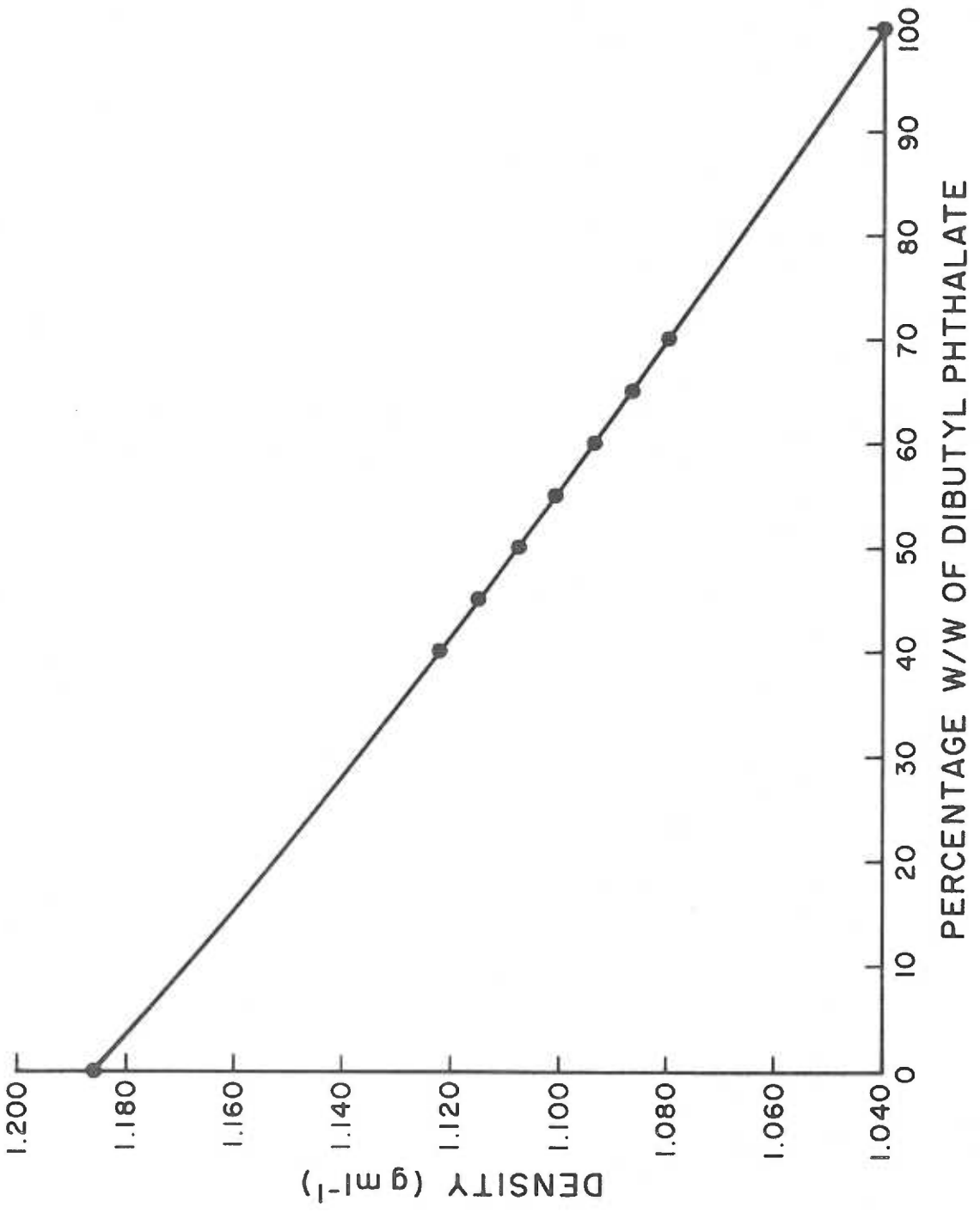
DENSITY (g ml⁻¹)
1.200
1.180
1.160
1.140
1.120
1.100
1.080
1.060
1.040
0
10
20
30
40
50
60
70
80
90
100
PERCENTAGE W/W OF DIBUTYL PHTHALATE

Figure 5-3. Density distribution of a whole population of human red blood cells as determined with phthalate esters.

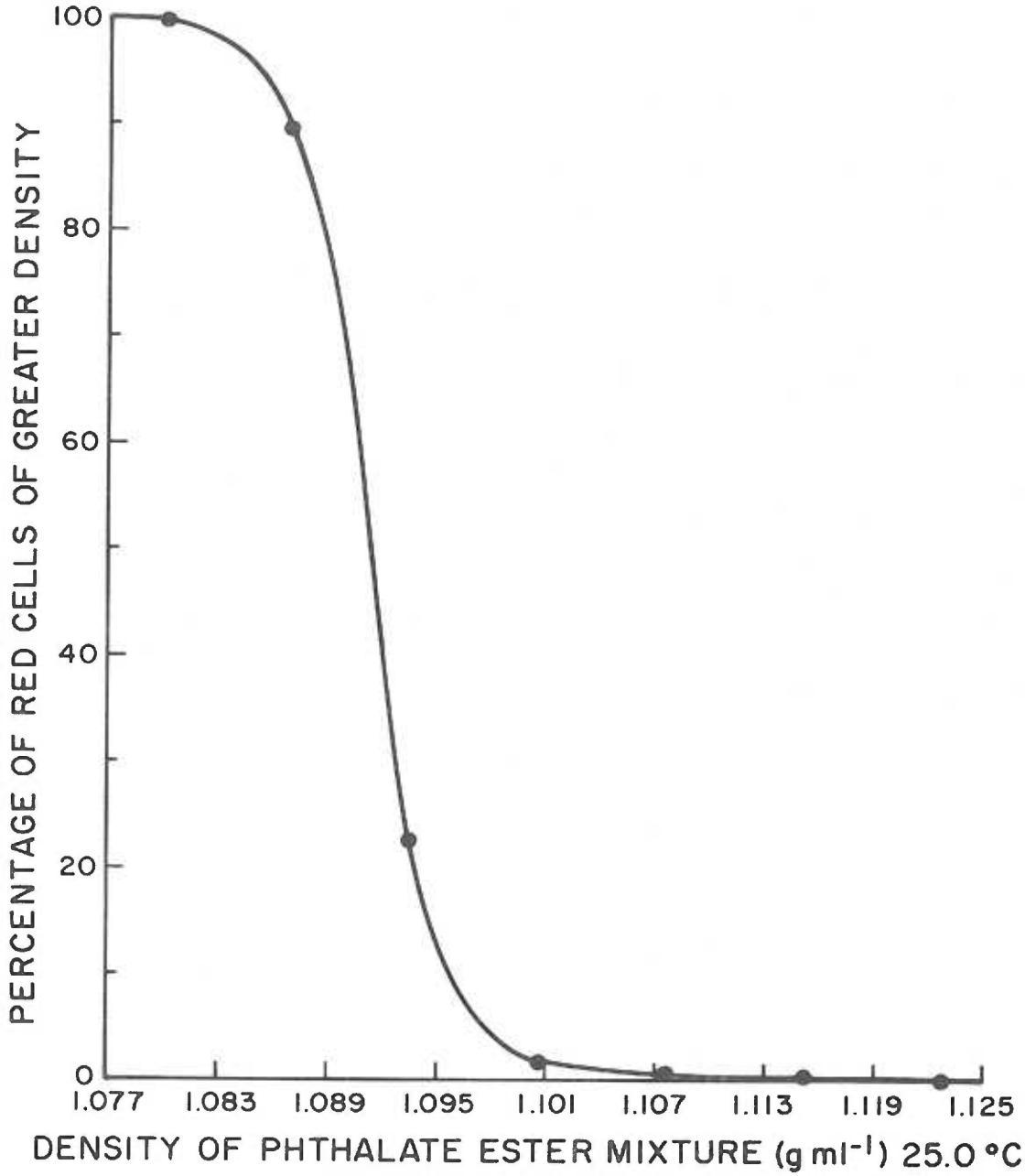
100
80
60
40
20
0
PERCENTAGE OF RED CELLS OF GREATER DENSITY
1.077
1.083
1.089
1.095
1.101
1.107
1.113
1.119
1.125
DENSITY OF PHTHALATE ESTER MIXTURE (g ml⁻¹) 25.0 °C

the least dense cells, i.e., the youngest cells, are never exposed to the ester. It is not inconceivable that these water immiscible esters may interact with the cell membrane and markedly alter its properties and concomitantly the electrokinetic properties of the cells as well. Experiments, the data of which are presented in Table 5-1, did not bear out this possibility. The electrophoretic mobilities of control cells and cells exposed to the esters, both at high and low salt concentrations, were identical. This, however, does not rule out other changes in the physicochemical properties of the cells which might not affect the electrophoretic mobility of the cells. Thus, as a rule, exposure of cells to such non-physiological conditions should, if possible, be avoided. This is one of the main reasons why an alternate density fractionation technique was also investigated.

Figure 5-4 depicts a representative standard curve for the cyanmethemoglobin assay. As can be seen, the absorbance is a linear function of the hemoglobin concentration.

The hematologic parameters for the density fractions obtained by the phthalate ester method are presented in Table 5-2, and those for the cell fractions obtained by the one-step high speed centrifugation method are given in Table 5-3.

The cells of the top fractions, with either separation technique, tended to have higher MCV, GOT, sialic acid and reticulocyte counts. Cells from the bottom density fractions, consistently, had lower MCV,

GOT, reticulocyte counts, as well as lower sialic acid levels. The MCHC increased in all instances in going from the less dense to the more dense cell fractions, whereas the MCH tended to be more variable.

Table 5-1. Electrophoretic mobility of human red cells at pH 7.4 and 25.0°C before and after exposure to dibutyl and dimethyl phthalate ester mixtures.

Treatment of RBC	Suspending Medium	Observed u ± S.D. (n)
None	0.015 M NaCl	-1.08 ± 0.03 (30)
None	0.015 M NaCl-0.247 M sorbitol	-2.35 ± 0.08 (30)
Exposure to phthalate, esters and fractionation conditions	0.15 M NaCl	-1.08 ± 0.04 (30)
Exposure to phthalate, esters and fractionation conditions	0.015 M NaCl-0.247 M sorbitol	-2.35 ± 0.07 (30)

The electrophoretic mobilities of freshly drawn human red cells and cells obtained by density centrifugation by the phthalate ester method and the one-step centrifugation method are shown in Table 5-4. The fractions at the extremes of the density range, i.e., cells which constitute less than 10% of the whole population, were electrophoretically characterized at ionic strengths of 0.150 and 0.030 g-ions·L^{-1} at 25.0°C, pH 7.4 ± 0.2. No significant differences in the mean electrophoretic mobilities at a given ionic strength were observed between any

Figure 5-4. A standard curve illustrating the linearity of the cyanmethemoglobin assay. The indicated amounts of a standard solution of cyanmethemoglobin were added to each sample and the assay was carried out as described in Section 5.2.1.

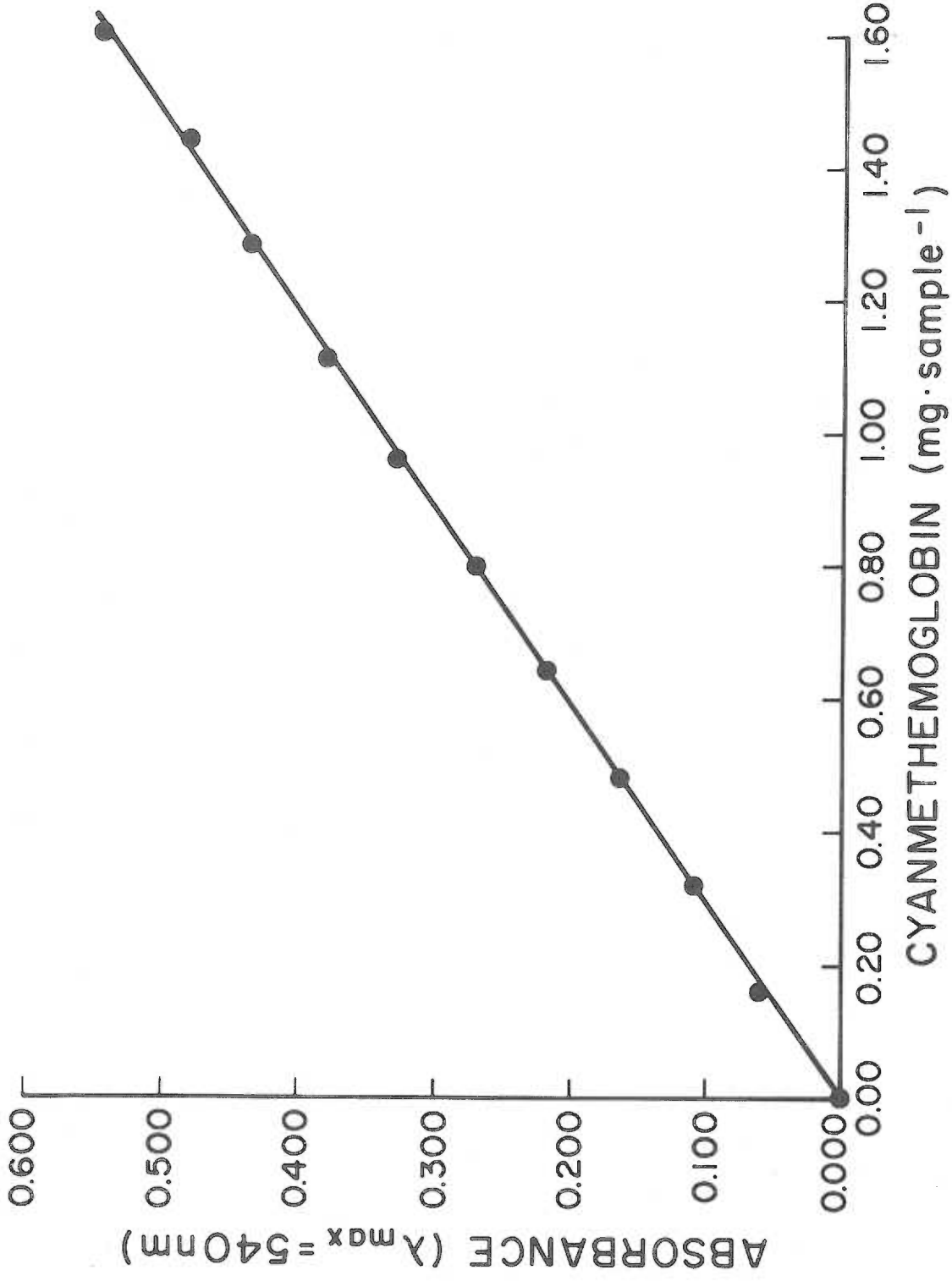
ABSORBANCE (λ_{max} = 540nm)
0.600
0.500
0.400
0.300
0.200
0.100
0.000
0.00
0.20
0.40
0.60
0.80
1.00
1.20
1.40
1.60
CYANMETHEMOGLOBIN (mg·sample^{-1})

Table 5-2. Hematologic characteristics of red cell fractions obtained by the phthalate ester method.

Exp. No.	Population Fraction	RBC Density[1]	Retics. (%)	MCH (pg)	MCV (fl)	MCHC ($g \cdot dl^{-1}$)	NANA[2] ($fg \cdot RBC^{-1}$)	GOT[3] ($IU \cdot RBC^{-1} \times 10^{11}$)
1	Top 6%	<1.085	5.5	31.5	96	32.8	20.1	--
	Whole	--	1.2	34.6	100	34.6	--	--
	Bottom 10%	>1.100	0.6	35.3	87	40.6	13.8	--
2	Top 5%	<1.085	6.7	37.2	104	35.8	20.8	16.9
	Whole	--	1.9	35.6	97	36.7	19.8	11.8
	Bottom 6%	>1.103	1.2	35.7	86	41.5	19.6	6.6
3	Top 7%	<1.081	3.0	33.4	98	34.1	21.2	13.5
	Whole	--	1.2	30.3	88	34.4	16.9	7.5
	Bottom 2%	>1.097	0.6	31.5	79	39.9	16.8	4.9

[1] Density listed is that of the phthalate ester mixture at 20°C.

[2] NANA: N-acetylneuraminic acid.

[3] GOT: Glutamic-oxaloacetic transaminase.

Table 5-3. Hematologic characteristics of red cell fractions obtained by the high speed centrifugation method described by Murphy (184).

Exp. No.	Population Fraction	Median Density	Retics. (%)	MCH (pg)	MCV (fl)	MCHC ($g \cdot dl^{-1}$)	NANA[1/] ($fg \cdot RBC^{-1}$)	GOT[2/] ($IU \cdot RBC \times 10^{11}$)
4	Top 5%	1.095	6.3	31.8	95	33.5	18.4	9.4
	Whole	1.102	3.8	32.3	92	35.5	17.6	5.2
	Bottom 5%	1.107	1.8	33.0	82	40.2	16.6	4.3
5	Top 5%	1.095	6.6	27.4	87	31.5	17.8	10.7
	Middle 90%	1.103	1.2	27.2	80	34.0	16.0	3.9
	Bottom 5%	1.104	0.5	27.6	77	35.8	15.9	2.0
6	Top 5%	1.098	6.3	30.4	89	34.2	17.8	9.7
	Whole	1.104	2.1	33.1	87	38.0	17.3	6.1
	Bottom 5%	1.107	0.4	33.2	79	42.0	16.2	4.8
7	Top 5%	1.096	-	26.5	89	29.9	20.3	9.7
	Whole	1.102	-	27.1	85	31.9	17.2	5.0
	Bottom 5%	1.106	-	26.5	77	34.4	16.3	3.5

[1/] NANA: N-acetylneruaminic acid.

[2/] GOT: Glutamic-oxaloacetic transaminase.

Table 5-4. Electrophoretic mobilities of fresh human red cells fractionated on the basis of density.

Exp. No.[1]	Population Fraction	Electrophoretic Mobility ($\mu m\ sec^{-1}\ V^{-1}\ cm$) ± S. D.[2]	
		0. 15 M NaCl	0. 03 M NaCl
1	Whole	-1. 09 ± 0. 05 (10)	-1. 77 ± 0. 10 (46)
	Top 6%	-1. 10 ± 0. 06 (30)	-1. 72 ± 0. 11 (56)
	Bottom 10%	-1. 10 ± 0. 06 (30)	-1. 72 ± 0. 09 (46)
2	Whole	-1. 10 ± 0. 05 (48)	-1. 74 ± 0. 09 (12)
	Top 3%	-1. 09 ± 0. 07 (60)	-1. 71 ± 0. 09 (50)
	Bottom 4%	-1. 09 ± 0. 06 (30)	-1. 70 ± 0. 07 (26)
	Bottom 7%	-1. 11 ± 0. 05 (32)	-1. 72 ± 0. 09 (28)
3	Whole	-1. 09 ± 0. 05 (40)	-1. 76 ± 0. 08 (42)
	Top 7%	-1. 09 ± 0. 07 (20)	-1. 74 ± 0. 06 (20)
	Bottom 2%	-1. 12 ± 0. 08 (20)	-1. 73 ± 0. 12 (20)
4	Whole	-1. 10 ± 0. 04 (24)	-1. 76 ± 0. 09 (20)
	Top 5%	-1. 10 ± 0. 07 (20)	-1. 82 ± 0. 07 (20)
	Bottom 5%	-1. 11 ± 0. 07 (20)	-1. 84 ± 0. 09 (20)
5	Whole	-1. 08 ± 0. 06 (36)	-1. 79 ± 0. 09 (32)
	Top 5%	-1. 08 ± 0. 04 (20)	-1. 77 ± 0. 10 (20)
	Middle 90%	-1. 08 ± 0. 06 (28)	-1. 79 ± 0. 08 (20)
	Bottom 5%	-1. 10 ± 0. 06 (28)	-1. 78 ± 0. 07 (20)
6	Whole	-1. 09 ± 0. 07 (40)	-1. 74 ± 0. 10 (30)
	Top 5%	-1. 05 ± 0. 08 (20)	-1. 72 ± 0. 09 (20)
	Bottom 5%	-1. 07 ± 0. 08 (20)	-1. 70 ± 0. 09 (20)

[1] Experiments 1-3, fractionation by phthalate ester method; experiments 4-6, fractionation by the high speed centrifugation method described by Murphy. The samples were coded such that the observer was unaware of the sample origin.

[2] Mean mobility ± sample standard deviation; the number of individual cells measured appears in parentheses.

of the fractions of the whole populations analyzed. In these experiments, the operator of the electrophoresis equipment was unaware of the identity of the fractions being analyzed so as to minimize the possibility of errors arising from operator bias. In addition to the author, a number of individuals from this laboratory were able to corroborate these results.

The sialic acid levels were estimated in addition to the TBA method, by the alkaline Ehrlich method, and the resorcinol procedure. The recovery of sialic acid was tested experimentally by adding known amounts of sialic acid to a red cell suspension and to the red cell incubation buffers (PBS) in the absence of cells. The samples were incubated for one hour at 37°C and assayed for sialic acid. No substantial differences in the amounts of sialic acid recovered were observed for any of the three assay methods. Hemolysis of red cells was shown not to interfere in the TBA assay system. The completeness of removal of sialic acid from red cells by VCN was determined by retreating VCN-modified red cells with VCN. Supernatant fluids from such retreated cell suspensions gave 0.1-0.4 $fg \cdot RBC^{-1}$ of TBA-positive material. Trichloroacetic acid treatment, plus ether extraction of the supernatant fluids from VCN digests, did not produce significant decreases in either the level of sialic acid assayed by the TBA method or the absorbance ratio (Abs 549/Abs 532), which is indicative of the absence of significant levels of interfering substances.

These experiments also established that no significant losses of sialic acid occurred during any of the assay procedures.

5.7 Discussion

Reliable methods for separating red cell populations according to age are required in order to describe the biochemical and biophysical changes that erythrocytes undergo during the aging process *in vivo*. Over the years a variety of techniques have been used, the most common involving centrifugal separation of cells on the basis of differences in their density.

Various polymeric additives have been used to aid in the centrifugal separation of cells. For example, the use of discontinuous density gradients of albumin (176) or Stractan 2, an arabino-galactan polysaccharide (192) have resulted in the successful separation of old and young red cells. Danon and Marikovsky (193) on the other hand, have used phthalate ester mixtures to separate red cells on the basis of density. In selecting a separation procedure it must be borne in mind that macromolecular additives which promote red cell aggregation or immiscible fluids which may interact with the red cell membrane are less desirable candidates for the fractionation of red cells than methods such as those described by Rigas and Koler (174) or Murphy (175). Stratification of erythrocytes according to cell age has been demonstrated by centrifugal fractionation combined with $^{59}Fe^{+2}$ and

^{14}C-glycine labeling of red cells in vivo (176). As discussed by Weed and Reed (194) both losses in hemoglobin and volume may accompany red cell aging. If MCHC is the major determinant of separation during centrifugation, and if there is a discontinuity in the rate of change of MCH with MCV toward the end of the life span of the red cell, a range of MCHC values (densities) would be produced for cells of the same age. Data on normal rabbit cells in which the membrane was labeled with ^{125}I and the hemoglobin with ^{51}Cr indicated a more rapid loss of ^{51}Cr then ^{125}I near the end of the normal red cell life span (195). Thus, whereas cells from the least dense regions may be regarded as young cells, cells from the most dense fractions probably represent a range in age of older cells. That this conclusion is reasonable may also be seen from the following analysis. Figure 5-3 shows that approximately 90% or more of the red cells are distributed through a rather narrow density range of about 0.013 $g \cdot ml^{-1}$. If the red cell loses only about 5% of its mass of hemoglobin on aging, in the absence of a concomitant change in volume, the resulting density change (~0.006 $g \cdot ml^{-1}$) is sufficient to shift the cell from the extreme dense to the central region of the density distribution. Such a mechanism would tend to mask any changes in cell properties which may occur during the last few days of the life span of the cells. In addition, such small changes in hemoglobin content would be difficult to quantitate, since the magnitude of these changes is close to the limits of precision

and accuracy of current methodologies for cell counting and measuring hemoglobin concentration.

In this study, trends of MCHC and MCV for the different cell fractions, the data for which are shown in Tables 5-2 and 5-3, are in agreement with those reported for cells fractionated according to their density (175, 176, 185, 196). Sass et al. (180), have examined different levels of a column of centrifuged red cells for various enzyme activities and have concluded that GOT provides the most sensitive indicator of cell age. Accordingly, GOT activities were used as indicators of cell age in this study. The basis for the decrease in GOT activity with increasing age is not known. For example, it is not clear whether the decrease in activity represents an inactivation of the enzyme with age, or its physical loss from the system, or whether it is due to decreased levels of its cofactor, pryidoxal phosphate (197). Some enzyme activity losses may be attributed to the metamorphosis of the reticulocyte to the erythrocyte. However, how much of the markedly elevated levels of GOT activity are due to the higher levels of reticulocytes in the upper fractions remains a matter of conjecture. Thus, the hematological characteristics of the red cell fractions obtained by either the phthalate ester method or the one-step high speed centrifugation method compare favorably with other methods reported in the literature and indicate a successful fractionation according to in vivo cell age.

5.7.1 The Relationship between Cell Age and Charge Density

Danon and Marikovsky (155) first reported a difference in surface charge density between young and old red cells separated on the basis of age by means of a discontinuous density gradient. Later, Yaari (156) obtained similar results for human red cells using water immiscible mixtures of dimethyl and dibutyl phthalate for density fractionation. These observations have gained wide acceptance in the hematological literature, particularly since these results suggest a plausible mechanism for the removal of effete cells from the circulation.

Employing two density fractionation procedures, red cells from the extremes of their density distribution were examined by electrophoresis at two ionic strengths. The data, summarized in Table 5-4, unexpectedly showed no experimentally significant mobility differences between the extreme red cell populations. The expected mobility differences should have been easily detected, as may be seen from Fig. 5-5 in which Yaari's data have been repolotted (broken line) and compared with our own data at physiological ionic strength (solid line). Yaari's data suggest that the electrophoretic mobility is a monotonic function of cell density, whereas our data indicate that the electrophoretic mobility is essentially invariant with cell age, at least over the central 90-95% of the red cell distribution. The coefficients of

Figure 5-5. Mean electrophoretic mobility of human red cells as a function of density. ● Yaari's data (156); stippled boxes, range of mean mobilities for data in Table 5-1; vertical bars, ± SD calculated from Yaari's data. Percentages refer to percentage of the total red cell population. Whole population point ± SD derived from Yaari's data.

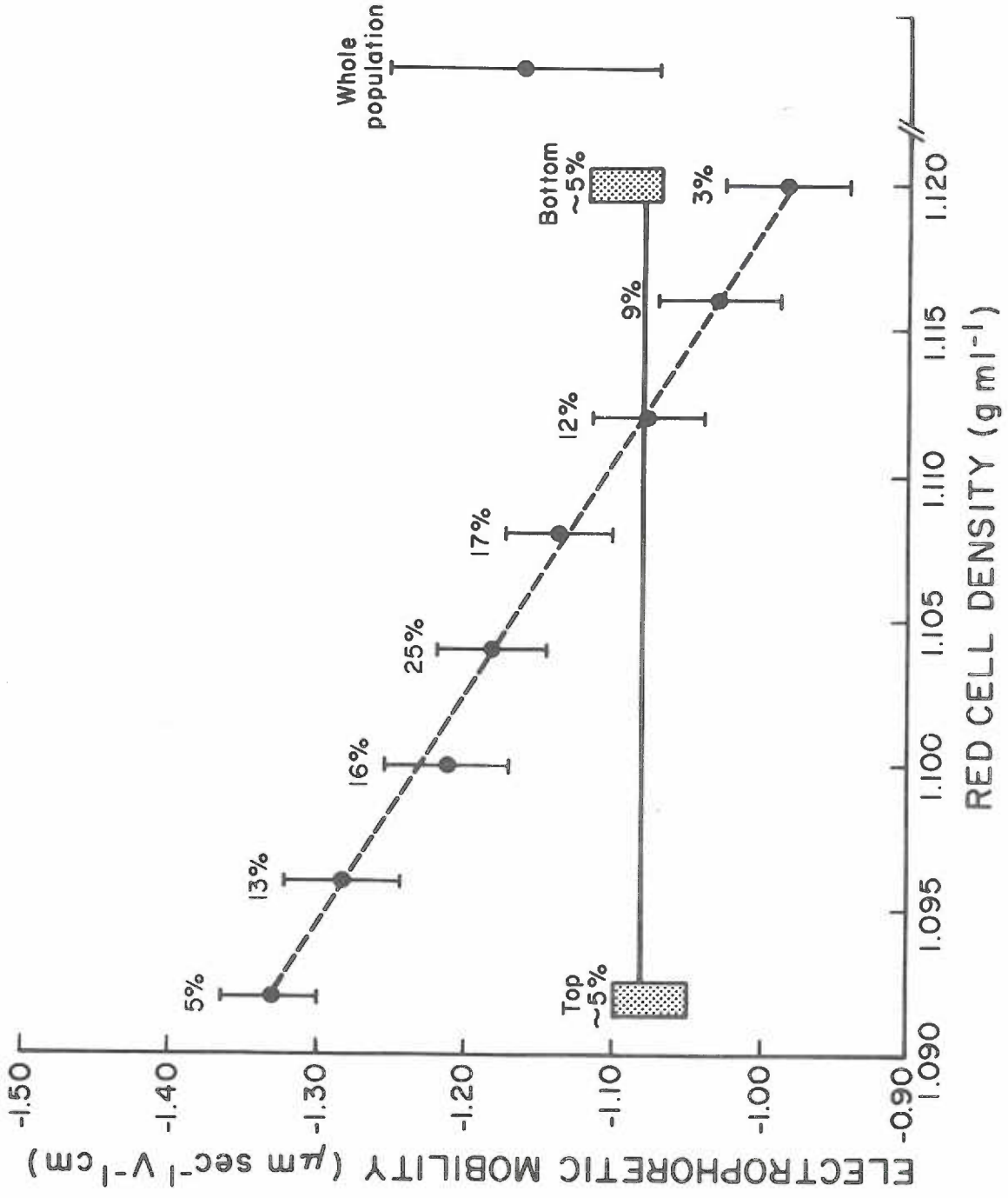
ELECTROPHORETIC MOBILITY (μm sec⁻¹ V⁻¹cm)
-1.50
-1.40
-1.30
-1.20
-1.10
-1.00
-0.90
1.090
1.095
1.100
1.105
1.110
1.115
1.120
RED CELL DENSITY (g ml⁻¹)
Whole population
Bottom ~5%
Top ~5%
5%
13%
16%
25%
17%
12%
9%
3%

variation for the data sets in Table 5-4 average 5.5%. It is probable that much of the variation is due to instrumental factors rather than appreciable dispersity of mobilities of the cell population. Thus, the differences in mobility reported by Danon and Marikovsky (155), Yaari (156), and Marikovsky (198) if real, ought to have been detected. Objections that the data base is insufficient for the above conclusions to be drawn seem unfounded when viewed in context with the following additional findings.

At the time that this work was in progress, Luner and Szklarek (199) reported observations similar to ours, namely, that the electrophoretic mobility of red cells was independent of cell density and thus, presumably, cell age. Similar observations were reported by Ware (200). Luner and Szklarek carried out electrophoresis of erythrocyte density fractions by the continuous flow streak deflection method using the Kolin endless belt electrophoresis apparatus (201). If electrophoretic heterogeneity between cell samples were present it would have been evidenced by progressive sample band broadening and by actual band splitting if the samples were made up of cells having multimodel mobility distributions on passage through the electrical field of the instrument. Ware, applying laser Doppler velocimetry (LDV) (202) to the problem of measuring the electrophoretic mobility distributions of cells was also unable to demonstrate heterogeneity in the mobility of red cells density fractionated by ultracentrifugation. These

observations by three independent groups (200) employing different electrophoresis instrumentation, suspending media, and density fractionation procedures provide a strong case for the invariance of the mobility of red cells of different densities and of different ages. It should be emphasized that endless belt electrophoresis, as well as LDV, are population methods, i.e., the mobility of a large number of cells is simultaneously being monitored in contrast to analytical particle electrophoresis where the mean mobility of a cell population is derived from measurements on individual cells which are then averaged.

In order to compare the levels of sialic acid per red cell, found in this study (Tables 5-2 and 5-3), with values reported in the literature, a list was compiled, and the values were converted, where possible, into the same units, i.e., $fg \cdot RBC^{-1}$ for sialic acid per red cell. The results are presented in Table 5-5. As can be seen, there is extreme variability even in the results reported for unfractionated red cell populations, where values ranged between 6.3 and 22 fg sialic acid per red cell, a variation of more than 300%.

The divergent results given in Table 5-5 for human red blood cells may have arisen in one or a combination of three ways: (1) elevation in NANA values originating from the contribution of interfering substances in the supernatant fluids; (2) losses of sialic acid during purification procedures intended to eliminate interfering substances;

Table 5-5. Total NANA levels reported for human red cells and subpopulations obtained by density centrifugation.

Cell Population	NANA[1] Released by	NANA Assay by	Reported NANA	Calc.[2] NANA $(fg\ RBC)^{-1}$	Ref. No.
Whole	Acid	TBA	223 nmole/ml RBC	6.3	203
	Acid	TBA	237 nmole/ml RBC	6.7	164
	VCN	Resorcinol	89 $\mu g/10^{10}$ RBC	8.9	91
	Acid	Resorcinol	1.17 pg $\times 10^{-2}$/RBC	11.7	204
	VCN, Acid	TBA-Resorcinol	135 μg/ml RBC	12.2	142
	Acid	TBA	140 μg/ml RBC	12.7	205
	---	---	19.2 mg/100 ml RBC	17.4	206
	---	---	2.2×10^{-14} g/ghost	22	207
Whole	Acid, NANAase[3]	TBA	348 ng/mg Hb	10.4	
Top 20%	Acid, NANAase[3]	TBA	386 ng/mg Hb	11.6	159
Bottom 11%	Acid, NANAase[3]	TBA	327 ng/mg Hb	9.8	
Whole	Acid	TBA	1.72 μmole/g Hb	16.0	
Top 10%	Acid	TBA	1.89 μmole/g Hb	17.5	160
Bottom 10%	Acid	TBA	1.54 μmole/g Hb	14.3	
Top 14%	Acid	TBA	20.7 $\mu g/10^9$ RBC	20.7	158
Bottom 14%	Acid	TBA	18.9 $\mu g/10^9$ RBC	18.9	

[1] NANA: N-acetylneuraminic acid.

[2] Conversions were made assuming a NANA molecular weight of 309.3, MCH of 30 pg, and 1.1×10^{10} RBC ml^{-1} packed cells.

[3] *Clostridium perfringens* neuraminidase.

or (3) erroneous assumptions or inaccurate supporting data used in calculating or normalizing the results.

Schauer et al. (203) comment that ether extraction of the supernatant fluids from neuraminidase-treated red cells for removal of lipid, and ion exchange clean-up (adsorption of sialic acid to an anion exchange resin with subsequent elutiation for formic acid) are both required to eliminate interfering substances in the TBA assay system. When these measures were not taken, they report that results were elevated up to 200%, with indications of interfering chromophores in the TBA assay based on aberrant absorption spectra in the 510-540 nm region. As a result of the problems evident in the published literature, studies were designed that would establish the validity, accuracy, and reproducibility of our quantitation techniques for erythrocyte sialic acid. The use of three independent NANA assay methods, the alkaline Ehrlich (36), resorcinol (190), and TBA assays (36), made it unlikely that interfering substances would influence each procedure in exactly the same way. Thus the agreement obtained between results by the different methods under given conditions is a strong indication that the values for sialic acid were not influenced significantly by interfering substances.

The average value of 17.8 ± 1.2 fg sialic acid per red cell released by VCN from whole human red cell populations agrees well with those reported by Cohen et al. (160) and Greenwalt and Steane

(158). Like Greenwalt and Steane (158) no evidence of interfering substances could be found by spectral examination of the chromophores produced in the TBA assays. Attempts to extract any interfering substances by TCA and ether treatments had no significant influence on the TBA results. The assayed NANA values from the alkaline Ehrlich and resorcinol assays were within 20% of the TBA assays. Therefore it is concluded that the 2.8-fold difference between the results here and those of Jancik et al. (164) and Schauer et al. (203) is not explained by interfering substances.

The data presented in Tables 5-2 and 5-3 show that the least dense, or youngest cells, contained an average of 12% more neuraminidase susceptible sialic acid than the old cells (19.5 ± 1.4 versus 17.1 ± 1.3 $fg \cdot RBC^{-1}$) even though no significant differences in electrophoretic mobility were observed. As shown in Section 1.3, the electrophoretic mobility is a reflection of the surface charge density of the cell. The apparent discrepancy between constant surface charge density during aging and simultaneous decreases in the levels of membrane associated sialic acid can be largely accounted for by the decrease in surface membrane area which accompanies loss of portions of the red cell membrane during its long journey through the circulation. Analytical data in the literature which indicate decreases in the total amount of many membrane components but a constancy in the ratios of the components to one another lend support to the loss of membrane

hypothesis. For example, Canham (196) has estimated the mean surface area and the volume of red cells were about 10% less than those for cells from the top 20% fraction (phthalate ester method). Similar reductions in red cell size with increasing age in vivo have also been reported by Piomelli et al. (176) and Van Dilla and Spalding (184) as well as having been confirmed here. The decreases in size taken together with the approximately constant MCH values (also in agreement with results reported elsewhere) account for the average 16% increase in the MCHC values of cells in going from the top to the bottom density fractions (see Tables 5-2 and 5-3). The magnitude of the changes in these physical parameters (volume, surface area, and MCHC) are comparable to the extent of the changes which occur in the chemical composition of the cells. A loss of phospholipid with cell age have been described by Westerman et al. (208), however these workers found no change in the phospholipid content per unit surface area. Similarly, Cohen et al. (160) found a decrease in both cholesterol and phospholipid as well as membrane protein however, there was no alteration in the cholesterol:phospholipid phosphorus ratios. Winterbourn and Batt (209) found no age-related alterations in the relative amounts of the major membrane lipids. These results strongly suggest that during red cell aging, portions of the membrane may be lost without disproportionate removal of any particular membrane constituent. In light of all of these considerations it is not difficult to

envision how loss of sialic acid may accompany aging of human erythrocytes without resulting in a change in the surface concentration of sialic acid or a change in the electrophoretic mobility of the cells.

However, a major obstacle to lending full credence to this interpretation have been electron micrographs of old and young human red cells treated with electron dense, positively charged colloids, such as colloidal iron oxide or cationized ferritin, showing old cells to have a diminished label density in comparison to young cells (119, 210). The quantitative aspects of colloidal iron binding in the ultrastructural visualization of acidic groups such as sialic acid on cell surfaces was called into question by Weiss a number of years ago (211), primarily because of the low pH (~1.8) at which the labeling is accomplished. At this pH many of the acidic groups having a pK greater than pH 2.0, would be protonated and thus would be unlikely to react with positively charged particles. To circumvent these objections, Danon et al. (210) used cationized ferritin for labeling either native or glutaraldehyde pretreated old and young erythrocytes at physiological pH and ionic strength. Cationized ferritin was prepared from horse spleen ferritin by reaction of the protein carboxyl groups with N, N dimethyl-1, 3 propanediamine. If native cells were labeled a considerable degree of agglutination took place which could be diminished by prefixing the cells with glutaraldehyde. The agglutination was attributed to bridging of the cell surfaces by the ferritin

complexes. It is unclear as to why human red cells agglutinated to a greater extent than rabbit red cells. In any case, it was shown that young rabbit cells were labeled with a uniform dense deposition of ferritin particles, whereas old cells showed particles deposited irregularly in clusters. The number of cationized ferritin particles on the old rabbit cells per unit length of transversely sectioned membranes was ~28% lower than on young rabbit cells (210). Treatment of the cells with neuraminidase from Vibrio cholerae reduced the number of particles associated with the membrane drastically by either the iron oxide or the cationized ferritin labeling method (119, 210). One puzzling feature of these results is the apparent similarity in labeling density of both human and rabbit erythrocytes since the surface charge density of these two cell types as measured by cellular electrophoresis is markedly different (-1.08 versus -0.48 $\mu m\ sec^{-1}\ V^{-1}\ cm$) (49).

It is also not clear why a loss of 10-15% of the sialic acid upon cell aging should lead to an approximate change of 30% in the labeling density of colloidal iron. The size of the particles which are employed to label the cells should also be taken into consideration. Another drawback to use of colloidal iron is that particle size is difficult to control and the diameters may range between 30-40 Å (212). Thus, one particle may cover up to 1300 $Å^2$ of cell surface. The difficulties concerning size heterogeneity is circumvented by the use of ferritin. However, ferritin is even larger, occupying a space of ~55 Å diameter

or ~2400 $\mathring{A}^2$ of surface area (213). The negative charges at the surface of the red cell are unlikely to be evenly distributed. Instead they probably occur in clusters at the terminal sites of the major sialoglycoproteins (glycophorin) of the red cell. It has been estimated that there are approximately 5×10^5 copies of glycophorin per red cell (214). Assuming, for the moment, that all of the sialic acid of the cell is associated with glycophorin, then ~60 molecules of sialic acid would be associated with each molecule of glycophorin, assuming that there are 15 fg of sialic acid per red cell. The molecular weight of glycophorin is less than one-tenth that of ferritin (213, 214) such that one molecule of ferritin could easily associate with more than one glycophorin molecule. As a result, if these molecules were to rearrange in the plane of the membrane it would become difficult to distinguish the effects of charge loss from charge rearrangement. In fact, recently Marikovsky et al. (215) have demonstrated that changes in label density comparable to those seen in old and young red cells (using cationized ferritin) result on mere transformation of red cell shape and presumably surface charge topography. Very simply, these authors considered that the lateral mobility of integral membrane proteins (216), such as the sialylglycoprotein of the red cell (111) is severely restricted (217, 218, 219), although recent studies have shown that these proteins are not totally immobile (220, 221, 222).

By hypothesizing that the integral membrane proteins are associated with the red cell cytoskeleton and utilizing cationized ferfitin as a cell surface charge topography probe, Marikovsky et al. (215) were able to show that a 27% decrease in labeling density resulted in transforming the normally shaped discocyte to an echinocytic, crenated shape in hypertonic media. They furthermore showed that the change was reversible, i.e., on resuspending the crenated echninocytic forms in isoosmotic media the label density returns to control values. It seems apparent that on crenation the proteins cluster and one ferritin particle associates with more protein molecules than when the cell is normally shaped. These results, depicted in Fig. 5-6 (215), may be compared with very similar appearing photographs obtained on density fractionated human cells in Fig. 5-7 and density fractionated rabbit cells in Fig. 5-8 taken from the work of Danon and Marikovsky (119), who made the assertion that the labeling density changes were the result of a decrease in surface charge density. However, surface charge density changes and surface charge topography changes are entirely different phenomena. The former would affect the electrophoretic mobility and the latter would not. This is borne out by the fact that the electrophoretic mobility of crenated cells such as those shown in Fig. 5-6 is identical to that of discocytes. This is consistent with the fact that particle electrophoretic mobility is only a reflection of its total charge density and not the arrangement of charge on the

Figure 5-6. Marikovsky et al. 's (215) data illustrating the influence of red cell shape on surface charge topography. Left column: Scanning electron micrograph, x1000; Center column: Thin section electron micrograph of cross-sectioned, cationized ferritin (CF) labeled cell surfaces, x100,000; Right column: Freeze fracture deep-etch electron micrographs of CF particles on red cell surfaces x100,000.

a) Normal discocytes in isotonic sodium chloride medium. The even coverage of the cell surfaces with CF particles should be noted. The iron core of the CF particles (~55 Å diameter) are visualized in the thin section (center column) and the CF particles are visualized in their entirety in the freeze fracture replica (right column).

b) Crenated red cells: CF particles are reduced in number. At identical magnifications CF particles appear relatively small where they are closely packed together because of the small size of their metal caps (compare a and b in the right column).

c) Shape-reverted red cells which were crenated in hypertonic sodium chloride medium and then resuspended in isotonic sodium chloride. CF labeling has reverted to the typical pattern for discocytes (compare with a).

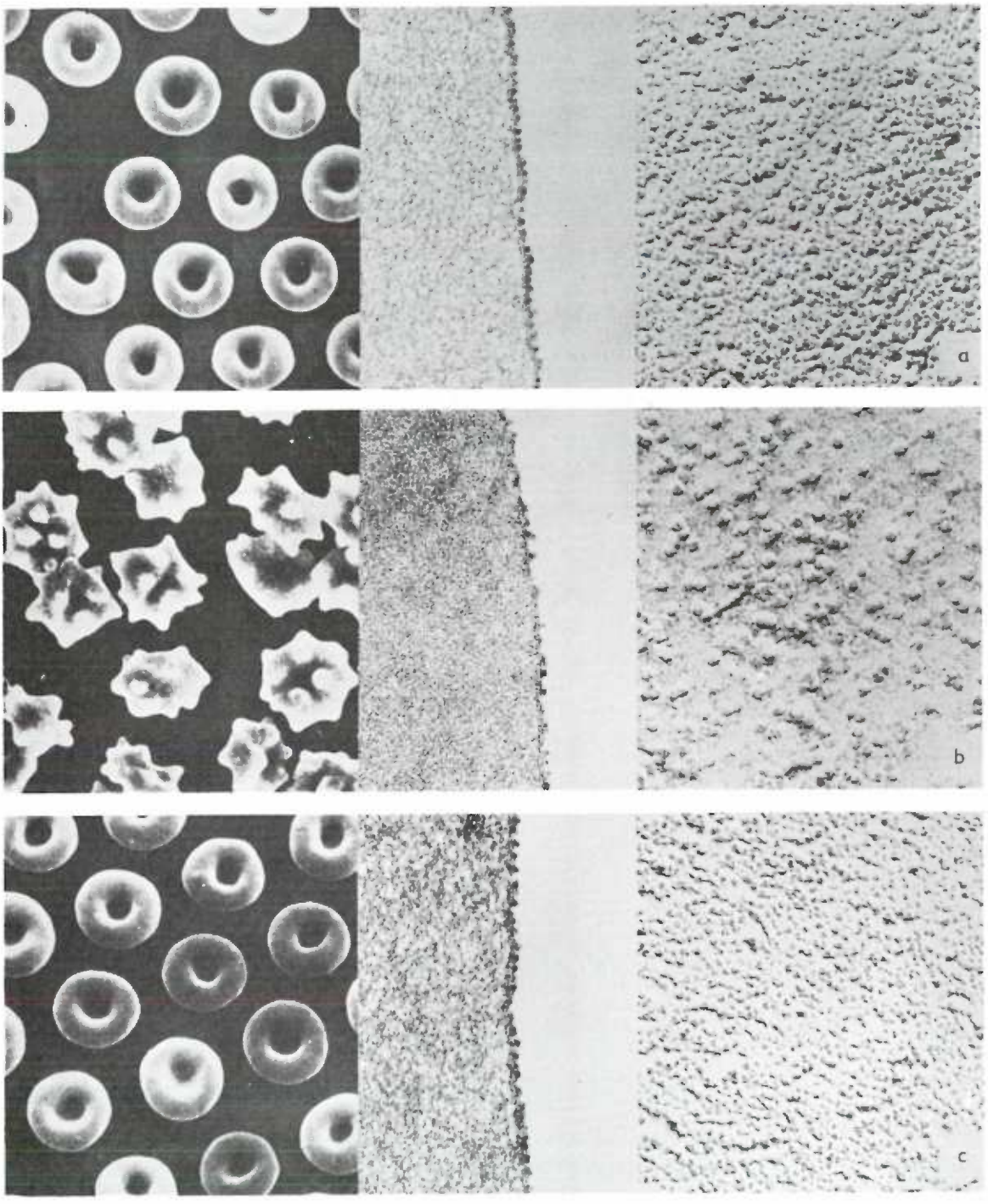
a
b
c

Figure 5-7. Data of Marikovsky and Danon (119).

1: A human red cell from a young fraction of cells, separated by the phthalate ester method, fixed in glutaraldehyde, and labeled with a positively charged colloidal iron suspension. Colloidal particles are uniformly distributed along the membrane surface. x20, 000.

2: Human red cells from an old fraction separated by the phthalate ester method, fixed in glutaraldehyde, and labeled with a positive colloidal iron suspension. Iron particles are deposited irregularly, leaving gaps on the membrane surface. x20, 000.

3: Unseparated whole population of red cells treated with neuraminidase and labeled with colloidal iron. Deposition of colloidal iron particles is similar in amount and disposition to that of an old human red blood cell. x20, 000.

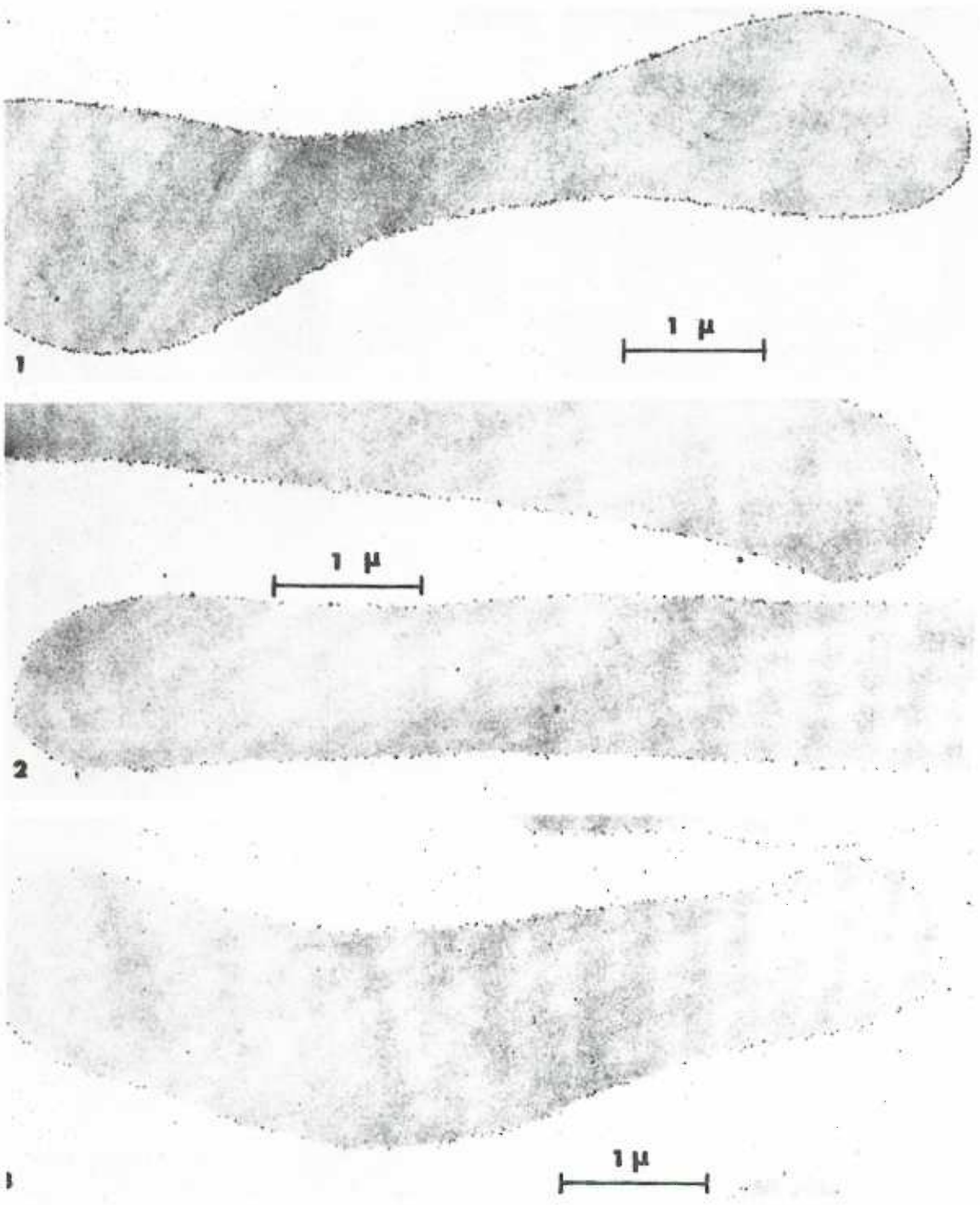
1 μ
1
1 μ
2
1 μ

Figure 5-8. Data of Marikovsky and Danon (119).

4: A cell from an unseparated whole population of human red cells treated with neuraminidase at twice the concentration as were those cells shown in Figure 5-7:3. After treatment with the enzyme the cells were fixed with glutaraldehyde and labeled with a positive colloidal iron suspension. Deposition of colloidal particles on the membrane surface is practically absent. x20, 000.

5: Young rabbit red cells, labeled with colloidal iron, showing a deposition similar to that of young human red cells. (Note however that the surface charge density of rabbit cells, as determined by electrophoresis is about half that of human red cells). x20, 000.

6: Old rabbit red cells, labeled with positive colloidal iron, showing particles deposited irregularly, leaving unlabeled gaps on the membrane surface. x20, 000.

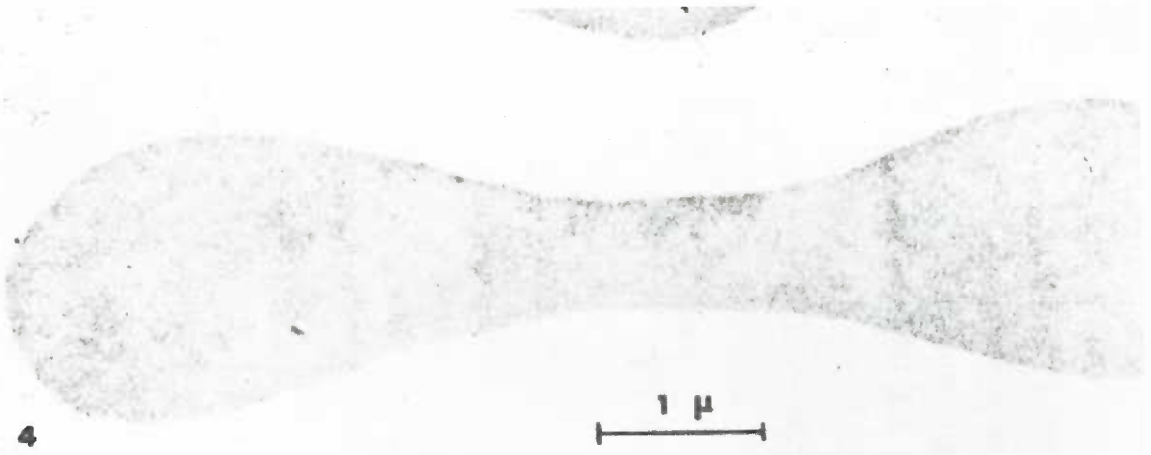

4

5

6

surface. Thus, labeling of red cells, or any other cell type, with positively charged colloids is, at best, a rather nonspecific method for assessing cell surface charge density. The method is more than likely, more sensitive to charge topography changes than to actual differences in zeta potential or charge density.

Another approach which has been invoked as providing evidence for charge differences between old and young red cells is the rate of aggregation of cells as produced by poly-L-lysine, where the rate has been found to be greater for old cells than young cells (119, 223, 224). The experiment consists of suspending density separated cells in barbital buffered saline in the presence of poly-L-lysine (MW 38, 000). The rate of agglutination as measured by the percent light transmission in a Fragiligraph, Model D-2, (Elmedix Ltd., Tel Aviv) is determined over a period of 12 minutes. The more cells that agglutinate, the less turbid the suspension will be and the less light will be scattered; viz., more light will be transmitted. Figures 5-9a and 5-9b show data redrawn from the work of Marikovsky and Danon (119) and Marikovsky et al. (215). The interpretation for the results shown in Fig. 5-9a was that old cells, because of their purported lower charge density, interacted and flocculated (aggregation due to intercellular polymer bridging) more readily than young cells. The interpretation for the results depicted in Fig. 5-9b was that the increased rate of agglutination of crenated red cells, as opposed to normal discocytes,

Figure 5-9. The rate of aggregation of human red blood cells by poly-L-lysine mol. wt. 38,000.

a) Agglutination curves of red cells from a young fraction of phthalate ester separated cells (o) and cells from an old fraction (●). Data of Marikovsky and Danon (119).

b) Rate of agglutination of glutaraldehyde fixed normal discocytes (o) and crenated red cells (●). Data of Marikovsky et al. (215).

The absolute magnitude of the light transmission is to a large degree a function of the cell concentration of the samples and is thus not significant in a comparison of data in a) and b). Most important is the absolute difference in light transmission between samples at t = 12 minutes. This difference appears to be almost identical in the two cases.

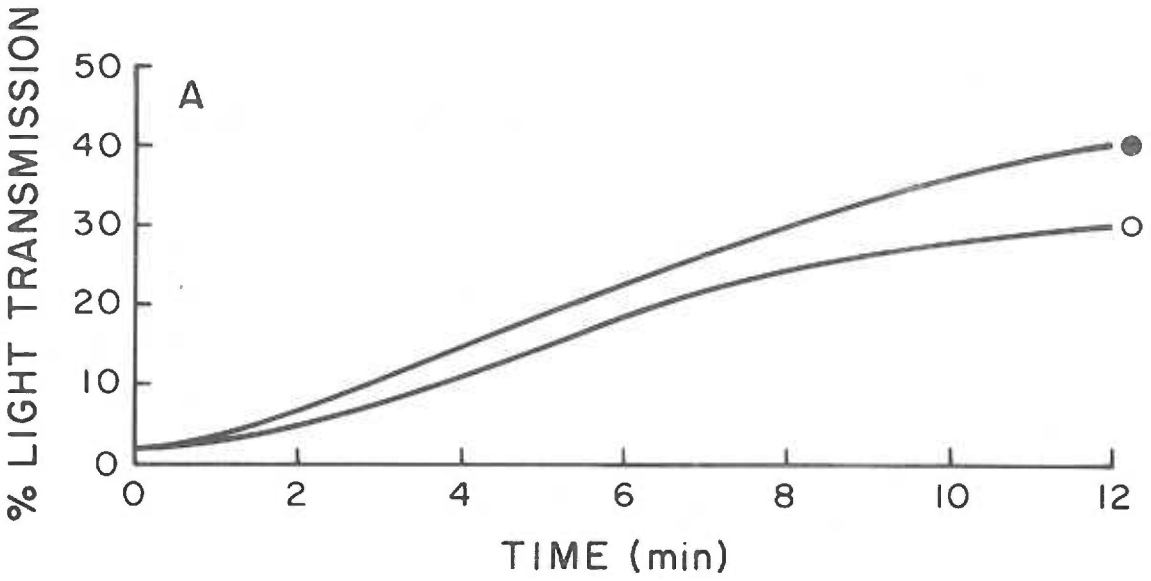
% LIGHT TRANSMISSION
A
50
40
30
20
10
0
0
2
4
6
8
10
12
TIME (min)

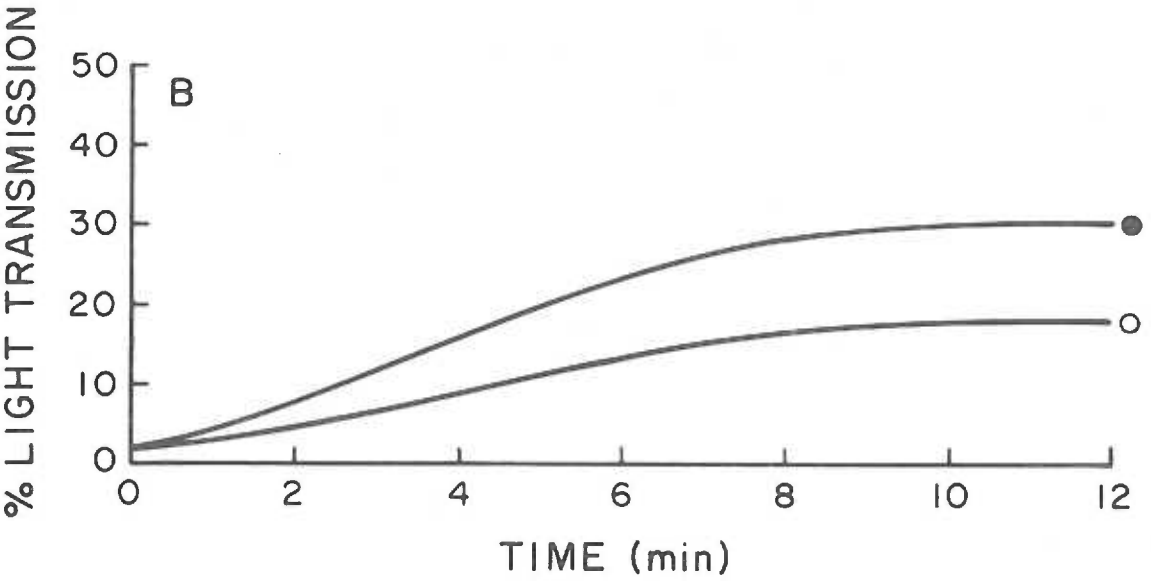
% LIGHT TRANSMISSION
B
50
40
30
20
10
0
0
2
4
6
8
10
12
TIME (min)

was due to a change in cell surface charge topography, viz., a two dimensional change in the topography of integral membrane glycoproteins. The similarity between the two sets of data (Fig. 5-9a, b) is striking, which also points out the insensitivity of this technique to surface charge density changes.

The changes in the hematological parameters and the chemical composition of the cells on aging as well as the results of labeling membranes from old and young cells with positively charged colloids, and the interaction of old and young cells with polylysine suggest a reordering or restructuring of membrane components within red cells as they age. In other words, cell surface charge topography changes may accompany red cell aging. Changes, as a result of aging, in the two dimensional arrangement of integral membrane glycoproteins within the cell cytoskeleton may arise as a result of membrane loss (160) and are certainly within the realm of possibility. These types of changes may also be responsible for the different membrane properties of old cells even if the proportions of their major components are not altered. Additional evidence for differences in the surfaces of old, as opposed to young cells, is provided by differences in their partitioning behavior in two phase aqueous polymer systems (225), agglutinability toward antisera (226), binding of lectins (120), phagocytosis by autologous macrophages (165), membrane permeability to ions (227), and mechanical properties of the membrane (228, 229). Now that surface

charge density of red cells has been shown to be invariant under the conditions under which many of these measurements have been made, explanation for these age-related variations, other than differences in surface charge density between old and young cells, must be sought. For example, one area which has received relatively little attention is the role of sulfhydyl (-SH) groups in erythrocyte aging. In general, sulfhydyl groups have an important function in determining and stabilizing the primary structure of proteins. In the red cell membrane ~5% of the sulfhydyl groups are associated with glycophorin and the remainder are associated with the Band 3 protein (230, 231, 232), which is the putative mediator of membrane anion transport (233). A variety of hemolytic processes in vivo may be produced if membrane SH groups are blocked by either organic or inorganic reagents (234, 235). It has been shown in several studies that red cell membrane SH groups are involved with transport of d-glucose as well as small charged molecules into and out of red cells (230, 235, 236, 237). Since the red cell is constantly exposed to high levels of oxygen and thiol groups are easily oxidized, one might hypothesize that a deterioration of the transport processes accompanies red cell aging. The oxidized thiol groups may then also serve as signals to the reticuloendothelial system, e.g., indicating a senescent cell or providing points of interaction with plasma macromolecules which in turn adsorb to the cell and signal its effeteness (165).

CHAPTER 6

INFLUENCE OF NEURAMINIDASE ON THE PERIPHERAL ZONE STRUCTURE OF THE HUMAN ERYTHROCYTE

As shown in the last chapter, the surface charge density of red cells remains constant throughout most of their life span implying that the net number of sialyl residues per unit area of membrane also remains constant. However, the constancy of mobility is only suggestive, since desialylation could occur by protease action whereby there could be a one to one replacement of sialyl carboxyl groups by carboxyl residues present in the peptide backbones of cell surface glycoproteins (e.g. from glutamyl or aspartyl residues) (238). In order to establish which mechanisms of sialic acid loss predominates, Vibrio cholerae neuraminidase (VCN) was utilized to exhaustively desialylate density fractionated human red cells with the rationale that the enzyme would only release sialyl residues and thereby simply eliminate the contribution of sialyl carboxyl groups to the negative surface charge of the cell. Accordingly, any differences in the number of non-sialyl carboxyl groups could then be detected by electrophoresis.

Furthermore, the diminished levels of sialic acid in senescent red cells has kindled speculation that loss of sialic acid during the in vivo life of the red cell constitutes a normal determinant of red cell life span (239). Many investigators have found that reinjection of autologous red cells treated in vivo with neuraminidase results in a

markedly shortened red cell life span in a variety of animals, including dogs and goats (123), mice (240), rabbits (163), and rats (162), as well as humans (164). In addition to studies on the biological roles of sialic acid on red cells as well as other cell types (241), VCN has been used extensively to elucidate the contribution of sialic acid to the physicochemical properties of the cell surfaces. Interpretation of all these studies requires a knowledge of the specificity of neuraminidase action on the red cell and the extent of alterations in addition to desialylation brought about by action of the enzyme.

6.1 Materials and Methods

6.1.1 Blood Collection and Processing

Blood was drawn by venipuncture from healthy male and female adult human donors and anticoagulated with disodium ethylene diamine tetraacetate dihydrate (EDTA, 4 mM final concentration). The blood was centrifuged at 2000 g at room temperature and the supernatant plasma and buffy coat material was aspirated and discarded. The red cell pack was washed three times in about 25 volumes of 0.15 M aqueous sodium chloride solution buffered to pH 7.4 ± 0.2 with sodium bicarbonate (standard saline). Residual buffy coat material was carefully aspirated after each wash. Red cells were density fractionated by the one-step centrifugation method (175) described in Section 5.1.3.

6.1.2 Neuraminidase Treatment of Erythrocytes

Vibrio cholerae neuraminidase, prepared according to Schick and Zilg (189), was manufactured by Behringwerke AG (Marburg/Lahn FGR) and may be purchased from Calbiochem-Behring Corp. (La Jolla, CA). The enzyme was supplied in 0.05 M sodium acetate buffer, pH 5.5, containing 0.15 M NaCl and 0.01 M $CaCl_2$ (enzyme buffer) in 1 ml vials containing 500 units of activity where one unit hydrolyzes 1 μg N-acetylneuraminic acid from α_1-acid glycoprotein in 15 minutes at 37°C. A VCN preparation (500 units · ml^{-1}) having approximately a 40% higher specific activity was obtained as a gift from Dr. F.R. Sciler of Behringwerke AG, Marburg/Lahn, FGR. This enzyme preparation was homogeneous on sodium dodecylsulphate polyacrylamide gel electrophoretic analysis, (SDS-PAGE), and further, the bands did not split on isoelectric focusing (189). Both the commercial enzyme as well as the more highly purified preparation had molecular weights in the region of 90,000-95,000 as determined by SDS-PAGE. These values are in close agreement with results obtained by others (242). The enzyme does not dissociate into subunits, either in the presence of 8 M urea or sulfhydryl group reagents such as mercaptoethanol (189).

The standard VCN treatment consisted of washing standard washed packed red cells in approximately 20 volumes of the media to

be used during the enzyme treatment followed by their suspension in that medium to a hematocrit of about 20%. Hematocrits and red cell concentrations were measured as described previously in Section 2.5.

The cell suspensions were transferred to Corex glass centrifuge tubes (either 25 ml or 30 ml tubes were utilized). The mass of the suspension was determined such that the total number of red cells incubated, as well as the total amount of sialic acid released per red cell could be determined as shown in Section 2.6. Treatment of red cells with VCN was initiated by addition of the enzyme to the cell suspension which had been equilibrated to the incubation temperature in a water bath. Control suspensions were incubated alongside the test samples in the same manner except that an equivalent volume of pH 5.5 enzyme buffer was added instead of enzyme. Fresh VCN solutions were utilized for each experiment and they were dispersed using either glass syringes (Hamilton) or glass pipettes. Different enzyme concentrations (expressed in enzyme units per 10^{10} red cells), incubation media, and incubation times were employed at either 0°C or 37°C which will be detailed below. During the incubation, cell suspension samples were mixed a minimum of three times per hour in order to maintain red cells evenly suspended.

Supernatant fluids were recovered from the incubation mixtures after centrifugation for five minutes at 2500 g at either room temperature or 0-4°C. Aliquots were assayed for their sialic acid content by the

thiobarbituric acid method (TBA) (36). The results were computed as fg sialic acid released per cell as described, or as percent of total release, where the total releasable sialic acid was the observed quantity released at 37°C in three hours by ≥ 60 units VCN per 10^{10} red cells.

Soluble VCN activity was measured by determining the amount of sialic acid released from N-acetyl-neuraminlactose (NAN-LAC) obtained from Calbiochem-Behring Corp., A grade, by the TBA method. The assay procedure consisted of utilizing 3.16×10^{-7} mole NAN-LAC per assay, usually in a volume of ≤ 250 µl of enzyme buffer. This substrate sample was incubated with an aliquot of 250 µl of sample containing ≤ 10 units (as defined by the manufacturer) of VCN at 37°C for 15 to 60 minutes. The reaction was terminated by the addition of the strongly acidic periodate reagent employed in the TBA assay method for free sialic acid. Appropriate enzyme, substrate and reagent blanks were juxtaposed.

6.1.3 Determination of Protein Concentration of VCN Preparations

The protein concentration of the VCN preparations was measured by three methods: 1) binding of protein to Amidoschwartz 10B according to the method of Shaffner and Weissman (38); 2) binding of protein to Coomassie Brilliant Blue G-250 according to Bradford (40); and 3) measurement of protein nitrogen by the microkjeldahl procedure

using Nessler's reagent according to the method of Campbell et al. (41) (see Section 2.7).

6.1.4 Immobilization of VCN on Sepharose 4B

Neuraminidase was coupled to CNBr activated Sepharose 4B (Pharmacia). The reaction between proteins and the gel is thought to involve reaction of free primary amino groups of the protein and cyclic imidocarbonates present on the gel (243, 244). This reaction tends to proceed better at alkaline pH where most of the amino groups are not protonated. Since VCN is supplied in a pH 5.5 buffer, 5 ml were dialysed overnight in 0.65 cm, #8 dialysis tubing (VWR Scientific) against ~500 ml of 0.50 M aqueous NaCl-0.1 M $NaHCO_3$ at 4°C. Dry Sepharose (0.5 g) was reconstituted on a coarse sintered glass filter using a total of 100 ml of a 1 mM solution of HCl. To determine the efficiency of VCN coupling, 100 µl aliquots of the enzyme solution were assayed for protein to determine its initial and final concentration after coupling, according to the method of Bradford (40).

Coupling was carried out with ~3.85 ml VCN in a 25 ml Erlenmeyer flask at room temperature with gentle agitation for 2 hours, after which the VCN-gel mixture was transferred to a cold room at 4°C. The mixture was agitated overnight. The gel was then washed and reacted for 2 hours with 1 M ethanolamine in water to block excess active groups on the gel. This was followed by five alternate washes

with 1.0 M aqueous NaCl-0.10 M sodium acetate, pH 4.0 and 1.0 M NaCl-0.10 M $NaHCO_3$, pH 9.0 to desorb and wash away any uncoupled residual protein. Finally, the gel was washed with enzyme buffer and stored therein at 4°C. A procedure very similar to that given above has been described for coupling VCN to Sepharose by Corfield et al. (245).

The activity of the immobilized VCN was assayed by incubation of the derivatized Sepharose 4B with the soluble substrate N-acetylneuraminlactose. Appropriate reagent blanks, enzyme blanks and standard samples were run together. Typically, 0.250 g of the coupled Sepharose 4B were incubated for 60 minutes at 37°C with 3.00 ml of standard saline and sufficient neuraminlactose to provide ~0.65 μmole of releasable sialic acid. After the incubation 100 μl aliquots were drawn and assayed for free sialic acid by the TBA method.

6.1.5 Treatment of Human Red Blood Cells with Immobilized VCN

Both native and formaldehyde fixed erythrocytes were treated with the insolubilized VCN. A red cell suspension, having a hematocrit of about 20%, was incubated on a roller type agitator with about 1 g of gel in a Corex centrifuge tube for 16 hours. The supernatant fluid was recovered by filtering the cells through Whatman No. 1 filter paper with slight suction. The gel was recovered, washed, and

reutilized in other experiments. The red cells were recovered by centrifugation, and electrokinetically characterized in 0.150 g-ions $\cdot L^{-1}$ ionic strength NaCl media buffered to pH 7.4 with aqueous 0.150 M $NaHCO_3$. Samples were then fixed with formaldehyde and subjected to electrophoretic analysis. The supernatant fluid was assayed for sialic acid released, which was expressed in fg sialic acid released per cell based on the original number of red cells incubated, which was determined as described previously. In order to determine the correct supernatant volume, the amount of fluid trapped by the gel before addition of the red cell suspension, had to be determined. This was accomplished by transferring a reconstituted sample of the gel to a calibrated test tube which was weighed before and after heating for one hour at 120°C. The amount of water driven off was calculated as a volume of water per ml of gel. Due to considerable hemolysis, the supernatant fluids were treated with trichloroacetic acid (TCA) to precipitate the protein. The final TCA concentration was ~12% w/v. A control incubation, consisting of red cells incubated with Sepharose 4B only was also included.

Human red cells fixed with formaldehyde, as described by Heard and Seaman (56), were also treated with the immobilized VCN as explained above. In addition, an aliquot of the cells was subsequently treated with the soluble enzyme. Further samples were incubated with the soluble enzyme only. The amounts of sialic acid released by

the individual treatment regimes were calculated on a per cell basis. The cells were also electrophoretically characterized in a sodium chloride containing medium having an ionic strength of 0.150 g-ions $\cdot L^{-1}$.

6.1.6 Formaldehyde Treatment of Erythrocytes

Formaldehyde solutions for cell fixation were prepared from paraformaldehyde (Matheson Coleman and Bell) either by direct dissolution of paraformaldehyde or by collection of formaldehyde gas as described in Section 4.1.1.1. Control or VCN-treated cells were washed twice in ~20 volumes of standard saline and once in an aqueous solution of 0.120 M NaCl-25.4 mM $NaH_2PO_4 \cdot 7H_2O$-4.6 mM $NaH_2PO_4 \cdot H_2O$ (pH 7.5, PBS). The cell packs were suspended in ~50 volumes of 0.500 M formaldehyde in PBS (ph 7.4, 765 mOsmoles $\cdot kg^{-1}$) and stored at room temperature for at least one week before use in further experiments.

6.1.7 Analytical Particle Electrophoresis

Electrophoretic mobilities of cells were measured according to the methods outlined in Section 3.5. Some experiments required measurements to be made at low temperatures. This was accomplished by maintaining the water bath temperatures at 0.2 ± 0.2°C by the addition of ice. Suspending media consisted of either 0.150 M

aqueous NaCl or 0.030 M aqueous NaCl-0.220 M sorbitol, the pH of which was adjusted to the indicated values with aqueous solutions of HCl, NaOH or $NaHCO_3$ made up to the corresponding ionic strength and where appropriate, rendered isotonic with sorbitol.

Data were collected on the relationship between the electrophoretic mobility and the pH of the suspending medium for native and fixed erythrocytes before and after VCN treatment. During the collection of pH-mobility data the suspension pH was measured both before and after electrophoresis and was found to vary by less than 0.1 pH unit. The pH meter (PHM-28, Radiometer, Copenhagen) was calibrated with standard buffer solutions, the pH values of which were within 2 pH units of the suspension pH, so as to minimize false readings due to pH meter electrode asymmetries.

In order to obtain valid pH-mobility data the mobility measurements were made such that the criterion of electrophoretic reversibility was fulfilled (64). For example, exposure of red cells to extreme nonphysiological pH and ionic strength conditions may lead to irreversible changes in the electrokinetic properties of the cells. Many of these changes are time dependent however, such that the range of ionic strength or pH over which the cells are electrokinetically reversible may be extended by very rapid performance of measurements. In the work to be described the range of pH was established over which the cells displayed electrokinetic stability. After electrophoretic

measurements of cells at a particular nonphysiological pH value were made, they were centrifuged and washed twice in 0.150 M aqueous $NaCl-NaHCO_3$, pH 7.4 ± 0.2, and electrophoretically characterized. Whether cells suspended in media of less than physiological ionic strength were electrokinetically reversible was tested by centrifuging and washing them twice in 0.030 M aqueous $NaCl-NaHCO_3$, pH 7.4, followed by resuspension for electrophoresis.

6.1.8 Assay for Proteolytic Activity in VCN Preparations

The presence of proteolytic activity in the VCN preparations was checked with Azocoll as outlined by Seaman et al. (246). One vial of VCN containing 500 units of activity was added to a suspension of Azocoll (5 $mg \cdot ml^{-1}$), an insoluble collagen dye conjugate in standard saline and incubated for one hour with the inclusion of appropriate blanks. After incubation, the Azocoll substrate was filtered off and the absorbance of the solution was measured at 580 nm. Under these conditions 100 $\mu g \cdot ml^{-1}$ trypsin results in an absorbance of ~0.50.

A much more sensitive assay, based on a method described by Bjerrum (247) was also utilized. The method consists of preparing 1% w/v agar diffusion plates containing a bovine casein substrate preparation in a Tris buffered physiological saline solution, pH 7.2. If protease activity is present in the samples to be tested, diffusion into the substrate gel is accompanied by digestion of the casein. This

forms a transparent ring around the sample wells in a turbid appearing gel. The size of the ring is a measure of the proteolytic activity of the sample. The sensitivity of the assay using trypsin is reported to be similar to that reported by Sevier (267) using ^{125}I labeled solid phase protein substrates. Trypsin activity may be measured on samples containing as little as 0.5 μg trypsin per ml.

The presence of protease activity in Behringwerke VCN solutions was tested for by employing an assay kit supplied by BioRad Laboratories. Up to 12.5 units of VCN (25 μl) were incubated for up to 28 hours together with appropriate blanks and a positive control sample, the latter supplied by the manufacturer.

6.1.9 Reversible Blocking of Cell Surface Amino Groups by Dimethylmaleic Anhydride and Maleic Anhydride

The reaction of derivatives of maleic anhydride with primary amino groups are highly specific (248, 249). Butler et al. (249, 250) were the first to use maleic anhydride as a reversible blocking reagent for protein amino groups. The maleyl groups were, however, inconveniently difficult to remove. As a result, various derivatives of maleic anhydride were tested for their suitability, as blocking reagents by Dixon and Perham (251). They found that 2, 3 dimethylmaleic anhydride reacted with amino groups between pH 8-9 but hydrolysed extremely easily, whereas citraconic anhydride adducts had

intermediate stability. Mehrishi (252) introduced these reagents as probes to be used for the determination of the presence and quantitation of amino groups at cell surfaces by cellular electrophoresis. The positive charge of amino groups on reaction with these reagents is replaced by the negative charge of the carboxyl group of the hydrolyzed anhydride as shown by the following scheme:

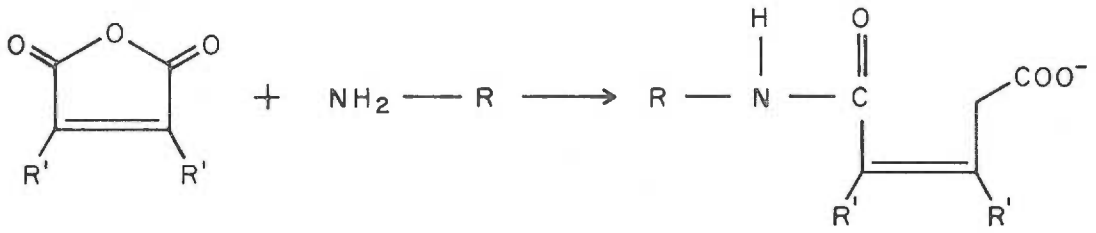

$R' = -CH_3$ or $-H$

Thus, in electrophoretic terms, the anhydride-amino group reactions are twice as sensitive as the formaldehyde-amino group reaction in which the positive charge is simply blocked. In the work here, both maleic or 2,3-dimethylmaleic anhydride (Aldrich Chemical Co., MA and DMA, respectively) were utilized as blocking reagents. Initially, reaction conditions recommended by Mehrishi (252) were tried. This involved addition of up to 100 µl of a 0.100 M ethanolic DMA solution to a 10 ml of a red cell suspension in 0.150 M aqueous NaCl-$NaHCO_3$ pH 6.8, containing ~1 x 10^7 red cells per ml of suspension. This resulted in a DMA concentration of $\leq$ 1 x 10^{-3} M or ~1 x 10^{-13} moles DMA per red cell. Cell concentrations were adjusted using the Electrozone-Celloscope cell counting equipment described

previously. The electrophoretic mobility of native control and VCN treated, as well as formaldehyde fixed control and VCN treated cells was determined within 10-15 minutes after addition of DMA. Similar experiments were carried out by adding DMA to the red cell suspending medium which had previously been adjusted to pH 8.3 ± 0.2 with 0.150 M $NaHCO_3$ and/or 0.015 M NaOH. To this solution test red cells were added such that a cell concentration of ~1 x 10^7 cells per ml was obtained. The pH of the suspension was stabilized and maintained at ~ pH 8.0 by addition of 0.150 M NaOH. This was required to neutralize excess hydrolysed DMA. After ~5 minutes mobility measurements were made. Appropriate controls were included to determine whether ethanol alone would have any effect on the electrophortic mobilities of the cells at the concentrations used. The concentrations of DMA were optimized by utilizing 0.250 M DMA and increasing the concentrations until the maximum electrophoretic mobility change was attained. The reversibility of the reactions was tested by first treating cells with DMA at ~ pH 8.0 and then washing them twice and incubating them up to 10 minutes with 0.150 M aqueous NaCl, the pH of which had been adjusted to pH 6.0 with 0.150 M HCl. The cells were then centrifuged and resuspended in standard saline and electrokinetically characterized. Similar experiments were carried out with 0.25 M MA in dioxane at 0.150 and 0.015 g-ions · L^{-1} ionic strength sodium chloride media. These conditions are similar to those

described by Donner and Mehrishi recently (252). The reaction of MA with amino groups is more vigorous and the adducts are not labile except at very low pH values which would be unsuitable for erythrocytes. Appropriate control samples containing dioxane were included to observe the effects, if any, of the solvent on the electrophoretic mobilities of red cells at the concentrations employed in the experiments.

6.2 Results

The protein concentration of the purchased VCN solutions as measured by both dye binding methods was 10 μg/ml. The protein nitrogen concentration from the microkjeldahl assay was 1.94 μg/ml which corresponds to 12 μg protein · ml^{-1} assuming an average nitrogen content of 16% w/w. Absolutely no proteolytic activity was detectable in the VCN preparations either by the Azocoll method or the agar diffusion method.

The quantities of NANA released from red cells treated for one hour at 37°C with VCN at concentrations ranging from 1.5 to 350 units per 10^{10} red cells are shown in Fig. 6-1 with the resulting electrophoretic mobilities of the cells in standard saline at 25.0°C. Relatively low concentrations of enzyme (~40 units per 10^{10} red cells) released ~90% of the total sialic acid in one hour at 37°C in both 0.150 M NaCl buffered with 0.01 M sodium phosphate to pH 7.4 and

Figure 6-1. Sialic acid release and electrophoretic mobilities for red cells treated for one hour at 37°C with different concentrations of Vibrio cholerae neuraminidase: O, ● sialic acid release and □ , ■ mean electrophoretic mobilities in standard saline, 25°C. Open symbols refer to cells treated in pH 7.4, 0.010 M potassium phosphate buffered 0.144 M NaCl and closed symbols refer to cells treated in Ca-saline.

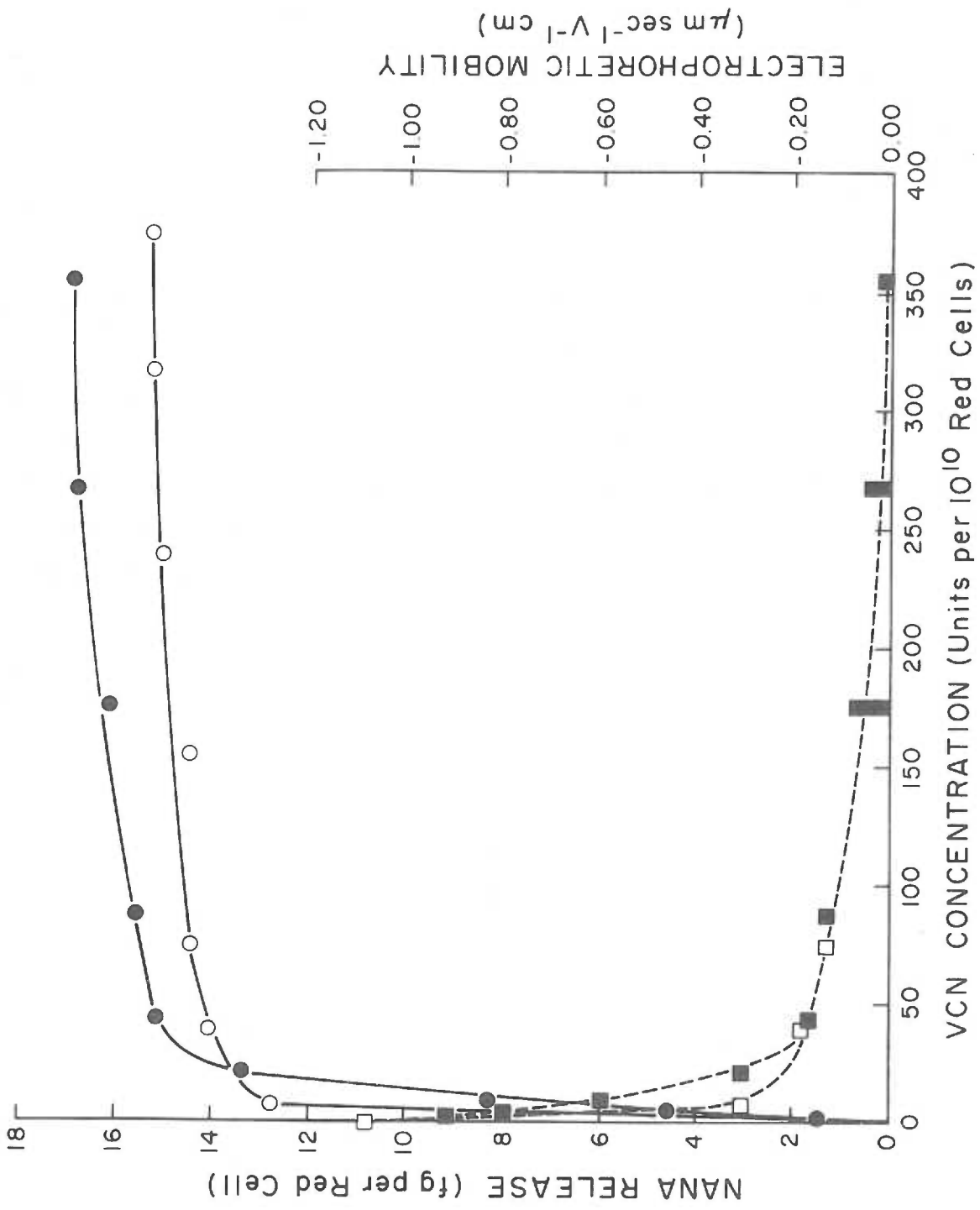
NANA RELEASE (fg per Red Cell)
0
2
4
6
8
10
12
14
16
18
VCN CONCENTRATION (Units per 10^{10} Red Cells)
0
50
100
150
200
250
300
350
400
ELECTROPHORETIC MOBILITY
(μm sec^{-1} V^{-1} cm)
0.00
-0.20
-0.40
-0.60
-0.80
-1.00
-1.20

0.150 M NaCl-0.005 M $CaCl_2$ (Ca-saline) and reduced the mobilities of the cells by about 80% to ~ -0.5 μm $sec^{-1}V^{-1}$ cm in standard saline. With higher levels of enzyme the mobilities of the cells approached zero so that accurate mobility measurements were difficult to collect. A mobility of ~ zero in standard saline at 25.0°C appeared to represent the "endpoint" of the VCN treatment. This result was obtained for cells treated at 37°C with high concentrations of VCN (700 units per 10^{10} red cells) for one hour as well as for cells treated for three hours with 60 units per 10^{10} red cells.

Figure 6-2 illustrates the influence of formaldehyde treatment on the electrophoretic mobilities at two ionic strengths for those cell samples in Fig. 6-1 which were treated with different concentrations of VCN in Ca-saline. Red cells treated with increasing concentrations of VCN up to 350 units VCN per 10^{10} red cells show a decrease in electrophoretic mobility with increasing concentration of VCN in both 0.030 M NaCl-0.200 M sorbitol and in standard saline. However, upon fixation with formaldehyde the mobility increases to yield values which are then constant for all cells which had been treated with VCN concentrations between 20 and 350 units VCN per 10^{10} red cells. As may be seen from Fig. 6-2, the increase in mobility in 0.150 M NaCl as a result of the formaldehyde treatment was most pronounced for the cells from which 50% or more of the sialic acid had been removed, whereas the increase in 0.030 M NaCl-0.220 M sorbitol was most pronounced

Figure 6-2. Influence of formaldehyde treatment on the electrophoretic mobilities of VCN-treated human red cells. Open symbols provide the mean mobilities in 0.030 M NaCl-0.220 M sorbitol (□) and standard saline (○) at 25°C for the cell samples (from Figure 6-1) treated in Ca-saline with the indicated quantities of VCN; and the corresponding closed symbols represent the mobilities of those cell preparations following treatment with formaldehyde.

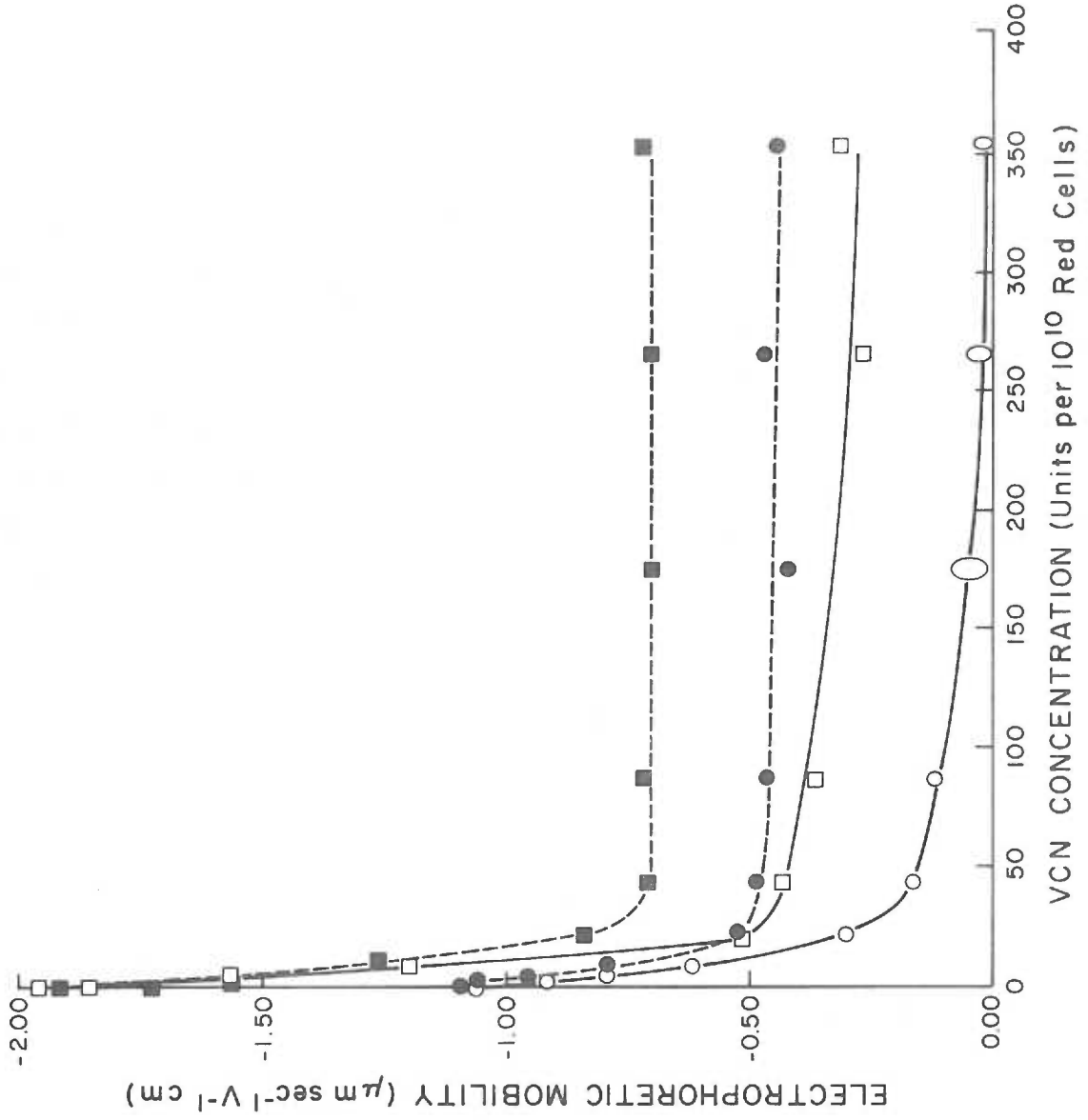
ELECTROPHORETIC MOBILITY (μm sec^{-1} V^{-1} cm)
-2.00
-1.50
-1.00
-0.50
0.00
0
50
100
150
200
250
300
350
400
VCN CONCENTRATION (Units per 10^{10} Red Cells)

for cells from which $\geq 80\%$ of their sialic acid had been removed. Formaldehyde treatment produced no experimentally significant changes in the mobilities of control cells.

The dependence of mobility on suspending medium pH was examined for VCN treated native red cells in 0.150 M NaCl. It was observed that where the mobilities of the VCN-treated cells were only slightly negative at neutral pH, they became significantly more negative at pH value of ~9. At pH values less than 5.0-5.5 the mobilities of the cells became positive. The mobility increases at ~ pH 9 where characteristic of the desialylated cells and deviate from the behavior of the native cells which show no mobility increase in this pH region.

Figure 6-3 shows the pH mobility profiles following aldehyde treatment of cells which had been treated for one hour at 37°C with enzyme buffer (control), a low level of enzyme (8.7 units per 10^{10} red cells) which produced ~50% sialic acid release, and a high level of enzyme (350 units per 10^{10} red cells) which provided complete release of sialic acid. The pH for zero charge of the cells moved to successively higher pH values with increased desialylation. The pH at which the mobility is reduced to zero for fixed nondesialylated red cells is at pH 1.5 and 3.0 for 0.150 M NaCl and 0.030 M NaCl-0.220 M sorbitol, respectively. There is a small upward inflection in mobility which is associated with enzyme treatment in the pH 10-11 region, at both ionic strengths, which is indicative of positive surface groups. The range

Figure 6-3. pH-mobility profiles for formaldehyde stabilized red cells. In A, the suspending medium is 0.150 M NaCl and in B, 0.030 M NaCl-0.220 M sorbitol: O control cells; □ 50% desialylated with 8.7 unites per 10^{10} red cells (Figure 6-1); and Δ 100% desialylated with 350 units per 10^{10} red cells (Figure 6-1). The solid curves cover the region of electrokinetic stability and the dashed curves indicate the regions of instability where the cells do not display their original mobility values at pH 7 following exposure to the indicated pH. Mobilities were measured at 25°C.

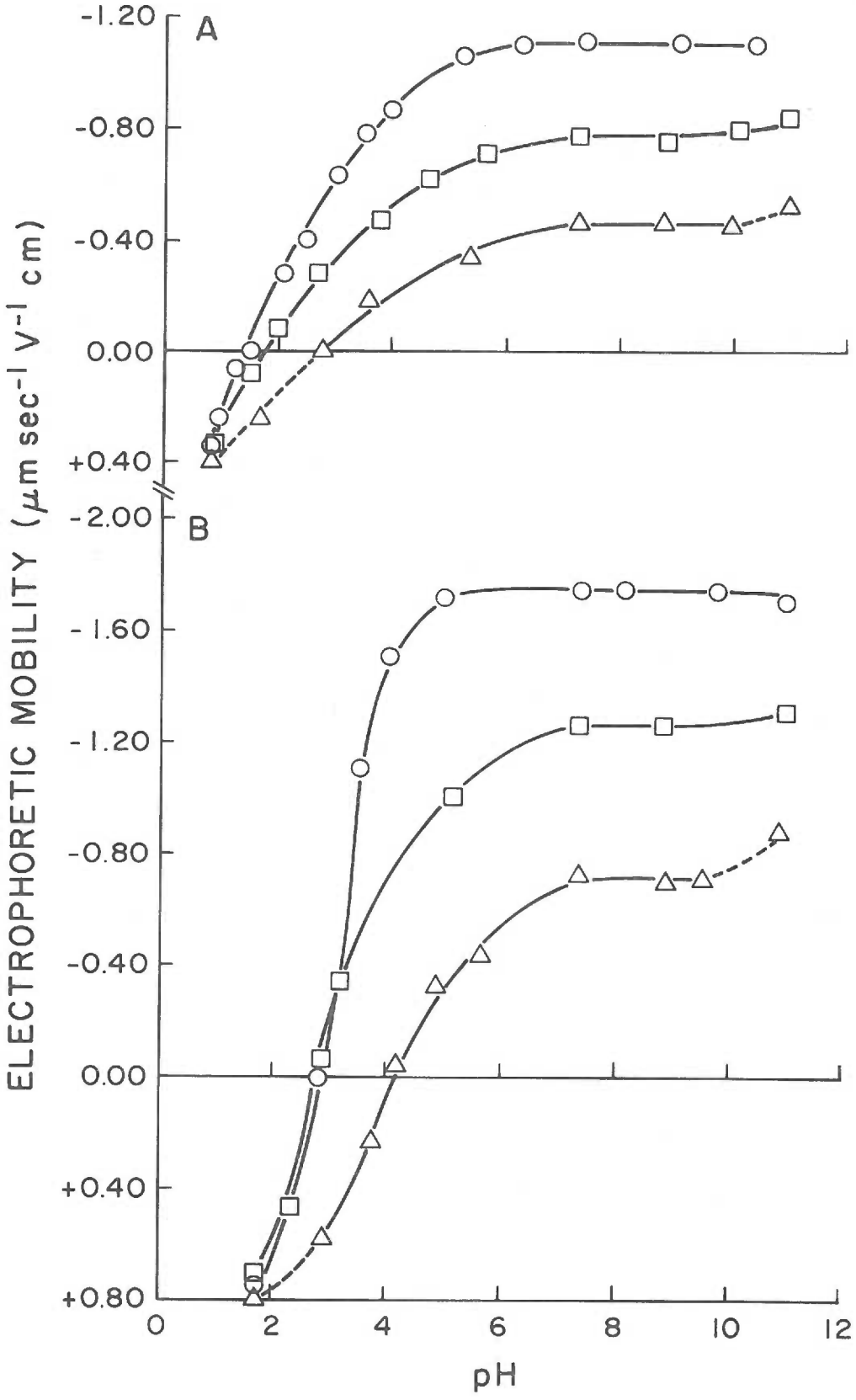
A
B
-1.20
-0.80
-0.40
0.00
+0.40
-2.00
-1.60
-1.20
-0.80
-0.40
0.00
+0.40
+0.80
0
2
4
6
8
10
12
pH
ELECTROPHORETIC MOBILITY (μm sec⁻¹ V⁻¹ cm)

of pH over which electrokinetic stability was observed, decreased for the completely desialylated cells. Where the control and partially desialylated cells were stable for at least 15 minutes at pH values of ~1 to 11, the fully desialylated cells were stable only in the region from pH 3 to 10. Outside this region of stability, readjustment of the pH to neutrality resulted in significantly higher negative mobilities than those originally observed.

VCN treatment of formaldehyde fixed red cells produced a smaller decrease in electrophoretic mobility than was observed for native red cells. Treatment of fixed cells for up to four hours at 37°C with 200 units per 10^{10} red cells reduced their mobilities at neutral pH to -0.34 $\mu m\ sec^{-1}\ V^{-1}\ cm$ at 0.150 g-ions $\cdot L^{-1}$ ionic strength and -0.68 $\mu m\ sec^{-1}\ V^{-1}\ cm$ at 0.030 g-ions $\cdot L^{-1}$ ionic strength. These values approximate those observed for desialylated cells following aldehyde treatment (Fig. 6-2). Refixation of the enzyme treated fixed cells did not significantly alter their mobilities at neutral pH.

The effects of VCN and the neuraminidase preparation of higher specific activity on the electrokinetic properties of native red cells were also compared. Following incubations for two or four hours at 37°C with 220 units VCN per 10^{10} red cells, no significant differences were observed between the preparations with regard to the amount of sialic acid released or the electrophoretic mobilities of the cells in standard saline prior to or following formaldehyde treatment. Each

preparation reduced the mobilities of the cells to approximately zero.

The possibility that adsorption of a component of the preparation other than VCN might occur at 37 °C such that repeated exposure of the preparation to untreated RBC would deplete the component, was tested by incubating cells for one hour at 37 °C with 270 units VCN per 10^{10} red cells. The cell suspension was centrifuged and the collected supernatant fluid was likewise incubated with a volume of fresh cells adjusted to give the same calculated concentration of enzyme assuming no depletions. Two such supernatant fluid transfers were performed and the mobilities of each cell batch and the sialic acid content in each supernatant fluid was determined. Complete release of sialic acid was observed for all three incubations. The mobilities of all three cell preparations approached zero (< -0.1 μm sec^{-1} V^{-1} cm) at 25.0 °C in standard saline. Formaldehyde treatment raised these mobilities to -0.46 μm sec^{-1} V^{-1} cm.

Figure 6-4 illustrates the observed mobilities and percent sialic acid release for cells incubated $\leq$ 45 minutes with 60 units of VCN per 10^{10} red cells at 0 °C in Ca-saline. The incubation periods were termed nominal since the enzyme adsorbed extensively to the cell surface and therefore it was not possible to terminate the action by dilution and washing of the cells. The manipulations involved in preparing the samples for sialic acid assays and conducting electrophoretic measurements took about five minutes. Consequently, the difference

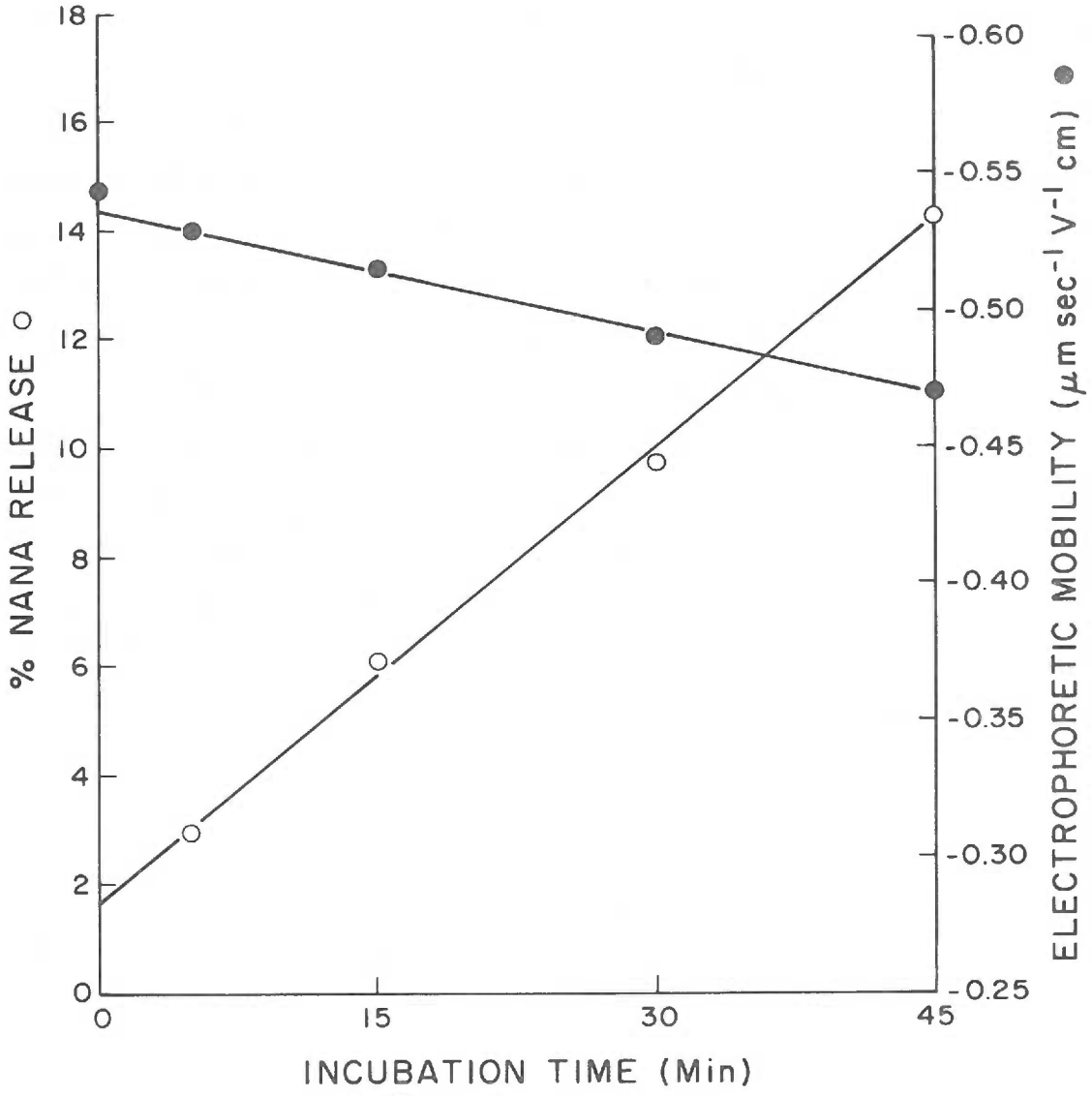
% NANA RELEASE ○
ELECTROPHORETIC MOBILITY (μm sec⁻¹ V⁻¹ cm) ●
INCUBATION TIME (Min)
0
2
4
6
8
10
12
14
16
18
-0.60
-0.55
-0.50
-0.45
-0.40
-0.35
-0.30
-0.25
0
15
30
45

between the nominal and actual incubation times for each curve is of the order of five minutes.

The enzyme was much more active at 0°C than expected. After 45 minutes about 15% of the releasable sialic acid was removed. During this period the extent of removal was a linear function of incubation time. Associated with the linear release of sialic acid at 0°C was a linear decrease in the mobility of the cells. Extrapolation of the mobility curve to zero time gave a mobility value equal, within experimental error, to the control value. Under these conditions active enzyme was adsorbed to the red cells. Assay of the supernatant fluid of the five minute incubation mixture of VCN activity demonstrated only ~5% of the amount of enzyme originally added to the mixture. Also, the presence of active enzyme on the cells was indicated by sialic acid released at 37°C from cells incubated with enzyme at 0°C, washed at 0°C, and then incubated at 37°C. The red cell pack from the five minute incubation mixture was washed three times with 20 volumes of standard saline at 0°C. Following washing, the mobility of the sample was ~6% lower than observed immediately after the five minute incubation. Incubation of the washed cells for 90 minutes at 37°C in Ca-saline resulted in a 90% removal of the sialic acid which remained on the cells after the five minute incubation and reduced their mobilities to < -0.1 $\mu m\ sec^{-1}\ V^{-1}\ cm$ in standard saline at 0°C. Formaldehyde treatment of this cell sample raised its mobility from

< -0.1 to -0.27 μm $sec^{-1} V^{-1}$ cm in standard saline at 0°C.

Incubation of native human red cells with immobilized VCN for 16 hours, dropped their mobility from -1.08 μm $sec^{-1} V^{-1}$ cm to -0.30 μm $sec^{-1} V^{-1}$ cm in 0.150 g-ions $\cdot L^{-1}$ ionic strength sodium chloride medium. On fixation with formaldehyde the mobility increased to -0.62 μm $sec^{-1} V^{-1}$ cm. The amount of sialic acid released (7.7 fg per red cell) with the solid state enzyme and the corresponding electrophoretic mobility of the cells, i.e., 0.30 μm $sec^{-1} V^{-1}$ cm is in good agreement with results obtained with the soluble enzyme (see Fig. 6-1).

Treatment of formaldehyde fixed red cells with the immobilized VCN for 16 hours resulted in the release of a very similar amount of sialic acid as was liberated from the native cells, namely, 7.8 fg per red cell. The mobility of these fixed cells in 0.150 M aqueous NaCl was 0.66 μm $sec^{-1} V^{-1}$ cm. Thus, the order of treatment, i.e., formaldehyde fixation, followed by treatment with the coupled enzyme or vice versa made no significant difference in the final mobility values. This was also found to be true for the soluble enzyme. Further treatment of the solid state VCN treated cells with soluble VCN released an additional 5.8 fg sialic acid per red cell. Thus, the total amount of sialic acid released per red cell was 13.6 fg. This agreed well with a total of 13.9 fg per red cell released from a control sample of red cells from the same individual using the soluble VCN preparation only.

A series of sample treatments with VCN were also conducted at 0°C and 37°C in order to establish whether such treatments at temperatures much lower than those of the lipid phase transition for the cell membrane influenced the anomalous electrokinetic effects of VCN treatments observed at 37°C. Incubation at 0°C for four days produced complete sialic acid release and reduced the mobility of the cells to zero at 0°C, whereas the control cells were unaffected. The treated cells became positive at < pH 4 and more negative at pH values of ~9 or more as do those treated at 37°C. Thus, the peculiar effects of VCN on the cells are observed at 0°C as well as at 37°C.

Treatment of the top 5%, bottom 5% and a whole-population sample of density fractionated human red cells with 600-700 units VCN per 10^{10} red cells for one hour at 37°C uniformly reduced their mobilities to nearly zero in standard saline.

An attempt to identify the cationic charge groups at the surfaces of VCN treated cells was made by treating them with amino group-specific reagents. Only VCN treated red cells reacted with dimethylmaleic anhydride (DMA) as exhibited by an increase in the anodic electrophoretic mobility of the cells, which indicated the presence of free amino groups at the surfaces of these cells. Both native and formaldehyde fixed control red cells, as well as VCN treated cells which had been subsequently treated with formaldehyde, showed no increase in mobility on exposure to DMA. The maximum observable

increase in mobility of VCN treated native cells on treatment with DMA was from < -0.1 μm sec^{-1} V^{-1} cm to -0.37 μm sec^{-1} V^{-1} cm. This change was obtained by treatment of the cells at pH 8.0 ± 0.2 with 2.44 x 10^{-12} moles DMA per red cell. To obtain these concentrations ≤ 100 μl of DMA in ethanol was utilized per 10 ml of cell suspension. The resultant concentrations of ethanol were shown not to have an effect on the mobilities of the cells. The reactions were found to be completely reversible, i.e., short incubation of the cells at ~ pH 6 and subsequent resuspension in pH 8.0 media, caused the electrophoretic mobilities of the VCN treated cells to return to control values. Mere washing of the cells in pH 8.0 media did not result in a reversal of the reaction.

The actual conditions, under which the DMA reaction with free amino groups is reported to go to completion, are more drastic than those which could be employed with the red cells, i.e., the optimum pH for the reaction lies closer to 9-9.5 than to pH 8. VCN treated red cells are barely stable at pH 9. Therefore, it was decided to use the more vigorous maleic anhydride reagent which may be employed at physiological pH (253). The MA adduct is, however, much less labile than the DMA adduct, so for red cells the MA reaction is not reversible. However, for quantitation of the number of free amino groups present at the VCN treated red cell surface the reagent is ideally suited. Approximate quantitation of the number of amino groups per cell was

carried out by converting the change in mobility of red cells treated with MA to a change in charge density with the aid of Eq. 1-33. The results are expressed in terms of electron charges gained per red cell. The effective number of electrons gained per red cell is actually twice the number of amino groups present since reaction of one amino moiety with one molecule of MA results in the gain of two electron charges. The results are presented in Table 6-1. It is of special interest to note the small but significant number of amino groups demonstrated to be present on native human erythrocytes (~4.5×10^5 groups per red cell). An even more striking feature is the large number of free amino groups which appear in the peripheral zone of the cell following treatment with VCN (~5.6×10^6 groups per red cell). It should be pointed out that the number of amino groups calculated to be at the surface of the red cell represents a minimum since there can be no assurance that the reaction with MA is complete.

6.3 Discussion

This study developed from an interest in establishing the nature of the decreases in the sialic acid content of human red blood cells during *in vivo* aging. Balduini et al. (254) observed altered sialic acid contents for glycopeptides from density fractionated human red cells and suggested that desialylation of specific membrane glycoproteins accompanied aging. Cohen et al. (160) reported decreases of

Table 6-1. Quantitation of cationic groups on native and VCN treated RBC with maleic anhydride (MA) and formaldenyde.

RBC Experiment	I[1]	u[2] ($\mu m\ sec^{-1}\ V^{-1}\ cm$)	σ[3] e^-/RBC($\times 10^{-6}$)	$\Delta\sigma$[4] e^-/RBC($\times 10^{-6}$)	Minimum Apparent Number of Amino Groups ($\times 10^{-6}$)
Control	0.15	-1.09	13.0	0.9	0.45
Control-MA		-1.16	13.9		
VCN	0.15	-0.05	0.6	5.6	2.80
VCN-MA		-0.52	6.2		
VCN	0.15	-0.05	0.59	4.9	4.9
VCN-CH_2O		-0.46	5.45		
Control	0.015	-2.13	10.8	0.40	0.20
Control-MA		-2.82	11.2		
VCN	0.015	-0.65	2.4	1.6	0.80
VCN-MA		-1.07	4.0		
VCN	0.015	-0.65	2.38	1.05	1.1
VCN-CH_2O		-0.93	3.43		

[1] Ionic strength expressed in g-ions $\cdot L^{-1}$.

[2] Electrophoretic mobility.

[3] Charge density of erythrocytes (RBC) calculated using Gouy-Chapman Theory, expressed as electron charges per red cell. Each electron charge is assumed to correspond to one charged functional group. The surface area of a red cell was taken to be 163 μm^2 (49).

[4] Effective number of electrons gained per red cell on reaction of amino groups with MA. Reaction of one amino moiety with one molecule of MA results in the gain of two electron charges.

comparable magnitude in the sialic acid, membrane protein and lipid contents of density fractionated human red cells and suggested that membrane fragments were lost during aging. A resolution of which mechanism is responsible for the reported decreases in sialic acid content of senescent cells would have a major impact on views of the role of sialic acid as a determinant of red cell life span and on the use of neuraminidase in such studies.

As stated in the introduction to this chapter, the constancy in mobility of red cells over their life span suggests that the net number of sialyl residues remains constant per unit area of membrane. In order to establish which mechanism of sialic acid loss predominated, VCN was used to exhaustively desialylate density fractionated human cells with the rationale that the enzyme would only release sialyl residues and thereby simply eliminate the contribution of sialyl carboxyl groups to the negative surface charge of the cell. Accordingly, any differences in the number of nonsialyl carboxyl groups could then be detected by electrophoresis. When the electrophoretic mobilities of VCN treated old and young red cell fractions were compared, no differences were observed. The mobility of each fraction was reduced to about zero and was markedly increased by subsequent formaldehyde treatment. This behavior indicated that treatment of human red cells with VCN led to alterations of the cell surface in addition to desialylation and prompted directing the work towards elucidating the nature of

the changes produced in the molecular structure of the peripheral zone of whole populations of human erythrocytes as a result of interaction with VCN.

Formaldehyde fixation of erythrocytes extends the range of conditions over which they may be examined by electrophoresis (56). Fixation of native human red cells with formaldehyde does not produce any significant changes in their electrokinetic properties over the range of conditions where the cells are electrokinetically stable (56, 64), and aldehyde treatment has been used to examine cell surfaces for the presence of positive surface groups (117, 255).

Electrokinetic data obtained on VCN treated human erythrocytes before and after aldehyde treatment indicate that they have lost their polyanionic character (Fig. 6-2). However, the lack of specificity of the formaldehyde reaction has precluded the identification of the exact nature of the positive groups at the surface. Haydon and Seaman (113) using an earlier Behringwerke VCN preparation on human erythrocytes also found an increase in mobility on fixation of the enzyme treated cells, but attributed the appearance of cationic groups on the cell surface to the action of proteases in the VCN preparation. The authors found that if red cells were first treated with aldehyde, then VCN and finally again with aldehyde, the increase in mobility was smaller than for VCN modified native red cells fixed with aldehyde. The smaller increase in mobility of the fixed cells modified by VCN was attributed

to reduced proteolysis of the aldehyde fixed cells.

There is considerable evidence for adsorption of neuraminidase to the red cell surface starting with the work of Ada and French (256) who used adsorption of neuraminidase to RBC at 0°C for purification of the enzyme. Sedlacek and Seiler (257) found a fluoroisothiocyanate conjugated rabbit anti-VCN antibody that binds to VCN pretreated human erythrocytes, thus, also indicating VCN adsorption. Further evidence for adsorption of VCN to human red cells was provided by Lüben et al. (258) using a radiolabeled VCN preparation. Weiss (259) has pointed out that very low concentrations of VCN lead to complete release of sialic acid from human erythrocytes, but that the electrophoretic mobility of the neuraminidase treated cells decreases progressively further when treated with larger and larger amounts of VCN. He suggested that these observations may arise from the adsorption of VCN to the cell surfaces.

Due to the variety of methods used to prepare earlier VCN preparations and the paucity of published experimental detail with regard to enzyme treatment procedures, sample preparations, surface modification procedures, etc., a direct comparison of much of the previously reported data appeared unwise. For this reason the studies illustrated in Figs. 6-1 through 6-3, were conducted in order to establish whether the VCN preparation currently marketed by Behringwerke increased the cationic behavior of the cells as had been

described previously. Both the marketed preparation and the purified material with higher specific activity produced red cells with appreciable cationic characteristics. The isoelectric point of VCN modified native red cells in 0.15 M NaCl fell around pH 5.5 in agreement with Eylar et al. (142) and aldehyde treatment markedly increased the mobilities of the desialylated cells.

Assay of the stock Behringwerke VCN for protein consistently indicated a level of about 10 $\mu g \cdot ml^{-1}$, i.e., 10 μg per 500 units VCN. Now 50 units VCN per 10^{10} red cells is sufficient for complete desialylation in one hour at 37°C. Assuming a molecular weight of 90,000 for the VCN (260) this corresponds to approximately 1000 VCN molecules per red cell. Even if all the VCN were to adsorb this would be insufficient to produce the observed cationic character of the VCN treated cells. This was demonstrated experimentally by adsorbing large amounts of available VCN onto the red cells, i.e., at 0°C (Fig. 6-4) which does not change their electrokinetic properties significantly as a result of adsorption per se. This is further borne out by the fact that the electrokinetic properties of red cells treated with immobilized VCN are very similar to those of red cells treated with the soluble enzyme.

In previous reports a lack of purity of the enzyme preparation has been suggested as the source of the appearance of positive groups (113). Current preparations of VCN are reported by Behringwerke to

be free of protease, aldolase and phospholipase C activities and recently Lamont and Isselbacher (261) reported no detectable protease activity by VCN on radiolabeled hemoglobin. As indicated, protease contamination could not be dected in these studies either. Furthermore, the low protein content of the VCN preparation makes it extremely improbable that a trace contaminant could be present at a level sufficient to produce the observed cationic character of the VCN treated cells by a mechanism such as proteolysis. For example, in treatments of 10^{10} red cells with 60 units of VCN for three hours at 37°C, cationic groups appear but only ~1 μg total VCN protein is in the incubation medium.

Adsorption of proteins derived from the cells may be involved. However adsorption of hemoglobin to the surface of the desialylated cell is not supported by the studies of Piper (262) who noted that partial desialylation of human RBC with Vibrio cholerae neuraminidase markedly reduced the binding of hemoglobin and/or albumin and complete desialylation eliminated the binding of these proteins.

On treatment of VCN modified red cells with the specific amino group reagent maleic anhydride it was found that ~57% of the cationic groups which appear at physiological ionic strength are free amino groups. This is based on the assumption that formaldehyde treatment eliminates 100% of all cationic groups (see Table 6-1). At low ionic

strength free amino groups appear to account for ~73% of all cationic groups.

The most likely explanation for the apparently smaller number of cationic groups which appear to be present at the cell surfaces at low ionic strength as opposed to high ionic strength is that more negative groups, e.g., protein carboxyl groups which are situated deep within the peripheral zone, contribute to the overall charge properties of the cells on expansion of the double layer.

As shown in Table 6-1 a small number of positive groups do exist at the red cell surface. These groups have heretofore remained undetected by electrophoretic methods, which has previously led to the conclusion that the human erythrocyte is essentially a macropolyanion. Earlier studies which sought to block the positive groups lacked sensitivity and any changes which occurred were within the limits of experimental error of the techniques used.

Seaman and Uhlenbruck (263) discussed changes which can occur in the structure of the peripheral zone of red cells as a result of exposure to enzyme preparations. From our experimental data the adsorption of VCN or other components in the preparation, action of other enzymes in the preparation and the adsorption of hemoglobin from lysed cells in the suspension are all processes which are very unlikely to account for the observed cationic character of VCN treated cells. A possibility not considered by Seaman and Uhlenbruck (263) is

the effect of endogeneous red cell enzymes which may be activated by the increase in surface pH which accompanies desialylation, or by structural rearrangement of the peripheral zone. Protease (264) and phospholipase activities (265) have been indicated to be present in human red cells.

Nonenzymatic mechanisms which may account for the peculiar effects of VCN on the cell surface following desialylation include conformational changes of the molecular structure of the peripheral zone of the cell, adsorption of cellular components to the cell surface, redistribution of ions at the cell-medium interface and shifts in the location of the electrophoretic plane of shear. It has also been suggested that the carbohydrates at the cell surface interact by hydrogen bonding to form a lattice over the entire cell surface (266) and that removal of sialic acid residues could produce dramatic changes in such a structure.

While the mechanism of the appearance and the nature of the cationic groups on the surfaces of VCN treated human red cells remain unresolved, these studies indicate the following characteristics of the process:

a. The process occurs at 0°C as well as 37°C and appears to reach an electrophoretically measured endpoint.
b. The final electrophoretic mobilities at neutral pH are essentially the same for red cells treated with both formaldehyde

and VCN regardless of the order of treatment even though the mobilities of the VCN treated cells may be nearly zero prior to aldehyde treatment.

c. The appearance of cationic groups becomes pronounced during the removal of the last 30% of the VCN susceptible sialic acid residues.

d. The appearance of cationic groups does not represent the adsorption of components of the VCN preparation on the cell surface but rather the appearance of cell derived components which were previously not detectable by electrophoresis and aldehyde modification.

e. The agent in the VCN preparation which initiates the process is adsorbed to red cells at 0°C and probably represents VCN since the use of highly purified preparations also initiates the process.

The evidence presented here and by others introduces significant ambiguities into the interpretation of red cell studies where VCN has been used with the intent of removing sialic acid residues without altering other physicochemical properties of the cell surface. Until the process is understood, the results of experiments employing VCN in studies on the contribution of sialic acid to the physicochemical properties of the erythrocyte membrane and various cell contact phenomena must be interpreted with caution.

CHAPTER 7

CONCLUSIONS

1. The electrophoretic mobility and consequently the charge density of human erythrocytes is not a function of cell age.
2. The sialic acid content of young cells is ~10-15% higher than in old cells.
3. The apparent discrepancy between constant surface charge density during aging accompanied however by loss of membrane associated sialic acid is largely accounted for by the decrease in surface membrane area which is associated with loss of portions of the red cell membrane during aging.
4. Loss of membrane on aging of red cells is supported by a decrease in mean cellular volume, an increase in mean cellular hemoglobin concentration, an increase in cell density and approximately constant mean cellular hemoglobin values in going from young to old cells.
5. The mean value for the sialic acid content is 17.7 ± 1.5 fg per red cell. Reports that the actual absolute value was ~300% lower were investigated as to their validity. These reports were not substantiated.
6. Desialylation of erythrocytes with neuraminidase from Vibrio cholerae (VCN) is not limited to simple removal of sialic acid.

7. Desialylation with VCN is accompanied by an emergence of cationic charge groups at the electrophoretic surface of the erythrocytes which are not present prior to enzyme treatment.

8. The positive groups appear at the red cell surface after treatment of the cells with VCN immobilized on a solid support and the electrophoretic mobility of red cells with large amounts of VCN adsorbed to their surfaces is not different from native cells. Thus, the appearance of the positive groups cannot be attributed to VCN adsorption.

9. The enzyme preparation is free from detectable protease activity. Furthermore, the low protein content of the VCN preparation makes it extremely improbable that a trace contaminant would be present in a sufficient quantity to produce the observed cationic character by a mechanism such as proteolysis.

10. The cationic groups which appear after VCN treatment are of endogenous, i.e., cellular, origin.

11. Approximately 60% of the cationic groups at physiological ionic strength appear to be free amino groups.

12. A small but electrophoretically significant number of free amino groups exist in the peripheral zone of the native human erythrocyte.

13. The role which the appearance of amino and other positive charge groups in the cell periphery may play in the in vivo and/or in

vitro sequestration and phagocytosis of VCN treated cells and its relationship, if any, to red cell aging remains to be established.

14. Formaldehyde fixation of erythrocytes for purposes of cell stabilization and surface modification using solutions prepared by direct dissolution of commercially available paraformaldehyde in water or suitably buffered saline results in impure solutions which produce cells which have significantly different electrophoretic properties from native cells at low ionic strengths.

15. The basis for the electrophoretic differences between cells fixed in formaldehyde solutions prepared either directly from paraformaldehyde or by generating formaldehyde gas, is the presence of metallic impurities in commercially available paraformaldehyde preparations.

16. The impurities and thus, the anomalous electrokinetic properties of the fixed cells may be eliminated by generating formaldehyde gas from paraformaldehyde by heating the latter to 203-210°C or, alternatively, the impurities may be removed by addition of ethylenediamine tetraacetate dihydrate to fixative solutions prepared directly from paraformaldehyde.

17. The conductivity of native red cells is negligible. The conductivity of formaldehyde fixed erythrocytes is small but measurably greater than that of native erythrocytes.

18. The actual amount of current carried by native or fixed red cells in electrophoresis, however, is ~6 orders of magnitude less than that carried by the suspending medium. Thus, the increase in conductivity on fixation of cells is insignificant in terms of how much current either native or fixed cells carry under conditions encountered in cellular electrophoresis.

19. The packing efficiency factor for formaldehyde fixed cells is 0.65 as measured by a polymer dilution technique.

20. The electroosmotic fluid flow in cellular electrophoresis chambers constructed from glass may be dramatically reduced to about zero by coating the glass walls with diethylaminoethyl (DEAE) methylcellulose.

21. The stability of the electrophoresis chamber coating may be enhanced by crosslinking the gel with epichlorohydrin.

22. The effectiveness of the coating in eliminating the zeta potential of a glass surface may be varied by controlling the degree of DEAE derivatization of the gel.

BIBLIOGRAPHY

1. Reuss, F. F. Sur un nouvel effet de l'électricité galvanique. Mem. Soc. Imp. Nat. Moskou, 1809. 2, 327-337.

2. Wiedemann, G. Über die Bewegung von Flüssigkeiten im Kreise der geschlossenen galvanischen Säule. Poggendorff's Ann. Phys. Chem., Ser. 2, 1852. 87, 321-352.

3. Quincke, G. Ueber eine neue Art electrischer Ströme. Poggendorff's Ann. Phys. Chem., Ser. 2, 1859. 107, 1-47.

4. Dorn, E. Ueber die Fortführung der Electricität durch strömendes Wasser in Röhren und verwandte Erscheinungen. Wied. Ann., 1880. 10, 46-76.

5. Quincke, G. Über die Fortführung materieller Theilchen durch strömende Electricität. Poggendorff's Ann. Phys. Chem., Ser. 2, 1861. 113, 513-598.

6. Kühne, W. Ueber die chemische Reizung der Muskeln and Nerven und Ihre Bedeutung für die Irritabilitatsfrage. Reichert, Archiv, 1860. 315-354.

7. Smoluchowski, M. Przyczynek do teoryi endosmozy elektrycznej i niek tó rych zjawisk pokrewynch (Contribution à la théorie de l'endosmose électrique et de quelques phénomenes corrélatifs). Bull. Int. Acad. Sci. Cracovie, 1903. NV (1), 182-199.

8. Dukhin, S.S. & Derjaguin, B.V. Equilibrium double layer and electrokinetic phenomena. In E. Matijevic (Ed.) Surface and colloid science. Vol. 7. New York: John Wiley, 1974. (pages 49-272)

9. Overbeek, J. Th. G., & Wiersema, P.H. The interpretation of electrophoretic mobilities. In M. Bier (Ed.) Electrophoresis theory, methods, and applications. Vol. 2. New York: Academic Press, 1967. (pages 1-52)

10. Shaw, D.J. Electrophoresis. London: Academic Press, 1969. (pages 4-26).

11. Overbeek, J. Th. G., & Bijsterbosch, B. H. The electrical double layer and the theory of electrophoresis. In P. G. Righetti, C. J. Van Oss & J. W. Vanderhoff (Eds.) Electrokinetic separation methods. Amsterdam: Elsevier/North-Holland, 1979. (pages 1-32)

12. Debye, P., & Hückel, E. Bemerkungen zu einem Satze über die kataphoretische Wanderungsgeschwindigkeit suspendierter Teilchen. Phys. Z., 1924. 25, 49-52.

13. Henry, D. C. The cataphoresis of suspended particles. Part I. - The equation of cataphoresis. Proc. R. Soc. London, Ser. A., 1931. 133, 106-129.

14. Morrison, F. A., Jr. Electrophoresis of a particle of arbitrary shape. J. Colloid Interface Sci., 1970. 34, 210-214.

15. Abramson, H. A. Electrophoretic phenomena and their application to biology and medicine. New York: Chemical Catalog Co., 1934. (pages 100-135)

16. Furchgott, R. F., & Ponder, E. Disk-sphere transformation in mammalian red cells. II. The nature of the anti-sphering factor. J. Exp. Biol., 1940. 17, 117-127.

17. Seaman, G. V. F., & Pethica, B. A. A comparison of the electrophoretic characteristics of the human normal and sickle erythrocyte. Biochem. J., 1964. 90, 573-578.

18. Abramson, H. A. Modification of the Northrup-Kunitz microcataphoresis cell. J. Gen. Physiol., 1929. 12, 469-472.

19. Hunter, R. J., & Alexander, A. E. Surface properties and flow behavior of kaolinite. Part I. Electrophoretic mobility and stability of kaolinite sols. J. Colloid Sci., 1963. 18, 820-832.

20. Stigter, D. On the viscoelectric effect in colloidal solutions. J. Phys. Chem., 1964. 68, 3600-3602.

21. Lijklema, J., & Overbeek, J. Th. G. On the interpretation of electrokinetic potentials. J. Colloid Sci., 1963. 16, 501-512.

22. Gouy. Sur la constitution de la charge électrique a la surface d'un électrolyte. J. Phys. (Paris), 1910. 9, 457-468.

23. Chapman, D. L. A contribution to the theory of electrocapillarity. Philos. Mag., 1913. 25, 475-481.

24. Lewis, G.N., & Randall, M. The activity coefficient of strong electrolytes. J. Am. Chem. Soc., 1921. 43, 1112-1154.

25. Haydon, D.A. The electrical double layer and electrokinetic phenomena. Recent Prog. Surf. Sci., 1964. 1, 94-158.

26. Haydon, D.A. The surface charge of cells and some other small particles as indicated by electrophoresis. I. The zeta potential-surface charge relationships. Biochim. Biophys. Acta, 1961. 50, 450-457.

27. British standard methods for the determination of the viscoeity of liquids in C.G.S. units. London: British Standards House, 1957. (pages 1-62)

28. Weast, R.C. (Ed.) Handbook of chemistry and physics. (57th Ed.) Cleveland: Chemical Rubber Co., 1976. (pages F11 and F51)

29. Weast, R.C. (Ed.) Handbook of chemistry and physics. (57th Ed.) Cleveland: Chemical Rubber Co., 1976. (page F7)

30. Young, H.D. Statistical treatment of experimental data. New York: McGraw-Hill, 1962. (pages 1-172)

31. Grover, N.B., Naaman, J., Ben-Sasson, S., & Doljanski, F. Electrical sizing of particles in suspension. I. Theory. Biophys. J., 1969. 9, 1398-1414.

32. Kachel, V., Metzger, H., & Ruhenstroth-Bauer, G. Der Einfluss der Partikel Durchtrittsbahn auf die Volumenverteilungskurven nach dem Coulter-Verfahren. Z. Gesamte Exp. Med., 1970. 153, 331-347.

33. Brooks, D.E. Theoretical and experimental studies on the interaction of neutral polymers with cell surfaces. Unpublished doctor's dissertation, Univ. Oregon Medical School, 1971.

34. Waravdekar, V.S., & Saslaw, L.D. A method of estimation of 2-deoxyribose. Biochim. Biophys. Acta, 1957. 24, 439.

35. Warren, L. The thiobarbituric acid assay of sialic acids. J. Biol. Chem., 1959. 234, 1971-1975.

36. Aminoff, D. Methods for the quantitative estimation of N-acetylneuraminic acid and their application to hydrolysates of sialomucoids. Biochem. J., 1961. 81, 384-392.

37. Paerels, G.B., & Schut, J. The mechanism of the periodate-thiobarbituric acid reaction of sialic acids. Biochem. J., 1965. 96, 787-792.

38. Shaffner, W., & Weissmann, C. A rapid, sensitive, and specific method for the determination of protein in dilute solution. Anal. Biochem., 1973. 56, 502-514.

39. Tanford, C., & Roberts, G.L. Phenolic hydroxyl ionization in proteins and bovine serum albumin. J. Am. Chem. Soc., 1952. 74, 2509-2575.

40. Bradford, M.M. A rapid and sensitive method for the quantitation of microgram quantities of protein utilizing the principle of protein-dye binding. Anal. Biochem., 1976. 72, 248-254.

41. Campbell, D.H., Garvey, J.S., Cremer, N.E., & Sussdorf, D.H. Methods in immunology. New York: W.A. Benjamin, 1963. (pages 53-57)

42. Seaman, G.V.F. Microelectrophoresis of red blood cells. Unpublished doctor's dissertation, Univ. Cambridge, 1958.

43. Weiss, L. Effect of temperature on cellular electrophoretic mobility phenomena. J. Nat. Cancer Inst., 1966. 36, 837-847.

44. Ambrose, E.J. Cell electrophoresis. London: J. & A. Churchill, Ltd., 1965. (pages 1-204)

45. Brown, H.C., & Broom, J.C. Studies in microcataphoresis. I. Technique. Proc. R. Soc. London, Ser. B., 1936. 119, 231-244.

46. Abramson, H.A. Electrokinetic phenomena and their application to biology and medicine. New York: Chemical Catalog Co., Inc., 1934. (pages 256-282)

47. Mehrishi, J.N. Molecular aspects of the mammalian cell surface. In J.A.V. Butler & D. Noble (Eds.) Progress in biophysics and molecular biology. Vol. 25. Oxford: Pergamon Press, 1972. (pages 1-68).

48. Smith, M.E., & Lisse, M.W. A new electrophoresis cell for microscopic observations. J. Phys. Chem., 1936. 40, 339-412.

49. Seaman, G.V.F. Electrokinetic behavior of red cells. In D. MacN. Surgenor (Ed.) The red blood cell. (2nd Ed.) Vol. 2. New York: Academic Press, 1975. (pages 1135-1229)

50. Alexander, A.E., & Saggers, L. A simple apparatus for quantitative electrophoretic work. J. Sci. Instrum., 1948. 25, 374-375.

51. Bangham, A.D., Flemens, R., Heard, D.H., & Seaman, G.V.F. An apparatus for microelectrophoresis of small particles. Nature (London), 1958. 182, 642-644.

52. Seaman, G.V.F., & Heard, D.H. A microelectrophoresis chamber of small volume for use with biological systems. Blood, 1961. 18, 599-604.

53. Henry, D.C. A source of error in micro-cataphoretic measurements with a cylindrical-bore cell. J. Chem. Soc., 1938. 42, 997-999.

54. Seaman, G.V.F. Electrophoresis using a cylindrical chamber. In E.J. Ambrose (Ed.) Cell electrophoresis. London: J. & A. Churchill, Ltd., 1965. (pages 4-21)

55. Shaw, D.J. Electrophoresis. London: Academic Press, 1969. (pages 27-42)

56. Heard, D.H., & Seaman, G.V.F. The action of the lower aldehydes on the human erythrocyte. Biochim. Biophys. Acta, 1961. 53, 366-374.

57. Lamb, H. On the theory of electric endosmose and other allied phenomena, and on the existence of a sliding coefficient for a fluid in contact with a solid. Phil. Mag., 1888. 25, 52-70.

58. Seaman, G.V.F., & Brooks, D.E. Analytical cell electrophoresis. In P.G. Righetti, C.J. Van Oss & J.W. Vanderhoff (Eds.) Electrokinetic separation methods. Amsterdam: Elsevier/North-Holland, 1979. (pages 95-109)

59. Tiselius, A. A new apparatus for electrophoretic analysis of colloidal mixtures. Trans. Faraday Soc., 1937. 33, 524-531.

60. Altug, I., & Hair, M.L. Cation exchange in porous glass. J. Phys. Chem., 1967. 71, 4260-4263.

61. Strickler, A., & Sacks, T. Focusing in continous-flow electrophoresis systems by electrical control of effective cell wall zeta potentials. Ann. N.Y. Acad. Sci., 1973. 209, 497-514.

62. Van Oss, C.J., Fike, R.M., Good, R.J., & Reinig, J.M. Cell microelectrophoresis simplified by the reduction and uniformization of electroosmotic backflow. Anal. Biochem., 1974. 60, 242-251.

63. Brooks, D.E., & Seaman, G.V.F. The effect of neutral polymers on the electrokinetic potential of cells and other charged particles. I. Models for the zeta potential increase. J. Colloid Interface Sci., 1973. 43, 670-686.

64. Heard, D.H., & Seaman, G.V.F. The influence of pH and ionic strength on the electrokinetic stability of the human erythrocyte membrane. J. Gen. Physiol., 1960. 43, 635-654.

65. Andrade, J.D. Interfacial phenomena and biomaterials. Med. Instrum. (Baltimore), 1973. 7, 110-120.

66. Lee, L.H. Wettability and conformation of reactive polysiloxanes. J. Colloid Interface Sci., 1968. 27, 751-760.

67. Porath, J., Janson, J.-C., & Låås, T. Agar derivatives for chromatography, electrophoresis and gel-bound enzymes. I. Desulphated and reduced cross-linked agar and agarose in spherical bead form. J. Chromatogr., 1971. 60, 167-177.

68. Ma, S.M., Gregonis, D.E., Van Wagenen, R., & Andrade, J.D. Streaming potential studies on gel-coated glass capillaries. Polym. Prepr. Am. Chem. Soc. Div. Polym. Chem., 1975. 16, 421-423.

69. Peterson, E.A., & Sober, H.A. Chromatography of proteins. I. Cellulose ion-exchange adsorbants. J. Am. Chem. Soc., 1956. 78, 751-755.

70. Ragetli, H.W.J., & Weintraub, M. Agar derivatives for gel electrophoresis requiring reduced endosmotic flow. Biochim. Biophys. Acta, 1966. 112, 160-167.

71. Schell, H.D., & Ghetie, V.F. New medium-strength and strong and basic agarose ion exchangers. Rev. Roum. Biochim., 1972. 9, 165-177.

72. King, E.J., & Wootton, I.D.P. Micro-analysis in medical biochemistry. London: J. & A. Churchill Ltd., 1958. (pages 50-55)

73. Flodin, P. Dextran gels and their application in gel filtration. Unpublished doctor's dissertation, Univ. Uppsala, 1962.

74. March, J. Advanced organic chemistry: Reactions, mechanisms, and structure. New York: McGraw-Hill, 1968. (pages 307 and 319)

75. Bangham, A.D., Pethica, B.A., & Seaman, G.V.F. The charged groups at the interface of some blood cells. Biochem. J., 1958. 69, 12-19.

76. Seaman, G.V.F., & Pethica, B.A. The electrophoretic characteristics of the human normal and sickle erythrocyte. In Solid/liquid interface and cell/water interface, Proceedings of the Second International Congress on Surface Activity. London: Butterworths, 1957. (pages 277-287)

77. Hjertén, S. Free zone electrophoresis. Uppsala: Almqvist and Wiksells Boktryckeri AB, 1967. (page 51)

78. Peterson, E.A. Cellulosic ion exchangers. Amsterdam: North-Holland, 1970. (pages 236-237)

79. Hartley, G.S., & Roe, J.W. Ionic concentrations at interfaces. Trans. Faraday Soc., 1940. 36, 101-109.

80. Abramson, H.A. Electrokinetic phenomena. I. The adsorption of serum proteins by quartz and paraffin oil. J. Gen. Physiol., 1929. 13, 169-177.

81. Chattoraj, D.K., & Bull, H.B. Electrophoresis of adsorbed protein. J. Am. Chem. Soc., 1959. 81, 5128-5133.

82. Mehrishi, J.N., & Seaman, G.V.F. Temperature dependence of the electrophoretic mobility of cells and quartz particles. Biochim. Biophys. Acta, 1966. 112, 154-159.

83. Allen, R.E., Rhodes, P.H., Snyder, R.S., Barlow, G.H., Bier, M., Bigazzi, P.E., Van Oss, C.J., Knox, R.J., Seaman, G.V.F., Micale, F.J., & Vanderhoff, J.W. Column electrophoresis on the Apollo-Soyuz Test Project. Sep. Purif. Methods, 1977. 6, 1-59.

84. Eggerth, A.H. Changes in the stability and potential of cell suspensions. I. The stability and potential of bacterium coli. J. Gen. Physiol., 1924. 6, 63-71.

85. Eggerth, A.H. Changes in the stability and potential of cell suspensions. II. The potential of erythrocytes. J. Gen. Physiol., 1924. 6, 587-596.

86. Kozawa, S. Cataphoresis and hemolysis. Biochem. Z., 1914. 60, 146-158.

87. Abramson, H.A. Electrokinetic phenomena. III. The "isoelectric point" of normal and sensitized mammalian erythrocytes. J. Gen. Physiol., 1930. 14, 163-177.

88. Bungenberg de Jong, H.G. Reversal of charge phenomena, equivalent weight and specific properties of the ionised groups. In H.R. Kruyt (Ed.) Colloid science. Vol. 2. New York: Elsevier, 1949. (pages 259-334)

89. Few, A.Y., Gilby, A.R., & Seaman, G.V.F. An electrophoretic study on structural components of Micrococcus lysodeikticus. Biochim. Biophys. Acta, 1960. 38, 130-136.

90. Winkler, K.C., & Bungenberg de Jong, H.G. Structure of the erythrocyte-membrane. Arch. Néerl. Physiol., 1940-41. 25, 431-508.

91. Cook, G.M.W., Heard, D.H., & Seaman, G.V.F. Sialic acids and the electrokinetic charge of the human erythrocyte. Nature (London), 1961. 191, 44-47.

92. Seaman, G.V.F., & Heard, D.H. The surface of the washed human erythrocyte as a polyanion. J. Gen. Physiol., 1960. 44, 251-268.

93. Ponder, E. Effects produced by trypsin on certain properties of the human red cell. Blood, 1951. 6, 350-356.

94. Chapelle, E.W., & Luck, J.M. The decarboxylation of amino acids, proteins and peptides by N-bromosuccinimide. J. Biol. Chem., 1957. 229, 171-179.

95. Cook, G.M.W., Heard, D.H., & Seaman, G.V.F. A sialomucopeptide liberated by trypsin from the human erythrocyte. Nature (London), 1960. 188, 1011-1012.

96. Cornforth, J.W., Daines, M.E., & Gottschalk, A. Synthesis of N-acetylneuraminic acid (lactaminic acid, O-sialic acid). Proc. Chem. Soc., 1957. 25-26.

97. Cornforth, J.W., Firth, M.E., & Gottschalk, A. The synthesis of N-acetylneuraminic acid. Biochem. J., 1958. 68, 57-61.

98. Gottschalk, A. The influenze virus neuraminidase. Nature (London), 1958. 181, 377-378.

99. Gottschalk, A. Neuraminidase: The specific enzyme of influenza virus and Vibrio cholerae. Biochim. Biophys. Acta, 1957. 23, 645-646.

100. Burnet, F.M., McCrea, J.F., & Stone, J.D. Modification of human red cells by virus action. I. The receptor gradient for virus action in human red cells. Br. J. Exp. Pathol., 1946. 27, 228-236.

101. Ada, G.L., & Stone, J.D. Electrophoretic studies of virus-red cell interaction. Mobility gradient of cells treated with viruses of the influenza group and the receptor-destroying enzyme of V. cholerae. Br. J. Exp. Pathol., 1950. 31, 263-274.

102. Klenk, E., & Uhlenbruck, G. Über ein neuraminsäurehaltiges Mucopepteid aus Rindererythrocytenstroma. Hoppe-Seyler's Z. Physiol. Chem., 1958. 311, 227-233.

103. Klenk, E., & Lempfried, H. Über die Natur der Zellreceptoren für das Influenzavirus. Hoppe-Seyler's Z. Physiol. Chem., 1957. 307, 278-283.

104. Klenk, E. Neuraminic acid. In G. E. W. Wolstenholme & H. O'Connor (Eds.) Chemistry and biology of mucopolysacchardies. Boston: Little, Brown & Co., 1958. (pages 296-313)

105. Drezeniek, R., Bogel, K., & Rott, R. On the classification of bovine parainfluenza 3 viruses. Virology, 1967. 31, 725-727.

106. Huang, R. T., & Ohrlich, M. Substrate specificities of the neuraminidases of Newcastle disease and fowl plague viruses. Hoppe-Seyler's Z. Physiol. Chem., 1972. 353, 318-322.

107. Drezeniek, R. Wechselwirkungen zwischen Myxovirus und Zelloberflächen. I. Veränderungen der Zelloberfläche durch Myxovirus. Z. Med. Mikrobiol. Immunol., 1970. 155, 315-334.

108. Constantopoulos, A., & Najjar, V. A. The requirement for membrane sialic acid in the stimulation of phagocytosis by the natural tetrapeptide, tuftsin. J. Biol. Chem., 1973. 248, 3819-3822.

109. Den, H., Malinzak, D. A., & Rosenberg, A. Cytotoxic contaminants in commercial Clostridium perfringens neuraminidase preparations purified by affinity chromatography. J. Chromatogr., 1975. 111, 217-222.

110. Steck, T. L., Weinstein, R. S., Strauss, J. H., & Wallach, D. F. H. Inside-out red cell membrane vesicles: Preparation and purification. Science, 1970. 168, 255-257.

111. Marchesi, V. T., Furthmayr, H., & Tomita, M. The red cell membrane. Annu. Rev. Biochem., 1976. 45, 667-698.

112. Seaman, G. V. F., Vassar, P. S., & Kendall, M. J. Electrophoretic studies on human polymorphonuclear leukocytes and erythrocytes: The binding of calcium ions within the peripheral regions. Arch. Biochem. Biophys., 1969. 135, 356-362.

113. Haydon, D. A., & Seaman, G. V. F. Electrokinetic studies on the ultrastructure of the human erythrocyte. I. Electrophoresis at high ionic strengths-the cell as a polyanion. Arch. Biochem. Biophys., 1967. 122, 126-136.

114. Seaman, G. V. F., & Cook, G. M. W. Modification of the electrophoretic behaviour of the erythrocyte by chemical and enzymatic methods. In E. J. Ambrose (Ed.) Cell electrophoresis. London: J. & A. Churchill, Ltd., 1965. (pages 48-65)

115. Seaman, G.V.F., & Swank, R.L. The influence of electrokinetic charge and deformability of the red blood cell on the flow properties of its suspensions. Biorheology, 1967. 4, 47-59.

116. Knox, R.J., Nordt, F.J., Seaman, G.V.F., & Brooks, D.E. Rheology of erythrocyte suspensions: Dextran mediated aggregation of deformable and nondeformable erythrocytes. Biorheology, 1977. 14, 75-84.

117. Vassar, P.S., Hards, J.M., Brooks, D.E., Hagenberger, B., & Seaman, G.V.F. Physicochemical effects of aldehydes on the human erythrocyte. J. Cell Biol., 1972. 53, 809-818.

118. Pease, D.C. Histochemical techniques for electron microscopy. New York: Academic Press, 1964. (pages 1-381)

119. Marikovsky, Y., & Danon, D. Electron microscope analysis of young and old red blood cells stained with colloidal iron for surface charge evaluation. J. Cell Biol., 1969. 43, 1-7.

120. Marikovsky, Y., Lotan, R., Lis, H., Sharon, N., & Danon, D. Agglutination and labeling density of soybean agglutinin on young and old human red blood cells. Exp. Cell Res., 1976. 99, 453-456.

121. Corry, W.D., & Meiselman, H.J. Modification of erythrocyte physicochemical properties by millimolar concentrations of glutaraldehyde. Blood Cells, 1978. 4, 465-480.

122. Yee, J.P., & Mel, H.C. Kinetics of glutaraldehyde fixation of erythrocytes: Size, deformability, form, osmotic and hemolytic properties. Blood Cells, 1978. 4, 485-497. (Abstract)

123. Aminoff, D., Bell, W.C., Fulton, I., & Ingebrigtsen, N. Effect of sialidase on the variability of erythrocytes in circulation. Am. J. Hematol., 1976. 1, 419-432.

124. Carstensen, E.L., Aldridge, W.G., Child, S.Z., Sullivan, P., & Brown, H.H. Stability of cells fixed with glutaraldehyde and acrolein. J. Cell Biol., 1971. 50, 529-532.

125. Walker, J.F. Formaldehyde. New York: Reinhold, 1967. (pages 483-510)

126. Fricke, H. A mathematical treatment of the electric conductivity and capacity of disperse systems. Phys. Rev., 1924. 24, 575-587.

127. Ponder, E. Hemolysis and related phenomena. New York: Grune and Stratton, 1948. (page 60)

128. International Union of Pure and Applied Chemistry. Tests recommended in the 5th report of the commission on analytical reactions. 1964.

129. Moskowitz, M., & Carb, S. Surface alteration and the agglutinability of red cells. Nature (London), 1957. 180, 1049-1050.

130. French, D., & Edsall, J.T. The reactions of formaldehyde with amino acids and proteins. Adv. Protein Chem., 1945. 2, 277-333.

131. Fraenkel-Conrat, H., & Olcott, H.S. The reaction of formaldehyde with proteins. V. Cross-linking between amino and primary amide or guanidyl groups. J. Am. Chem. Soc., 1948. 70, 2673-2684.

132. Levy, M. Equilibria in the formol titration. J. Biol. Chem., 1933. 99, 767-779.

133. Fraenkel-Conrat, H., Cooper, M., & Olcott, H.S. The reaction of formaldehyde with proteins. J. Am. Chem. Soc., 1945. 67, 950-954.

134. Horning, E.C., & Horning, M.G. Methone derivatives of aldehydes. J. Org. Chem., 1946. 11, 95-99.

135. Saunders, F.L. Adsorption of methyl cellulose on polystyrene latexes. J. Colloid Interface Sci., 1968. 28, 475-480.

136. Walker, J.F. Formaldehyde. New York: Reinhold, 1967. (pages 502-503)

137. Bowes, J.H., & Carter, C.W. The reaction of glutaraldehyde with proteins and other biological materials. J.R. Microsc. Soc., 1965. 85, 193-200.

138. Walker, J.F. Formaldehyde. New York: Reinhold, 1967. (pages 52-82)

139. Schwan, H.P. Electrical properties of tissue and cell suspensions. In J.H. Lawrence, & C.A. Tobias (Eds.) Advances in biological and medical physics. New York: Academic Press, 1967. (pages 147-209)

140. Carstensen, E.L., Fuhrmann, G.F., Smearing, R.W., & Klein, L.A. The influence of conductivity on the electrophoretic mobility of red blood cells. Biochim. Biophys. Acta., 1968. 156, 394-402.

141. Bull, H.B., & Söllner, K. Mercury emulsions prepared with the aid of ultrasonic waves. Kolloid Z., 1932. 60, 263-268.

142. Eylar, E.H., Madoff, M.A., Brody, O.V., & Oncley, J.L. The contribution of sialic acid to the surface charge of the erythrocyte. J. Biol. Chem., 1962. 237, 1992-2000.

143. Warren, L. The distribution of sialic acids in nature. Comp. Biochem. Physiol., 1963. 10, 153-171.

144. Ledeen, R.W., & Yu, R.K. Chemistry and analysis of sialic acid. In A. Rosenberg, & C.L. Schengrund (Eds.) Biological roles of sialic acid. New York: Plenum Press, 1976. (pages 1-57)

145. Jancik, J., & Schauer, R. Sialic acid--a determinant of the lifetime of rabbit erythrocytes. Hoppe-Seyler's Z. Physiol. Chem., 1974. 355, 395-400.

146. Wintzer, G., & Uhlenbruck, G. Topochemische Anordnung von Gangliosiden in der Erythrozytenmembran. Z. Immunitätsforsch. Allerg. Klin. Immunol., 1967. 133, 60-67.

147. Kóscielak, J., Plasek, A., Górniak, H., Gardas, A., & Gregor, A. Structures of fucose-containing glycolipids with H and B blood-group activity and of sialic acid and glucosamine-containing glycolipid of human erythrocyte membrane. Eur. J. Biochem., 1973. 37, 214-225.

148. Van Deenen, L.L.M., & de Gier, J. Chemical composition and metabolism of lipids in red cells of various animal species. In C. Bishop, & D.M. Surgenor (Eds.) The red blood cell. (1st Ed.) New York: Academic Press, 1964. (pages 243-307)

149. Dische, Z. Amino sugar-containing compounds in mucoses and in mucous membranes. In E. A. Balazs & R. W. Jeanloz (Eds.) The amino sugars. Vol. 2A. New York: Academic Press, 1965. (pages 115-140)

150. Ashwell, G., & Morell, A. G. The role of surface carbohydrate in the hepatic recognition and transport of circulating glycoproteins. Adv. Enzymol., 1974. 41, 99-128.

151. Morell, A. G., Van Den Hamer, C. J. A., Scheinberg, I. H., & Ashwell, G. A. Physical and chemical studies on ceruloplasmin. IV. Preparation of radioactive, sialic acid-free ceruloplasmin labeled with tritium on terminal D-galactose residues. J. Biol. Chem., 1966. 241, 3745-3749.

152. Morell, A. G., Gregoriadis, G., Scheinberg, I. H., Hickman, J., & Ashwell, G. The role of sialic acid in determining the survival of glycoproteins in the circulation. J. Biol. Chem., 1971. 246, 1461-1467.

153. Berlin, N. I., & Berk, P. D. The biological life of the red cell. In D. MacN. Surgenor (Ed.) The red blood cell. (2nd Ed.) Vol. 2. New York: Academic Press, 1975. (pages 957-1019)

154. Beck, W. S. Iron metabolism and hypochromic anemias. In W. S. Beck (Ed.) Hematology. Cambridge, Mass.: MIT Press, 1973. (pages 27-50)

155. Danon, D., & Marikovsky, Y. Différence de charge électrique de surface entre érythrocytes jeunes et âgés. C. R. Acad. Sci., Ser. D., 1961. 253, 1271-1272.

156. Yaari, A. Mobility of human blood cells of different age groups in an electric field. Blood, 1969. 33, 159-163.

157. Danon, D., Marikovsky, Y. & Skutelsky, E. The sequestration of old red cells and extruded erythroid nuclei. In B. Ramot (Ed.) Red cell structure and metabolism. New York: Academic Press, 1971. (pages 23-38)

158. Greenwalt, T. J., & Steane, E. A. Quantitative haemagglutination. IV. Effect of neuraminidase treatment on agglutination by blood group antibodies. Br. J. Haematol., 1973. 25, 207-215.

159. Baxter, A., & Beeley, J.G. Changes in surface carbohydrate of human erythrocytes aged in vivo. Biochem. Soc. Trans., 1975. 3, 134-136.

160. Cohen, N.S., Ekholm, J.E., Luthra, M.G., & Hanahan, D.J. Biochemical characterization of density-separated human erythrocytes. Biochim. Biophys. Acta, 1976. 419, 229-242.

161. Balduini, C.L., Ricevuti, G., Sosso, C., Ascari, E., Brovelli, A., & Balduini, C. In vivo behaviour of neuraminidase-treated rabbit erythrocytes and reticulocytes. Acta Haematol., 1977. 57, 178-187.

162. Aminoff, D., Vorder Bruegge, W.F., Bell, W.C., Sarpolis, K., & Williams, R. Role of sialic acid in survival of erythrocytes in the circulation: Interaction of neuraminidase-treated and untreated erythrocytes with spleen and liver at the cellular level. Proc. Nat. Acad. Sci. U.S.A., 1977. 74, 1521-1524.

163. Marikovsky, Y., Elazar, E., & Danon, D. Rabbit erythrocyte survival following diminished sialic acid and ATP depletion. Mech. Ageing Dev., 1977. 6, 233-240.

164. Jancik, J., Schauer, R., & Streicher, H-J. Influence of membrane-bound N-acetylneuraminic acid on the survival of erythrocytes in man. Hoppe-Seyler's Z. Physiol. Chem., 1975. 356, 1329-1331.

165. Kay, M.M.B. Mechanism of removal of senscent cells by human macrophages. Proc. Nat. Acad. Sci. U.S.A., 1975. 72, 3521-3525.

166. Key, J.A. Studies on erythrocytes with special reference to reticulum, polychromatophilia and mitochondria. Arch. Intern. Med., 1921. 28, 511-549.

167. Borum, E.R., Figueuroa, W.G., & Perry, S.M. The distribution of Fe^{59}-tagged human erythrocytes in centrifuged specimens as a function of cell age. J. Clin. Invest., 1957. 36, 676-679.

168. Chalfin, D. Differences between young and mature rabbit erythrocytes. J. Cell. Comp. Physiol., 1956. 47, 215-239.

169. Dameshek, W., & Schwartz, S.O. Hemolysins as the cause of clinical and experimental hemolytic anemias with particular reference to the nature of spherocytosis and increased fragility. Am. J. Med. Sci., 1938. 196, 769-792.

170. Stephens, J.G. Surface and fragility differences between mature and immature red cells. J. Physiol., 1940. 99, 30-48.

171. Walter, H., & Albertsson, P-Å. Fractionation of red blood cells by multiple sedimentation at unit gravity. Exp. Cell Res., 1971. 67, 218-220.

172. Beutler, E., Blume, K.G., Kaplan, J.C., Löhr, G.W., Ramot, B., & Valentine, W.N. International Committee for Standardization in Haematology: Recommended methods for red-cell enzyme analysis. Br. J. Haematol., 1977. 35, 331-340.

173. Bishop, C., & Van Gastel, C. Changes in enzyme activity during reticulocyte maturation and red cell aging. Haematologica, 1969. 3, 29-41.

174. Rigas, D.A., & Koler, R.D. Ultracentrifugal fractionation of human erythrocytes on the basis of age. J. Lab. Clin. Med., 1961. 58, 242-246.

175. Murphy, J.R. Influence of temperature and method of centrifugation on the separation of erythrocytes. J. Lab. Clin. Med., 1973. 82, 334-341.

176. Piomelli, S., Lurinsky, G., & Wasserman, L.R. The mechanism of red cell aging. I. Relationship between cell age and specific gravity evaluated by ultracentrifugation in a discontinuous density gradient. J. Lab. Clin. Med., 1967. 69, 659-674.

177. Garby, L., & Hjelm, M. Ultracentrifugal fractionation of human erythrocytes as the basis of age. Blut, 1963. 9, 284-291.

178. Hjelm, M. Methodological aspects of current procedures to separate erythrocytes into age groups. In H. Yoshikawa & S.M. Rapoport (Eds.) Cellular and molecular biology of erythrocytes. Baltimore: University Park Press, 1974. (pages 427-444)

179. Turner, B.M., Fisher, R.A., & Harris, H. The age related loss of activity of four enzymes in the human erythrocyte. Clin. Chim. Acta, 1974. 50, 85-95.

180. Sass, M.D., Vorsanger, E., & Spear, P.W. Enzyme activity as an indicator of red cell age. Clin. Chim. Acta, 1964. 10, 21-26.

181. Herz, F., & Kaplan, E. A review: Human erythrocyte cholinesterase. Pediatr. Res., 1973. 7, 204-214.

182. Karmen, A. A note on the spectrophotometric assay of glutamic-oxalacetic transaminase in human blood serum. J. Clin. Invest., 1955. 34, 131-133.

183. Henry, R.J., Chiamori, N., Golub, O.J., & Berkman, S. Revised spectrophotometric methods for the determination of glutamic-oxaloacetic transaminase, glutamic-pyruvic transaminase, and lactic acid dehydrogenase. Am. J. Clin. Pathol., 1960. 34, 381-398.

184. Van Dilla, M.A., & Spalding, J.F. Erythrocyte volume distribution during recovery from bone marrow arrest. Nature (London), 1967. 213, 708-709.

185. Coopersmith, A., & Ingram, M. Red cell volumes and erythropoiesis. I. Age: density: volume relationship of normocytes. Am. J. Physiol., 1968. 215, 1276-1283.

186. Wilton, Å. An attempt to separate erythrocytes according to age by a new type of centrifuge. Acta Haematol., 1966. 35, 163-175.

187. Eilers, R.J. Notification of final adoption of an international method and standard solution for hemoglobinometry: specifications for preparation of standard solution. Am. J. Clin. Pathol., 1967. 47, 212-214.

188. Dacie, J.V., & Lewis, S.M. Practical hematology. (5th Ed.) New York: Churchill Livingstone, 1975. (pages 79-82)

189. Schick, H-J., & Zilg, H. Molecular properties of Vibrio cholerae neuraminidase. Proceedings of the Tenth International Congress of Biochemistry, 1976, 232. (Abstract)

201. Kolin, A., & Luner, S. J. Endless belt electrophoresis. In E.S. Perry & C.J. Van Oss (Eds.) Progress in separation and purification. New York: John Wiley, 1971. (pages 93-132)

202. Ware, B.R. Electrophoretic light scattering. Adv. Colloid Interface Sci., 1974. 4, 1-44.

203. Schauer, R., Corfield, A.P., Wember, M., & Danon, D. A micromethod for quantitative determination of acylneuraminic acids from erythrocyte membranes. Hoppe-Seyler's Z. Physiol. Chem., 1975. 356, 1727-1732.

204. Yachnin, S., & Gardner, F.H. Measurement of human erythrocyte neuraminic acid: Relationship to haemolysis and red blood cell virus interaction. Br. J. Haematol., 1961. 7, 464-475.

205. Durocher, J.R., Payne, R.C., & Conrad, M.E. Role of sialic acid in erythrocyte survival. Blood, 1975. 45, 11-20.

206. Manfredi, G. Determination of neuraminic acid in human red cells. Boll. Soc. Ital. Biol. Sper., 1960. 36, 447-449.

207. Juliano, R.L. The proteins of the erythrocyte membrane. Biochim. Biophys. Acta, 1973. 300, 341-378.

208. Westerman, M.P., Pierce, L.E., & Jensen, W.N. Erythrocyte lipids: A comparison of normal young and normal old populations. J. Lab. Clin. Med., 1963. 62, 394-400.

209. Winterbourn, C.C., & Batt, R.D. Lipid composition of human red cells of different ages. Biochim. Biophys. Acta, 1970. 202, 1-8.

210. Danon, D., Goldstein, L., Marikovsky, Y., & Skutelsky, E. Use of cationized ferritin as a label of negative charges on cell surfaces. J. Ultrastruct. Res., 1972. 38, 500-510.

211. Weiss, L. The topography of cell surface sialic acids and their possible relationship to specific cell interactions. Behring Inst. Mitt., 1974. 55, 185-193.

212. Gasic, G.J., Berwick, L., & Sorrentino, M. Positive and negative colloidal iron as cell surface electron strains. Lab. Invest., 1968. 18, 63-71.

213. Pierce, G.B., Sri Ram, J., Midgley, A.R., Jr. The use of labeled antibodies in ultrastructural studies. Int. Rev. Exp. Pathol., 1964. 3, 1-34.

214. Steck, T.L. The organization of proteins in the human red blood cell membrane. J. Cell Biol., 1974. 62, 1-19.

215. Marikovsky, Y., Khodadad, J.K., & Weinstein, R.S. Influence of red cell shape on surface charge topography. Exp. Cell Res., 1978. 116, 191-197.

216. Singer, S.J., & Nicolson, G.L. The fluid mosaic model of the structure of cell membranes. Science, 1972. 175, 720-731.

217. Peters, R., Peters, J., Tews, K.H., & Bahr, W. A microfluorimetric study of translational diffusion in erythrocyte membranes. Biochim. Biophys. Acta, 1974. 367, 282-294.

218. Loor, F., Forni, F., & Pernis, B. The dynamic state of the lymphocyte membrane. Factors affecting the distribution and turnover of surface immunogolobulins. Eur. J. Immunol., 1972. 2, 203-212.

219. Elgsaeter, A., & Branton, D. Intramembrane particle aggregation. I. The effects of protein removal. J. Cell Biol., 1974. 63, 1018-1036.

220. Gordon, J.A., & Marquardt, M.D. Erythrocyte morphology and clustering of fluorescent anti-A immunoglobulin. Nature (London), 1975. 258, 346-347.

221. Pinto da Silva, P., & Nicolson, G.L. Freeze-etch localization of Conconavalin A receptors to the membrane intercalated particles of human erythrocyte ghost membranes. Biochim. Biophys. Acta, 1974. 363, 311-319.

222. Cherry, R.J., Bürkli, A., Busslinger, M., Schneider, G., & Parrish, G.R. Rotational diffusion of band 3 proteins in the human erythrocyte membrane. Nature (London), 1976. 263, 389-393.

223. Danon, D. Biophysical aspects of red cell ageing. In Proceedings of the Eleventh Congress of the International Society of Hematology. Sydney: U.C.N. Blight Gov. Press, 1966. (pages 394-405)

224. Marikovsky, Y., Danon, D., & Katchalsky, A. Agglutination by polylysine of young and old red blood cells. Biochim. Biophys. Acta, 1966. 124, 154-159.

225. Walter, H., & Selby, F. W. Counter-current distribution of red blood cells of slightly different ages. Biochim. Biophys. Acta, 1966. 112, 146-153.

226. Greenwalt, T.J., Flory, L.L., & Steane, E.A. Quantitative haemagglutination. III. Studies of separated populations of human red blood cells of different ages. Br. J. Haematol., 1970. 19, 701-709.

227. La Celle, P.L., Kirkpatrick, F.H., Udkow, M.P., & Arkin, B. Membrane fragmentation and Ca^{+2} membrane interaction: Potential mechanisms of shape change in the senescent red cell. In M. Bessis, R.I. Weed & P.F. Leblond (Eds.) Red cell shape. New York: Springer, 1973. (pages 69-78)

228. Smith, B.D., La Celle, P.T., & La Celle, P.L. Elastic behavior of senescent human erythrocyte membranes. Biophys. J., 1977, 17, 28a. (Abstract)

229. Weed, R.I. The importance of erythrocyte deformability. Am. J. Med., 1970. 49, 147-150.

230. Cabantchik, Z.I., & Rothstein, A. Membrane proteins related to anion permeability of human red blood cells. I. Localization of disulfonic stilbene binding sites in proteins involved in permeation. J. Membr. Biol., 1974. 15, 207-226.

231. Cabantchik, Z.I., & Rothstein, A. Membrane proteins related to anion permeability of human red blood cells. II. Effects of proteolytic enzymes on disulfonic stilbene sites of surface proteins. J. Membr. Biol., 1974. 15, 227-248.

232. Knauf, P.A., & Rothstein, A. Chemical modification of membranes. I. Effects of sulfhydryl and amino reactive reagents on anion and cation permeability of the human red blood cell. J. Gen. Physiol., 1971. 58, 190-210.

233. Steck, T.L. The band 3 protein of the human red cell membrane: A review. J. Supramol. Struct., 1978. 8, 311-324.

234. Jacob, H.S., & Jandl, J.H. Effects of sulfhydryl inhibition on red blood cells. I. Mechanism of hemolysis. J. Clin. Invest., 1962. 41, 779-792.

235. Zipursky, A., Stephens, M., Brown, E.J., & Larson, P. Sulfhydryl groups of the erythrocyte membrane and their relation to glycolysis and drug-induced hemolytic anemia. J. Clin. Invest., 1974. 53, 805-812.

236. Vansteveninck, J., Weed, R.I., & Rothstein, A. Localization of erythrocyte membrane sulfhydryl groups essential for glucose transport. J. Gen. Physiol., 1965. 48, 617-632.

237. Ho, M.K., & Guidotti, G. A membrane protein from human erythrocytes involved in anion exchange. J. Biol. Chem., 1975. 250, 675-683.

238. Seaman, G.V.F., & Uhlenbruck, G. Die elektrophoretische Beweglichkeit von Erythrozyten nach Behandlung mit verschiedenen Enzymen und Antiseren. Klin. Wochenschr., 1962. 40, 699-700.

239. Bocci, V. The role of sialic acid in determining the life-span of circulating cells and glycoproteins. Experientia, 1976. 32, 135-140.

240. Landaw, S.A., Tenforde, T., & Schooley, J.C. Decreased surface charge and accelerated senescence of red blood cells following neuraminidase treatment. J. Lab. Clin. Med., 1977. 89, 581-591.

241. Jeanloz, R.W., & Codington, J.F. The biological role of sialic acid at the surface of the cell. In A. Rosenberg & C-L. Schengrund (Eds.) Biological roles of sialic acid. New York: Plenum Press, 1976. (pages 201-238)

242. Pye, J., & Curtain, C.C. Electrophoretic, sedimentation and diffusion behaviour of crystalline neuraminidase from Vibrio cholerae. J. Gen. Microbiol., 1961. 26, 423-425.

243. Axén, R., Dorath, J., & Ernback, S. Chemical coupling of peptides and proteins to polysaccharides by means of cyanogen halides. Nature (London), 1967. 214, 1302-1304.

244. Kågedal, L., & Akerstrom, S. Covalent binding of proteins to polysaccharides by cyanogen bromide and organic cyanates. I. Preparation of soluble glycine-, insulin- and ampicillin-dextran. Acta Chem. Scand., 1971. 25, 1855-1859.

245. Corfield, A.P., Beau, J-M., & Schauer, R. Desialylation of glycoconjugates using immobilized Vibrio cholerae neuraminidase: Preparation, properties and use of the bound enzyme. Hoppe Seyler's Z. Physiol. Chem., 1978. 359, 1335-1342.

246. Seaman, G.V.F., Jackson, L.J., & Uhlenbruck, G. The action of α-amylase preparations and some proteases on the surface of mammalian erythrocytes. Arch. Biochem. Biophys., 1967. 122, 605-613.

247. Bjerrum, O.J., Ramlau, J., Clemmesen, I., Ingild, A., & Bøg-Hansen, T.C. An artefact in quantitative immunoelectrophoresis of spectrin by proteolytic acitivity in antibody preparations. Scand. J. Immunol., Suppl. 2, 1975. 4, 81-88.

248. Gertler, A. Selective, reversible loss of elastolytic activity of elastase and subtilisin resulting from electrostatic changes due to maleylation. Eur. J. Biochem., 1971. 23, 36-40.

249. Butler, P.J.G., Harris, J.I., Hartley, B.J., & Leberman, R. Reversible blocking of peptide amino groups by maleic anhydride. Biochem. J., 1967. 103, 78-79.

250. Butler, P.J.G., Harris, J.I., Hartley, B.J., & Leberman, R. The use of maleic anhydride for the reversible blocking of amino groups in polypeptide chaings. Biochem. J., 1969. 112, 679-689.

251. Dixon, H.B.F., & Perham, R.N. Reversible blocking of amino groups with citraconic anhydride. Biochem. J., 1968. 109, 312-314.

252. Mehrishi, J.N. Positively charged amino groups on the surface of normal and cancer cells. Eur. J. Cancer, 1970. 6, 127-137.

253. Donner, M., & Mehrishi, J.N. The lymphocyte surface; differences in the surface chemistry of murine T lymphocytes of varying major histocompatibility haplotypes. Proc. R. Soc. London, Ser. B, 1978. 201, 271-284.

254. Balduini, C., Balduini, C.L., & Ascari, E. Membrane glycopeptides from old and young human erythrocytes. Biochem. J., 1974. 140, 557-560.

255. Seaman, G.V.F. The surface chemistry of the erythrocyte and thrombocyte membrane. J. Supramol. Struct., 1973. 1, 437-447.

256. Ada, G.L., & French, E.L. Purification of the receptor destroying enzyme of V. cholerae. Aust. J. Sci., 1950. 13, 82.

257. Sedlacek, H.H., & Seiler, F.R. Demonstration of Vibrio-cholerae neuraminidase (VCN) on the surface of VCN-treated cells. Behring Inst. Mitt., 1974. 55, 254-257.

258. Lüben, G., Sedlacek, H.H., & Seiler, F.R. Quantitative experiments on cell membrane binding of neuraminidase. Behring Inst. Mitt., 1976. 59, 30-37.

259. Weiss, L. Neuraminidase, sialic acids, and cell interactions. J. Nat. Cancer Inst., 1973. 50, 3-19.

260. Laver, W.G., Pye, J., & Ada, G.L. The molecular size of neuraminidase from Vibrio cholera (Strain 4Z). Biochim. Biophys. Acta, 1964. 81, 179-180.

261. Lamont, J.T., & Isselbacher, K.J. The effects of neuraminidase on Concanavalin A agglutination of erythrocytes: Evidence for adsorption of neuraminidase to erythrocyte membrane. J. Cell. Physiol., 1977. 90, 565-572.

262. Piper, W. Untersuchungen über die Wirkung des "Receptor-Destroying-Enzyme" auf menschliche Erythrocyten. Acta Haematol., 1957. 18, 414-428.

263. Seaman, G.V.F., & Uhlenbruck, G. The surface structure of erythrocytes from some animal sources. Arch. Biochem. Biophys., 1963. 100, 493-502.

264. Pennell, R.B. Composition of normal human red cells. In D. MacN. Surgenor (Ed.) The red blood cell. (Vol. 1) New York: Academic Press, 1974. (pages 93-146)

265. Van Deenen, L. L. M., & DeGier, J. Lipids of the red cell membrane. In D. MacN. Surgenor (Ed.) The red blood cell. (Vol. 1) New York: Academic Press, 1974. (pages 147-211)

266. Bretscher, M. S. Membrane structure: Some general principles. Science, 1973. 181, 622-629.

267. Sevier, E.D. Sensitive, solid phase assay of proteolytic activity. Anal. Biochem., 1976. 74, 592-596.